ESTIMATION OF DRIVER FATALITY RATIO USING COMPUTATIONAL MODELING AND OBJECTIVE MEASURES BASED ON VEHICLE INTRUSION RATIO IN HEAD-ON COLLISIONS

A Thesis by

Rajarshi Setpally

Bachelor of Technology, JNT University, 2008

Submitted to the Department of Mechanical Engineering
and the faculty of the Graduate School of
Wichita State University
in partial fulfillment of
the requirements for the degree of
Master of Science

December 2010

ESTIMATION OF DRIVER FATALITY RATIO USING COMPUTATIONAL MODELING AND OBJECTIVE MEASURES BASED ON VEHICLE INTRUSION RATIO IN HEAD-ON COLLISIONS

The following faculty members have examined the final copy of this thesis for form and content, and recommend that it be accepted in partial fulfillment of the requirement for the degree of Master of Science with a major in Mechanical Engineering.

_____
Hamid M. Lankarani, Committee Chair

_____
David N. Koert, Committee Member

_____
Krishna Krishnan, Committee Member

_____
Ramazan Asmatulu, Committee Member

DEDICATION

Mr. & Mrs. RaniLingareddy Setpally

Mr. & Mrs. ShirleyLakshmiNarsareddy Pennabadi

Dr. Hamid M. Lankarani

ACKNOWLEDGEMENT

Completing this research works was a challenge for me, it would not have been possible without the support, inspiration, encouragement and contribution of many entities. First of all I would like to thank Dr. Hamid Lankarani for his unconditional support and encouragement throughout my Masters program at Wichita State University. I heartily thank him for supporting me morally and on academic bases in different vicissitude. Without his support things would never been better than this.

My special thanks to Dr. David Koert for his love and support throughout my Master's program, I am very thankful to him for his unbelievable faith in me as a teaching assistant which helped me in re-identifying myself and work more efficiently. I would like to express my gratitude towards Dr. Krishna Krishnan and Dr. Ramazan Asmatulu for being my thesis committee members.

I am very much grateful to my Parents for their endless love and constant encouragement. I would also like to express my deepest gratitude and appreciation to my lovely sister and brother-in-law for their constant love, support and encouragement.

My sincere appreciations to Amarnath D, Rasoul M, Lavanya V, Rupali T for their help in countless and unmentionable way in completing my research work. Many thanks to my dearest friends Manikanta Bijju, Harish Muppalla, Shravan Sabbani, Mohith, Akhilesh, Anil, Srinivas, Rohitha, Kartheek A, Aneesha and Praneeth who shared with me their knowledge and friendship in every stage of my life. Finally I would like thank all my friends and colleagues for their understanding, support, assistance and cooperation.

ABSTRACT

In the last decade, the increase in usage of light trucks and vans (LTVs) has resulted in an increase in fatal injuries to the occupants of passenger cars for truck-car accidents, because of the aggressive nature of LTVs. To study the aggressive behavior of LTVs, National Traffic Highway Safety Administration (NHTSA) has developed an aggressivity metric (AM) for different vehicles in a specific impact configuration. These AM however does not produce consistent estimates when specific vehicle-to-vehicle impact categories are studied. Hence, NHTSA has introduced a Driver Fatality Ratio (DFR), based on the Fatality Analysis Reporting System (FARS) and General Estimating System (GES) crash Involvement statistics, which has produced good estimates of the aggressive behavior of vehicles in crashes.

The DFR proposed by NHTSA is based on the statistical data, which makes it difficult to evaluate DFR for other vehicle categories (e.g., crossovers, etc.), which are relatively new in the market as they do not have sufficient crash statistics. This research work proposes a new methodology based on computational reconstruction of impact crashes and objective measures to predict the DFR for any vehicle. The objective measures considered include the ratios of maximum intrusion, peak acceleration, and weight for the two vehicles in head-on collisions. Factors which directly influence fatal injuries to the occupants are identified and studied to develop a relation between these objective measures to the DFR. The proposed method is then validated for a range of LTVs against a passenger car, and is then used to predict the DFR for a cross category vehicle, a light pick-up truck, and a full-size car. Factors which influence these objective measures in predicting the DFR are discussed. Results from this study indicate that the ratio of intrusions produces a better estimate of the DFR and can be utilized in predicting fatality ratios for head-on collisions.

TABLE OF CONTENTS

TABLE OF CONTENTS (continued)

Chapter **Page**

LIST OF TABLES

LIST OF TABLES (continued)

LIST OF FIGURES

LIST OF FIGURES (continued)

Figure **Page**

LIST OF FIGURES (continued)

Figure **Page**

LIST OF FIGURES (continued)

Figure **Page**

LIST OF FIGURES (continued)

Figure **Page**

LIST OF FIGURES (continued)

Figure **Page**

LIST OF FIGURES (continued)

Figure **Page**

NOMENCLATURE

AM	Aggressivity Metric
COR	Coefficient of Restitution
CAD	Computer Aided Design
CAE	Computer Aided Engineering
DFR	Driver Fatality Ratio
EEVC	European Experimental Vehicle Committee
FARS	Fatality Analysis Reporting System
FMVSS	Federal Motor Vehicle Safety Standard
GES	General Estimating System
HIC	Head Injury Criteria
IIHS	Insurance Institute for Highway Safety
LTV	Light Truck and Van
MADYMO	Mathematical Dynamic Modeling
NHTSA	National Highway Traffic Safety Administration
NCAP	New Car Assessment Program
NCAC	National Crash Analysis Center
SUV	Sports Utility Vehicle
TTI	Thoracic Trauma Index
VC	Viscous Injury Response

CHAPTER 1

INTRODUCTION

1.1 Motivation

Human Life is the most valuable thing in this world and every human being in this world will always take preventive measures to protect his existence, especially during driving vehicles. In spite of the extreme attention and preventive measures there are always chances of fatal accidents. Much research has been done to protect the occupant involved in fatal accidents which made cars safer. When we compare the type of vehicles sold in the last decade to the period before it, it is evident that the sales of minivans, pickup trucks and sports utility vehicles are more when compared to the cars [1]. These LTVs are heavy, high ground clearance and are ruggedly constructed when compared with the passenger's cars on the road. These features of LTVs make them incompatible with passenger cars.

According to United States crash statistics, one third of all passenger cars in U.S. are LTVs and of all the vehicle collisions which occur in the US, over 50% accidents occur between LTVs and cars, out of which 81% of fatal injuries are in passenger cars [1]. From these statistics we can infer that LTVs and passenger cars are incompatible in road accidents, and LTVs are more aggressive when compared with cars.

This aggressiveness of LTVs over Passenger cars is measured by using a metric called aggressivity metric. This metric tells us how aggressive a particular type of LTV is when compared to passenger car which is given based on statistical data collected by FARS. This metric however does not produce reliable estimates in specific vehicle category, and hence the DFR is used to study the incompatibility between vehicles of specific category, which is also

based on FARS and GES. But the statistical data is not available for new cars and crossovers which motivated to do this research work to find out a way to predict the DFR of new vehicles.

1.2 Literature Review

Ever since the researchers realized that more than half of the accidents that occur in Unites States are because of the incompatibility between LTVs and passenger cars, researchers have explored different facets in this area. The following are some of the research work done by few individuals who contributed in developing this field of incompatibility between vehicles.

Gabler et al [2] focused on the factors which contribute for the incompatibility between vehicles, and found out that aggressivity metric will vary according to the vehicle weight, LTVs frontal structures are very stiff in comparison with passenger cars which make the LTVs to absorb less crash energy developed during vehicle crash.

Researchers like summers et al [3] have conducted extensive research in this field and also introduced a measure called as "Aggressivity Metric" (AM) and calculated for individual car classes and for different type of impact configurations. They also conducted a lot of experimental crash tests to find the relation between aggressivity metric and weight of the car, aggressivity metric and ride height of the car. They varied the height and weight of Chevy Lumina (passenger car) and Chevy K2500 (pickup truck) and crashed it against Honda Accord (target car) and found out that, increase in the weight of Chevy Lumina has high injury potential in the target car when compared with the increase in the ride height of the Chevy Lumina car. In the same way when a pickup truck Chevy K2500 is crashing against a Honda Accord car, increase in the ride height of K2500 has increased the injury potential in the target car when compared with increase in weight of Chevy K2500.

Gabler et al [4] proposed that the ideal compatibility scenario is achieved only when the crash energy is shared equally between two cars involved in an accident. They also proposed that high ride heights of the LTVs cause structural mismatch during frontal impacts, this structural mismatch leads to the under ride of the passenger car into LTV.

Joksh et al [5] proposed that weight, height of centre of Force, static stiffness can be correlated with the aggressivity metric. This study included that Aggressivity Metric of SUV is more dependent on its weight; whereas aggressivity metric of pickup Trucks are dependent on the ride height and static stiffness.

Joksh [6] has found out that aggressivity of SUV is higher than minivans or pick-up trucks. The report also discussed about the internal and external factors like drivers age, sex, vehicle weight, speed limit and so on.

Digges et al [7] have conducted experiments of crashing cars against load cell barrier and used the data from these barriers to predict vehicle compatibility. He conducted experiments on Jeep Grand Cherokee and Dodge Neon and found out that the load path of Grand Cherokee is much higher than Neon car which leads to geometric incompatibility in frontal impact scenario. For a crush of 250 mm, the amount of force exerted by neon is only half the amount of force exerted by Cherokee which indicates that when these two cars collide against each other most of the crash energy is absorbed by the Neon car. Height of the striking vehicle hood plays a vital role in the head injury criteria of the target passenger car.

Gabler et al [8] has proposed that the aggressivity of LTVs can be decreased by increasing the crashworthiness features of the passenger cars involving in crashes. Researchers have found out that LTVs are aggressive because of their greater weight, stiffer structure and higher ride height.

Les et al [9] proposed that vehicle mass, stiffness, frontal structure height and placement of key engine components in LTVs will play a crucial role in determining their aggressivity. They found out that vehicle wheel base, height of bonnet leading edge and bonnet length will also have an impact on aggressive behavior of vehicles.

Summers et al [10] have found out that in side impact crash scenarios weight of the bullet vehicle will not have a strong relation with neither the injury to occupants of vehicle nor the FARS and GES reported crash statistics. But he found out that during the oblique crash tests injury measures to the occupant are dependent on the weight of the vehicle and shows a good correlation with FARS reported data. The study concluded that in the frontal offset impacts along with the change in mass of the bullet vehicle there are other factors like geometric shape will have a strong impact on the injury to the occupants of the target car.

Gottumukkala [11] has conducted finite element simulation of Chevy C1500 (Bullet Car) crashing against Geo Metro (Target Car) and found out that decrease in the ride height and mass of the bullet car (Pickup Truck) reduced the injury risk in the target car's occupants. It was concluded by saying that both ride height and mass are two main factors which can directly influence the risk of injury and in turn the aggressivity metric too.

Yadav [12] in his research found out that in collision of a low floor transit bus against different range of vehicle, with increase in the weight of the bullet vehicle the injury potential of the occupant sitting in the transit is also increasing.

Bhagavatula [13] found out that use of air bag will prevent the occupant of a vehicle from svere neck injury during side impacts.

Krishnamurthy et al [14] have found out that the intrusion, combined injury index and internal energy ratio vary with change in mass, stiffness and the type of overlap occurring

between the vehicles. He also found out that mass of the vehicle is one factor which has a strong influence on the overall aggressivity of the pick-up trucks.

Maletz [15] found out that injury potential to the occupants sitting in the Geo Metro is higher than the occupant sitting in Ford Taurus.

Tay et al [16] have found out that, the focus of conventional occupant protection is mainly concentrated on increasing the crashworthiness which resulted in occupant protection and increase in vehicle size but this increase in size of the vehicle increases the overall driver fatality because of increase in aggressivity. The study found out large vehicles like SUV will increase the occupant protection but will have adverse effects than smaller cars because they are less aggressive. He also concluded that a profound shift in to smaller cars will reduce the overall accident fatalities.

Digges et al [17] have found out that vehicle weight will not adequately vary with vehicle stiffness and centre of force. Any vehicle can be high in weight but can still have less aggressivity because of its geometric incompatibility, in the same way an LTV can weigh less than a full size car but can still be more aggressive than it because of its high ride height and high frontal stiffness.

Latin et al [18] have found out in his research that risk of death to the drivers in the small and mid-size cars are same as the drivers of the SUV. The threat of injury for driver of small cars is the aggressive nature of the heavier vehicles where as the risk of injury for SUV is because of rollover chances as the centre of gravity will the high from the ground level when compared with the passenger cars. It was proposed in the study that a smaller car with all safety equipment like airbags, seatbelts can be safer than SUV in rollovers. Study evaluates that minivans are the safest vehicles than trucks and cars because they are build on full-size car chassis than a truck chassis.

It was found out that sports cars have the highest risk of injury because of it design. Pickup trucks are the vehicles with highest overall risk involved than any other vehicle because of its aggressive nature towards other vehicles and it can easily involve in rollover accidents. Pickups posses high risk to other because of its chassis stiffness and height. Quality of design of vehicle has more effect on the safety of the passengers than the weight of the vehicle.

As observed, almost all studies on the aggressivity of vehicles are either based on subjective statistical based data, or modeling a specific crash environment for two-car collisions. As, yet no study has been conducted which utilizes a general procedure for predicting the DFR for all category vehicles.

1.3 Objectives

The incompatibility of LTVs with passenger cars or aggressive behavior of LTVs are studied in this thesis using the DFR, which is based on the crash statistics such as the FARS reported fatalities and the GES reported crash involvements. As the DFR is dependent on the crash statistics, it is not possible to evaluate it for the new vehicles and crossovers, which do not fall into any conventional vehicle class because they have much quite less or no crash statistics available. The objective of this research is to utilize computational modeling and simulations and develop a new measure to predict DFR of a vehicle. The measures are based on the key factors which lead to fatal injuries to occupants of the vehicles in collisions. The methodology is validated with the DFR developed from the crash statistics. The new measure is then utilized to predict the DFR of the new and cross over vehicles.

CHAPTER 2

BACKGROUND

2.1 Impact Dynamics

Impact is a transmission of momentum from one body to another body during a very short span of time, resulting in high velocity changes of the vehicles in collision and small spatial changes during the collision process. The parameters which influence the impact response are [26]:

- Impact Velocity (↑ Velocity, ↑ Deformation and Crush)
- Structural Stiffness A, I (↑ Stiffness, ↑ Collision force)
- Material Properties E, S_y, S_u (Effects crush and COR)
- Contact Area and Shape (Effects Penetration and COR)

When a vehicle collides against an object, at higher velocities, intrusions and deformations are high in the vehicle. If the vehicle is made of materials which are quite stiff, then the collision force developed during crash will be high. The Coefficient of Restitution (COR) and the amount of crush a vehicle is dependent on the material properties of the vehicle and the amount of area which the vehicles made contact with colliding object and shape of the vehicle.

2.1.1 Crashworthiness

A study conducted on the impact performance of a vehicle colliding with any other object and has human being involved in the collision process is called as structural crashworthiness. From engineering side, crashworthiness can be defined as the ability of the vehicle to save its occupants during collision. Study of crashworthiness generally involves investigating structural damage of the car involved in collision, energy absorption capacity of the car during collision,

possible structural damage of the car when involved in collision, survivability of occupants in car during collision.

The desire behind the crashworthy structure is to build a vehicle which prevents the occupants from injuries when the vehicle is involved in an accident. To achieve this goal of occupant protection the main strategies which employed are:

1) Intrusions of the bullet object should be less in the target vehicle during collision. This is achieved only by having very strong vehicle compartment, A-pillar, B-pillar, C-pillar, strong roof, strong doors, and so on.
2) Impact energy is developed during the collision of vehicle against any object, the vehicle energy absorption capacity should be enough to absorb it and should not transfer force to the occupant compartment which results in injury to the occupant.
3) Vehicle stiffness is the third major factor which should be carefully governed while designing a safer vehicle. If a vehicle is manufactured with high stiffness, it experiences lower intrusions in it during collisions but due to high stiffness, the occupant of the vehicle experiences very high acceleration which can be fatal to the occupant.

2.1.2 Crash Severity

This crash severity is generally measured by using generated cabin accelerations and degree of cabin intrusions of the bullet vehicle on the target vehicle. Crash severity is further measured by using the Injury criteria on the occupants like HIC (Head Injury Criteria), TTI (Thoracic Trauma Index) and VC (Viscous Injury Response) [27].

Vehicle compatibility has a strong effect on the crashworthiness of the car. Compatible car collision are the collisions where the two vehicles have same load paths, vehicle stiffness and mass which results in lower cabin intrusions and accelerations and very less injury potential

to the occupants of the car. Compatible collision always leads to low crash severity and in the present day scenario compatible car crash is only possible between two identical cars from the same manufacturer. An incompatible collision occurs when the two vehicles in collision have different vehicle mass, collision stiffness and physical geometry that do not coincide with each other. This kind of incompatible collisions leads to quite higher injury potential to the occupant in the smaller car than in the bigger vehicle. A prime example for this kind of collision is an LTV striking a small passenger car. The following parameters play a crucial role in effecting crash severity:

- Vehicle mass incompatibility
- Vehicle collision stiffness incompatibility
- Vehicle geometry incompatibility
- Impact mode
- Closing speed

Mass of the vehicle is a very important factor in determining injury potential to the occupants in the vehicles involved in collisions. With the increase in the weight of the bullet car, the injury potential of the occupant in the target car increases. From this, one can state that fatality rate for an occupant sitting in a car is higher when the occupant is struck by an LTV, when compared with a passenger car. When a vehicle is involved in accidents, collision energy is developed which results in crush zone of the car which is low on frontal stiffness. The crush distance and crush force vary linearly in the crush zone and the collision force is given by the product of stiffness of the vehicle and crush.

Geometry of the vehicle also plays a crucial role in the injury potential of the occupant involved in collision. During various experiments, it has been demonstrated that different

vehicles with different frontal geometry when crashed against a load cell barrier produce different load paths. This difference in load paths results in incompatibility between vehicles and also geometric misalignment which may lead to fatal injuries to the occupants. For example, the load path of a Ford F250 and a Dodge Neon will very when they hit against a load cell wall. When these two vehicles collide against each other results in geometric misalignment and under-ride of neon into ford F250 [7].

Different impact modes will vary the injury potential of the occupant, for instance the injury potential of an occupant sitting in a car when struck in frontal direction will be different when the same occupant is struck in sideways. This is due to the variation in geometric shape, stiffness of the vehicle and crash energy absorption capacity on different sides. On an average when a vehicle frontal structure is involved in a collision it has almost 510 to 760 mm of crush zone after which the it starts intruding in to the occupant compartment. When we compare this to the side impact, the crush zone will be mere 200 to 300 mm. Rear collisions are again similar to the frontal impact where the crush zone will be almost the same as frontal impact [7].

2.2 Restraint System

When a car is involved in a crash against any object, first the car comes into contact with the object and then the occupant sitting in the car will come into the contact with car interior. In this case, if the occupant sitting in the car is not restrained (using seatbelt), the occupant will act as a projectile and keep moving forward which can lead to fatal injuries. Maximum number of motor vehicle fatalities occurs in frontal crashes, out of which two third of the people killed were unrestrained [15]. This indicates the importance of restraint system in vehicles. The most important restraint systems in vehicles are seatbelts and airbags which are discussed below.

2.2.1 Seat Belt

A seat belt or a safety belt restraints occupant sitting in the vehicle against sudden jerks or movements caused because of the vehicle collision with an object. This will prevent the occupant from hitting hard against the car interior when car crashes. This contact between occupant and car interior is called as second impact which can be prevented by using seat belts. These seat belts not only prevent us from second impact but also keep us in position or properly aligned with the airbag so that when it is deployed the face and airbag come into proper contact to prevent from head injury. In most of the passenger vehicles three point belt systems are used which has a lap belt and a shoulder belt. A worn seat belt always will hold the passenger in a proper way and prevent him from sliding or moving like a projectile when involved in a collision. These seatbelts are manufactured using elastic-plastic material to prevent from abrupt deceleration of the body. The seatbelt mechanism has two parts which are reactor, which tightens the belt after few milliseconds of impact and the other part is a pretensioner which makes sure that a constant force is absorbed during collision. According to NHTSA in the past decade almost 13000 lives are saved by seat belt and almost 7000 lives could have been saved if occupants wore seatbelts. In a further report NHTSA suggested that wearing seat belt will increase your chances of survival to 50% when involved in an accident [16].

2.2.2 Air Bag

An air bag is a safety device which is installed in a vehicle to prevent the occupant from hitting steering wheel or vehicle compartment during collision. From the year 1998 all the cars sold in US are employed with air bags in it and the statistics proved that the airbags have reduced the fatal accidents by at least 30% in these last 12 years [15]. Air bag consists of three parts, first part is a thin bag which is made of nylon and is folded into the steering wheel on driver side and

into the dashboard on the passenger side. This system also has a sensor which triggers the air bag to inflate within 15 to 50 ms after the impact or collision. The third part of this system is an inflation system which produces nitrogen and is filled in to the airbag. Failure in any one part out of these three constitutes of an airbag will lead to failure of airbag deployment during an event of collision which is highly dangerous the occupant of the vehicle, because occupant may come into contact with rigid occupant compartment of the vehicle which is highly dangerous.

2.3 Vehicle Aggressivity

2.3.1 Definition of Aggressivity

Compatibility of a vehicle is a combination of its "Crashworthiness" and "Aggressivity" with other vehicles on road. "Crashworthiness is capability of a vehicle to protect its occupants involved in crash. Whereas, aggressivity is a measure of how dangerous a vehicle can be in injuring occupants of the other vehicle involved in collision"[1]. In simple terms crashworthiness of a vehicle can be defined as self protection and decrease in aggressivity of a vehicle is generally referred to partner protection [1].

2.3.2 Approach

Vehicle incompatibilities may occur between two passenger cars, two LTVs and LTV to car, out of all the combination the most dangerous combination which has more number of fatalities registered statistics are for LTV to car crashes. In the year 1997, total number of fatalities occurred in all LTV to car crashes are 5373 out of which 4352 occurred only in the passenger car. In the same year out of the total 4459 fatalities in front impact modes, LTV to cars crashes (LTV was Bullet Vehicle) accounted for 62% (or 2765 deaths) of total fatalities. In side impact crash configuration, out of 4415 fatalities in that year, LTV to car crashes accounted for 57% (or 2536 deaths) of the total fatalities [1].

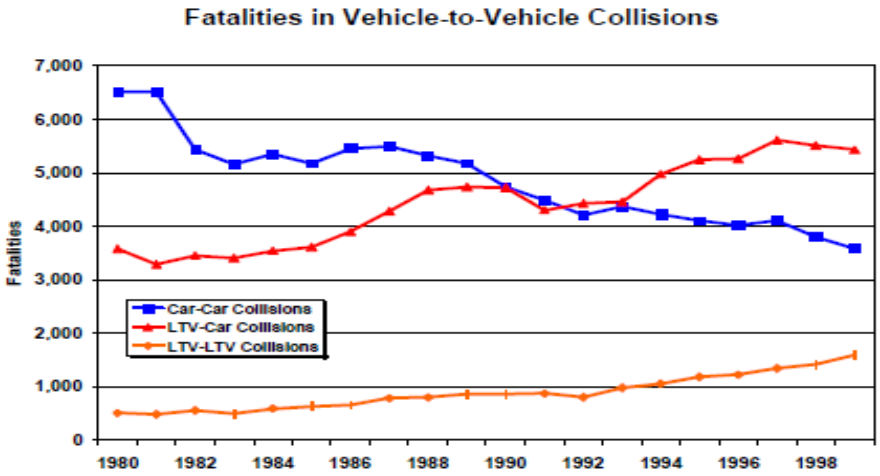

Figure 2.1: Fatalities in LTV to car crashes from year 1980 to year 1999 [9]

Figure 2.1 shows the fatalities occur in car to car crashes, car to LTV crashes and LTV to LTV crashes from the year 1980 to 1999 [9]. From this graph it is evident that the number of fatalities between two cars got decreased from the year 1980 to 1999, number of fatalities in LTV to LTV crashes were increased from year 1980 to 1999 but this increase in fatalities is very less when compared with the number of fatalities occurred in LTV to car crashes. Main reason behind these high fatalities is because of high sales and usage of LTVs. Figure 2.2 shows the increase in the number of LTV sales and Registration from the year 1980 to 1999 [9].

From these crash statistics, it is evident that a lot of incompatibility exists between these two classes of vehicles. This incompatibility may be because of the different type of load paths they exert when they involve in a crash or difference in mass or difference in ride height or due to any other factor. This incompatibility of an LTV over a smaller vehicle is generally expressed using a metric called as aggressivity metric. This aggressivity metric is generally calculated for LTVs using the crash statistics reported from FARS and GES. Figure 2.2 shows that the LTVs sales have increased from the year 1980 to 2000, simultaneously the sales of the passenger cars have decreased considerably. But during the impact LTVs are aggressive.

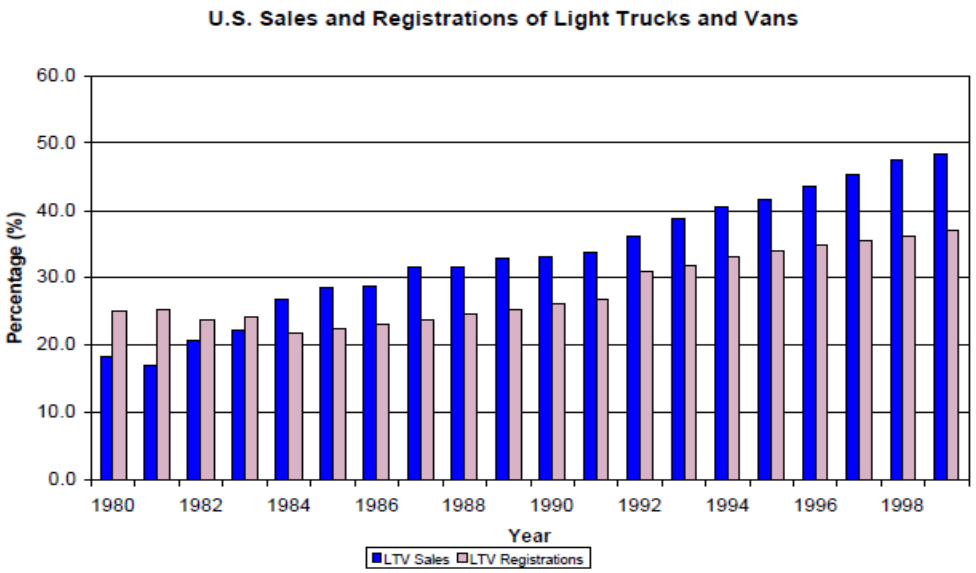

Figure 2.2: Percentage of sales and registrations of LTV from year 1980 to year 1999 [9]

2.3.3 Aggressivity Metric

Aggressivity metric has been evaluated using two different options which are proposed by NHTSA and are described here:

Option 1:

$$\text{Aggressivity} = \frac{\text{Fatalities in collision partner}}{\text{Registrations of subject vehicle}} \qquad (2.1)$$

This metric is developed by Hollowell and Gabler [5], which can be helpful in further research in the field. For each particular vehicle and model, the total numbers of fatalities in the collision partner are counted and then these fatalities are normalized by the total number of vehicle registration, normalization is done to prevent the vehicles with high registrations from high AM these fatalities in the subject vehicles are only taken for two vehicle crashes, where both vehicles are either car or an LTV. Using this method and examining all the statistics provided by FARS and GES Hollowell et al; found out that the LTVs are twice more aggressive than the passenger cars [1]. Within two years of proposing the first metric to predict aggressivity of a vehicle Hollowell et al has come out with a revised version of AM explained below.

Option 2:

$$\text{Aggressivity} = \frac{\text{Fatalities in collision partner}}{\text{Number of crashes of subject vehicle}} \qquad (2.2)$$

Gabler and Hollowell improved the aggressivity metric which they proposed earlier because in the previous method (option 1), the total number of fatalities where normalized against the number of vehicle registration, i.e. Aggressivity metric was dependent on the vehicle performance in terms of safety. However the accidents are generally dependent on the driver behavior. Generally aggressive drivers are more prone to accidents when compared with less aggressive drives. Considering this point Hollowell and Gabler proposed this new method where total number of fatalities in the collision partner was normalized by number of crashes in which the subject vehicle was involved. This "Aggressivity Metric" for a particular vehicle will be different in different impact modes. "Aggressivity Metric" for vehicle-to-vehicle crashes is shown from Figures 2.3 to 2.5 [9].

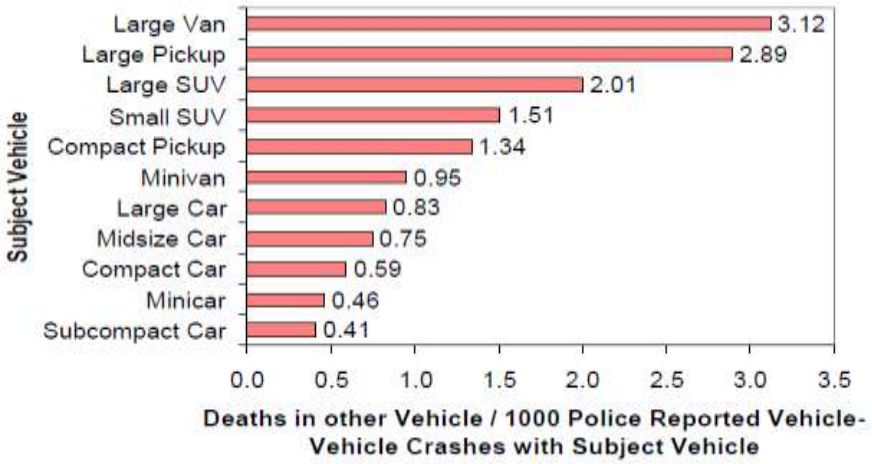

Figure 2.3: Aggressivity metric for vehicle-to-vehicle collisions [9]

Figure 2.3 shows the "Aggressivity Metric" for two-vehicle crashes in all impact modes (i.e., frontal, rear, side impact). It is evident that large van is the most aggressive vehicle and

subcompact car is the least aggressive vehicle. Aggressivity metric for all two vehicle crashes in frontal impact mode is shown in Figure 2.4.

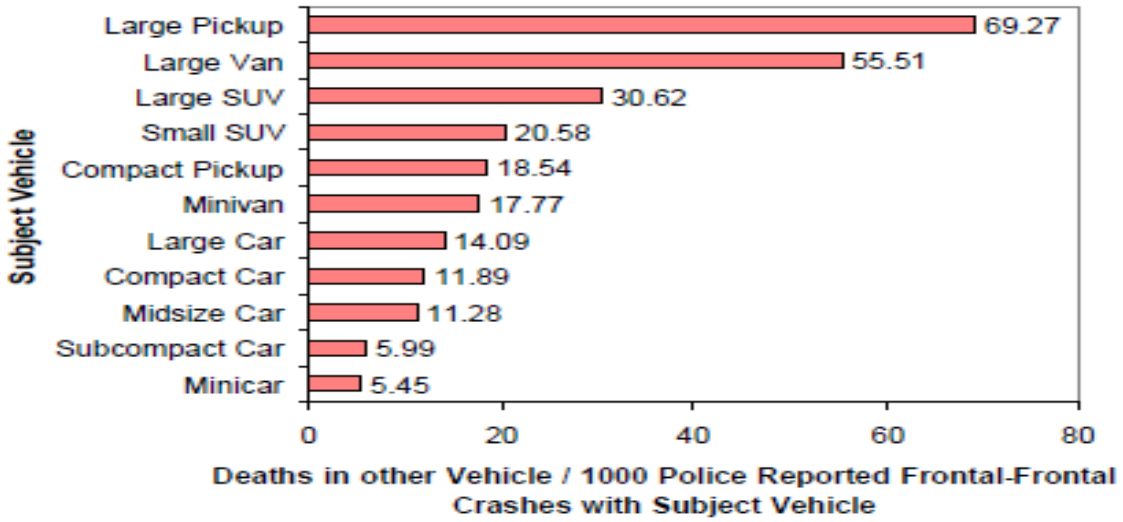

Figure 2.4: Aggressivity metric for vehicles in frontal impact mode [9]

Figure 2.4 shows the aggressivity metric of different vehicle class and it can be interpreted that large pickups have an AM of 69.27, which is high than a large van, which has an AM of 55.51. This is different when compared with the aggressivity metric in all impact modes where large van was more aggressive than large pickup. Aggressivity metric for all two-vehicle crashes in side impact modes is shown the Figure 2.5 [9]. From the figure, it is clear that the aggressivity of vehicles is much less when compared with the "Aggressivity Metric" of frontal impacts and the order of the vehicles from least to most aggressive vehicle is same as frontal AM All these "Aggressivity Metrics" are based on vehicle category and are calculated from statistics when each vehicle hit another vehicle in a particular impact mode. But it is always desirable to have aggressivity metric for a specific vehicle to another specific vehicle which will help us to understand the compatibility that exists between different specific vehicles.

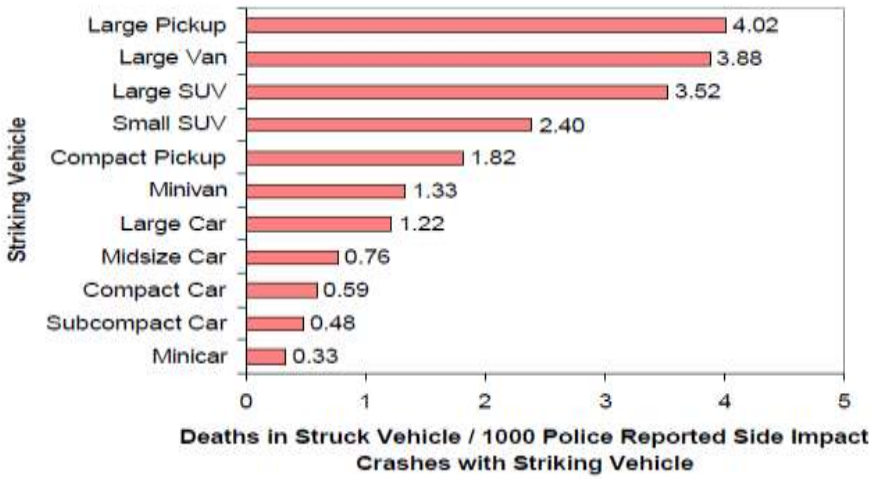

Figure 2.5: Aggressivity metric for vehicles in side impact mode [9]

The "Aggressivity Metric" when calculated for specific vehicle category produced values which were not reliable; instead of aggressivity metric they calculated the DFR for specific vehicles. These values are very reliable and are calculated for vehicles whose model year was at least 1990. In calculating the "Driver Fatality Ratio", driver age was also taken into consideration, drivers with age less than 25 and greater than 55 were eliminated in calculation [9]. All these calculations were done from the statistics reported by FARS. These driver fatality ratios are different for different mode of crash impact. Driver Fatality Ratio for Frontal - frontal LTV to car crashes are shown in Figure 2.6.

Figure 2.6, shows that if one person experiences a fatal injury in the compact pickup then 2.6 fatal injuries will occur in passenger car. Similarly it provides the fatality ratios for minivans, sports utility vehicle, full-size pickup and full-size van. It can be inferred that full-size pickup are the most dangerous out of all the LTVs which is in line with the aggressivity metric for the frontal impact which shows that Full-size van is most aggressive. Driver Fatality Ratios for the side impact of LTV-to-car crashes are shown in Figure 2.7 [9]. This Driver Fatality Ratio varies with the kind of crash configuration, such as side, frontal and rear impact scenarios.

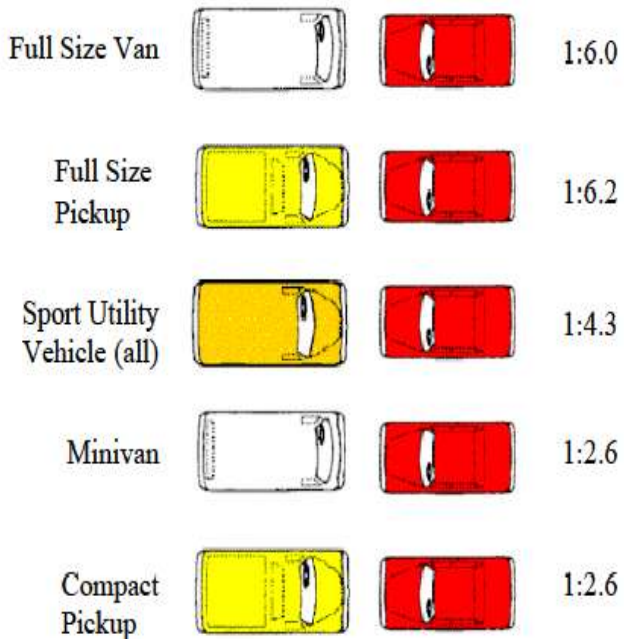

Figure 2.6: Driver Fatality Ratio in frontal impact mode [9]

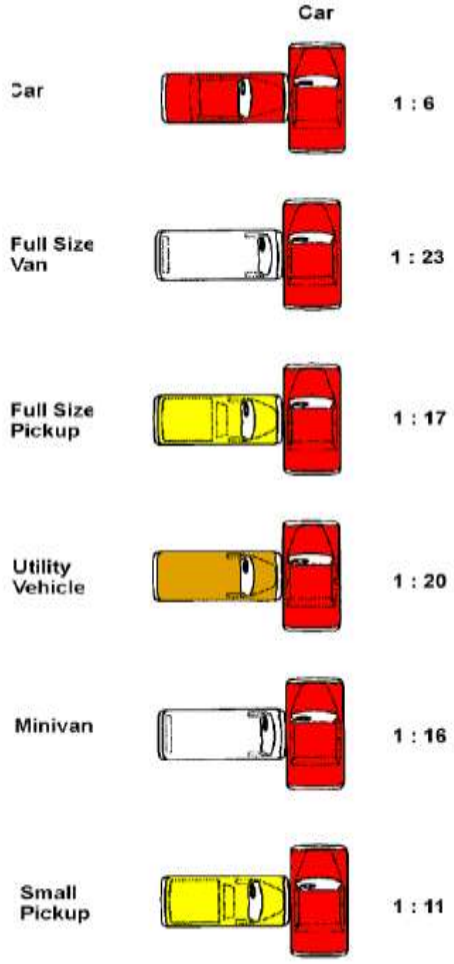

Figure 2.7: Driver Fatality Ratio in side impact mode [1]

From Figure 2.7, it is evident that the driver fatality ratio depends on the mode of impact, it can also be inferred that full-size van are the most aggressive vehicles with a fatality ratio of 1: 23 [side aggressivity].

2.3.4 Factors Causing Incompatibility

From all these preceding statistics, calculation and discussions it is evident that LTVs are more aggressive and incompatible with passenger car. The reason behind this incompatibility is because of design characteristics of LTV. Based on the physics of the problem, the three major factors which cause incompatibility seems to be:

1. Mass Incompatibility.
2. Stiffness Incompatibility.
3. Geometric Incompatibility.

2.3.4.1 Mass Incompatibility

According to law of conversation of momentum, during a collision the smaller vehicle has disadvantage when compared with a heavier vehicle and on an average all the LTVs are about 900 pounds heavier than passenger cars. This huge difference in weight between two cars creates a lot of incompatibility between them when they collide. Figure 2.8 shows the "Aggressivity Metric" as a function of mass for different vehicles. From the figure, it can be observed that as the mass of a car increases, it becomes more aggressive and becomes incompatible with cars. However there are few exceptions, for example a mid-size car weighing more than an SUV is less aggressive than an SUV, and an SUV weighing less than a mid-size car but SUV is more aggressive than the mid-size car. The reasons behind these exceptions are because of other factors like stiffness or geometric incompatibilities. The influence of geometric

incompatibility and stiffness incompatibility on the aggressive behavior of a vehicle is explained next.

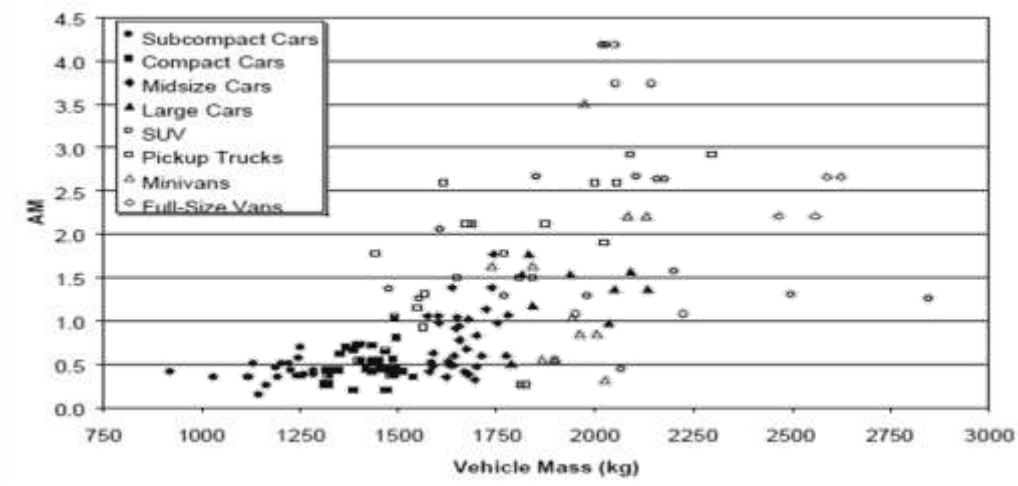

Figure 2.8: Variation of aggressivity metric with variation in mass of the vehicle [1]

2.3.4.2 Stiffness Incompatibility

LTVs are stiffer when compared with passenger cars. LTVs have a very stiff front rail design which makes it very incompatible with the cars. This high stiffness of LTVs makes the passenger car to absorb all the crash energy developed during the collision. From NHTSA's NCAP test results, the linear stiffness of some vehicles can be estimated by using equation [1].

$$k = (mv^2) / x^2 \tag{2.3}$$

Where, m is the mass of the vehicle, v is the initial velocity of the vehicle, x is the maximum dynamic crush distance. Figure 2.9 shows that an increase in the stiffness of a vehicle increases its "Aggressivity metric" as small. It can also be observed from Figure 2.9 that though for few mid-size cars the stiffness is higher than the LTVs, their "Aggressivity Metric" is not high and for few LTVs with lower stiffness than passenger cars, their Aggressivity Metric" is high, this indicates that there are other factors that govern the "Aggressivity Metric" like mass

incompatibility, and stiffness incompatibility. Many researchers have widely accepted and used equation proposed by NHTSA to calculate the dynamic stiffness of a vehicle involved in crash.

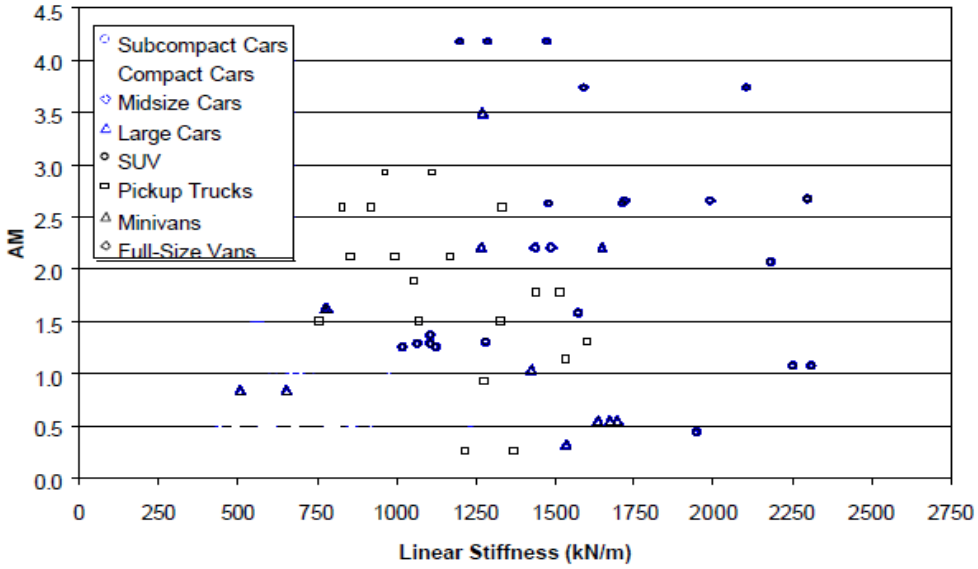

Figure 2.9: Variation of aggressivity metric with variation in linear stiffness [1]

From the stiffness equation provided by NHTSA, it is evident that stiffness of a vehicle and mass are related to each other, Figure 2.10 shows the variation of stiffness with increase in mass [1].

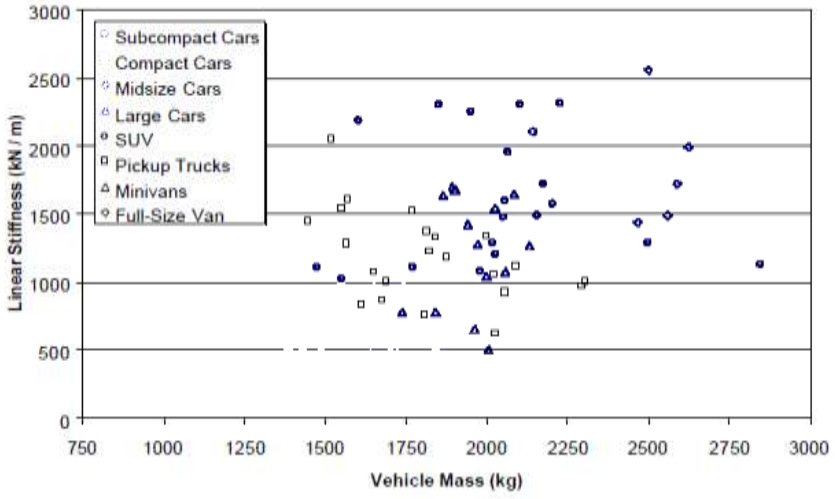

Figure 2.10: Variation of linear stiffness with variation in mass of the vehicle [1]

From Figure 2.10, it is apparent that for a particular weight, different range of stiffness is possible. For example, for a vehicle of 2000 kg, it is possible to have a linear stiffness varying from 500 kN/m to 2500 kN/m. This shows that the stiffness is not as dominant factor as compared with mass in influencing the aggressivity of a vehicle. For two-vehicles to be compatible, ultimate situation would be to share all the crash energy developed during the collision between them rather than forcing one car to absorb bulk of the crash energy developed.

2.3.4.3 Geometric Incompatibility

For all LTVs, the ride height is usually quite high when compared to the passenger cars to suite both on-and-off road conditions. This high ride height of LTVs leads to different load paths when compared to passenger cars and also when they collide, it will lead to a mismatch of ride height. This results in the under ride of the passenger car in to the LTV leading to fatal injuries to the occupant in the passenger car during frontal Impact modes. In case of side impact, if the ride height is very high, the LTV will override the car sill door and directly results in high passenger cabin intrusions.

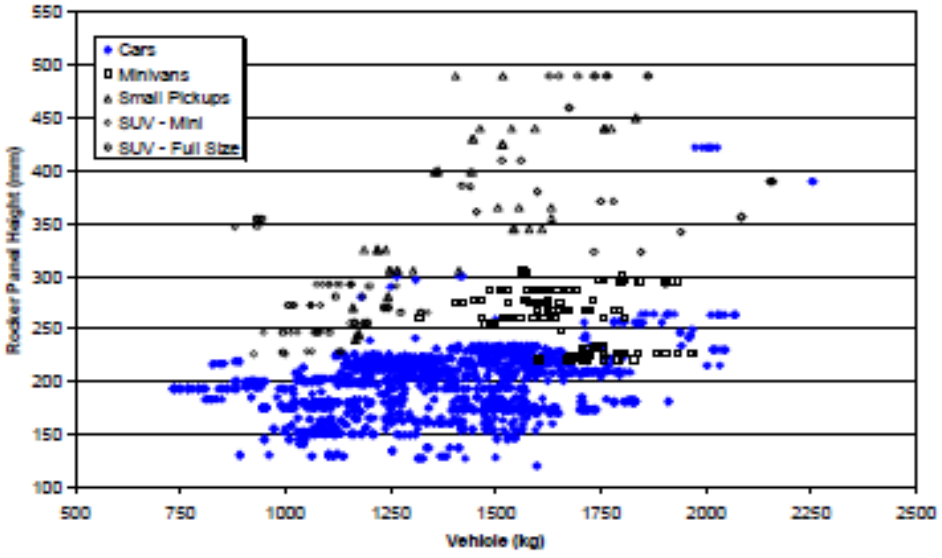

Figure 2.11: Variation of ride height with variation in mass of the vehicle [1]

Figure 2.11[1] shows how the ride height varies as the mass of the vehicle is increasing. It can be inferred from the Figure 2.11 that the ride height of the passenger cars is almost consistent with the vehicle mass with few exceptions, due to the bumper standard. As there is no bumper standard for LTVs, the ride height varies with increase in mass.

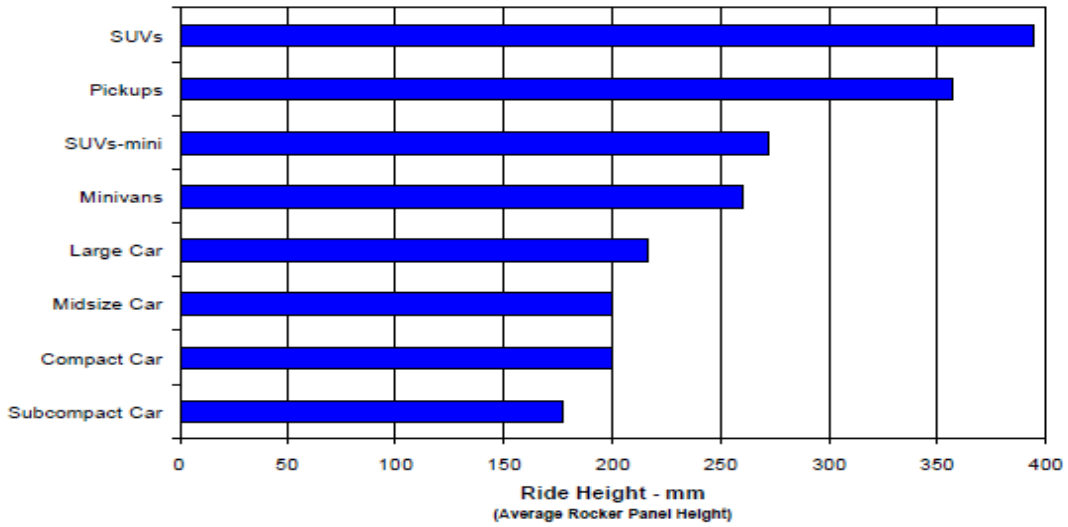

Figure 2.12: Ride height of different class vehicles [1]

Figure 2.12 [1] shows the average ride height of specific vehicle categories and it is clear that the SUVs ride quite high, and sub-compact cars ride low, when compared with other vehicles. This difference in ride height always result in geometric misalignment and results in high incompatibility between vehicles.

2.4 Crash Standards and Test Procedures

Different types of static and dynamic tests have been developed in the last few decades to fully evaluate the impact behavior of vehicles and the possible injuries to the occupants in the vehicles during impacts. The main ideology behind these test procedures is to provide maximum possible safety to the occupants during collision.

The most important crash test procedures are [15]:

1. FMVSS (Federal Motor Vehicle Safety Standard) [21]
2. NCAP (New Car Assessment Program) [21]
3. IIHS (Insurance Institute for Highway Safety) [20]
4. EEVC (European Experimental Vehicle Committee) [15]

In US, NHTSA takes care of the automotive standards. The NHTSA is a wing of US Department of Transportation (DOT), and NHTSA carry out several safety and crash tests of vehicles under National Traffic and Motor Vehicle Safety Act of 1966 and Highway Safety Act of 1966. Main job of NHTSA is to reduce driver fatalities during accidents in US. NHTSA has made legislation mandatory to carry safety test tests under title 49 of the US code of federal regulations. Each of these safety tests is different from one another to see the impact behavior of the vehicle during collisions [15].

2.4.1 FMVSS

There are a number of FMVSS regulations for different certification tests such as interior testing, dashboard testing, frontal impact, side impact, seats, seat belts, rear impact, rollover, head rest, roof crush and so forth [15]. There are specific standards for each type of testing like FMVSS 208 for occupant crash protection, FMVSS 209 for seat belt assemblies, FMVSS 201 for occupant protection in interior impact, FMVSS 205 for glazing materials, FMVSS 212 for windshield mounting, FMVSS 216 for roof crush resistance, FMVSS 219 windshield zone intrusion, FMVSS 203 for impact protection for driver from steering control system and so on. The most common crash test regulation out of all these regulations are the FMVSS 208 for Occupant Crash Protection (Frontal), FMVSS 214 Side Impact Protection, FMVSS 201 for occupant Protection in interior impact and FMVSS 213 for child restraint systems.

2.4.1.1 FMVSS 208

The main purpose of this standard is to reduce the number of fatalities and fatal injuries to occupants involved in frontal crash collisions. The standard test procedure involves frontal, angled and or offset vehicle test.

Full-Width Frontal Impact Test: In this test, a car is crashed against a flat rigid wall, with full-width contact of the car against the barrier. In this kind of test, a 50% Hybrid *III* dummy is used. Figure 2.13 shows this type of configuration [21].

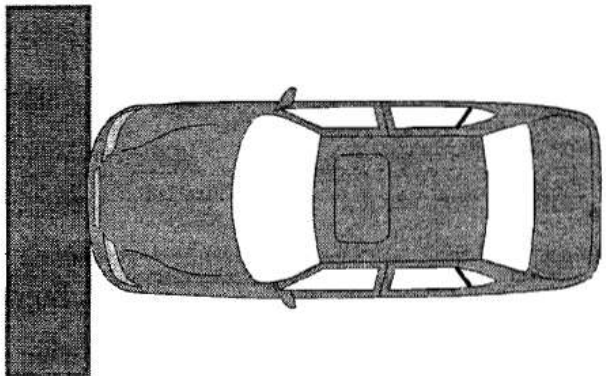

Figure 2.13: FMVSS208 full width frontal crash test configuration against flat rigid wall [21]

Full Width Frontal Impact Test: This type of test procedure is same as explained above; the only difference is the kind of barrier used. In this kind of test, a winkle rigid barrier is used. The configuration of this test is shown in Figure 2.14 [21].

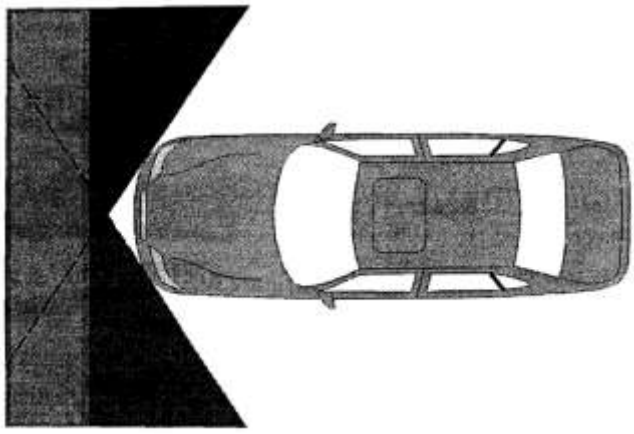

Figure 2.14: FMVSS208 full width crash test configuration against winkle rigid barrier [21]

Offset Frontal Impact Test: In this kind of test, only 40% of cars total width comes into contact with the barrier and the barrier is a deformable (generally honeycomb barrier is used). Car crashes in to this barrier at 35mph with a 50% hybrid *III* dummy. The test configuration for this kind of impact is shown in Figure 2.15 [21].

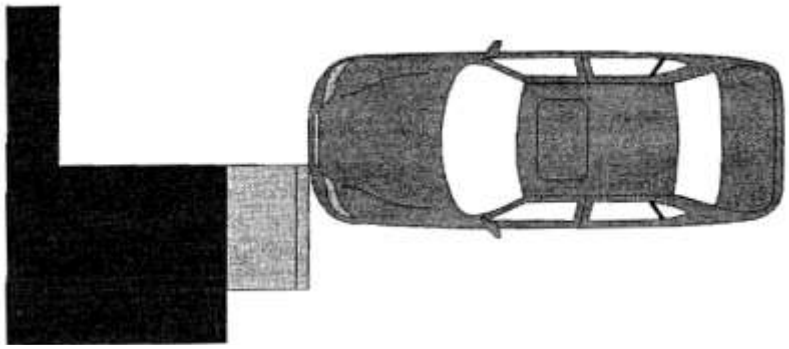

Figure 2.15: FMVSS208 Offset frontal crash test configuration against deformable barrier [21]

This standard allows only a certain amount of maximum load on different parts of the 50^{th} % dummy. If the load on these parts exceeds the limit specified, then those cars are said to violate FMVSS 208 standard. The pass/fail criteria in these standards are [27]:

1. The Head Injury Criteria for a 36 ms window (HIC 36) should not exceed 1000.
2. The femur load should not exceed 10 kN.
3. The maximum chest acceleration and deflection allowed are 60g's and 76 mm respectively.
4. Neck Injury Criteria value should not exceed 1.4

2.4.1.2 FMVSS 214

The reason behind establishing this standard is to protect the occupants in the vehicle during side impact crashes. In this type of test, the configuration is so build to create an intersection type of impact on the vehicle, then see the thoracic and pelvic area of the dummy for injuries on it and also to see the impact behavior of the vehicle in side impact. The test

configuration of this test is shown in the Figure 2.16. The maximum pass/fail which this standard allows or the performance limits are [27]:

- Thoracic Trauma Index TTI $< 85\ G$
- Pelvic Acceleration $< 130\ G$
- Head Injury Criteria HIC_{15} < 700 (not mandated in FMVSS 214)
- Viscous Criteria V*C $< 1.0\ m/s$ (not mandated in FMVSS 214)

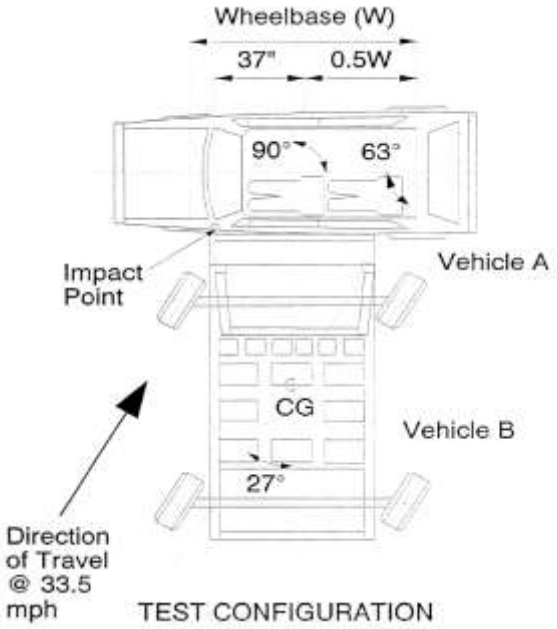

Figure 2.16: FMVSS214 side impact crash test configuration [20]

2.4.2 NCAP Tests

New Car Assessment Program (NCAP) was initiated by NHTSA in 1978 with the purpose to provide consumers a measure of the safety of a car in frontal impacts. The results from these tests were then rated on scale and then published for the consumers to see before they buy a vehicle. The crash test setup for the US NCAP test is shown in the Figure 2.17 [20]. A vehicle travelling at 35 mph hits a rigid barrier which is equivalent to a car travelling at 70 mph and

hitting another car of same weight. In this test, dummies are placed in the vehicle to evaluate the injury potential on the occupant during the crash.

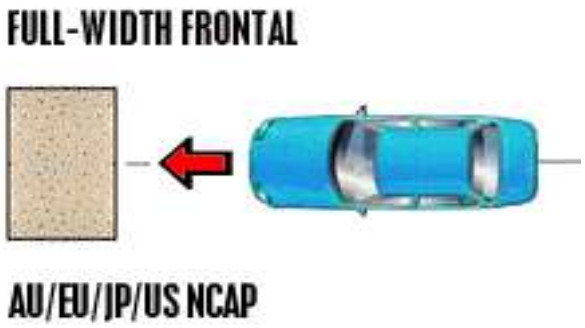

Figure 2.17: US NCAP test configuration

2.4.3 IIHS Test

Insurance Institute of Highway Safety (IIHS) is a nonprofit organization and funded by auto insures also conducts crash test to protect the damage to vehicle, occupants that still occur. The IIHS test differs from the NHTSA NCAP test. In the IIHS test, only 40% of the car width is exposed to the barrier travelling at 40 mph speed. By exposing 40% of the width to barrier, the structural strength of the vehicle can be studied in a better way, and moreover many real life accidents are mostly offset impacts. The rating system which the IIHS uses include four categories, as are:

- *Good* (best, green G)
- *Acceptable* (yellow A)
- *Marginal* (orange M)
- *Poor* (worst, red P).

Recently the IIHS introduced side-impact test, which is almost similar with NHTSA FMVSS 214, the only difference is that in IIHS test, the barrier travel normally to the vehicle at a speed of 42 mph. The test configurations for IIHS frontal offset and side impacts are shown in the Figure 2.18 [18].

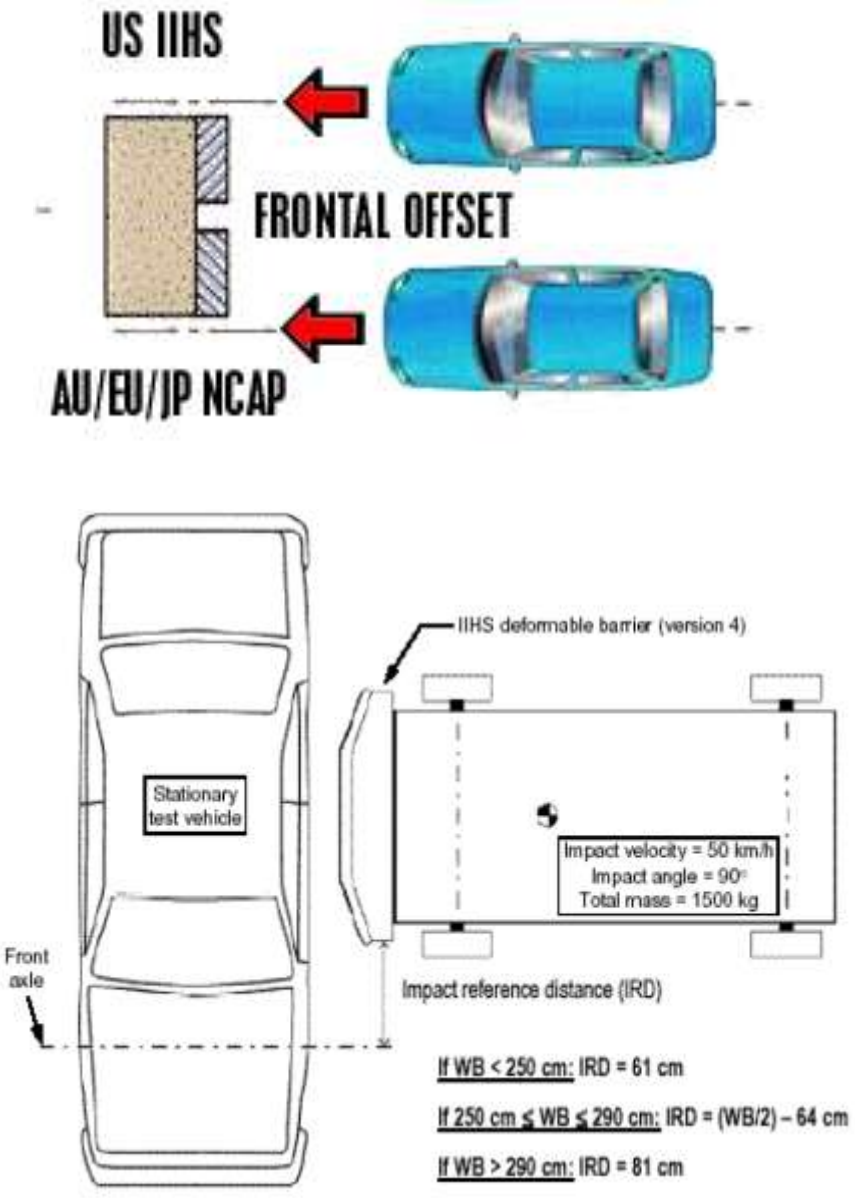

Figure 2.18: US IIHS frontal and side impact test configuration setup [18]

CHAPTER 3

COMPUTATIONAL TOOLS

Present day engineering and technology is vastly dependent on computational tools. These tools provide a unique and distinct advantage to product development. Few advantages of using computational tools out of many are:

- Product can be analyzed before building a prototype using finite element (FE) codes.
- Analysis of a product by these tools take less time in analyzing a product than building a prototype and assessing its functionality
- Cost spent on the analysis of a product is considerably reduced
- Analysis of product using these tools lead to higher efficiency of the product because many parametric studies can be conducted
- Finally a product can be optimized before it is sent to manufacturing stage

These advantages associated with computational tools makes them widely used in a product research and development stage. In this research work, the three computational tools have been utilized, namely :

1. HYPERMESH
2. LS-PREPOST
3. LS-DYNA

3.1 Pre/Post processors

In this research, the input deck (Key File) for the finite element analysis is created by using HyperMesh; finite element analysis was carried out by using LS-Dyna software, whereas the post processing of the results was carried out in LS-Prepost.

3.1.1 HyperMesh

The Altair HyperMesh is a widely used pre-processor used in the product design and development stage. This software provides and highly interactive and visual environment which helps greatly in the product design stage to the engineers. HyperMesh provide direct interface to different CAD and CAE systems which drives any firm to use it through the entire product development stage. HyperMesh can be used in modeling of solid geometry, modeling of surface, shell meshing, solid mesh generation, model morphing, automatic mid-surface generation, model setup, batch meshing and more [31].

HyperMesh has wide range of advantages like flexible interface to work with CAE and CAD environment; it can adapt itself to work in synchronization with any environment of product development. It is very robust tool which can be used in creating an input deck for finite element software minimizing time and cost spent. Different types of meshing are possible with this tool like shell, solid, tetra, hex, triangular, tet, CFD, SPH mesh and soon. All these types of meshing help us in reducing the surface modeling time, effort and money considerably. Using HyperMesh batch meshing is also possible so we can reduce time spent on meshing identical parts. Using HyperMesh we can assemble different parts of an assembly automatically. Morphing a model can also be done easily and most efficient way using HyperMesh.

HyperMesh is capable of importing complex CAD geometries created in different CAD software's like CATIA V4/V5, PRO-ENGINEER, PARASOLID, UNIGRAPHICS, STEP, ACIS and many more. There are numerous tools available in HyperMesh which can be used to clean up the imported geometries, can correct any kind of misalignments, and can manage boundaries between different surfaces which are very vital during the meshing of a model.

HyperMesh with a capability of importing geometries from different CAD software packages can also write input decks for a particular model for different finite element solvers like LS-DYNA, ABAQUS, RADIOSS, MADYMO. This feature allows us to use HyperMesh regardless of the finite element solver available. Altair HyperMesh has many new features available like mesh-flow, mid-Surfacing, auto-mesh using free-mesh, mesh-morphing, 1D element visualization, shrink wrap meshing and more.

3.1.2 LS-PrePost

LS-PrePost is a pre and post processor used to create and manage finite element models for solving in LS-Dyna [24]. LS-PrePost was designed especially for creating and editing a finite element model, which is further used for numerical analysis in LS-Dyna. PrePost can also be used for model visualization and keyword support [24].

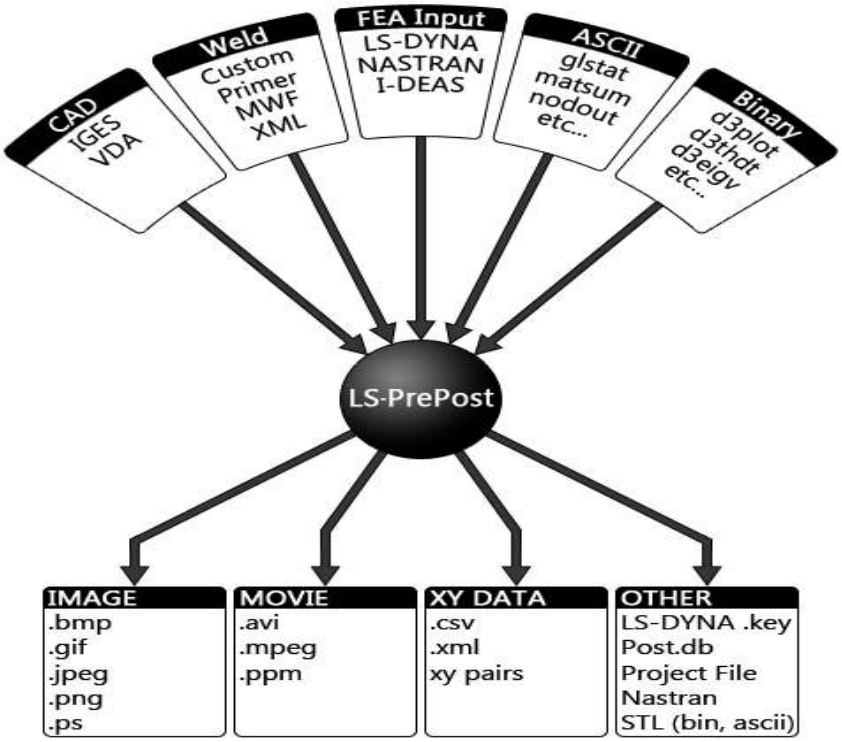

Figure 3.1: Features of LS-PrePost [24]

PrePost has number of advanced post processing features. Key pre and post processing features available with LS-PrePost are metal forming, roller hemming, airbag folding, dummy positioning, D3PLOT animation, engine mode animation and so on. Figure 3.1 shows the extensive features available in LS-PrePost.

3.2 LS-DYNA

LS-DYNA is an advanced multi-physics solver, which was originated in the year 1976 at Livermore National Laboratory by Hallquist. In the year 1976 it was developed for analyzing stress on a structure during impact loads [24]. From the year 1976 to till date LS-DYNA evolved as leading software used worldwide for many finite element analyses. LSTC has continuously improved DYNA from the year it started for solving much non-linear analysis like:

- Boundary conditions can be changed with more freedom like contact between parts that alter with time.
- Solving large deformation during analysis of sheet metal parts
- Deformation of elastic materials can be handled ideally using LS-Dyna.

LS-Dyna provides us large number of material models which can be used during analysis like elastic, kinematic/isotropic plasticity, thermo-elastoplastic, soil crushable and non crushable foam, high explosive burn, elastoplastic with fracture, laminated glass model, orthotropic crushable model, thermal orthotropic, piecewise linear isotropic plasticity, rigid, theromoelasroplastic, peicewise linear plastic, blatzo rubber and many more [32]. To run a FEA in DYNA, it requires a single command line driven executable file, enough disk space, command shell and an input file explaining the design component and the type of analysis you want to run on the part. Different pre and post processors are available to create an input deck for DYNA. HyperMesh and LS-PrePost are most widely used pre and post processors.

LS-Dyna has very wide range of application from crash analysis to ALE methods are more. A list of few applications of LS-DYNA is:

1. Automotive crash worthiness and occupant safety
2. Sheet metal forming
3. Metal forming applications
4. Aerospace applications
5. Drop testing
6. Electronic component design
7. Failure analysis
8. Earthquake engineering
9. Plastics, mold, and blow forming

Dyna is widely used in the automotive industry to test a vehicle crash behavior or strength of a vehicle during collisions to predict the safety factor of the car. In Sheet Metal forming applications, DYNA is used to analyze the stresses and deformation in a metal part. Dyna also provides facility to re-mesh the model during the analysis using r-adaptive method for accurate results and to save time. Metal forming applications of DYNA include hydro forming, metal stamping, forging and more. DYNA is widely used in aerospace industries to analyze failure criteria of a structure, to simulate a bird strike on a plane travelling at a particular elevation. LS-Dyna provides very huge variety of material cards, contact cards, and numerous amounts of other cards which does not restrict Dyna to any particular type of simulation. LS-Dyna is one of the most flexible FE packages available in the market.

CHAPTER 4

METHODOLOGY FOR PREDICTION OF DRIVER FATALITY

4.1 Method of Approach

The main idea behind this research is to develop a method to evaluate driver fatality ratio in terms of factors which cause fatal injuries to the occupants. The three main characteristic differences which exist between two incompatible vehicles are “Mass Incompatibility”, “Stiffness Incompatibility”, and “Geometric Incompatibility”.

Mass incompatibility and stiffness incompatibility make the smaller vehicle to absorb most of the crash energy developed during the collision. This absorption of crash energy results in high intrusions and high accelerations in the smaller vehicle. The last factor is the geometric incompatibility, which leads to an under ride potential of smaller vehicle into bigger vehicle. This may result in complete occupant compartment failure, which is quite dangerous to the occupants in smaller vehicle. These factors will directly influence the injury criteria of the occupant in the passenger car.

Driver Fatality Ratio (DFR) is the ratio of the drivers who experience fatal injuries in the two vehicles during collision. The Ratios are generally derived from the statistics reported by FARS and GES reporting systems and these calculations are used to understand the incompatibility between specific vehicle categories. The new method of approach for calculating Driver Fatality Ratio for specific vehicle category is to measure the ratios of major factors which influence the injury potential to the occupants in the collision. The incompatibilities between two vehicles directly lead to large intrusions and accelerations in the smaller vehicle. These two factors along with the weight ratios for all the vehicle are assessed in frontal impact modes to find a co-relation with the statistical Driver Fatality Ratio.

By using the same target car (passenger car) and varying the bullet car (each bullet car represent a particular class of LTVs), the following objective criteria are measured:

- Ratio of Intrusions
- Ratio of Accelerations
- Weight Ratios

These ratios are then compared with the statistical values for validation. After validating this new measure, it is then used to predict the Driver Fatality Ratio for different cars which do not have sufficient statistical data.

4.2 Vehicle Selection

In all the crashes the "Target Car" is the same and the bullet car is varied. Vehicles selected to represent different vehicle classes are shown in Figure 4.1. All these FE models are created by the NCAC of George Washington University and the finite element models are validated with US NCAP results and the finite element models are stable at different speeds [22].

Target Car:

Dodge Neon is selected to represent a passenger car.

Dodge Neon

FE Model of Dodge Neon

Bullet Cars

- Chevy S10 is used to represent a Compact Pick-up.

Chevy S10

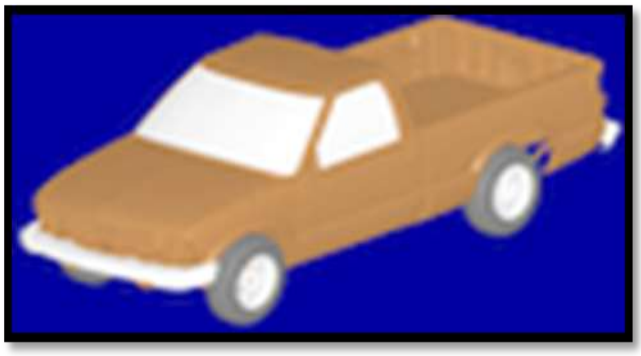

FE Model of Chevy S10

- Dodge Grand Caravan is used to represent a Minivan.

Dodge Grand Caravan

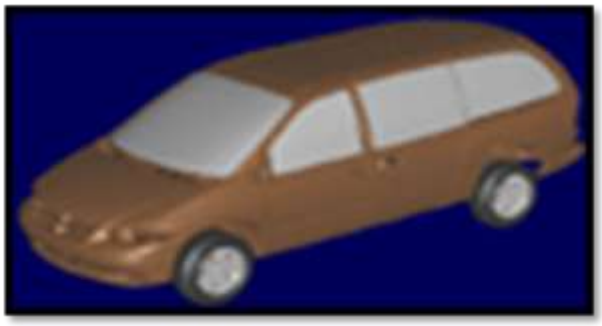

FE Model of Dodge Caravan

- Ford Explorer is used to represent a Sports Utility Vehicle.

Ford Explorer

FE Model of Ford Explorer

❖ Ford F250 is used to represent a Full Size Pick-up.

Ford F250

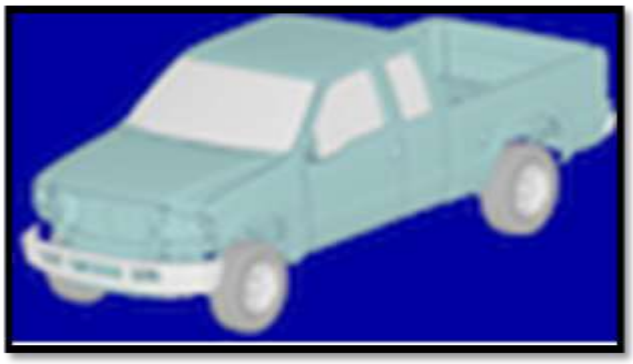

FE Model of Ford F250

❖ Ford Ecoline is used to represent a Full Size Van.

Ford Ecoline

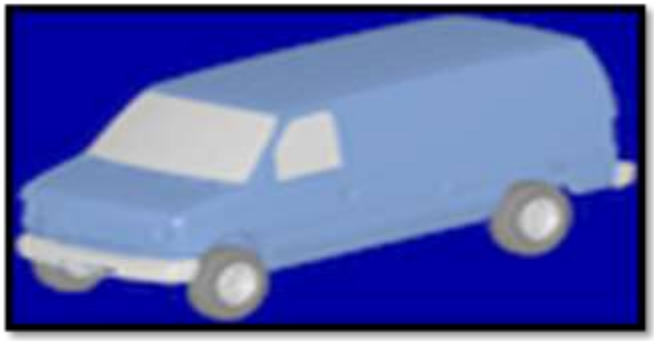

FE Model of Ford Ecoline

Figure 4.1: Vehicles selected to represent each vehicle of LTV category [22]

There are no specific crash test procedures or regulations available for incompatibility crashes between two vehicles, but all crashes are conducted according to US-NCAP regulation to some extent. The two vehicles are assumed to travel at 35 mph and collide in to each other with full width frontal interactions. Then the intrusions are measured at different parts according to the IIHS specifications, which are crucial in determining injury criteria to the occupant. Figure 4.2 shows the locations were intrusions are measures according to IIHS [20].

Figure 4.2: US IIHS intrusion measurement locations [20]

The finite element models which are used in this research work, do not have detailed occupant compartment design, and the maximum intrusions are measured on the firewall up on which these instrument panel are hung up. The maximum foot-well intrusions and the driver side A-pillar movement are also measured. Along with these, the ratio of left seat and right seat accelerations are also measured, as these accelerations also result in fatal injuries to the occupants. The ratio of intrusion at firewall, A-pillar and foot-well and acceleration ratios are then compared with the statistical data for validating the proposed method of approach. Figure 4.3 illustrates the details of the approach followed in this research work.

4.3 Methodology

The proposed approach for evaluating the DFR of a vehicle is to measure the ratios of peak intrusions, ratios of peak accelerations, and weight ratio between the bullet and target vehicles.

The equations 4.1 through 4.3 show the method of approach to evaluate these objective measures:

- Ratio of Intrusions = $\frac{\text{Maximum Intrusion in Bullet Vehicle}}{\text{Maximum Intrusion in Target Vehicle}}$ (4.1)

- Ratio of Accelerations = $\frac{\text{Peak Acceleration in Bullet Vehicle}}{\text{Peak Acceleration in Target Vehicle}}$ (4.2)

- Weight Ratio = $\frac{\text{Weight of Bullet Vehicle}}{\text{Weight of Target Vehicle}}$ (4.3)

Figure 4.3 outlines the method of approac in this research work. By having a constant target vehicles as a Dodge Neon and by varying the bullet vehicle, each bullet vehicle representing a specific LTV vehicle class, computation crash scenarios are conducted for the five cases. In each case, both vehicles are travelling at a speed of thirty five miles per hour and having full width frontal interaction according to U.S NCAP regulations. Objective measures including (Ratio of Intrusions measured at the locations specified by IIHS, Accelerations and left and right seat centre of gravities and Weight of two vehicles) are then calculated and then compared with statistical DFR for validation of the proposed method. Specific reasons are identified for the dominance of one vehicle on the other. This proposed new method is then applied to three different vehicles from different vehicle categories including a Toyota Rav4 representing a cross-over vehicle or compact style sports utility vehicle, a Chevrolet C1500 representing a light pick-up truck, and a Ford Taurus representing a full-size passenger car. Their DFR are then evaluated to study the impact of stiffness, geometric and mass incompatibility on the DFR of these three vehicles and finally the results are then interpreted.

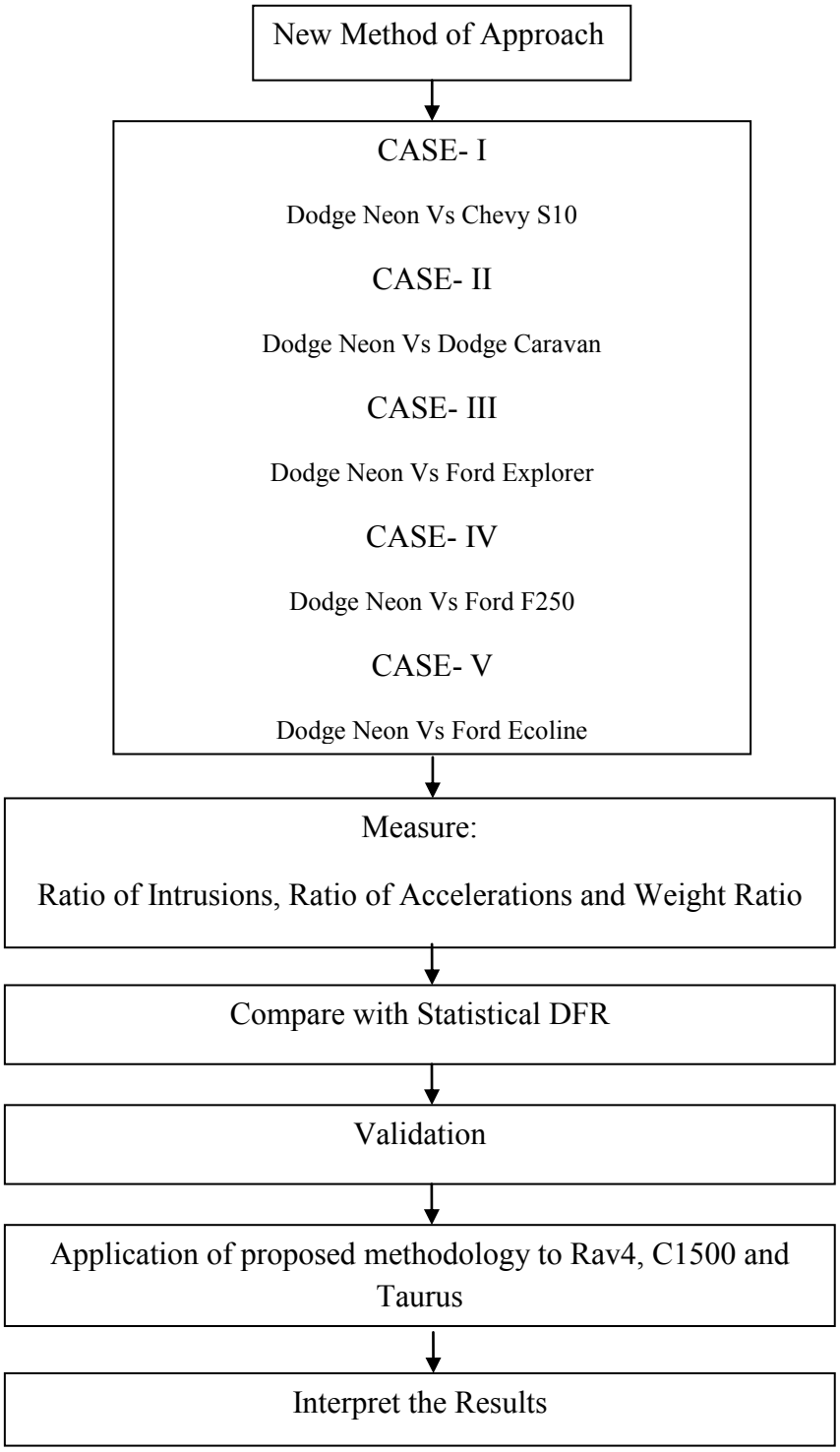

Figure 4.3: Methodology of proposed new method

CHAPTER 5

VALIDATION OF PROPOSED METHODOLOGY

The proposed methodology is validated by selecting a Dodge Neon as constant "Target Car" and crashing it against a range of LTVs as "Bullet Car". These computational crash impact scenarios are divided into five cases. Each case represents a crash simulation of a passenger car crashing against a particular class of LTV. The FE models used in all these cases are modeled by National Crash Analysis Centre and are open for public use. The detailed description of every FE model used is described and the conditions at which these crash simulations are conducted are also described.

5.1 CASE – I: Compact Pickup (Chevy S10) vs Passenger Car (Dodge Neon)

5.1.1 Model Description

Dodge Neon:

Finite element model of Dodge Neon is developed by (NCAC) based on 1996 Model Neon car. This model is developed by NCAC to be used mainly in the frontal mode of impacts. The mesh size or the elements are dense in the front portion when compared to the elements in the side and rear because there will not any significant deformation in the side and rear during frontal impacts. Figure 5.1 shows the FE model of the Dodge Neon [22].

Figure 5.1: Explored view of Dodge Neon FE model [15]

The material data which was used in developing this model was derived from coupon testing. The finite element model consists of 336 parts; each part of the FE model represents different part of the original car. Each part is given different material properties to suit the concerned part in the original car. Different materials used are BLATZ-KO_RUBBER, CRUSHABLE_FOAM,DAMPER_VISCOUS,ELASTIC,HONEYCOMB,PEICEWISE_LINEAR_PLASTIC, RIGID, SPOTWELD, SPRING_ELASTIC. There are 270768 elements in the model out of which 267786 elements are shell elements, 2852 are solid elements, and 122 are beam Elements. Different parts of the model are constrained by using 4195 spot welds, 8 revolute joints, 4 spherical joints. FE simulation of this model correlates with the NCAP test of the vehicle. This FE model is stable in full width frontal crash simulations travelling at 25, 30, 35 and 40 mph to check stability of the FE model. The Table 5.1 shows the summary of the FE model.

Table 5.1: FE model Summary of Dodge Neon

Number of parts	336
Number of Nodes	283859
Number of Solids	2852
Number of Beams	122
Number of Shells	267786
Number of Elements	270768

Chevy S10:

The FE model of Chevrolet S10 is developed by National Crash Analysis Center for frontal impacts based on a 1998 model Chevy S10. This model is also available in NCAC website which can be used for research purposes. The elements size in the frontal portion of the vehicle is very small when compared to the element size in the side and rear portion because the

intrusion in these areas is very less during head to head impacts. Figure 5.2 shows the FE Model of the Chevy S10 used to represent the compact pickup model.

The vehicle FE model has 346 parts; each part of the model depicts different parts of the original vehicle. The material properties of different parts are derived from the coupon testing. Different materials used in this FE model are SPOT WELD, SPRING ELASTIC, VISCOELASTIC, PIECEWISE LINEAR PLASTICITY, LOW DENSITY FOAM, and LINEAR_ELASTIC_DISCRETE_BEAM. There are 220409 elements in the FE model out of which 193 are beam elements, 22 are discrete elements, 212615 are shell elements, 3464 are solid elements. Different parts of the vehicle are constrained by one cylindrical joint, eighteen revolute joints, four spherical joints, four universal joints, three thousand sixty four spot welds.

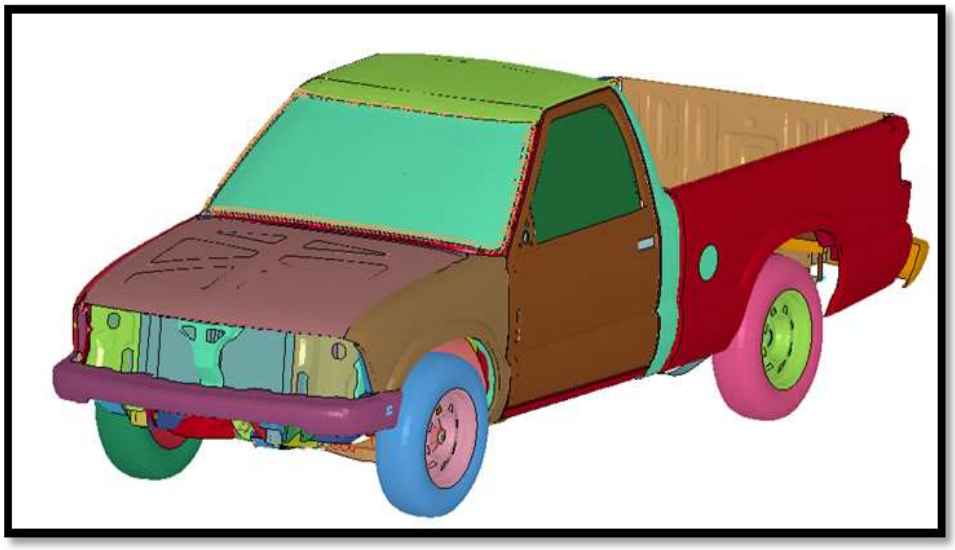

Figure 5.2: FE model of Chevy S10 [15]

The FE Model is validated against Chevy S10 NCAP test results and the vehicle is stable at 30, 35, 40 mph. The accelerations of the vehicle and the wall force exerted by this vehicle are comparable to NCAP test results. The Table 5.2 shows the summary of the FE Model.

Table 5.2: FE model summary of Chevy S10

Number of Parts	346
Number of Nodes	220499
Number of Solids	3156
Number of Beams	193
Number of Shells	203158
Number of Elements	220409

5.1.2 Crash Simulation

The two vehicles are positioned such that they have full width interaction during collision and the vehicles are placed as close as possible to reduce the computational time. The contact between two vehicles is defined by using "Automatic_Surface_to_surface" card. Static and dynamic friction are both given as 0.3 between the contact of two vehicles. Rigid wall planar cards are used between the contact of all tires and roads. Initial velocity of 35 mph is given to both vehicles and the Simulation termination time of 200 milliseconds is given with a time step of 10 milliseconds. The total computational time for simulation this crash scenario is almost 12 hours. Figure 5.3 shows the results of crash simulation between two vehicles at different time.

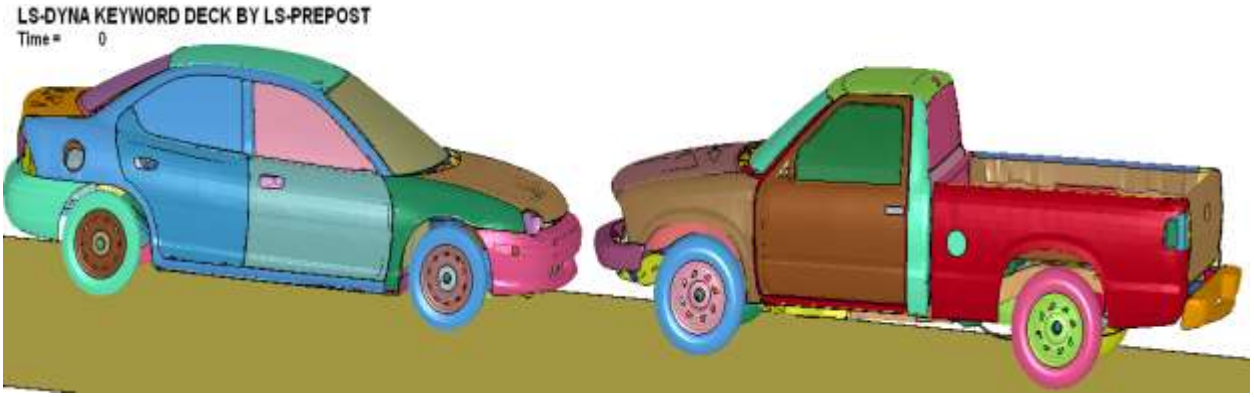

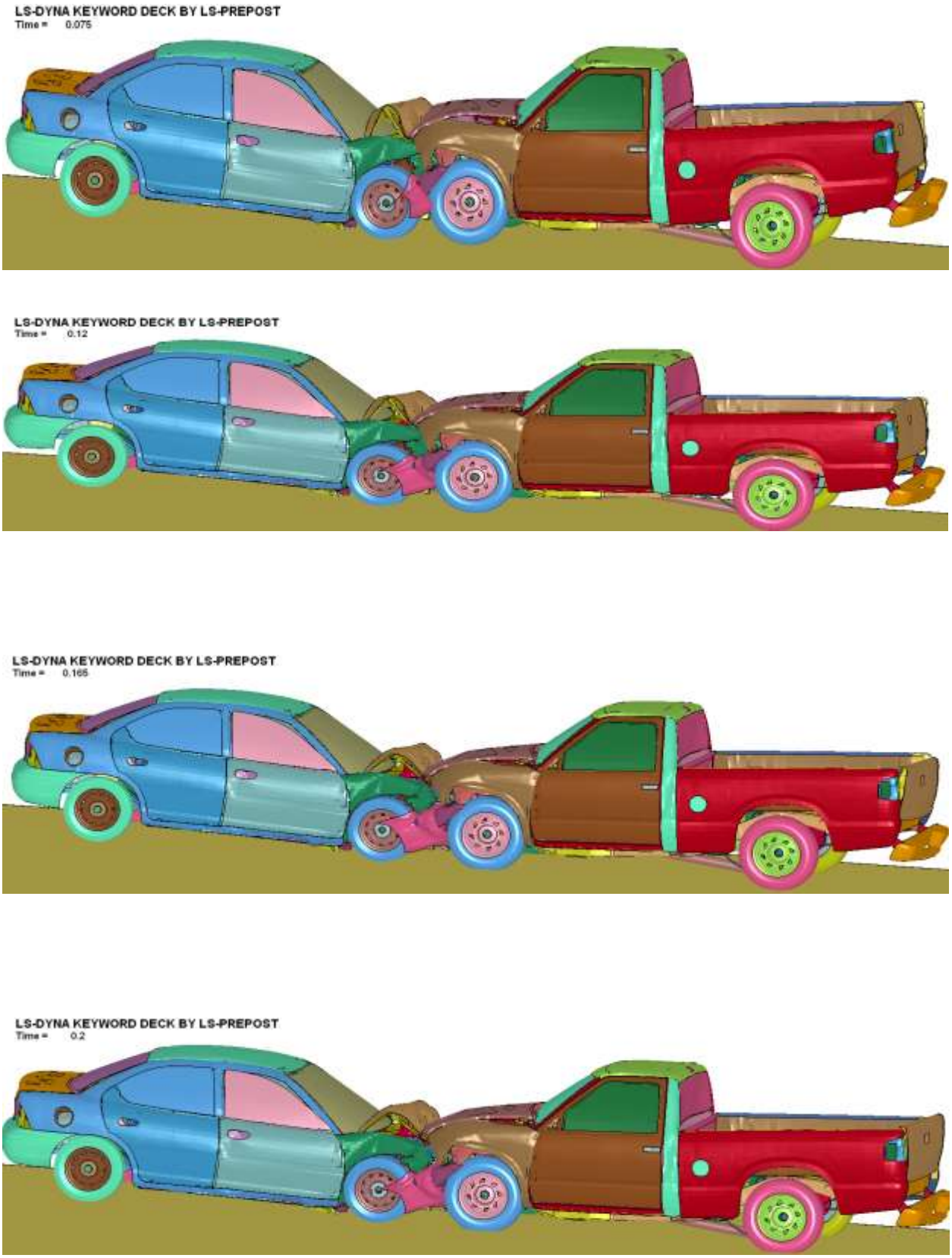

Figure 5.3: Animation sequence of Chevy S10 crashing against Dodge Neon

The two vehicles have come into contact with each other immediately because both were placed as close as possible. The maximum crush between the vehicles happened at 70 ms, after which the vehicles started to move away from each other. After the vehicles completely came off from contact between each other the firewall, driver side A-pillar, foot-well intrusions and accelerations of left and right seats are measured.

Intrusions in the firewall of Chevy S10:

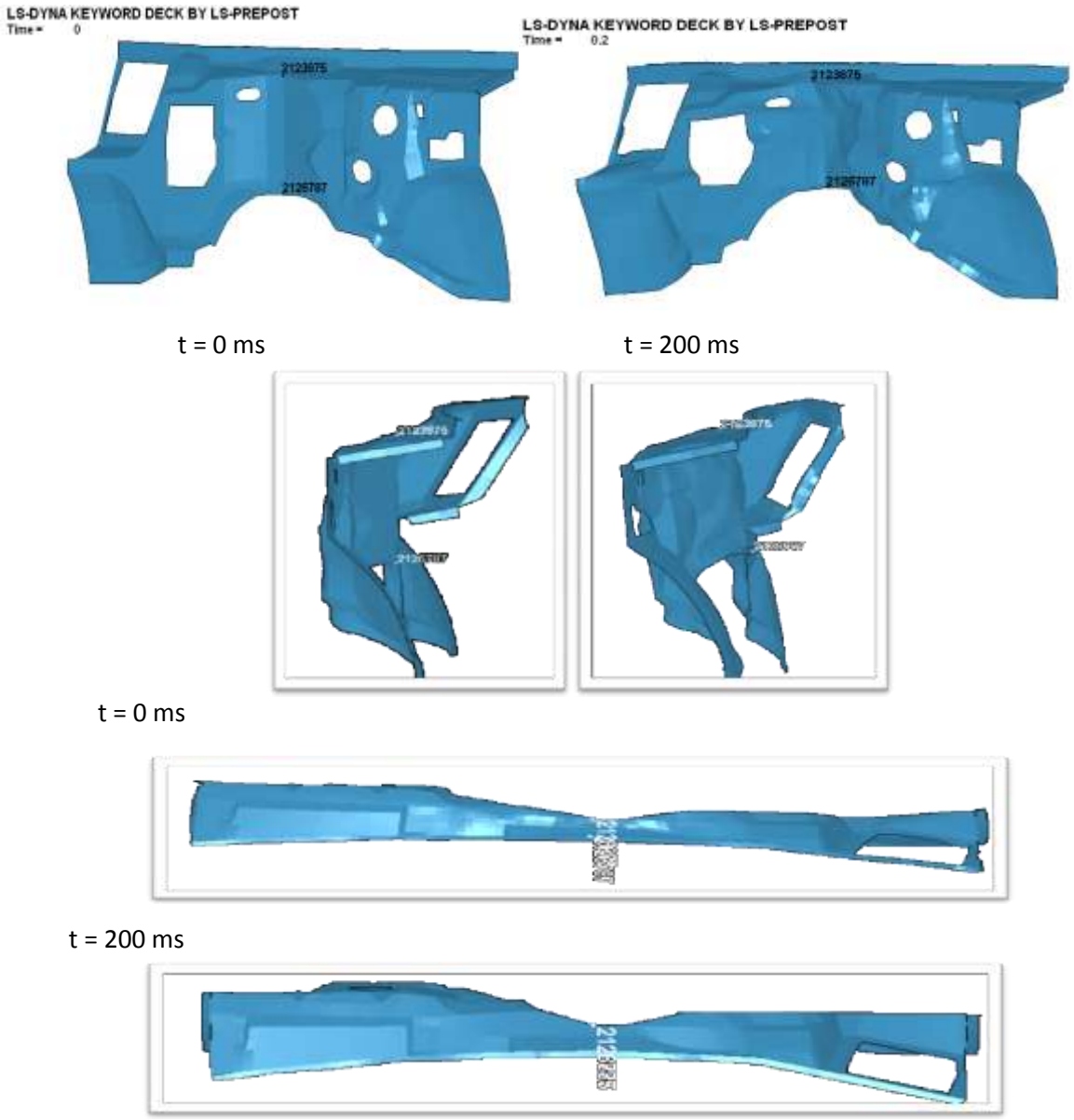

Figure 5.4: Animation sequence showing intrusion in firewall of S10 in CASE-I

From Figure 5.4, it can be observed that the maximum intrusion occurs approximately at node 2126787. The resultant displacement of the maximum intruded node is shown in the Figure 5.5. From the graph, maximum intrusion in the firewall of ChevyS10 in collision with a passenger car is measured as 53mm.

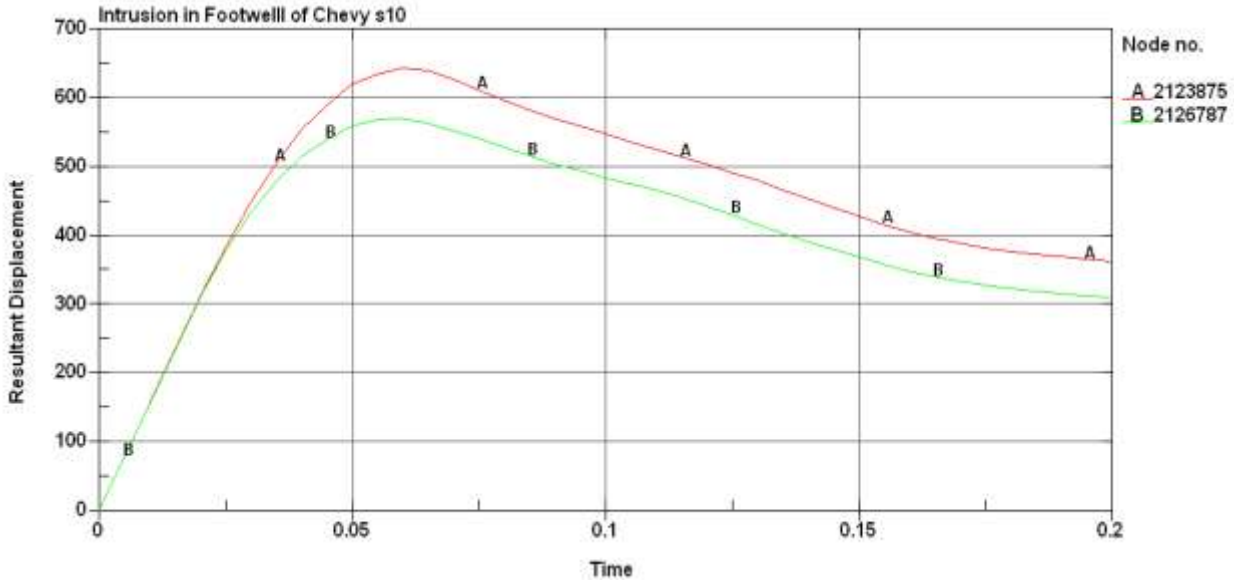

Figure 5.5: Maximum intrusion in firewall of S10 in CASE-I

Foot-well intrusion in chevy S10:

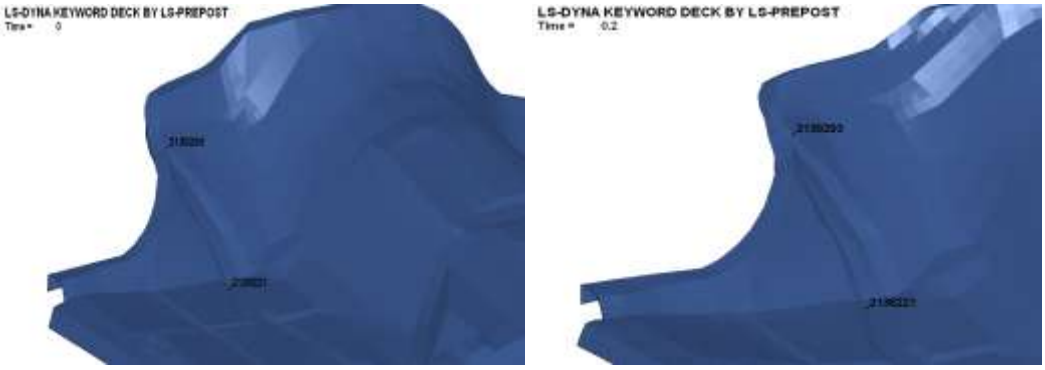

(a): Foot-well intrusion of Chevy S10 in Case-I (isometric view)

Figure 5.6: Animation sequence showing intrusion in foot-well of S10 in CASE-I
(a) isometric view (b) side view

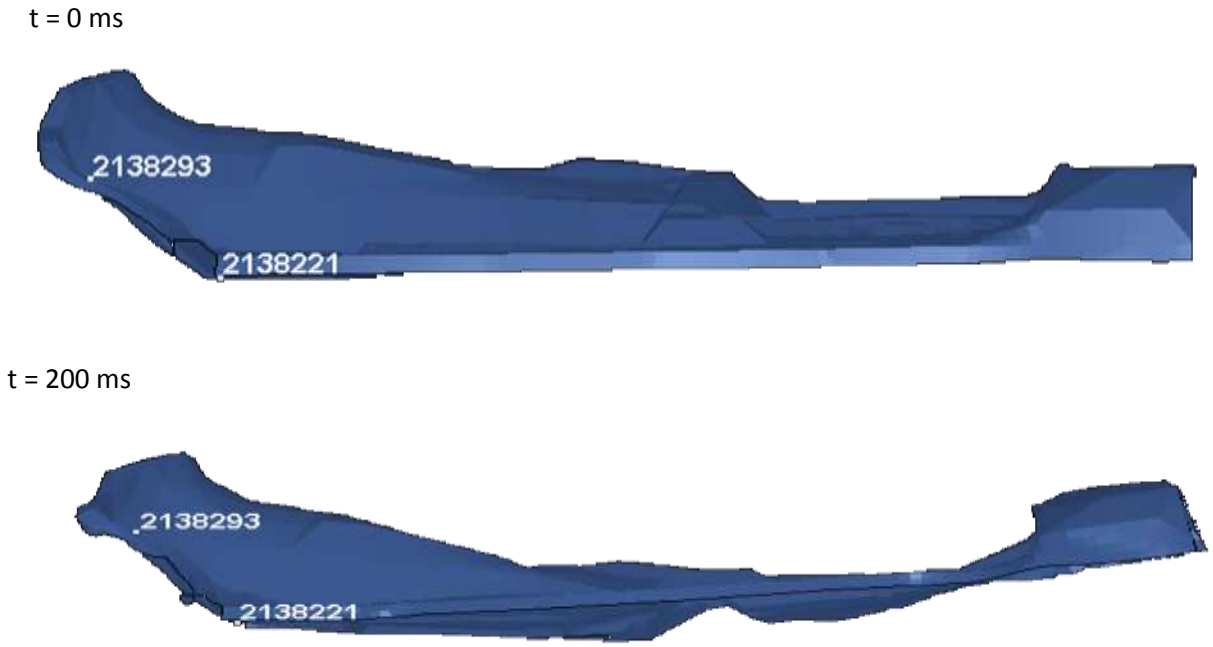

(b): Foot-well intrusion of Chevy S10 in Case-I (side view)

The maximum intrusion in the foot-well of Chevy s10 occurs at node 2138293 and the crash simulation is shown in Figure 5.6. The resultant displacement of this maximum intruded node is shown in the figure 5.7. From Figure 5.7, the maximum intrusion in the foot-well of Chevy S10 in collision with a passenger car is found to be 43mm.

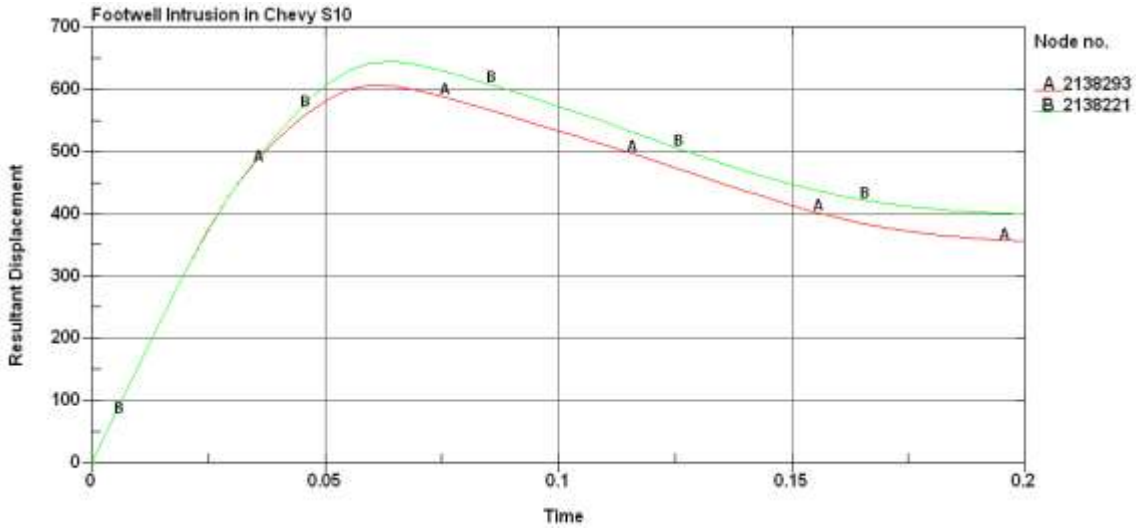

Figure 5.7: Maximum intrusion in foot-well of S10 in CASE-I

Driver side A-Pillar Intrusion in Chevy S10:

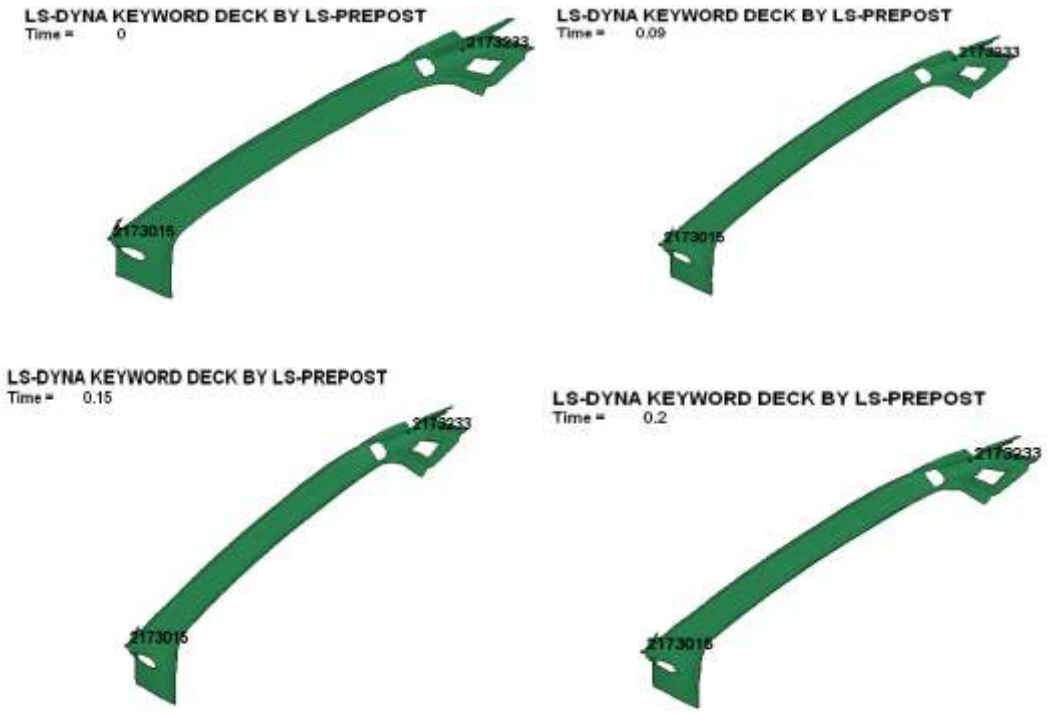

Figure 5.8: Animation sequence showing intrusion in driver side A-pillar of S10 in CASE-I

The node which had maximum rearward movement on the A-pillar of the Chevy S10 is node #2173015, and the animation sequence is shown in the Figure 5.8. The maximum displacement of this node is 17mm. Figure 5.9 shows the displacement of the node.

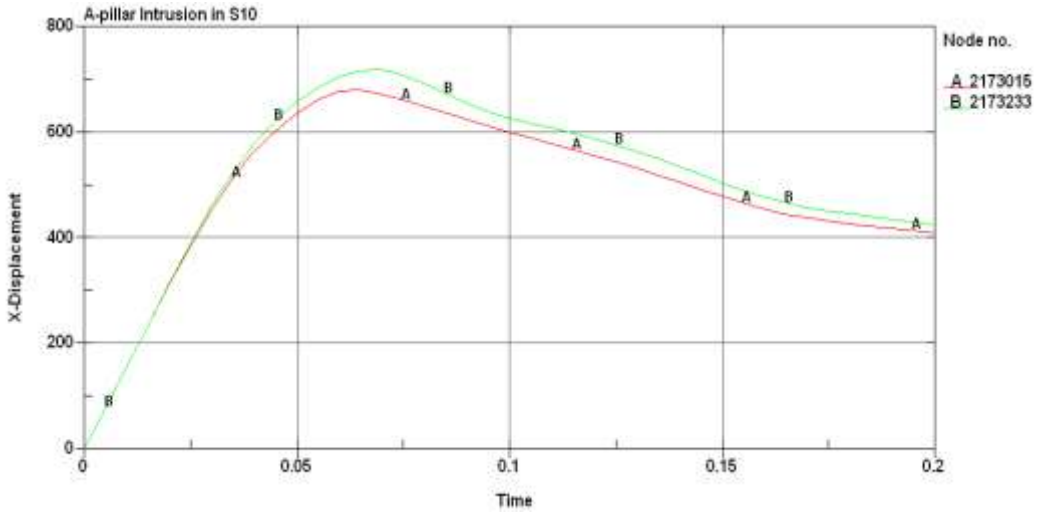

Figure 5.9: Maximum intrusion in driver side A-pillar of S10 in CASE-I

Firewall Intrusion in Dodge Neon:

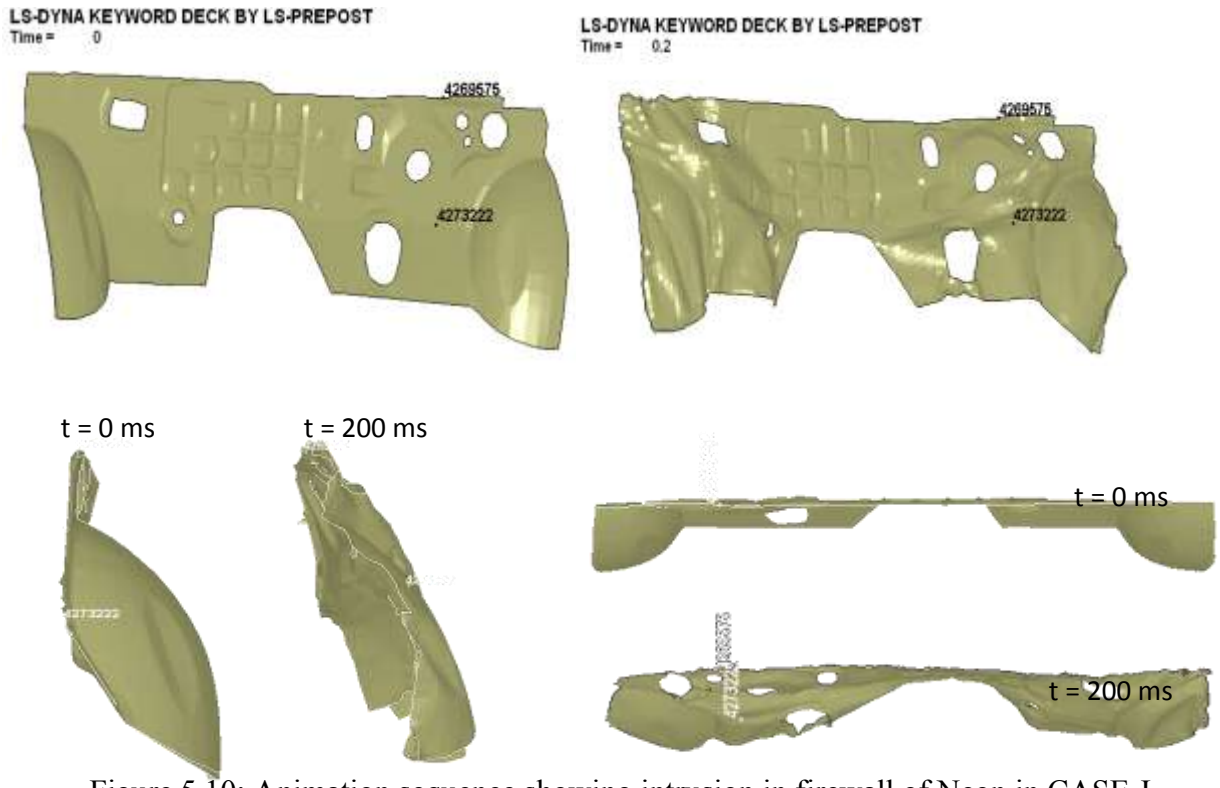

Figure 5.10: Animation sequence showing intrusion in firewall of Neon in CASE-I

From Figure 5.10, the maximum intrusion in the firewall of the Dodge Neon occurs approximately at Node # 4273222, the maximum displacement of this node is 130 mm, as is shown in the Figure 5.11.

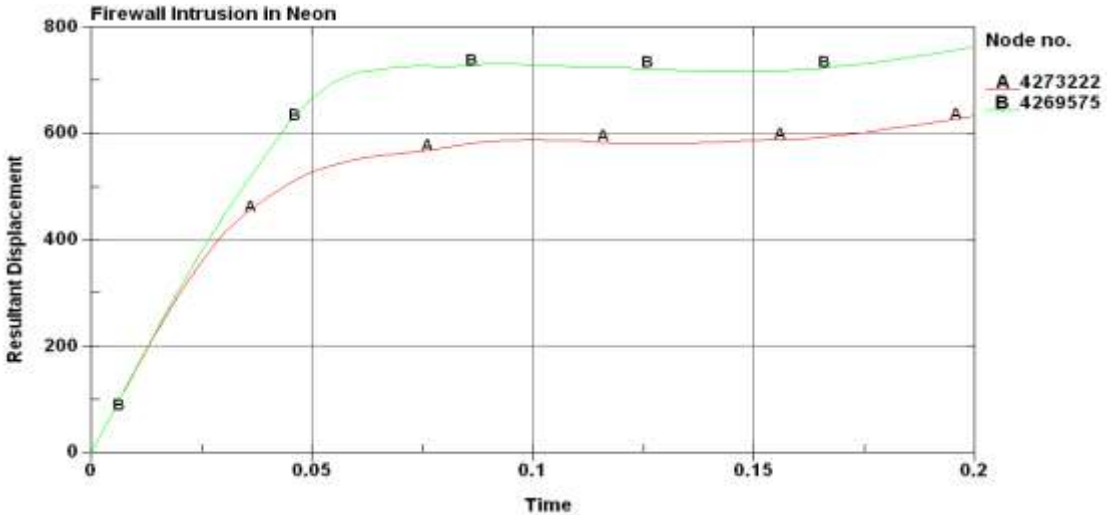

Figure 5.11: Maximum intrusion in firewall of Neon in CASE-I

Foot-well Intrusion in Chevy S10:

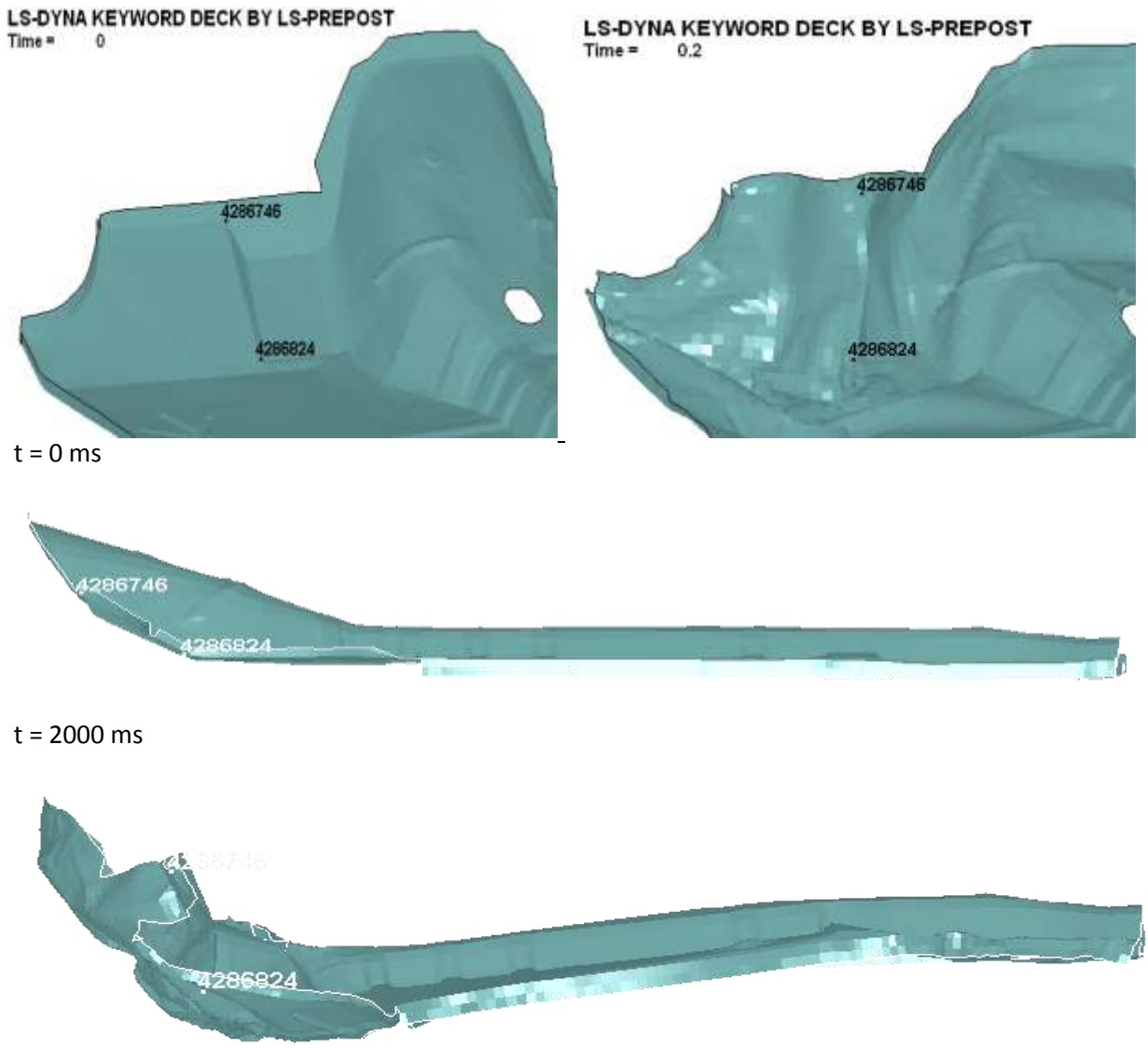

Figure 5.12: Animation sequence showing intrusion in foot-well of Neon in CASE-I

From the Figure 5.12, the maximum intrusion in the foot-well of the Dodge Neon occurs approximately at node # 4286746, the maximum displacement of this node is 104 mm, as is shown in the Figure 5.13.

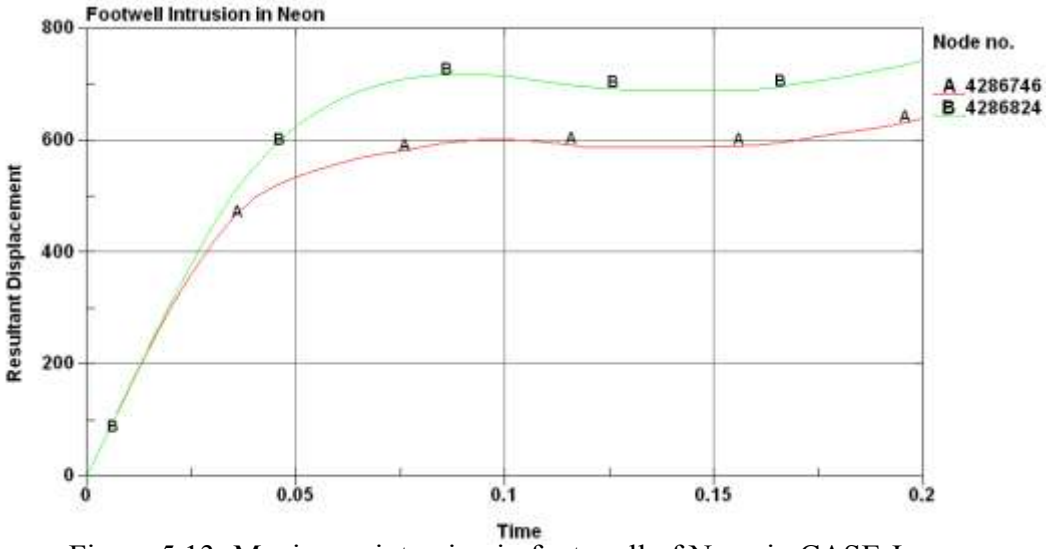

Figure 5.13: Maximum intrusion in foot-well of Neon in CASE-I

Driver side A-Pillar Intrusion in Dodge Neon:

Figure 5.14 shows the movement of A-pillar during the collision with a compact pickup.

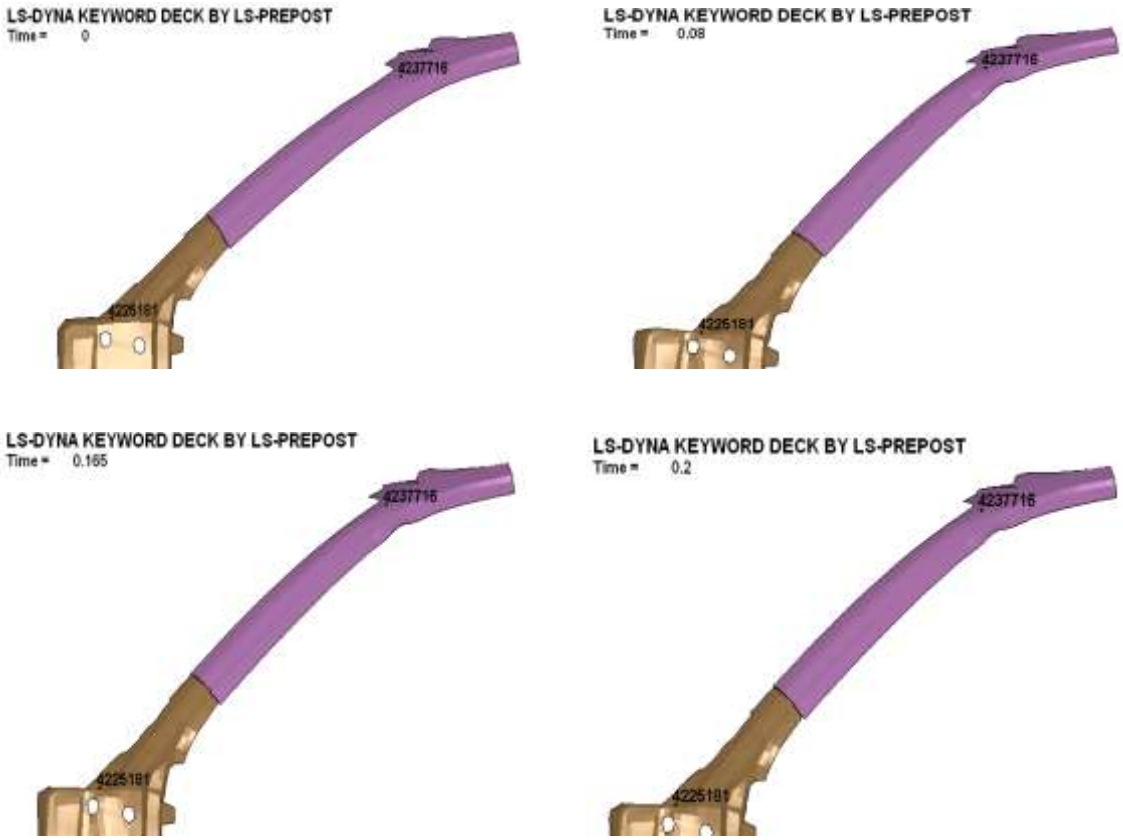

Figure 5.14: Animation sequence showing intrusion in driver side A-pillar of Neon in CASE-I

The node which had maximum rearward movement on the A-pillar of the Dodge Neon is node #4225181, the maximum displacement of this node is found to be 44mm. Figure 5.15 shows the displacement of the node with respect to time.

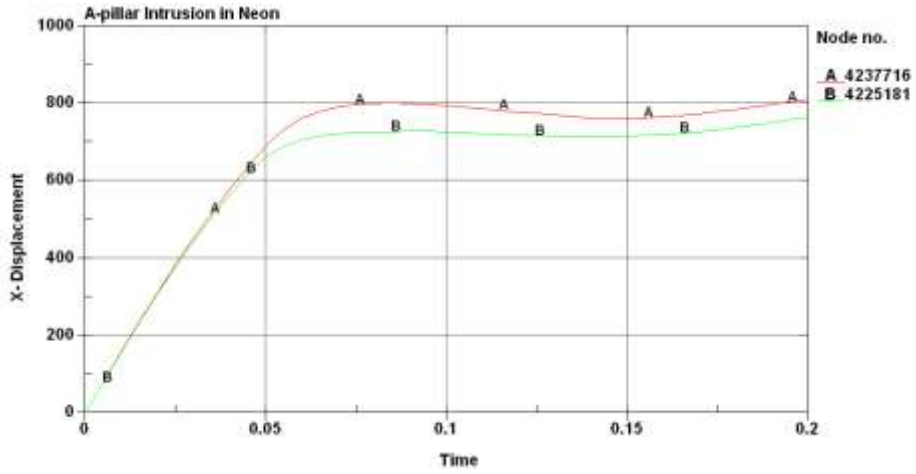

Figure 5.15: Maximum intrusion in driver side A-pillar of Neon in CASE-I

Figure 5.16 (a) and (b) shows the acceleration in the left and right seats of the Dodge Neon and Chevy S10. The figure also indicates the peak acceleration in the two vehicles.

LEFT and RIGHT Seat Acceleration:

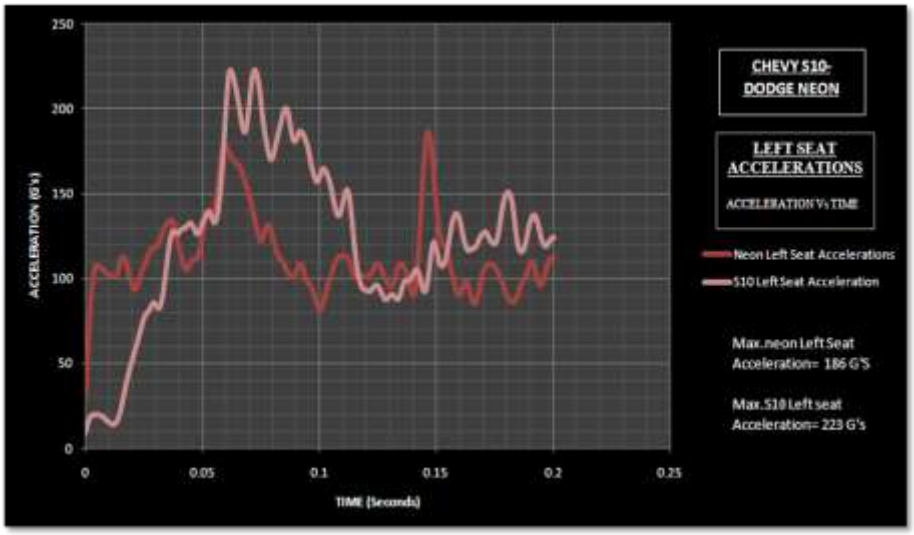

(a): Left seat acceleration in CASE-I

Figure 5.16: Left and Right seat acceleration in CASE-I
(a) Left seat (b) Right seat

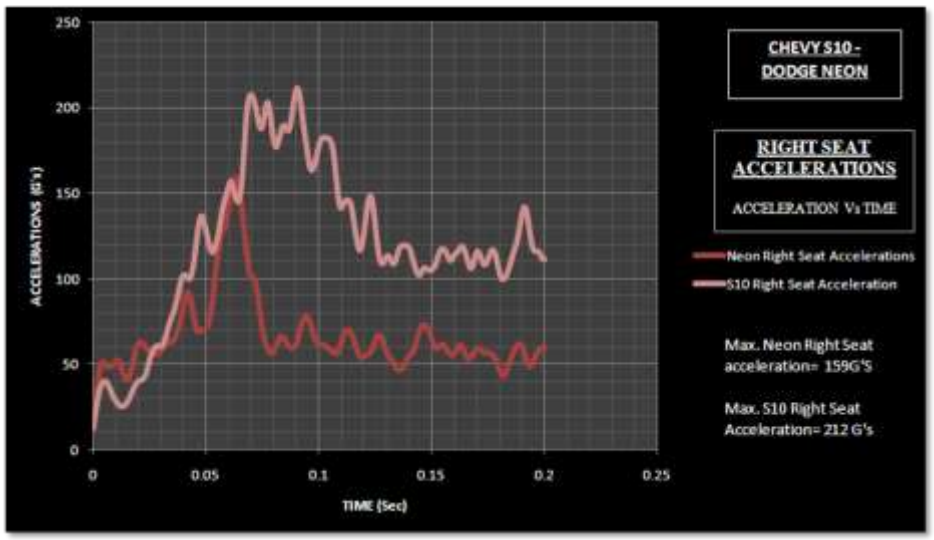

(b): Right seat acceleration in CASE-I

5.1.3 Discussion

In the above crash scenario of Chevy S10 (representing a compact Pick-up) colliding against Dodge Neon (representing Passenger car), the weight of Chevy S10 is less than the weight of dodge Neon, but the high intrusions in Dodge Neon indicates that even though S10 is lighter than Neon, it is stiffer than the passenger car. This indicates that stiffness incompatibility exists between two vehicles and as the weight of S10 is lighter than the weight of Neon, the Weight incompatibility does not exist in this case. The frontal geometry of Neon is completely different from the geometry of S10, this difference in the frontal geometry results in application of different load paths on each other, which will lead to geometric incompatibility. The ride height of S10 vehicle is approximately around 300mm where as the ride height of Neon car is approximately around 200mm. This difference in ride height will increase the geometric incompatibility even further; the difference in the ride height between two vehicles is around 100 mm which does not lead to under-ride of passenger car into the compact pick-up. In this case geometric and stiffness incompatibilities lead to more fatal injuries to the occupant of the

passenger car. The Table 5.3 shows the intrusions measured at the crucial location which can lead to fatal injuries to occupants. The left and right seat accelerations are also measured and tabulated. The Table 5.3 also shows the weight ratio, Firewall Intrusion ratio, Foot-well intrusion ratio, A-Pillar Intrusion ratio and, left and right seat acceleration ratios. The weight ratio of Chevy S10 to Dodge Neon is 0.8: 1, which does not coincide with statistical DFR (Driver Fatality Ratio) of 1: 2.6. The firewall, foot-well, A-pillar intrusion ratios are 1: 2.5, 1: 2.4, 1: 2.5 respectively which are almost the same as DFR of 1: 2.6. The left and right seat accelerations are: 1.2: 1, 1.3: 1, which again do not go with the DFR of 1: 2.6 because higher stiffness of S10 makes it to experience higher accelerations and low intrusions when compared with Dodge Neon car. Table 5.3 shows the summary of intrusion measured in S10 and Neon vehicles during collisions.

Summary of CASE- I:

Table 5.3: Summary of CASE-I

	S10	Neon
Firewall Intrusion (mm)	53	130
Foot well Intrusion (mm)	43	104
A-pillar Intrusion (mm)	17	44
Left seat Acceleration (G's)	223	186
Right seat Acceleration (G's)	212	159

Chevy S10 : Dodge Neon	Ratio
Ratio of Firewall Intrusion	1: 2.5
Ratio of Foot well Intrusion	1: 2.4
Ratio of A-pillar Intrusion	1: 2.5
Ratio of Left seat Acceleration	1.2: 1
Ratio of Right seat Acceleration	1.3 :1

5.2 CASE – II: Minivan (Dodge Grand Caravan) Vs Passenger Car (Dodge Neon)

5.2.1 Model Description

Dodge Neon: Described in Case I.

Dodge Grand Caravan:

The FE model of Dodge Grand Caravan is developed by National Crash Analysis Center for frontal impacts based on a 1997 model Caravan. This model is also available at free of cost in NCAC website which can be used for research purposes. This model can be used for research work in frontal impact modes. The elements size in the frontal portion of the vehicle is very small when compared to the element size in the side and rear portion because the intrusion in these areas is very less during head to head impacts. Figure 5.17 shows the FE Model of the Dodge Grand Caravan used to represent the minivan [22].

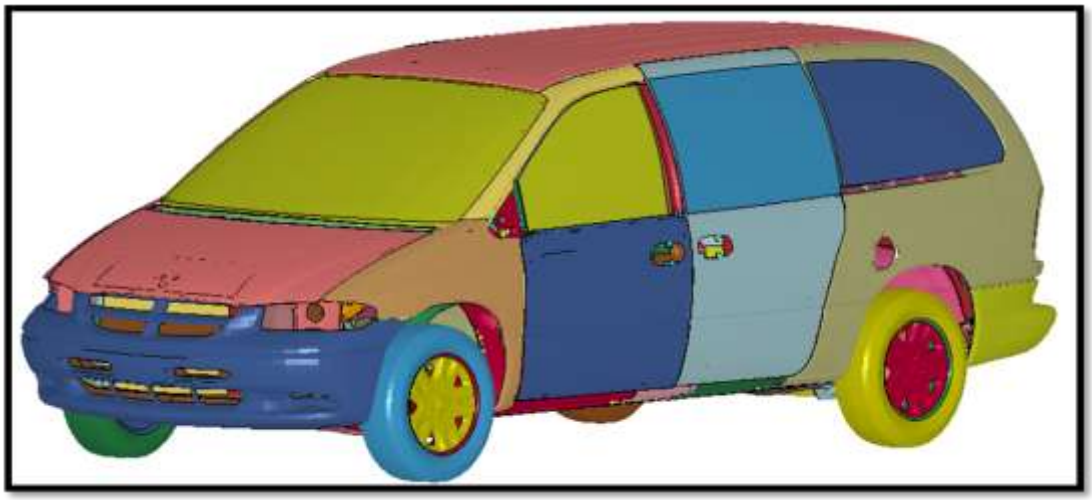

Figure 5.17: FE model of Dodge Grand Caravan

The vehicle FE model has 510 parts; each part of the model depicts different parts of the original vehicle. The material properties of different parts are derived from the coupon testing. Different materials used in this FE model are BLATZ-KO_RUBBER, DAMPER VISCOUS,

ELASTIC, HONEYCOMB, PIECEWISE LINEAR PLASTICITY and SPRING_ELASTIC. There are 333455 elements in the FE model out of which 35 are beam elements, 4 are discrete elements, 327163 are shell elements, 6253 are solid elements. Different parts of the vehicle are constrained by sixteen revolute joints, two spherical joints, five thousand fifteen spot welds. The FE Model is validates the Caravan NCAP test results and the vehicle is stable at 30, 35, 40 mph. The accelerations of the vehicle and the wall force exerted by this vehicle are comparable to NCAP test results. The Table 5.4 shows the summary of the FE Model.

Table 5.4: FE model summary of Dodge Grand Caravan

Number of Parts	510
Number of Nodes	344724
Number of Solids	6253
Number of Beams	35
Number of Springs	4
Number of Mass Elements	317
Number of Shells	327163
Number of Elements	333455

5.2.2 Crash Simulation

Two vehicles are positioned such that they have full width interaction during collision and the vehicles are placed as close as possible to reduce the computational time. The contact between two vehicles is defined by using “Automatic_Surface_to_surface “card. Static and dynamic frictions are both given as 0.3 between the contacts of two vehicles. Rigid wall planar cards are used between the contact of all tires and roads. Initial velocity of 35 mph is given to both vehicles and the Simulation termination time of 200 milliseconds is given with a time step of 10 milliseconds. The total computational time for simulation this crash scenario is almost 12 hours. Figure 5.18 shows results of crash simulation between the two vehicles at different times.

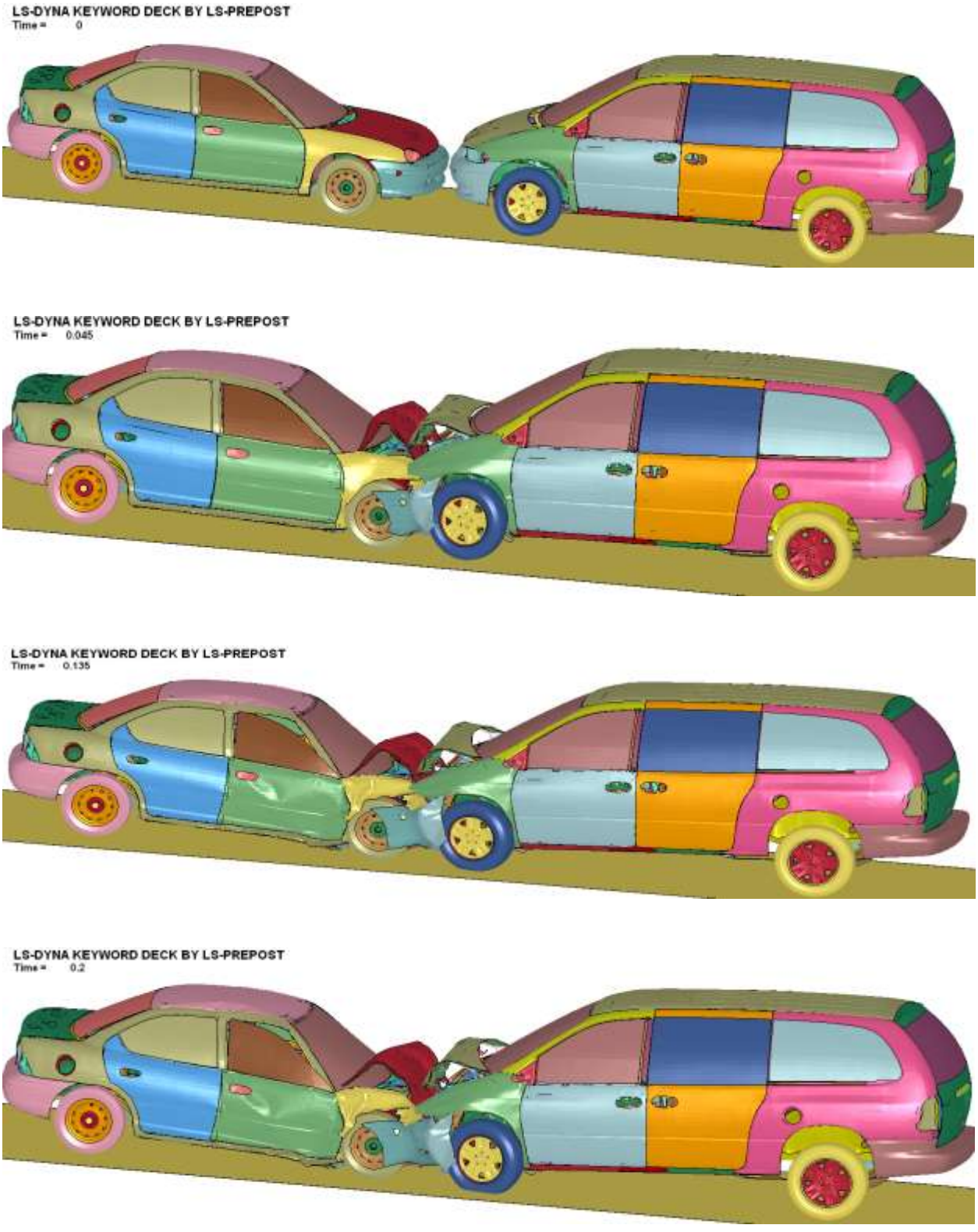

Figure 5.18: Animation of Dodge Caravan crashing against Dodge Neon

The two vehicles are placed as close as possible to each other to reduce calculation time. The maximum crush between the vehicles happenes at 85ms. After which the minivan is pushing the passenger car backwards. After reaching the maximum crush stage, maximum firewall, driver side A-pillar, foot-well intrusions and accelerations of left and right seat are measured for this crash. The Figure 5.19 below shows the intrusions in the firewall of Dodge Caravan.

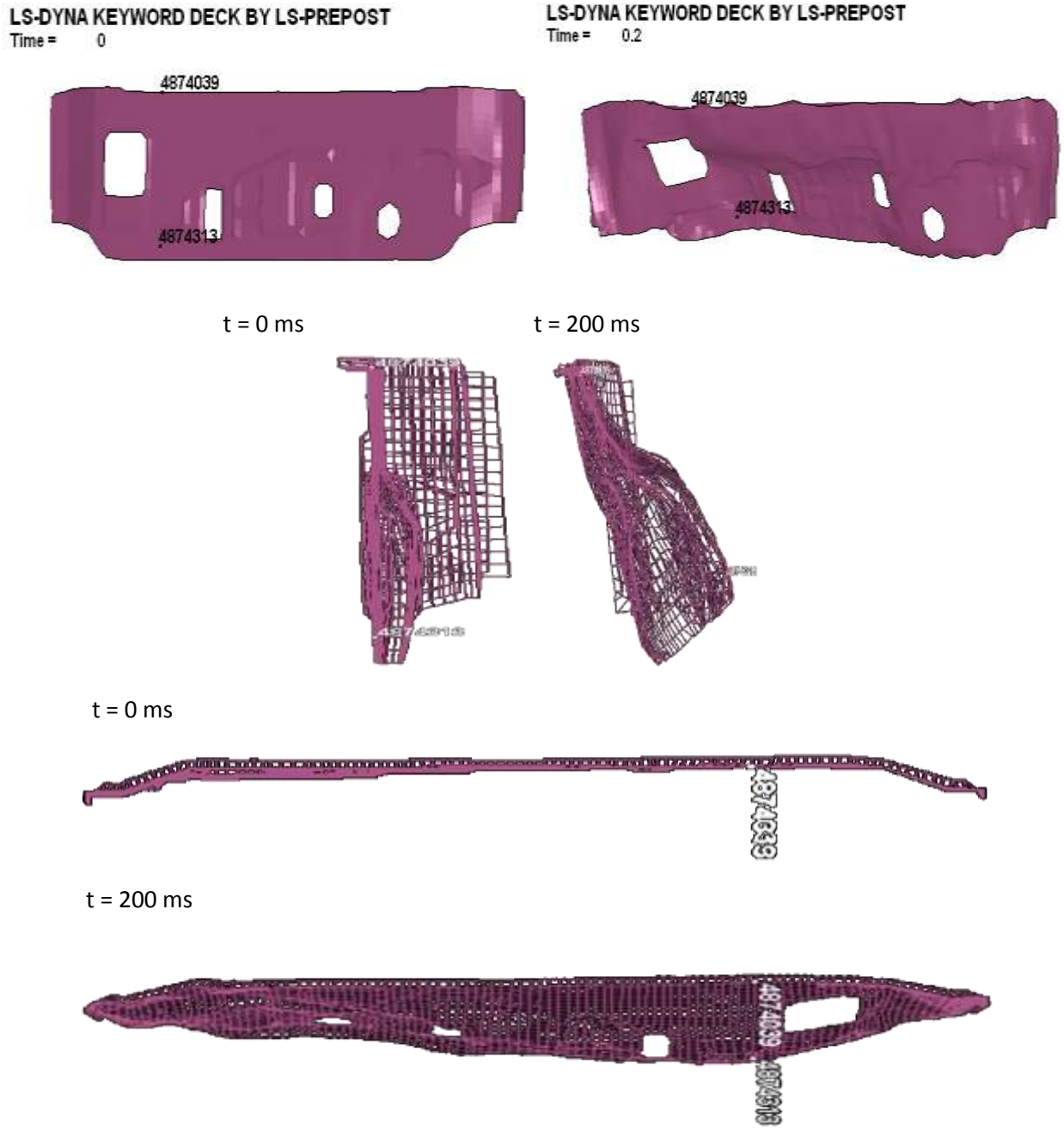

Figure 5.19: Animation sequence showing intrusion in firewall of Caravan in CASE-II

From Figure 5.19, it is evident that the maximum intrusion occurs approximately at node 4874313. The resultant displacement of the maximum intruded node is shown in the Figure 5.20. From the above graph, maximum intrusion in the firewall of Caravan in collision with a passenger car is measured as 234mm.

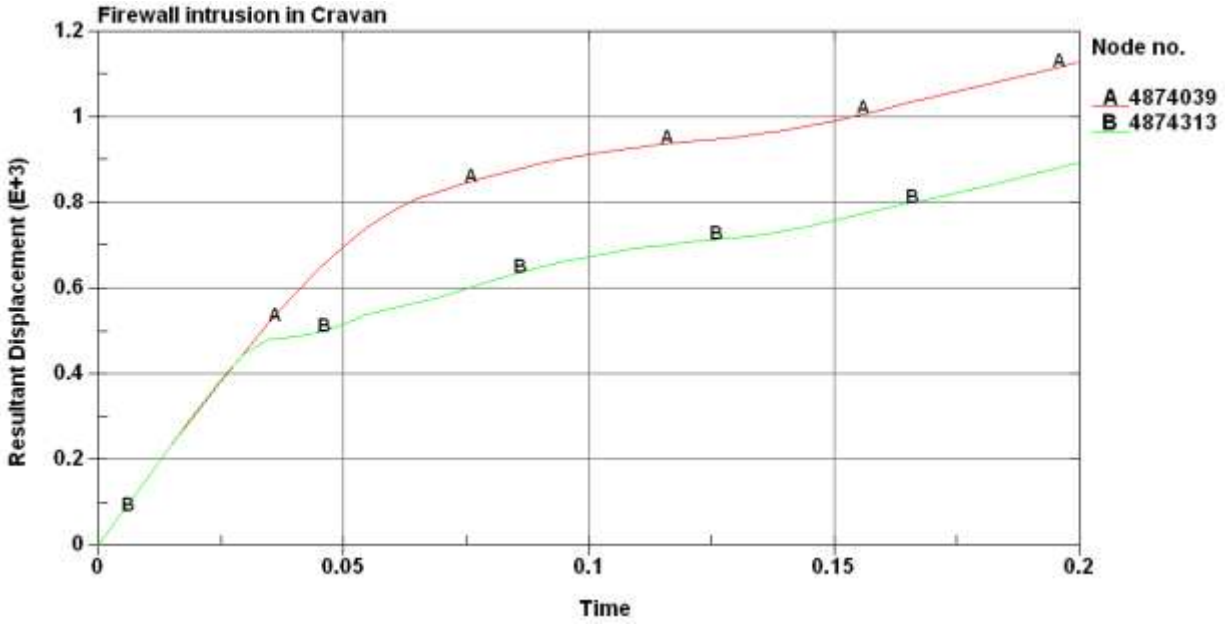

Figure 5.20: Maximum intrusion in firewall of Caravan in CASE-II

Foot-well Intrusion in Chevy S10:

(a): Intrusion in Foot-well of Caravan in CASE-II (isometric view)

Figure 5.21: Animation sequence showing intrusion in foot-well of Caravan in CASE-II
(a) isometric view (b) side view

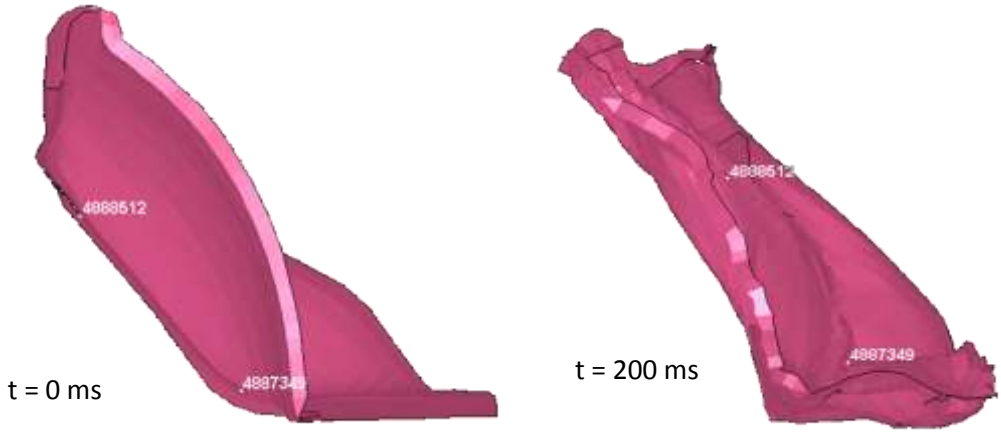

(b): Intrusion in Foot-well of Caravan in CASE-II (side view)

The maximum intrusion in the foot-well of Caravan occurs at node 4888512 and the animation sequence is shown in Figure 5.21. The resultant displacement of this maximum intruded node is shown in the Figure 5.22. From Figure 5.22, the maximum intrusion in the foot-well of Caravan in collision with a passenger car is found to be 48mm.

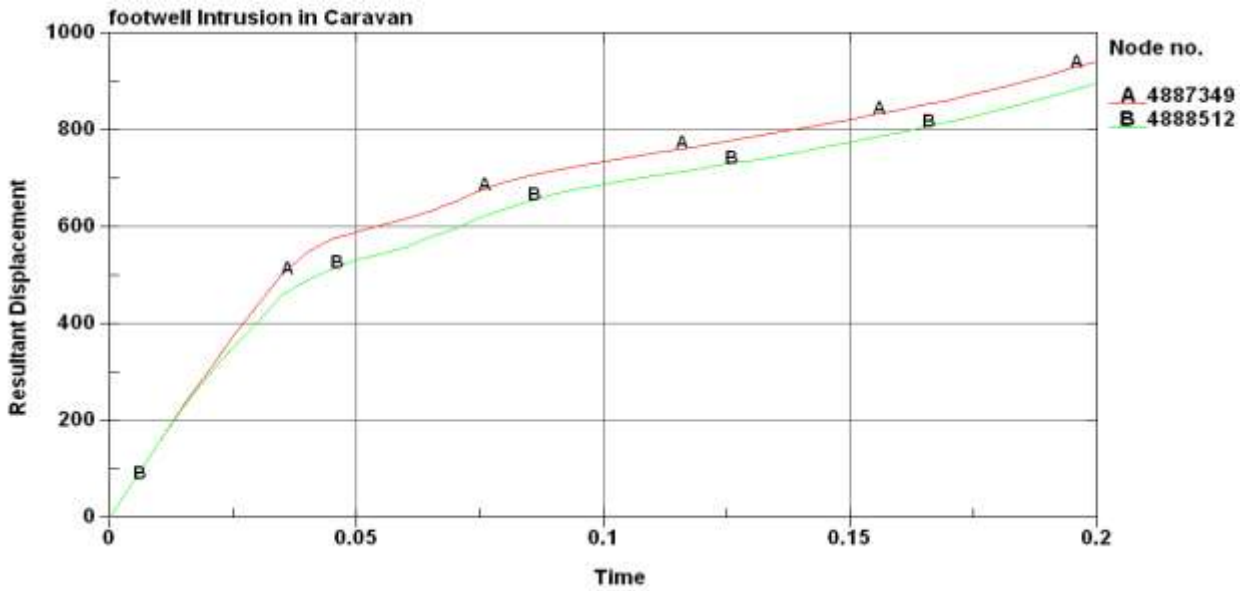

Figure 5.22: Maximum intrusion in foot-well of Caravan in CASE-II

Driver side A-Pillar Intrusion in Caravan:

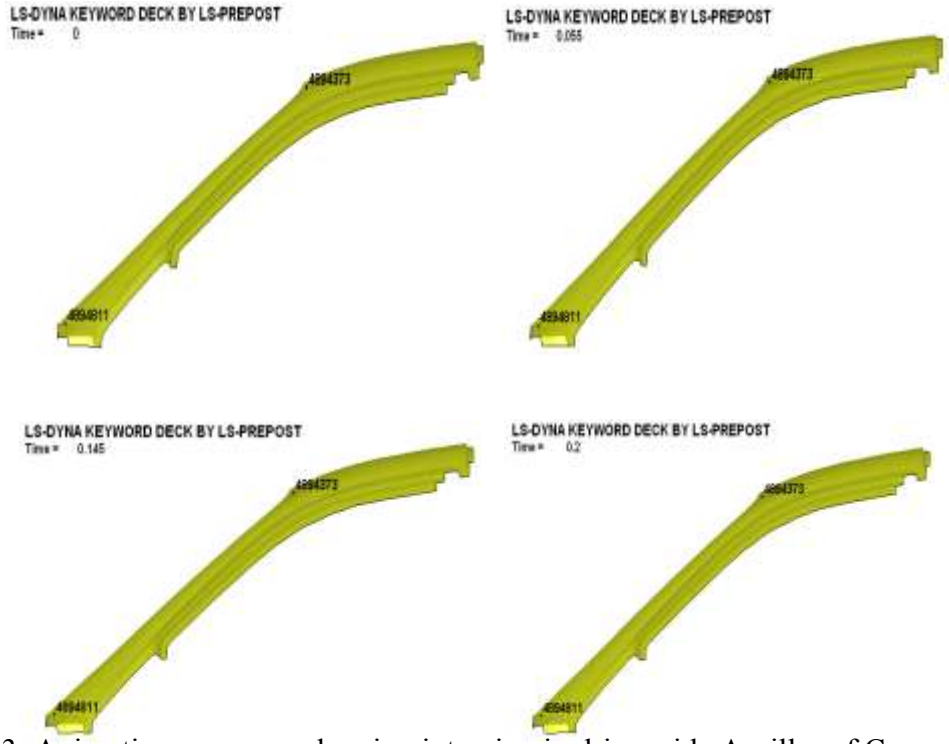

Figure 5.23: Animation sequence showing intrusion in driver side A-pillar of Caravan in CASE-I

From Figure 5.23, it can be observed that the node which had maximum rearward movement on the A-pillar of the Caravan is Node #4894811. The maximum displacement of this node is 30 mm and the Figure 5.24 shows the displacement of the node with respect to time.

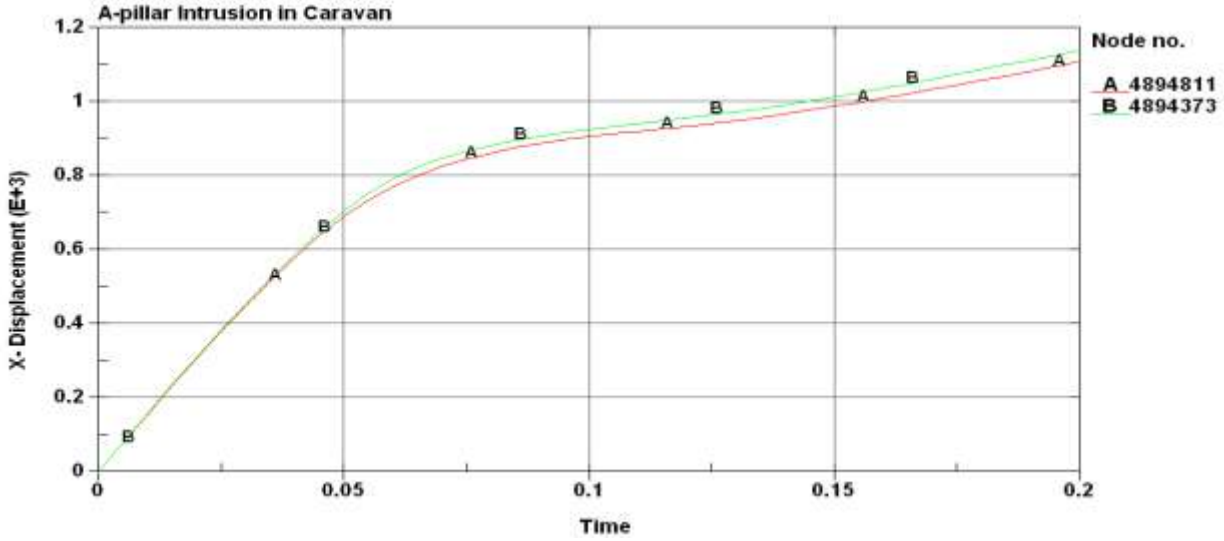

Figure 5.24: Maximum intrusion in driver side A-pillar of Caravan in CASE-II

Firewall Intrusion in Dodge Neon:

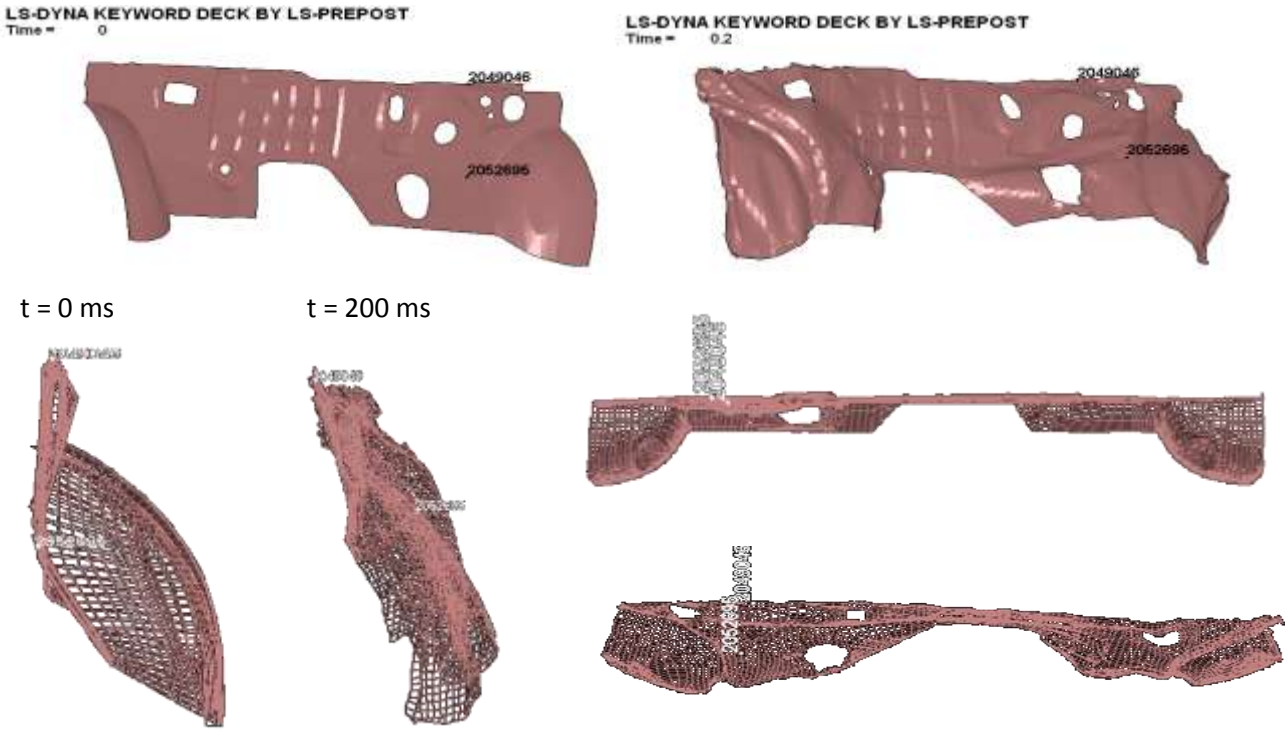

Figure 5.25: Animation sequence showing intrusion in firewall of Neon in CASE-II

From the Figure 5.25 the maximum intrusion in the firewall of the Dodge Neon occurs approximately at Node # 2052695, the maximum displacement of this node is 175 mm, as is shown in the Figure 5.26.

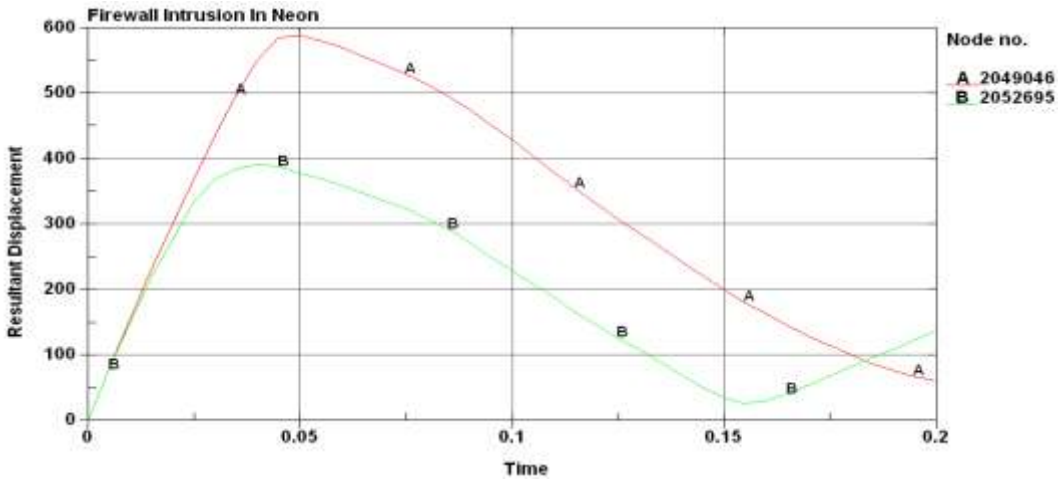

Figure 5.26: Maximum intrusion in firewall of Neon in CASE-II

Foot-well Intrusion in Neon

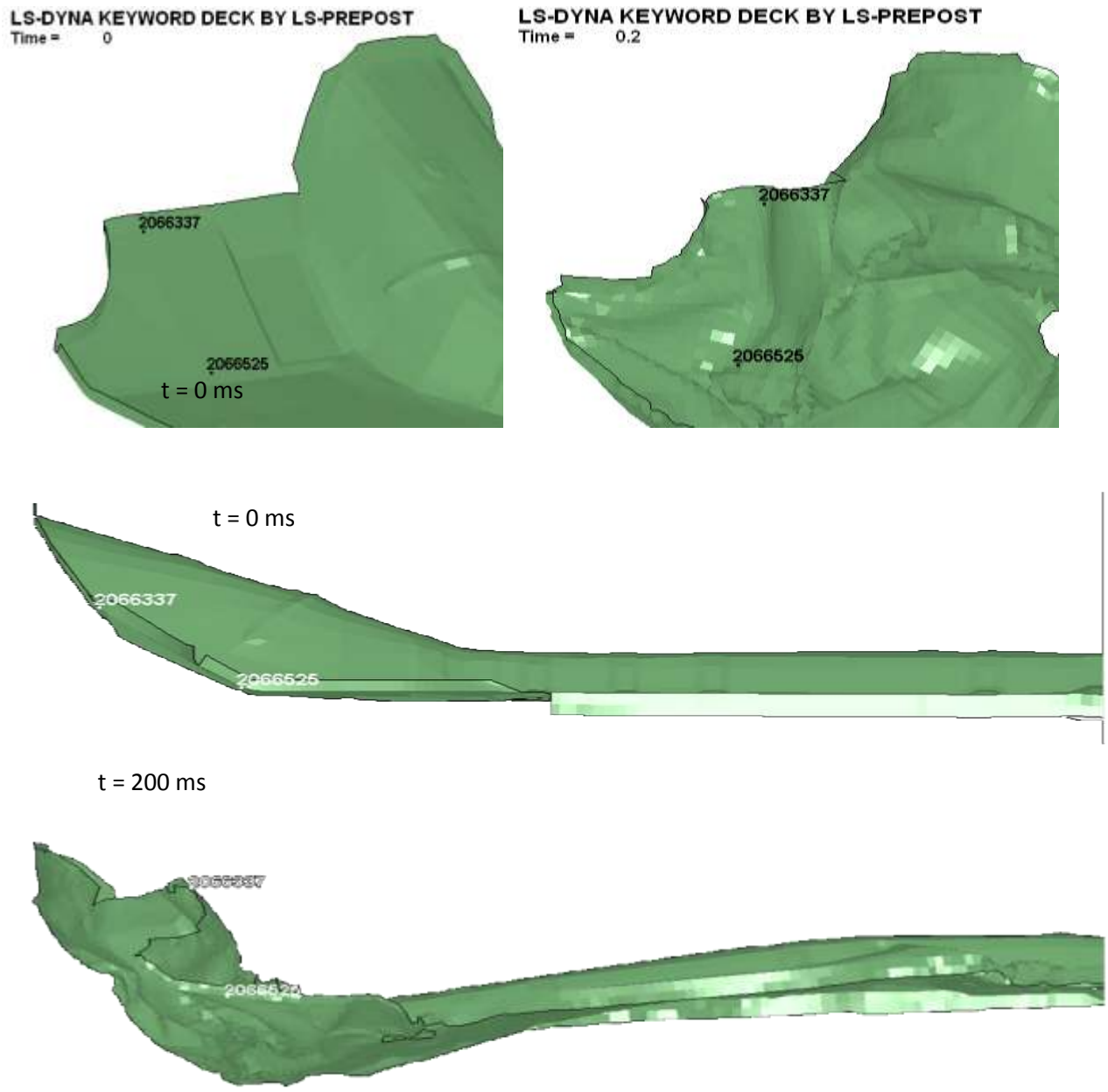

Figure 5.27: Animation sequence showing intrusion in foot-well of Neon in CASE-II

From the Figure 5.27, the maximum intrusion in the foot-well of the Dodge Neon occurs approximately at Node # 2066337, the maximum displacement of this node is 128 mm, as is shown in the Figure 5.28.

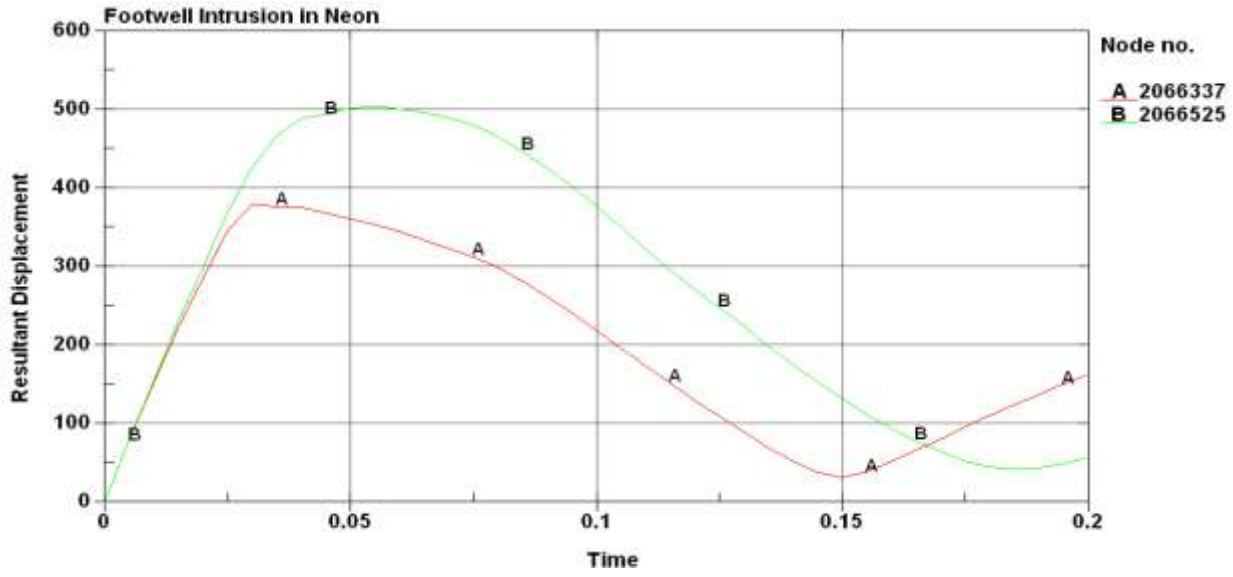

Figure 5.28: Maximum intrusion in foot-well of Neon in CASE-II

Driver side A-Pillar Intrusion in Dodge Neon:

The Figures 5.29 shows the movement of driver side A-pillar of Neon during the collision with a compact pickup.

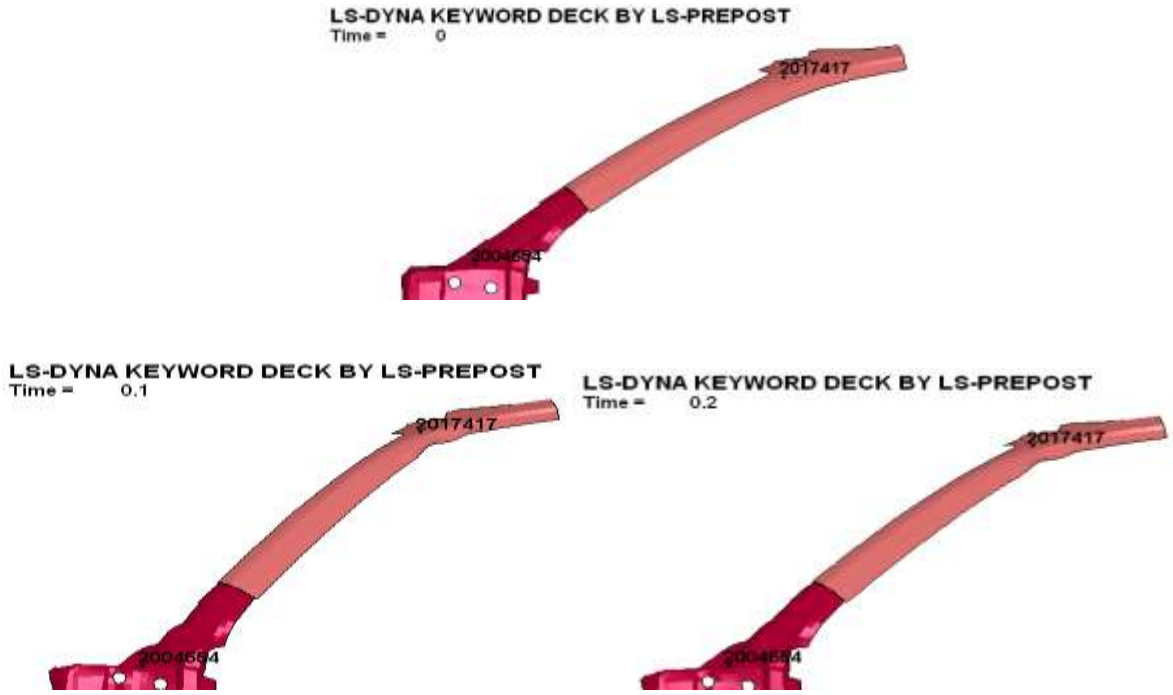

Figure 5.29: Animation sequence showing intrusion in driver side A-pillar of Neon in CASE-II

The node which had maximum rearward movement on the A-pillar of the Dodge Neon is node #2004654, the maximum displacement of this node is found to be 68mm. Figure 5.30 shows the displacement of the node with respect to time.

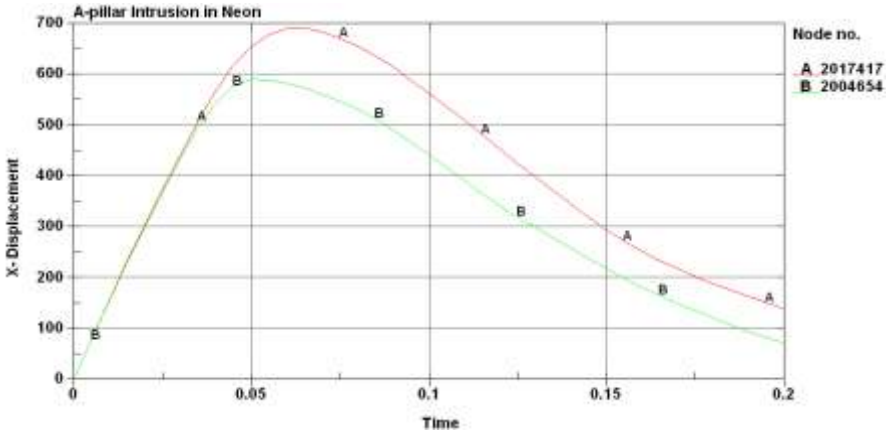

Figure 5.30: Maximum intrusion in driver side A-pillar of Neon in CASE-II

Figure 5.31 shows the left and right seat acceleration in the Dodge Neon and Dodge Caravan. The figure also shows the peak acceleration in the two vehicles.

LEFT and RIGHT Seat Accelerations:

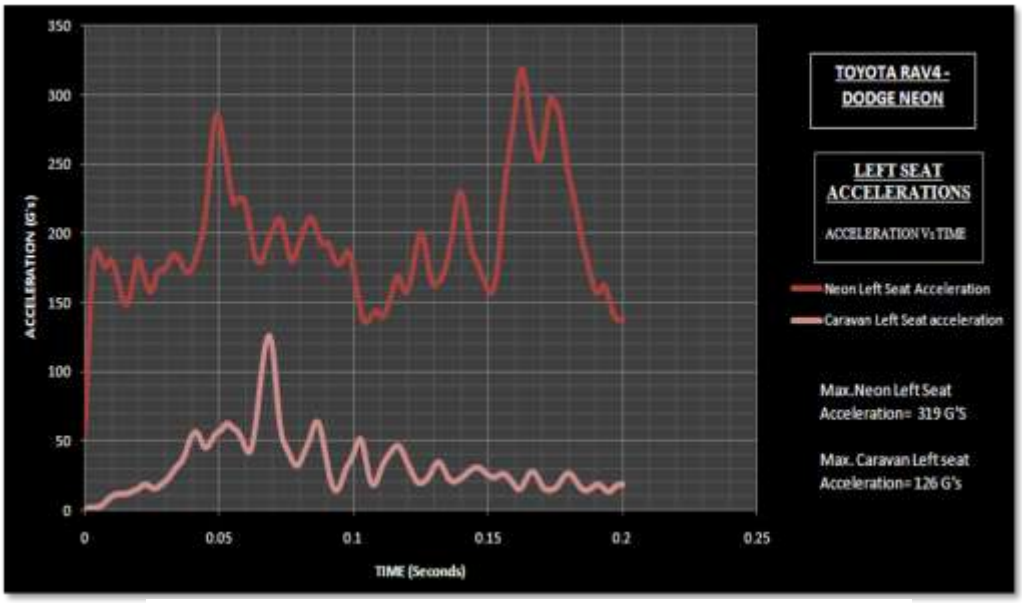

(a): Left seat acceleration in CASE-II

Figure 5.31: Left and Right seat acceleration in CASE-II
(a) Left seat (b) Right seat

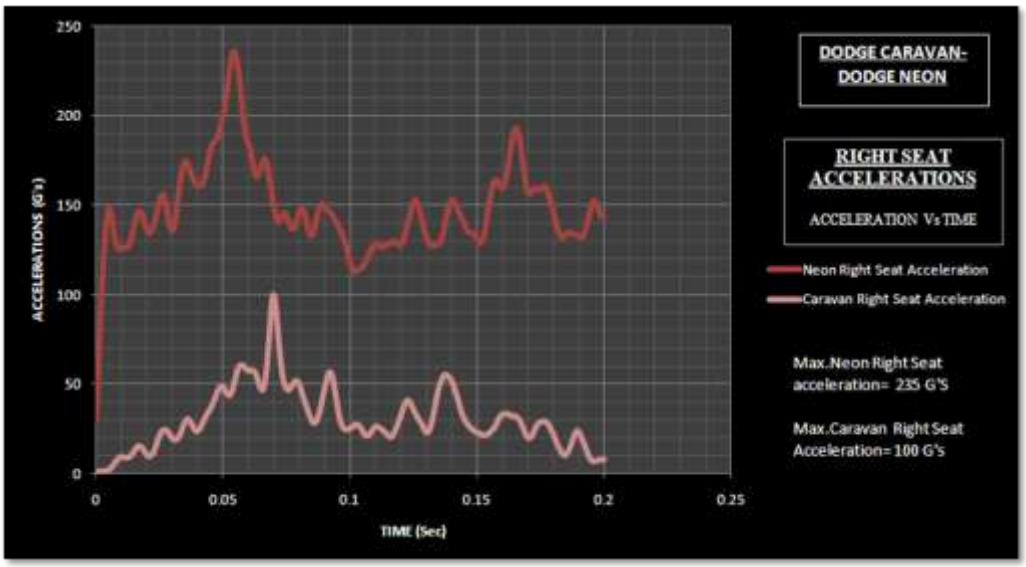

(b): Right seat acceleration in CASE-II

5.2.3 Discussion

In the crash Scenario of Dodge Grand Caravan (representing a Minivan) colliding against Dodge Neon (representing a Passenger car), the weight of the Caravan is 2000 Kgs where as weight of the Neon car is 1333 Kgs. This difference in weight between the two vehicles will lead to mass incompatibility between them which will result in high intrusions in the passenger car than the minivan. The ride height of Caravan and Neon are approximately 220 and 200mm respectively. The difference in the ride height of two vehicles is not huge, which prevents the small car from under riding in to minivan but the frontal geometric shape of minivan is completely different from the Neon car. The frontal engine arrangement and bonnet shape in the minivan is in an inclined position to ground rather than parallel to the ground. This type of arrangement will expose firewall directly and force the firewall to absorb the crash energy more than the firewall of the passenger car where the engine and bonnet shape will be more of parallel to the ground. This high absorption of crash energy by the firewall of Caravan will lead to higher intrusion than Neon. This difference in frontal geometric shape will lead to geometric

incompatibility and application of different type of load paths between them. In this case mass incompatibility will lead to higher intrusion at foot-well and A-pillar in the neon car than caravan but lower intrusion in the firewall because of the geometric shape of caravan. The stiffness of both cars is within acceptable range, which means there is no stiffness incompatibility between these two vehicles. The Table 5.5 below shows the firewall, foot-well and driver side A-pillar intrusion and left and right seat acceleration ratio. The weight ratio and firewall intrusion ratio of 1.5: 1 and 1.3: 1 respectively deviate from the statistical DFR of 1: 2.6 but the foot-well intrusion, A-pillar intrusion, left and right seat acceleration ratios of 1: 2.6, 1: 2.4, 1: 2.5, 1: 2.4 are comparable to the statistical DFR ratio of 1: 2.6.

Summary of CASE- II:

Table 5.5: Summary of CASE-II

	Caravan	Neon
Firewall Intrusion (mm)	234	175
Foot well Intrusion (mm)	48	128
A-pillar Intrusion (mm)	30	68
Left seat Acceleration (G's)	126	319
Right seat Acceleration (G's)	100	236

Dodge Caravan : Dodge Neon	Ratio
Ratio of Firewall Intrusion	1.3 : 1
Ratio of Foot well Intrusion	1: 2.6
Ratio of A-pillar Intrusion	1: 2.4
Ratio of Left seat Acceleration	1: 2.5
Ratio of Right seat Acceleration	1: 2.4

5.3 CASE – III: Sports Utility Vehicle (Ford Explorer) Vs Passenger Car (Dodge Neon)

5.3.1 Model Description

Dodge Neon: Described in Case I.

Ford Explorer:

The FE model of Ford Explorer is developed by National Crash Analysis Center for all impacts modes based on a 2003 model Explorer. This model can be used for research work in all impact configurations. The model is described detailed way in all sides of the vehicle making it useful in all impact scenarios. Figure 5.32 shows the FE Model of the Ford Explorer used to represent the SUV category.

Figure 5.32: Exploded view of Ford

The vehicle FE model has 791 parts; each part of the model depicts different parts of the original vehicle. The material properties of different parts are derived from the coupon testing. Different materials used in this FE model are BLATZ-KO_RUBBER, CRUSHABLE FOAM, DAMPER VISCOUS, ELASTIC, HONEYCOMB, PIECEWISE LINEAR PLASTICITY, SPRING NONLINEAR ELASTIC and SPRING_ELASTIC. There are 619161 elements in the FE model out of which 6 are beam elements, 42 are discrete elements, 585730 are shell elements, 33695 are solid elements. Different parts of the vehicle are constrained by thirty revolute joints, sixteen spherical joints, six thousand three hundred spot welds. The FE Model is validates the Ford Explorer NCAP test results and the vehicle is stable at 25, 30, 35, 40 mph. The

accelerations of the vehicle and the wall force exerted by this vehicle are comparable to NCAP test results. The Table 5.6 shows the summary of the FE Model.

Table 5.6: FE model summary of Ford Explorer

Number of Parts	791
Number of Nodes	632166
Number of Solids	33695
Number of Beams	48
Number of Shells	585418
Number of Elements	619161

5.3.3 Crash Simulation

Two vehicles are positioned such that they have full width frontal interaction during collision and the vehicles are placed as close as possible to reduce the computational time. The contact between two vehicles is defined by using "Automatic Surface to surface "card. Static and dynamic friction co-efficient are given as 0.3 between the contact of two vehicles. Rigid wall planar cards are used between the contact of all tires and roads. Initial velocity of 35 mph is given to both vehicles and the termination time of 200 milliseconds is given with a time step of 10 milliseconds. The total computational time for simulation this crash scenario is almost 200 hours. Figure 5.33 shows the results of crash simulation between the two vehicles at different times.

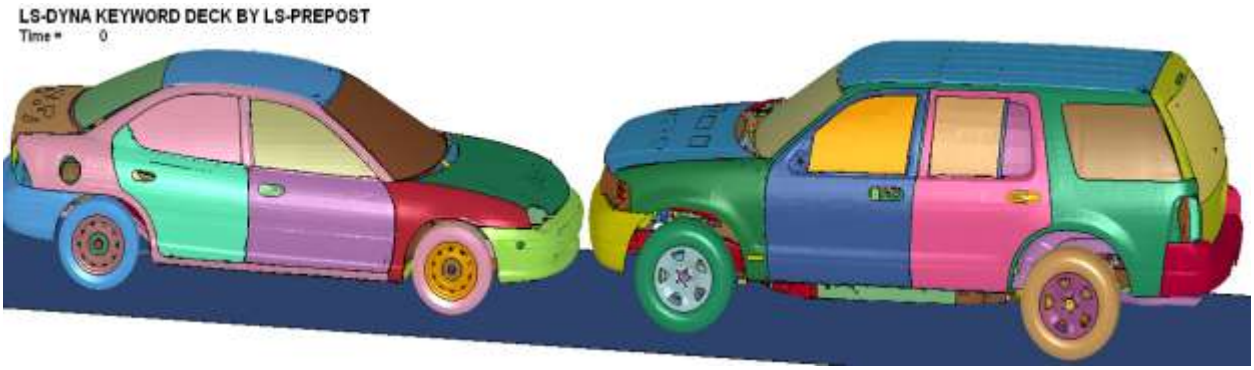

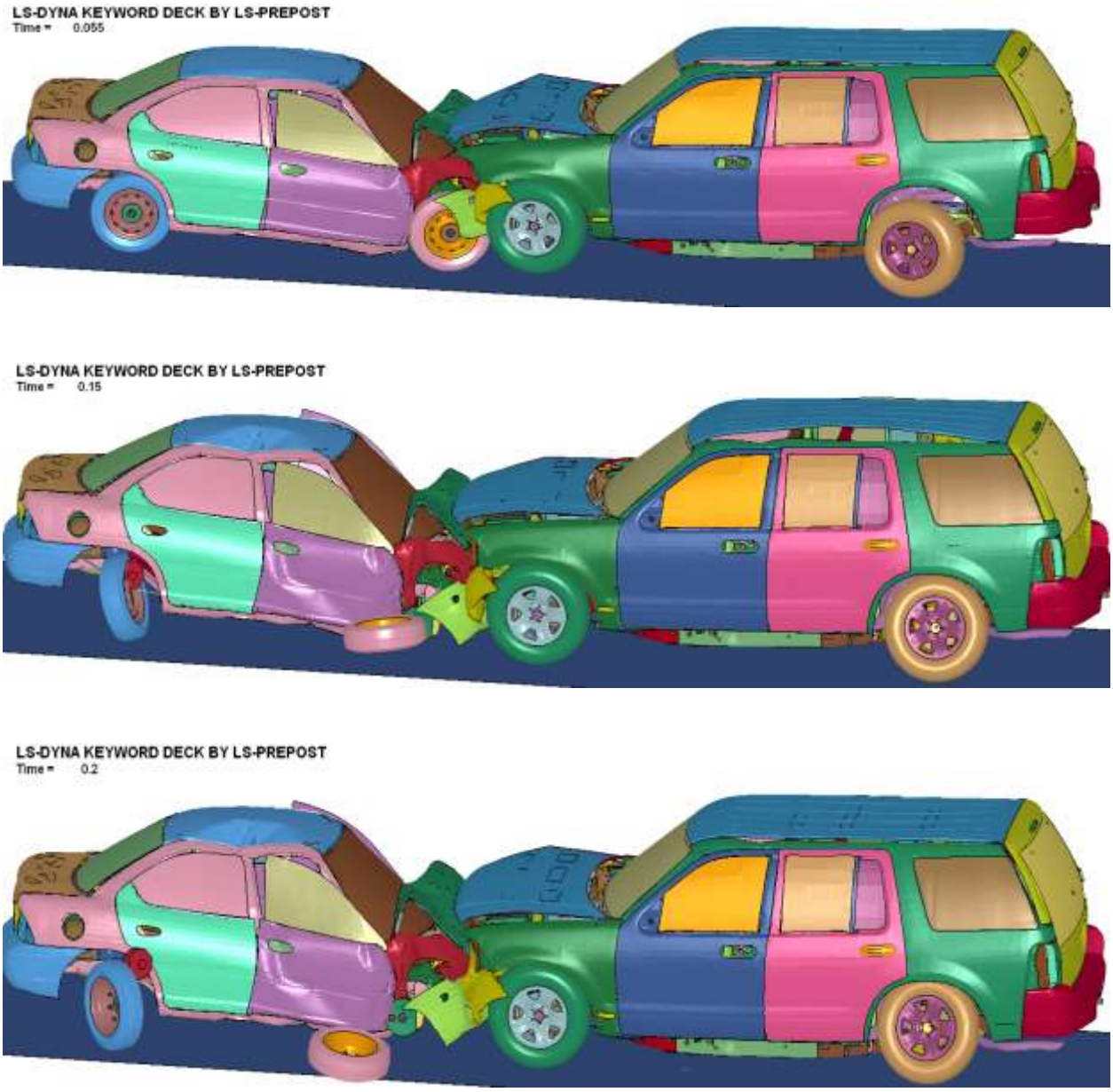

Figure 5.33: Animation of Ford Explorer crashing against Dodge Neon

The two vehicles are placed as close as possible to each other to reduce calculation time. The maximum crush between the vehicles happened at 95 ms, after which the SUV pushes the passenger car backwards. After reaching the maximum crush stage, firewall, driver side A-pillar, foot-well intrusions and accelerations of left and right seat are measured. Figure 5.34 shows the intrusions in the firewall of Explorer.

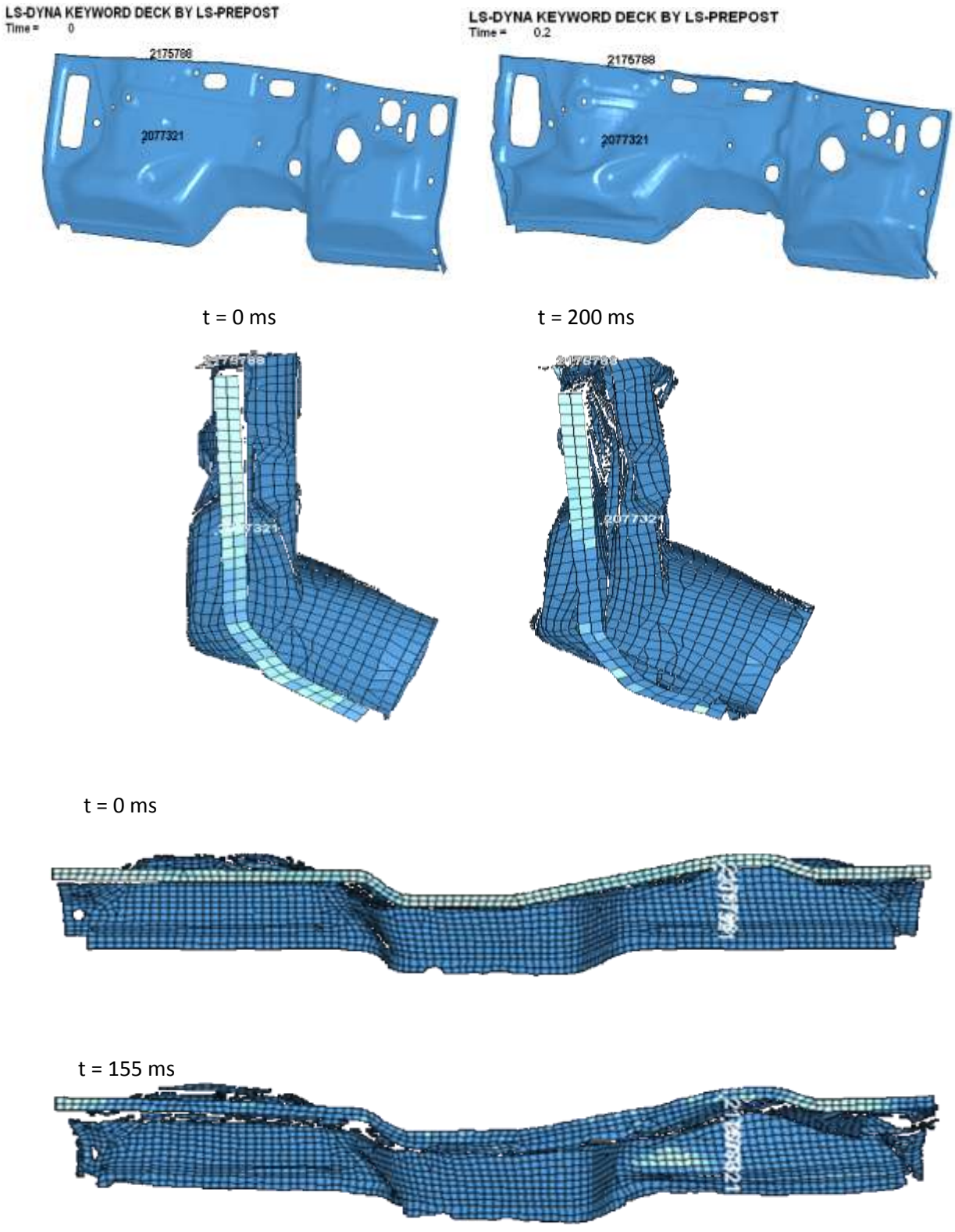

Figure 5.34: Animation sequence showing intrusion in firewall of Explorer in CASE-III

From Figure 5.34 it is evident that the maximum intrusion occurs approximately at Node 2077321. The resultant displacement of the maximum intruded node is shown in the Figure 5.35. From the Figure 5.35, maximum intrusion in the firewall of Explorer in collision with a passenger car is measured as 53 mm.

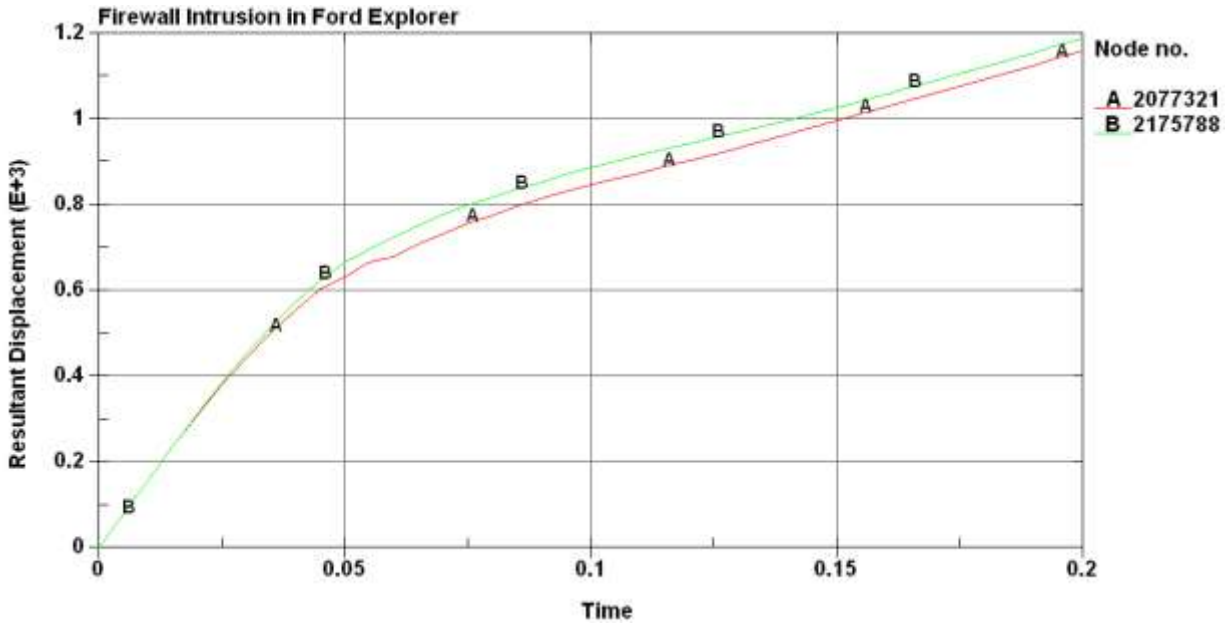

Figure 5.35: Maximum intrusion in firewall of Explorer in CASE-III

Foot-well Intrusion in Explorer:

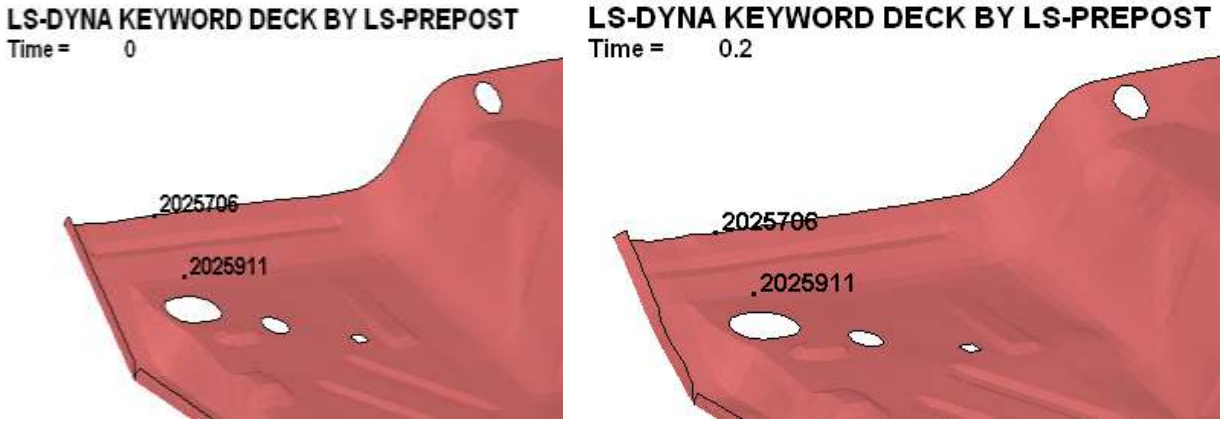

(a): Intrusion in Foot-well of Explorer in CASE-III (isometric view)

Figure 5.36: Animation sequence showing intrusion in foot-well of Explorer in CASE-III (a) isometric view (b) side view

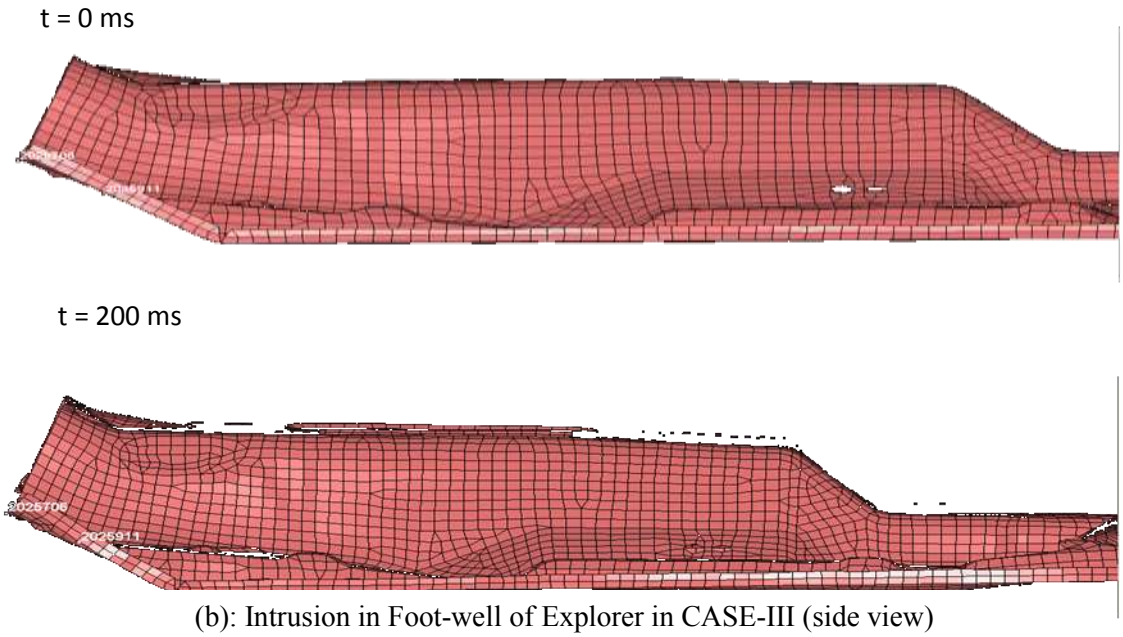

(b): Intrusion in Foot-well of Explorer in CASE-III (side view)

The maximum intrusion in the foot-well of Explorer occurs at node 2025911 and the animation sequence of intrusion is shown in Figure 5.36. The resultant displacement of this maximum intruded node is shown in the Figure 5.37. From Figure 5.7, the maximum intrusion in the foot-well of Explorer in collision with a passenger car is found to be 18mm.

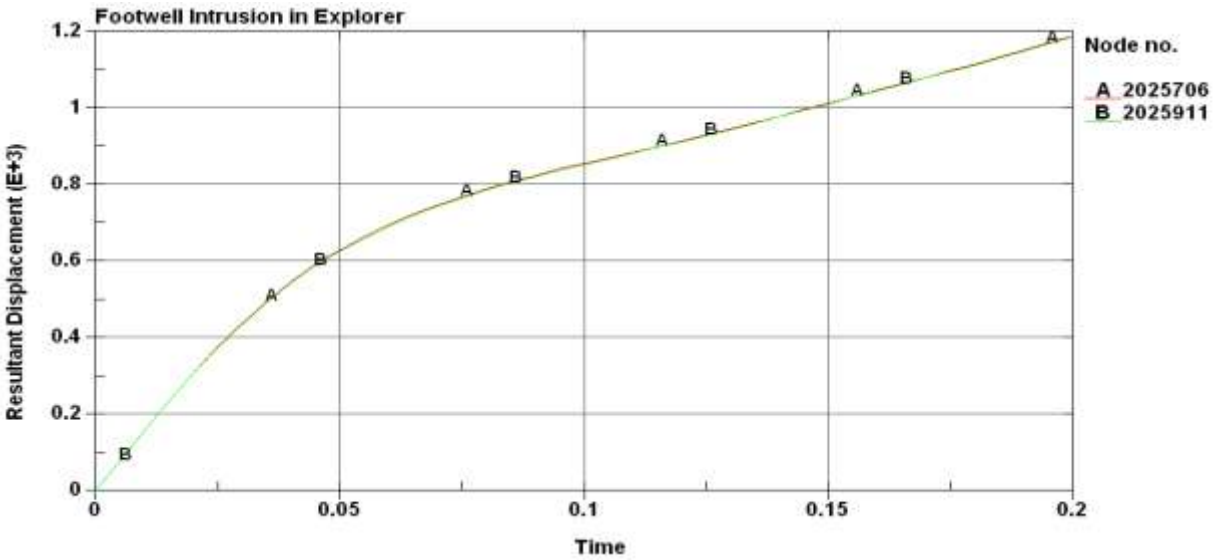

Figure 5.37: Maximum intrusion in foot-well of Explorer in CASE-III

Driver side A-Pillar Intrusion in Explorer:

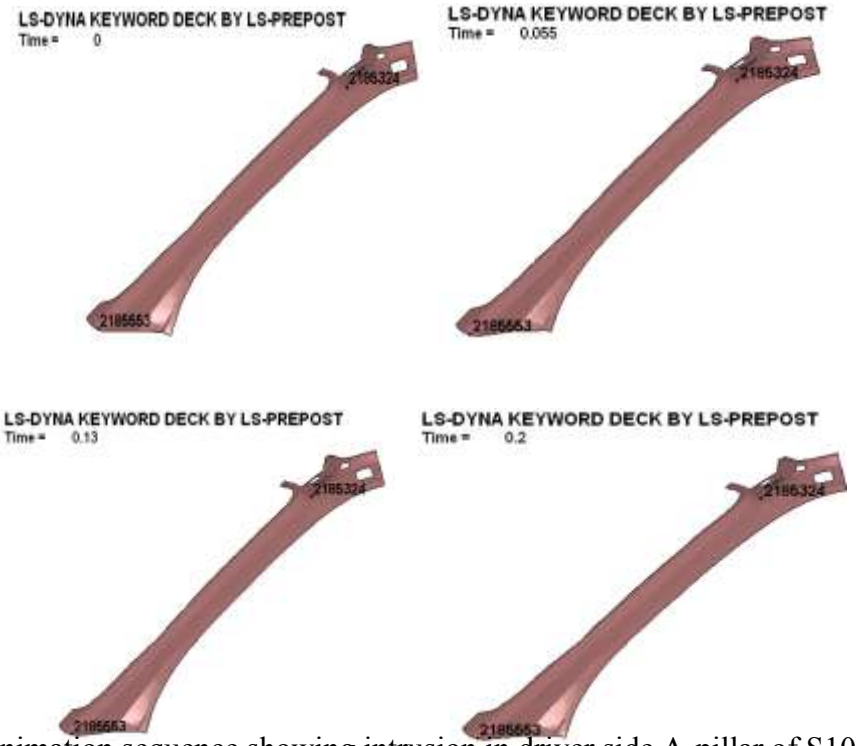

Figure 5.38: Animation sequence showing intrusion in driver side A-pillar of S10 in CASE-III

The node which had maximum rearward movement on the A-pillar of the Explorer is node #218553, the maximum displacement of this node is 31 mm and the Figure 5.39 shows the displacement of the node with respect to time.

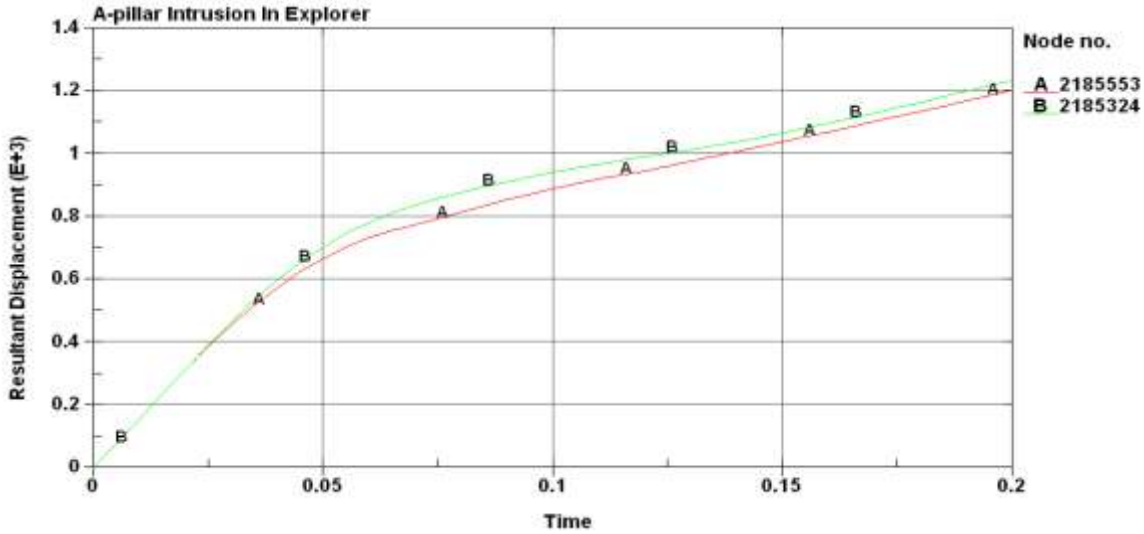

Figure 5.39: Maximum Intrusion in Driver Side A-Pillar of Explorer in CASE-III

Firewall Intrusion in Dodge Neon:

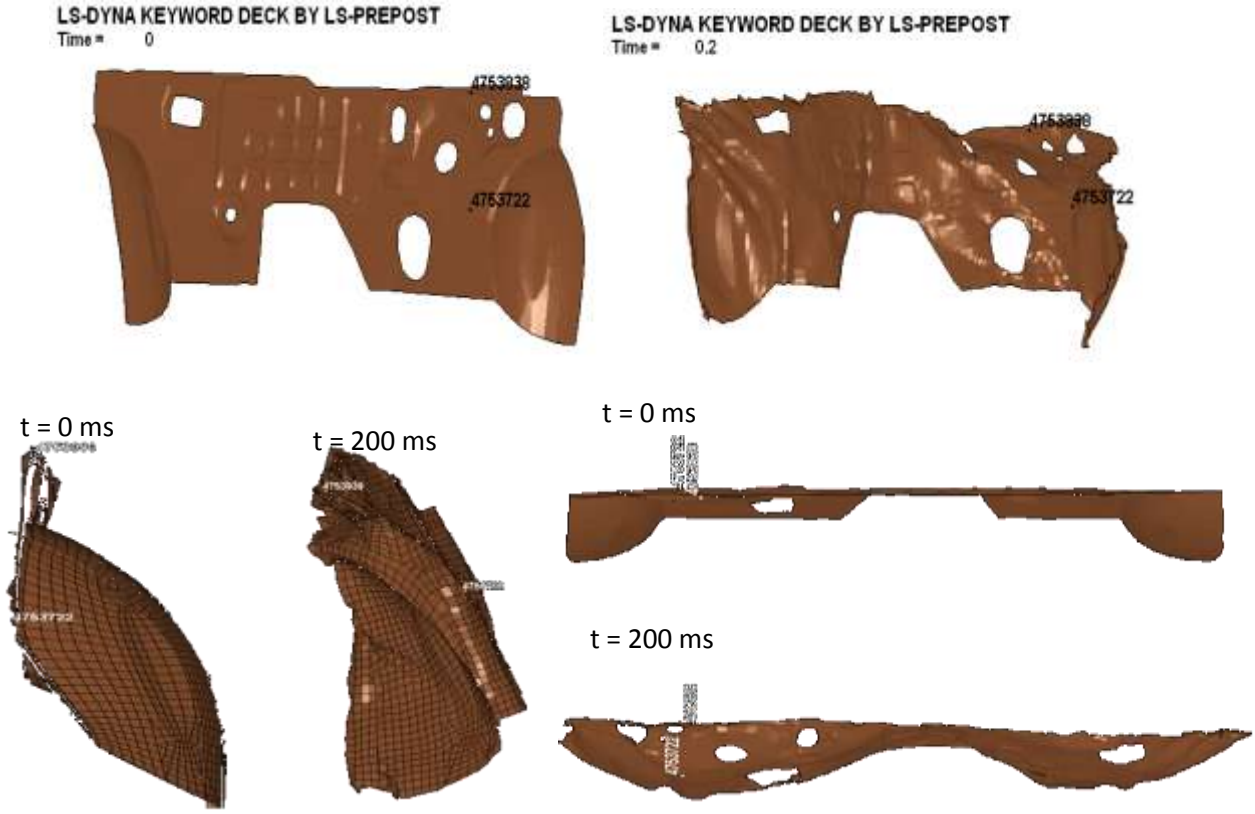

Figure 5.40: Animation sequence showing intrusion in firewall of Neon in CASE-III

From the Figure 5.40 the maximum intrusion in the firewall of the Dodge Neon occurs approximately at node # 4753722, the maximum displacement of this node is 226 mm, as is shown in the Figure 5.41.

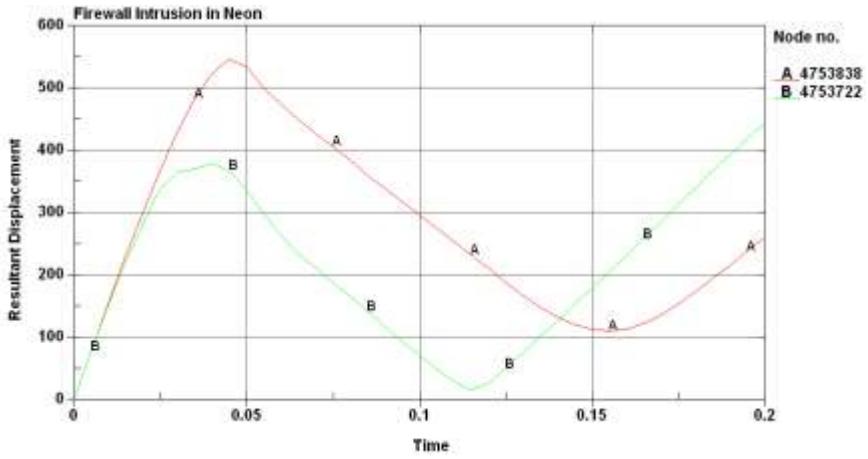

Figure 5.41: Maximum intrusion in firewall of Neon in CASE-III

Foot-well Intrusion in Neon:

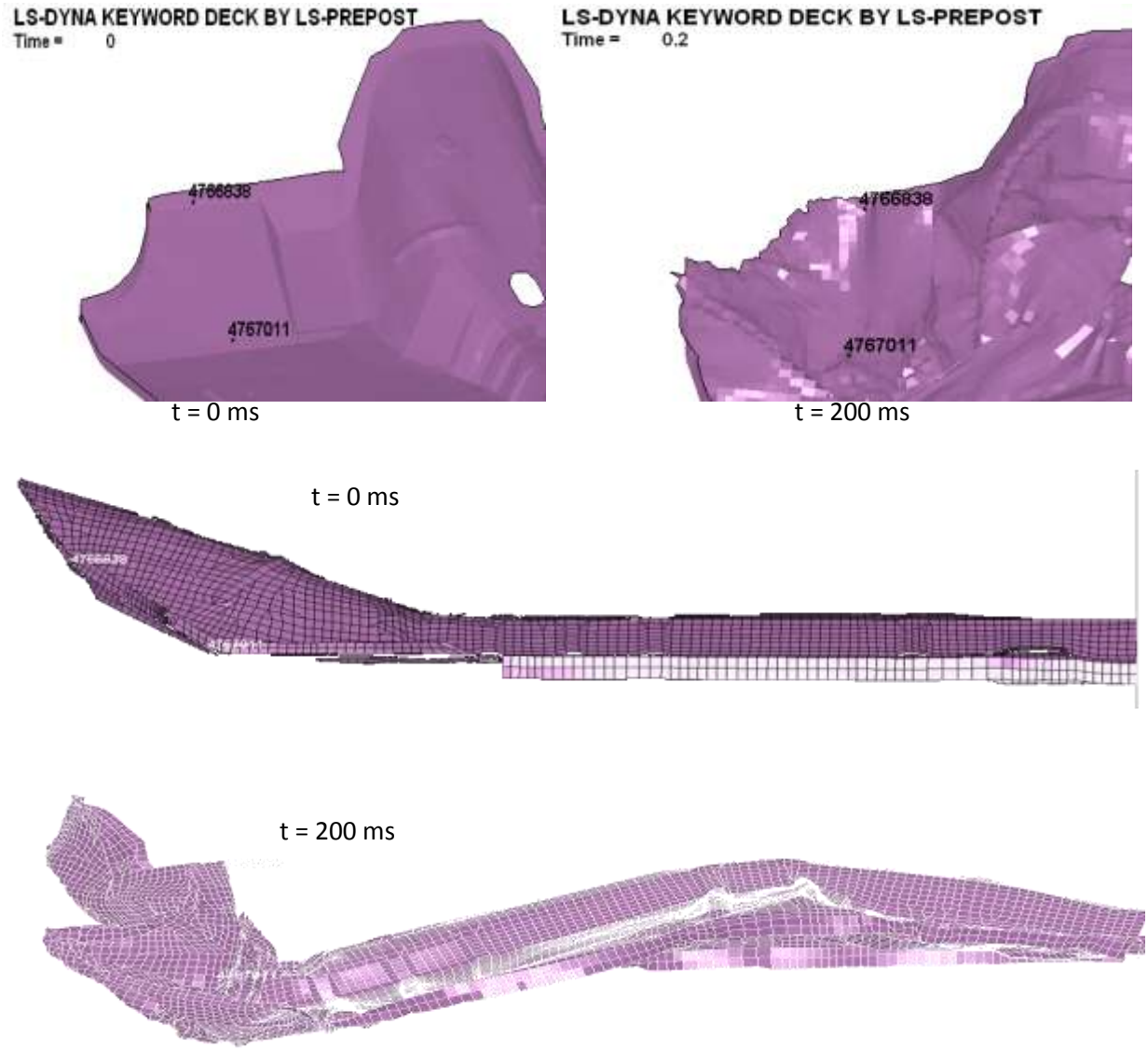

Figure 5.42: Animation sequence showing intrusion in foot-well of Neon in CASE-III

From the Figure 5.42, the maximum intrusion in the Foot-well of the Dodge Neon occurs approximately at node # 4766838, the maximum displacement of this node is 205 mm, as is shown in the Figure 5.43.

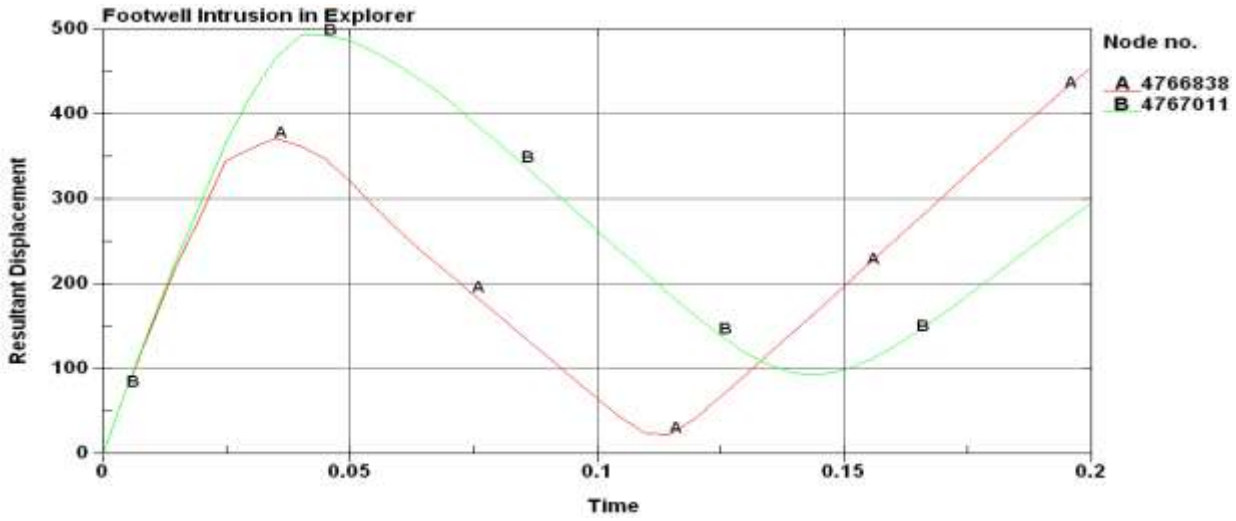

Figure 5.43: Maximum intrusion in foot-well of Neon in CASE-III

Driver side A-Pillar Intrusion in Dodge Neon:

The Figure 5.44 shows the movement of A-pillar during the collision with a compact pickup.

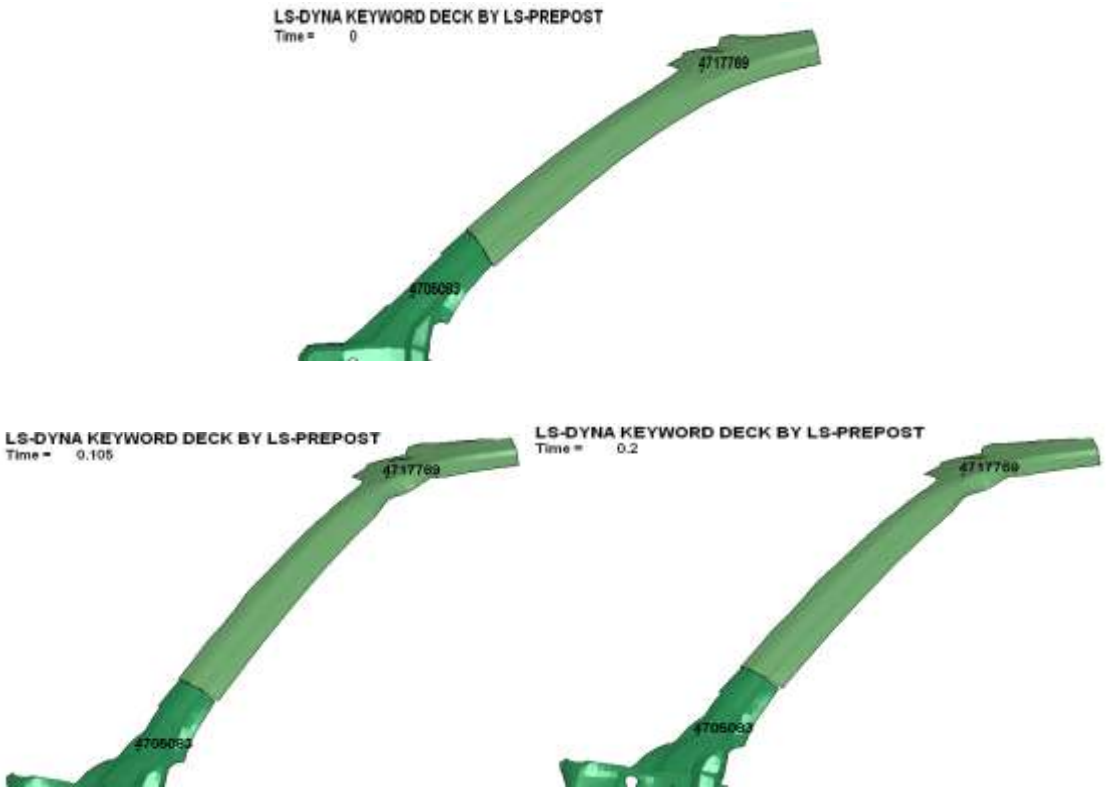

Figure 5.44: Animation sequence showing intrusion in driver side A-pillar of Neon in CASE-III

The node which had maximum rearward movement on the A-pillar of the Dodge Neon is node #4705083, the maximum displacement of this node is found to be 130mm. Figure 5.45 shows the displacement of the node with respect to time.

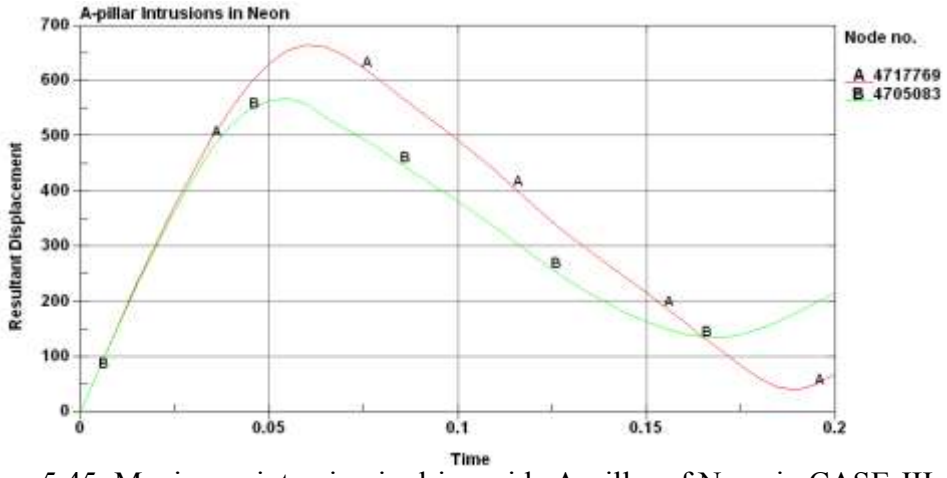

Figure 5.45: Maximum intrusion in driver side A-pillar of Neon in CASE-III

Figure 5.46 shows the left and right seat acceleration in the Dodge Neon and Ford Explorer. Peak acceleration in two vehicles is also shown in the figure.

LEFT and RIGHT Seat Acceleration:

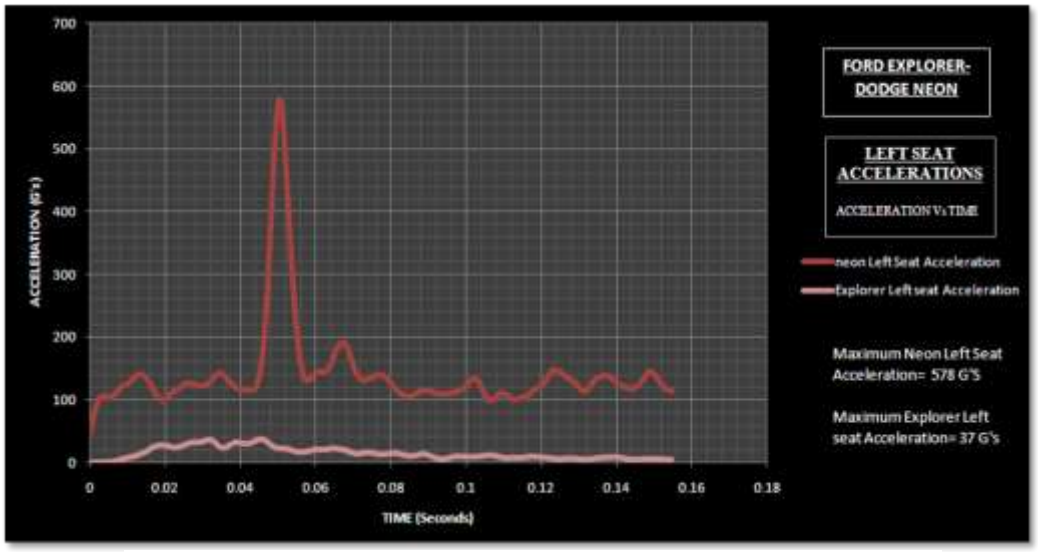

(a): Left seat acceleration in CASE-III

Figure 5.46: Left and Right seat acceleration in CASE-III
(a) Left seat (b) Right seat

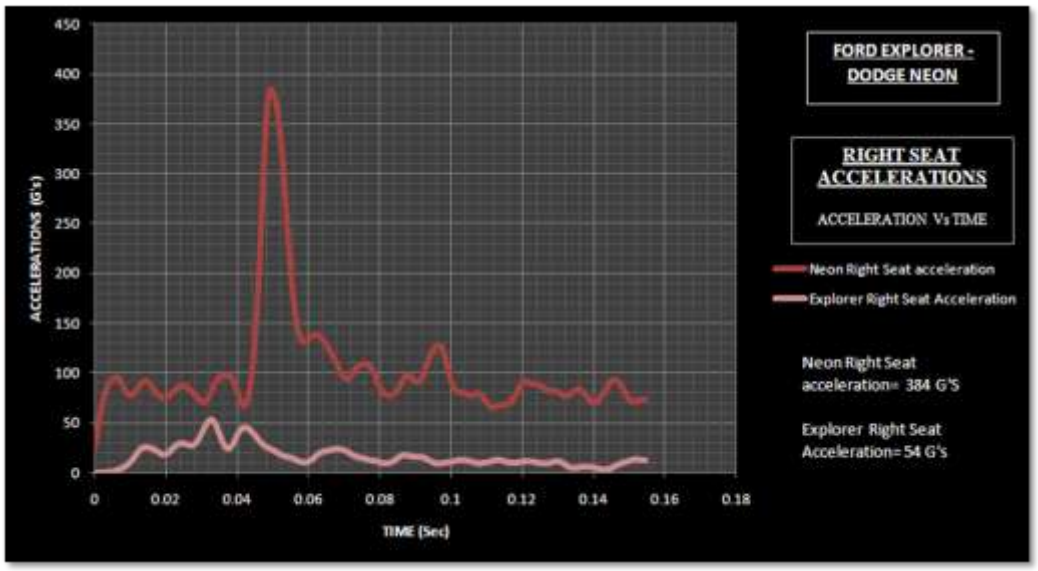

(b): Right seat acceleration in CASE-III

5.3.3 Discussion

In the above crash scenario of Ford Explorer (representing a SUV) and Dodge Neon (representing a Passenger car), the weight of Explorer is 2270 Kgs where as weight of the Neon car is 1333 Kgs. This difference in weight between the two vehicles will lead to mass incompatibility between them which in turn cause high intrusions in the passenger car than the SUV. The ride height of Explorer and Neon are 350 and 200mm. this difference of 150mm in ride height is just enough to prevent the passenger car in under riding into SUV. Any further increase in the difference of ride height will cause into sever geometric incompatibility between two vehicles. Since the difference in the ride heights and frontal geometry of two vehicles will results in application of different type of load paths between them, which will result in high fatal injuries to the occupants in passenger car than SUV. The SUV vehicle is stiffer than passenger car due to its high stiffness will force the passenger car to absorb most of the crash energy developed during the collision which will lead to higher intrusions in passenger car than SUV, this shows that stiffness incompatibility exists between these two vehicle categories. The Table

5.7 shows the maximum intrusions measured at the crucial location like firewall, foot-well and driver side A-pillar which can lead to fatal injuries to occupants. The left and right seat accelerations are also measured and tabulated. The Table 5.7 shows the firewall intrusion ratio, foot-well intrusion ratio, A-pillar intrusion ratio and, left and right seat acceleration ratios. The weight Ratio is way off from the DFR, whereas the left and right seat acceleration ratio and foot-well ratio does not co-relate with DFR because the SUV is very stiffer than passenger car. The firewall and driver Side A-Pillar Ratio of 1: 4.3 and 1: 4.2 respectively correlates with the statistical DFR of 1: 4.3.

Summary of CASE- III:

Table 5.7: Summary of CASE-III

	Explorer	Neon
Firewall Intrusion (mm)	53	226
Foot well Intrusion (mm)	18	205
A-pillar Intrusion (mm)	31	130
Left seat Acceleration (G's)	37	578
Right seat Acceleration (G's)	54	384

Ford Explorer : Dodge Neon	Ratio
Ratio of Firewall Intrusion	1: 4.3
Ratio of Foot well Intrusion	1: 11
Ratio of A-pillar Intrusion	1: 4.2
Ratio of Left seat Acceleration	1: 15
Ratio of Right seat Acceleration	1: 07

5.4 CASE – IV: Full Size Pick-up (Ford F250) Vs Passenger Car (Dodge Neon)

5.4.1 Model Description

Dodge Neon: Described in Case I.

Ford F250:

The FE model of Ford F250 is developed by National Crash Analysis Center for all impacts modes based on a 2006 model F250. This model can be used for research work in all impact modes. The model is described detailed way in all sides of the vehicle making it useful in all impact scenarios. Figure 5.47 shows the FE Model of the Ford Explorer used to represent the Full-size Pick-up category [22].

Figure 5.47: Exploded view of F250

The vehicle FE model has 871 parts; each part of the model depicts different parts of the original vehicle. The material properties of different parts are derived from the coupon testing. Different materials used in this FE model are BLATZ-KO_RUBBER, LOW_DENSITY_FOAM, VISCOELASTIC, DAMPER VISCOUS, ELASTIC, HONEYCOMB, PIECEWISE LINEAR PLASTICITY, SPRING NONLINEAR ELASTIC and SPRING_ELASTIC. There are 726759 elements in the FE model out of which 2305 are beam elements, 47 are discrete elements, 698372 are shell elements, 25905 are solid elements. Different parts of the vehicle are constrained by thirty four revolute joints, nine spherical joints, two cylindrical joints and two thousand four hundred and ninety seven spot welds. The FE Model is validates against Ford

F250 NCAP test results and the vehicle is stable at 25, 30, 35, 40 mph. The accelerations of the vehicle and the wall force exerted by this vehicle are comparable to NCAP test results. The Table 5.8 shows the summary of the FE Model.

Table 5.8: FE model summary of Ford F250

Number of Parts	871
Number of Nodes	738165
Number of Solids	25905
Number of Beams	2353
Number of Shells	698501
Number of Elements	726759

5.4.2 Crash Simulation

The two vehicles are positioned such that they have full width interaction during collision and the vehicles are placed as close as possible to reduce the computational time. The contact between two vehicles is defined by using "Automatic Surface to surface "card. Static and dynamic friction coefficients are both given as 0.3 between the contacts of two vehicles. Rigid wall planar cards are used between the contact of all tires and roads. Initial velocity of 35 mph is given to both vehicles and the Simulation termination time of 200 milliseconds is given with a time step of 10 milliseconds. The total computational time for this crash scenario is 200 hours. Figure 5.48 shows the results of crash simulation between two vehicles at different time.

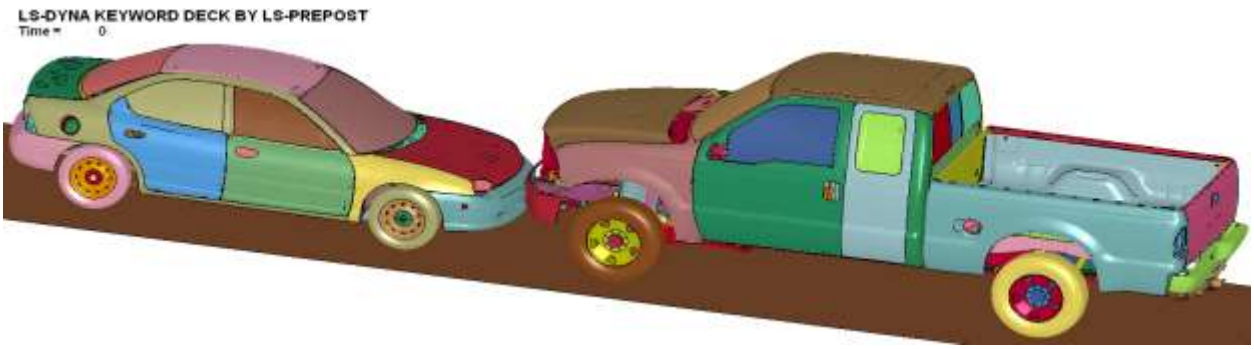

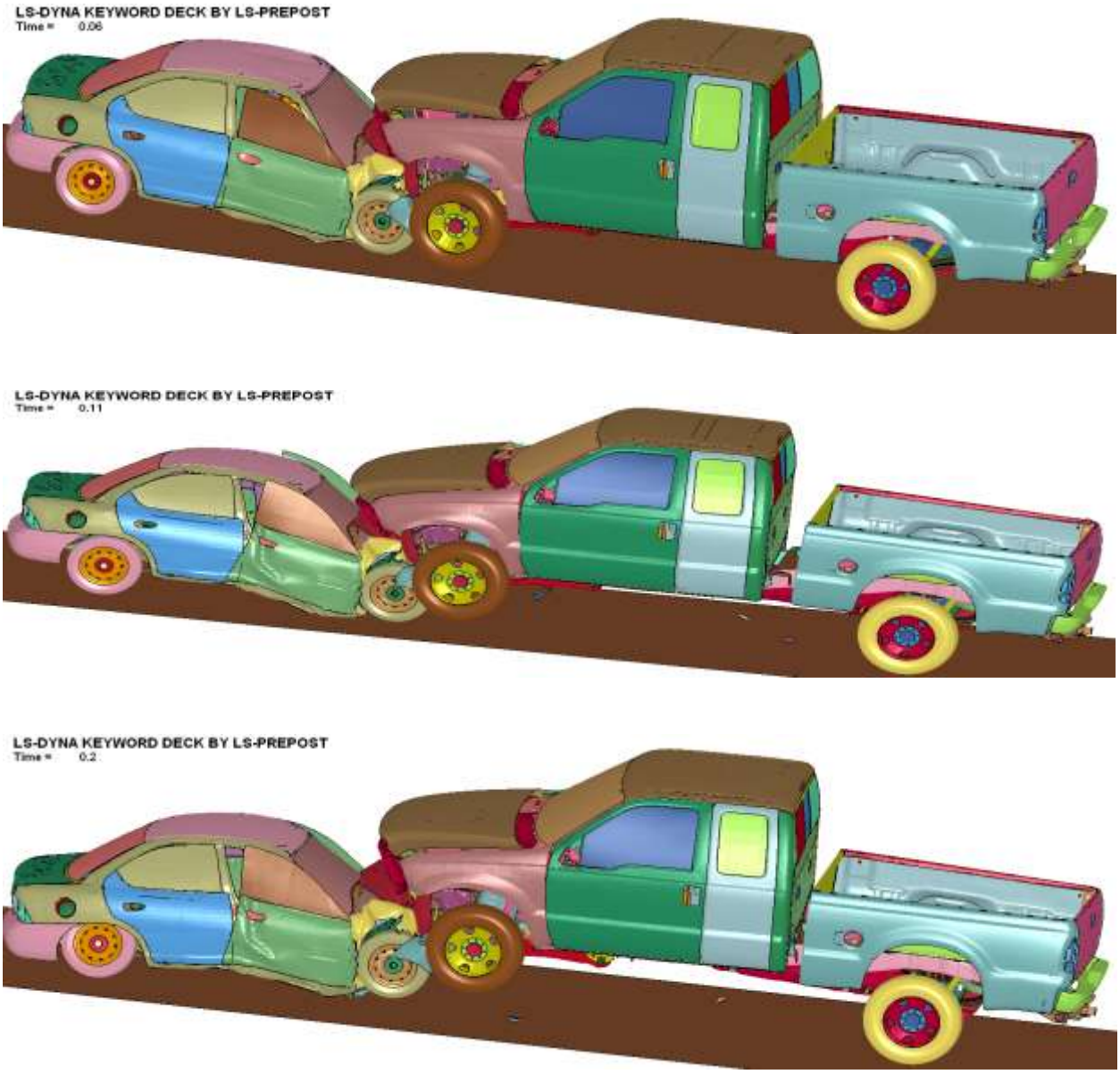

Figure 5.48: Animation of Ford F250 crashing against Dodge Neon

The two vehicles are placed as close as possible to each other to reduce calculation time. The maximum crush between the vehicles happened at 100ms, after which the small car (Neon) under rides in to Ford F250 vehicle. After reaching the maximum crush stage, firewall, driver side A-pillar, foot-well intrusions and accelerations of left and right seat are measured. Figure 5.49 shows the intrusions in the firewall of F250.

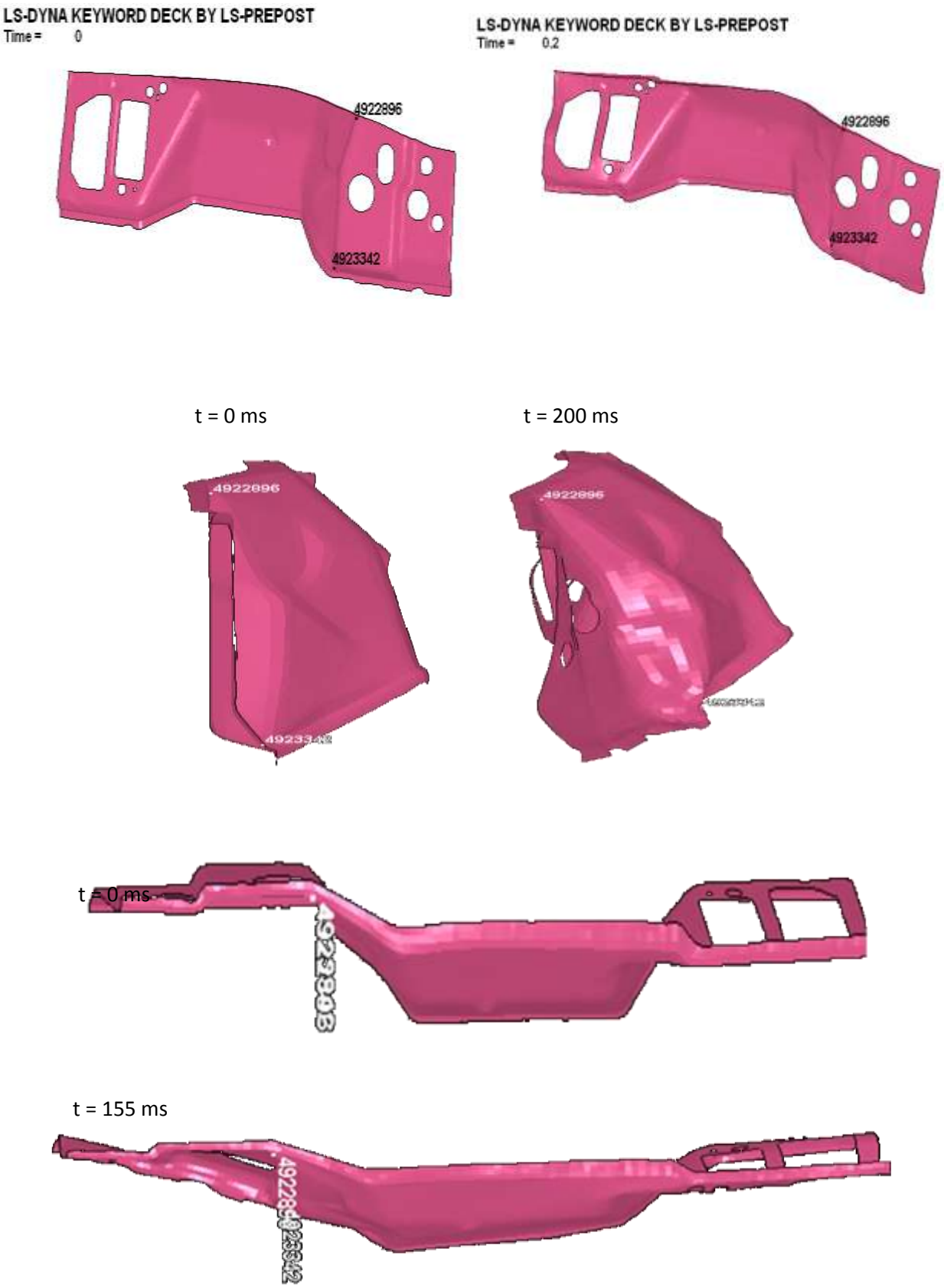

Figure 5.49: Animation sequence showing intrusion in firewall of F250 in CASE-IV

From Figure 5.49 it is apparent that the maximum intrusion occurs approximately at node 4923342. The resultant displacement of the maximum intruded node is shown in the Figure 5.50. From the above graph, maximum intrusion in the firewall of F250 in collision with a passenger car is measured as 116 mm.

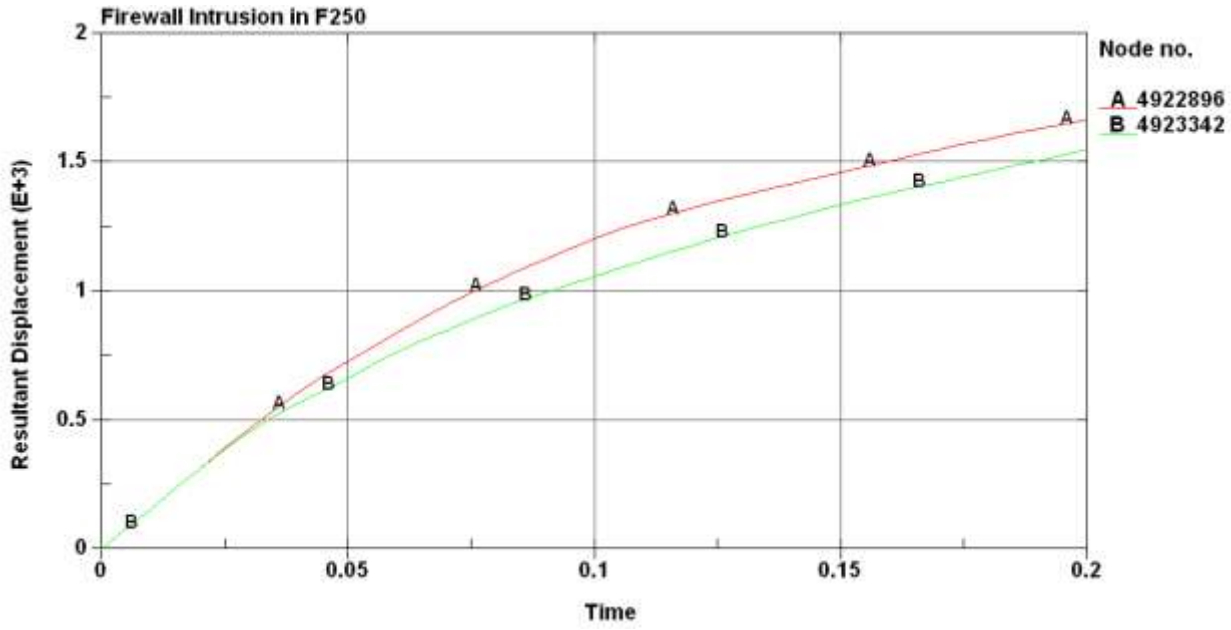

Figure 5.50: Maximum intrusion in firewall of F250 in CASE-IV

Foot-well Intrusion in F250:

(a): Intrusion in foot-well of F250 in CASE-IV (isometric view)

Figure 5.51: Animation sequence showing intrusion in foot-well of F250 in CASE-IV
(a) isometric view (b) side view

(b): Intrusion in foot-well of F250 in CASE-IV (side view)

The maximum intrusion in the foot-well of F250 occurs at node 4936640 and the animation sequence of the intrusion is shown in Figure 5.51. The resultant displacement of this maximum intruded node is shown in the Figure 5.52. From Figure 5.52, the maximum intrusion in the foot-well of F250 in collision with a passenger car is found to be 23mm.

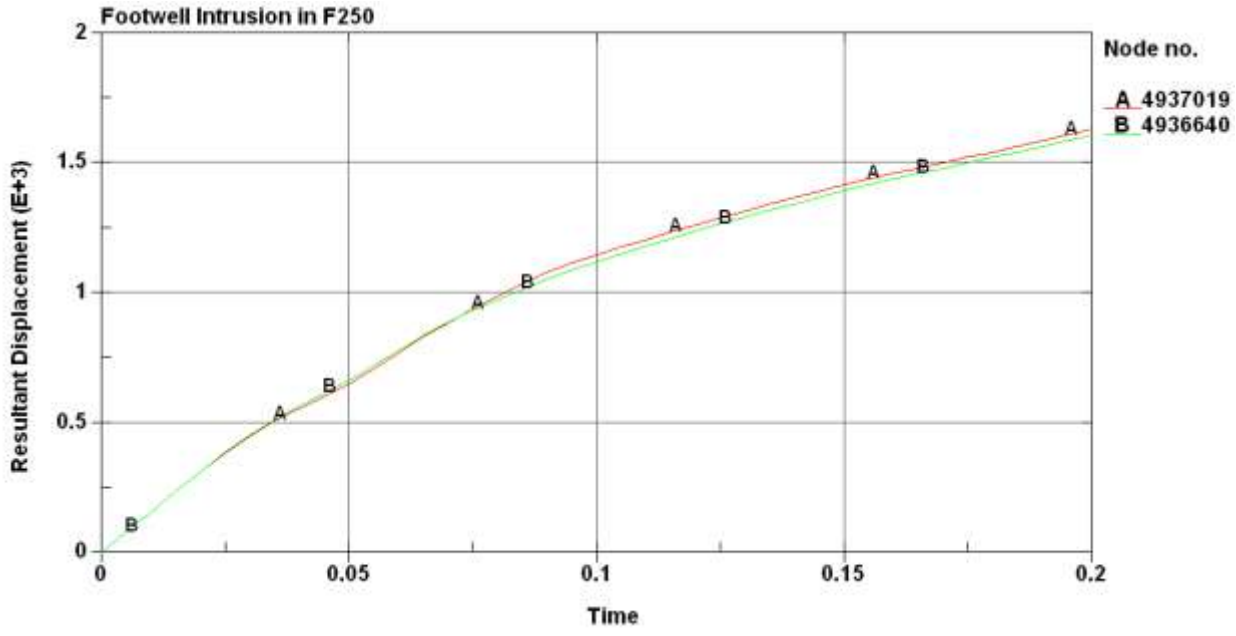

Figure 5.52: Maximum intrusion in foot-well of F250 in CASE-IV

Driver side A-Pillar Intrusion in F250:

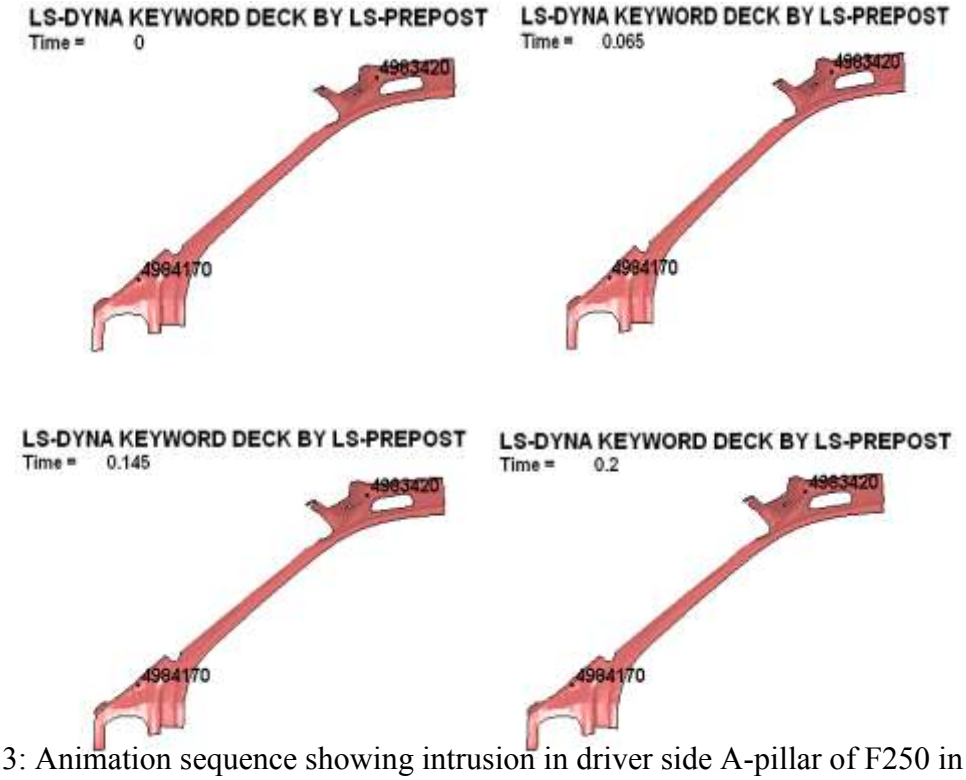

Figure 5.53: Animation sequence showing intrusion in driver side A-pillar of F250 in CASE-IV

From Figure 5.53 the node which had maximum rearward movement on the A-pillar of the F250 is Node #4984170, the maximum displacement of this node is 13 mm and the Figure 5.54 shows the displacement of the node with respect to time.

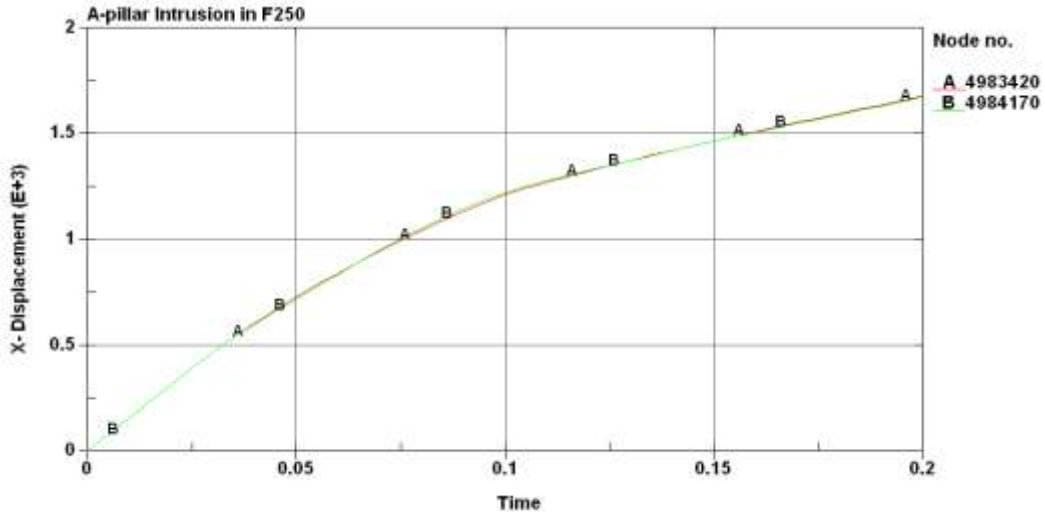

Figure 5.54: Maximum intrusion in driver side A-pillar of F250 in CASE-IV

Firewall Intrusion in Dodge Neon:

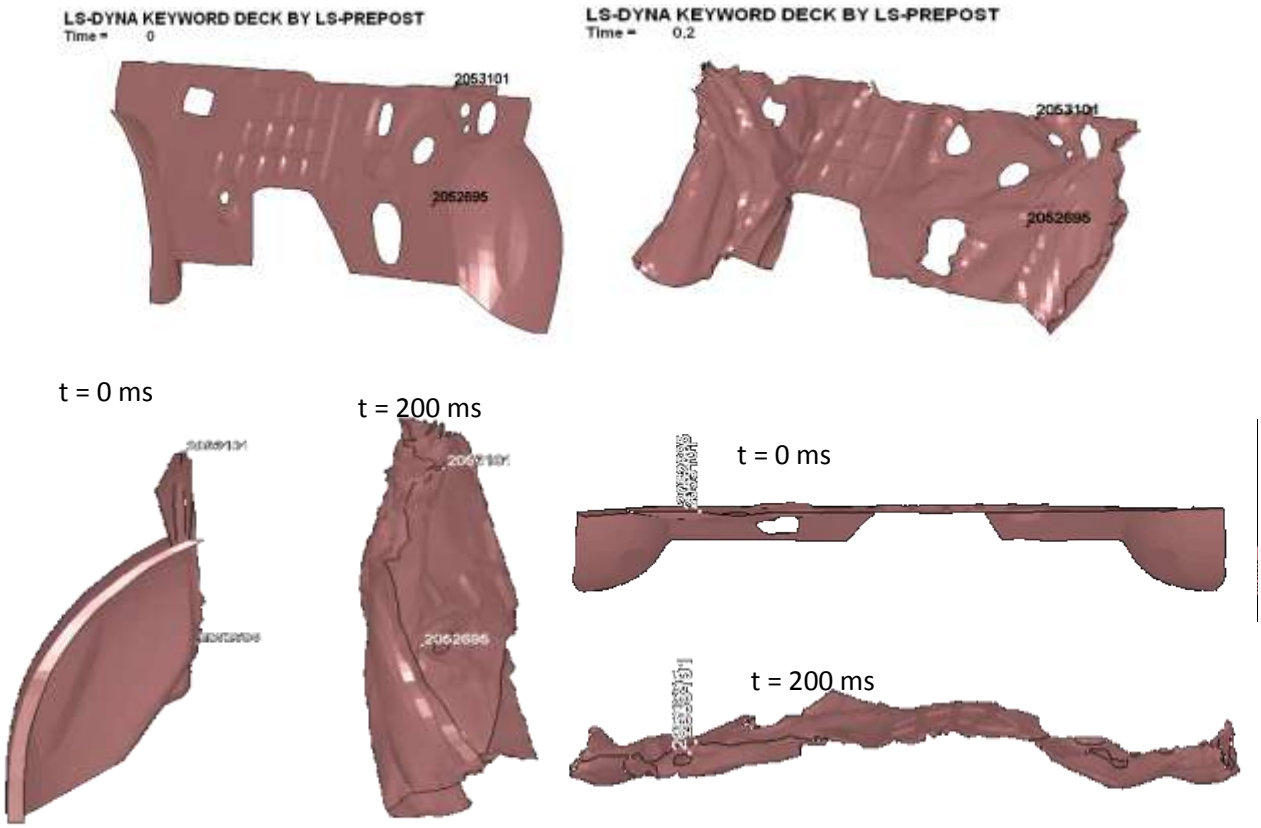

Figure 5.55: Animation sequence showing intrusion in firewall of Neon in CASE-IV

From the Figure 5.55 the maximum intrusion in the firewall of the Dodge Neon occurs approximately at node # 2052695, the maximum displacement of this node is 152 mm, as is shown in the Figure 5.56.

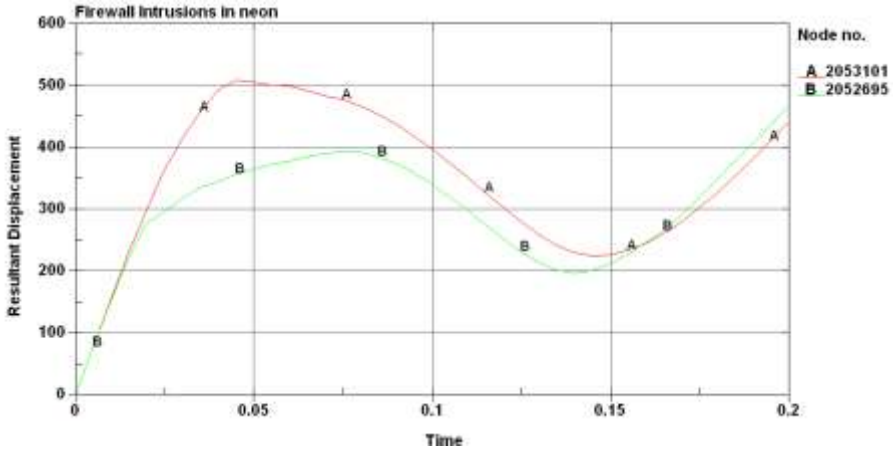

Figure 5.56: Maximum intrusion in firewall of Neon in CASE-IV

Foot-well Intrusion in Neon:

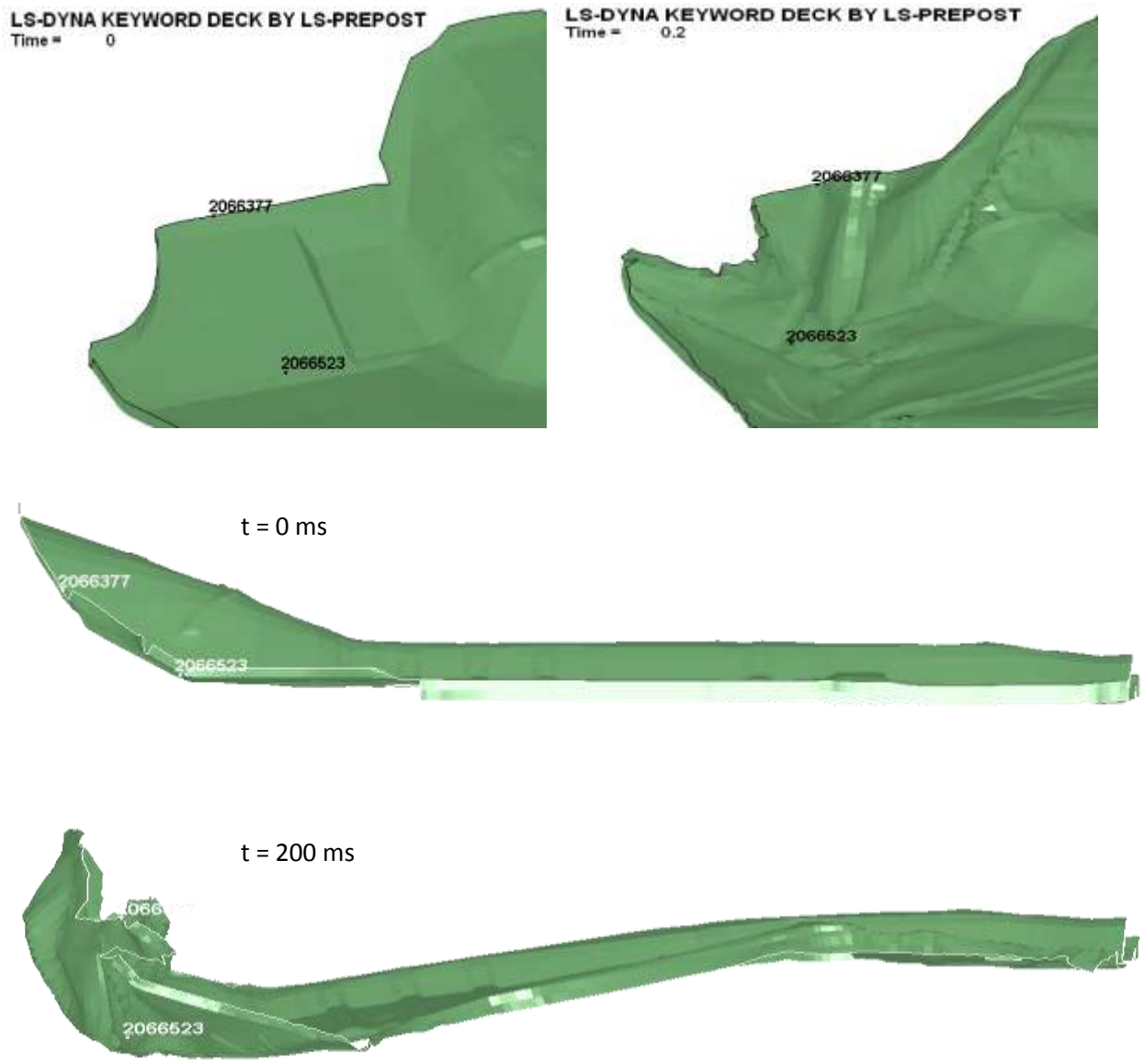

Figure 5.57: Animation sequence showing intrusion in foot-well of Neon in CASE-IV

From the Figure 5.57, the maximum intrusion in the Foot-well of the Dodge Neon occurs approximately at node # 2066523, the maximum displacement of this node is 146 mm, as is shown in the Figure 5.58.

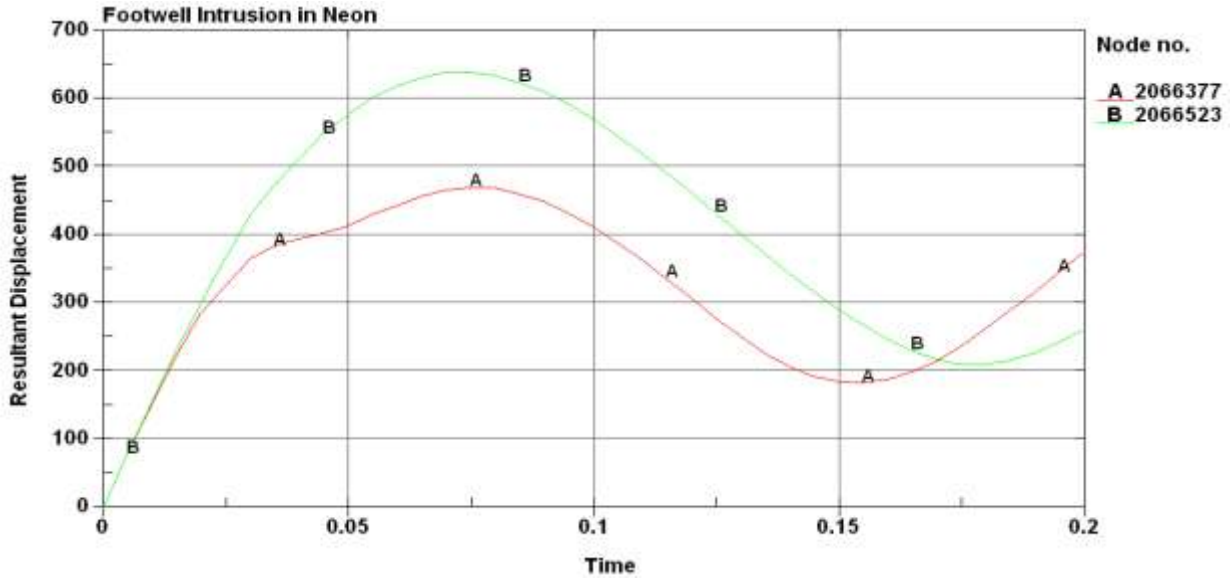

Figure 5.58: Maximum intrusion in foot-well of Neon in CASE-IV

Driver side A-Pillar Intrusion in Dodge Neon:

The Figure 5.59 shows the movement of A-pillar during the collision with a compact pickup.

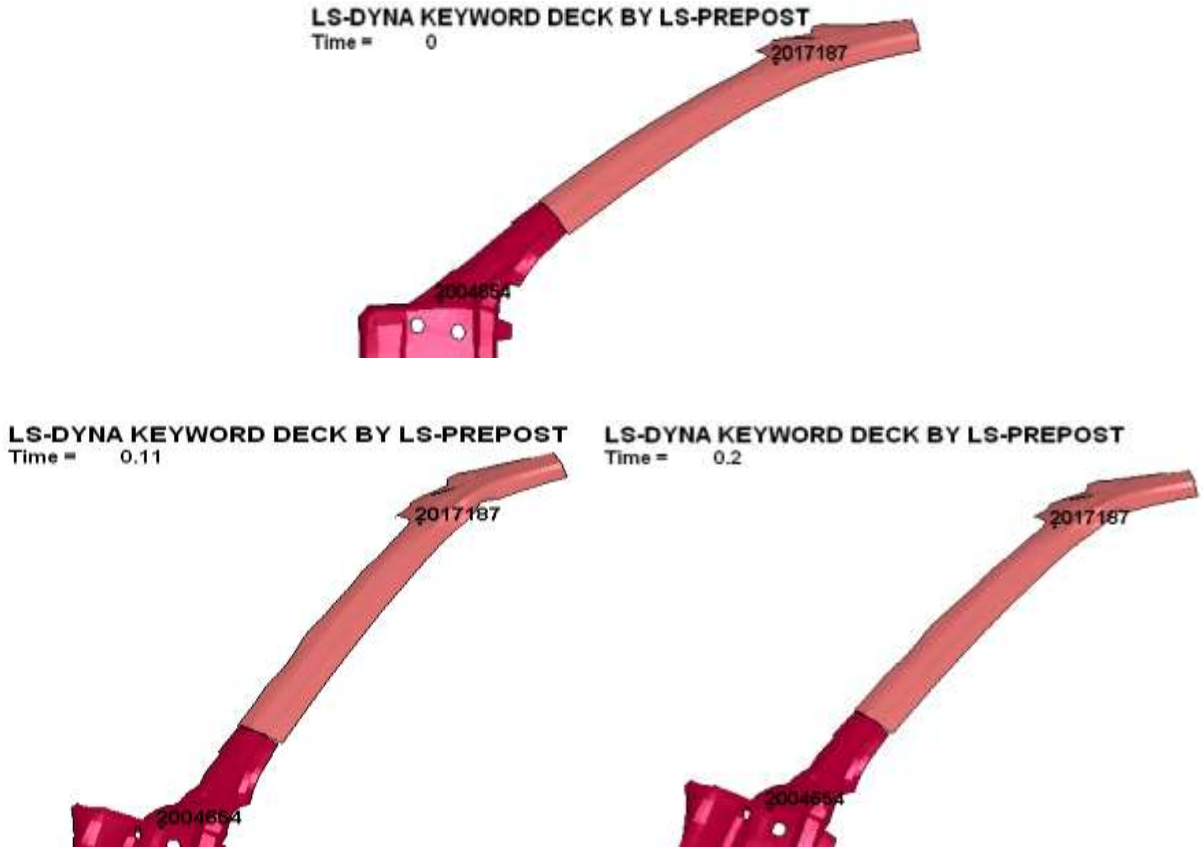

Figure 5.59: Animation sequence showing intrusion in driver side A-pillar of Neon in CASE-IV

The node which had maximum rearward movement on the A-pillar of the Dodge Neon is node #2004654, the maximum displacement of this node is found to be 156mm. Figure 5.60 shows the displacement of the node with respect to time.

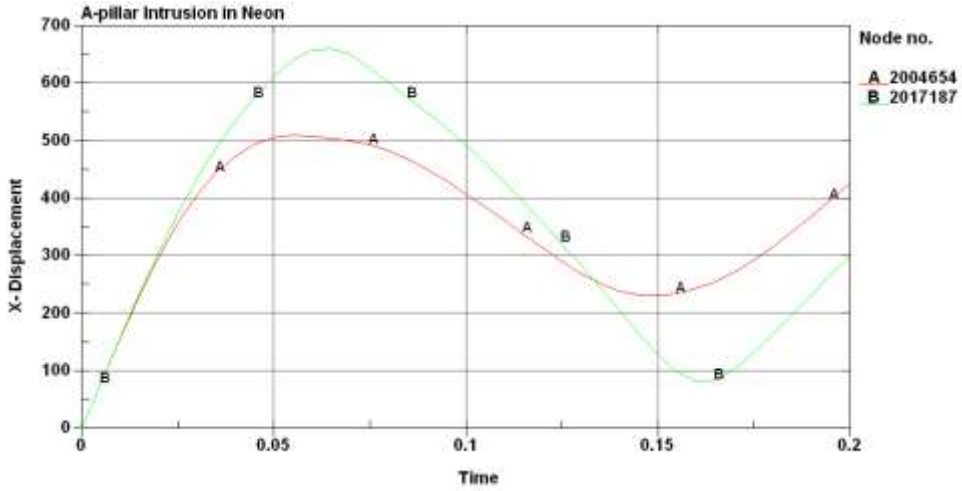

Figure 5.60: Maximum intrusion in driver side A-pillar of Neon in CASE-IV

Figure 5.61 shows the acceleration in the left and right seat acceleration in the Dodge Neon and Ford F250, the figure also shows the peak accelerations in the two vehicles.

LEFT and RIGHT Seat Acceleration:

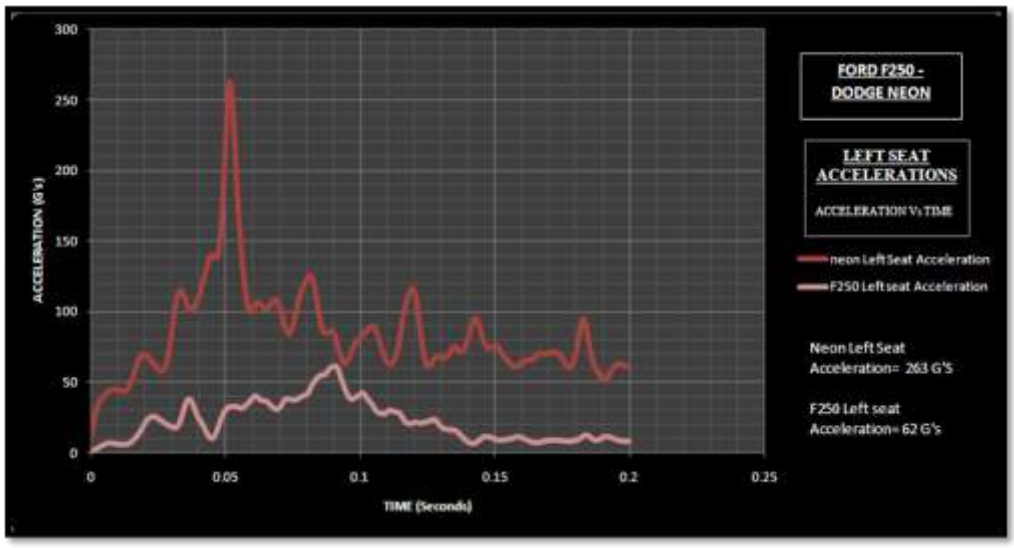

Figure 5.61 (a): Left seat acceleration in CASE-IV

Figure 5.61: Left and Right seat acceleration in CASE-IV
(a) Left seat (b) Right seat

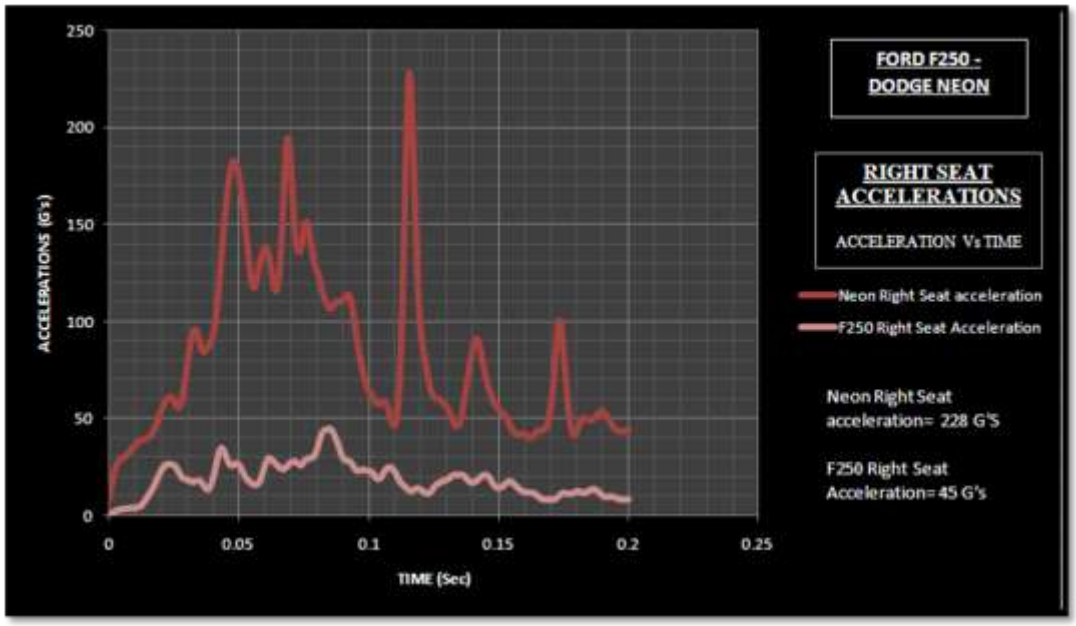

Figure 5.61 (b): Right seat acceleration in CASE-IV

5.4.3 Discussion

In the above crash scenario of Ford F250 (representing a full size pick-up) and Dodge Neon (representing a passenger car), the weight of F250 is 3066Kgs whereas weight of Neon is 1333 Kgs, that is F250 weighs twice more than the passenger car. This huge difference between two vehicles will lead to high mass incompatibility and consecutively lead to higher intrusions in the passenger car compared to full size pick-up. The ride height of Ford F250 is approximately around 465mm and ride height of Neon is approximately 200mm, the difference in ride height is 265mm which is very high. This high difference in ride height results in the under ride of the passenger car into the full size pick-up. Which will completely collapses the occupant compartment of the passenger car and in turn results in fatal injuries to the occupants where the chances of survival for the occupants in the passenger car are very little, this situation is considered as high geometric incompatibility. Since the Ford F250 is very bigger vehicle than the Dodge Neon, the stiffness of the F250 will be higher than the Neon leading to stiffness

incompatibility. Because of this high stiffness in F250, it will force Neon to absorb bulk of the crash energy developed during the collision. These three incompatibilities will result in fatal injuries to the occupants in the passenger car. The Table 5.9 shows the maximum intrusions measured at the crucial location like firewall, foot-well and driver side A-pillar which can lead to fatal injuries to occupants. The left and right seat accelerations are also measured and tabulated. The Table 5.9 also shows the weight ratio, firewall intrusion ratio, foot-well intrusion ratio, A-pillar intrusion ratio, left and right seat acceleration ratios. The weight ratio is way off from the DFR ratio and the firewall, driver side A-pillar intrusion ratio's is also different from the DFR ratio because the passenger car under rides into the pick-up. The left and right seat acceleration is different from the statistical DFR ratio due to the stiffness incompatibility.

Summary of CASE- IV:

Table 5.9: Summary of CASE-IV

	F250	Neon
Firewall Intrusion (mm)	116	152
Foot well Intrusion (mm)	23	146
A-pillar Intrusion (mm)	13	156
Left seat Acceleration (G's)	62	263
Right seat Acceleration (G's)	45	228

Ford F250 : Dodge Neon	Ratio
Ratio of Firewall Intrusion	1: 1.3
Ratio of Foot well Intrusion	1: 6.3
Ratio of A-pillar Intrusion	1: 12
Ratio of Left seat Acceleration	1: 4.3
Ratio of Right seat Acceleration	1: 5.1

5.5 CASE – V: Full Size Van (Ford Ecoline) Vs Passenger Car (Dodge Neon)

5.5.1 Model Description

Dodge Neon: Described in Case I.

Ford Ecoline:

The FE model of Ford Ecoline is developed by National Crash Analysis Center for all impacts modes based on a 1998 model Ecoline. This model can be used for research work in all impact modes. The model is described detailed way in all sides of the vehicle making it useful in all impact scenarios. Figure 5.62 shows the FE Model of the Ford Ecoline used to represent the Full-size van category [22].

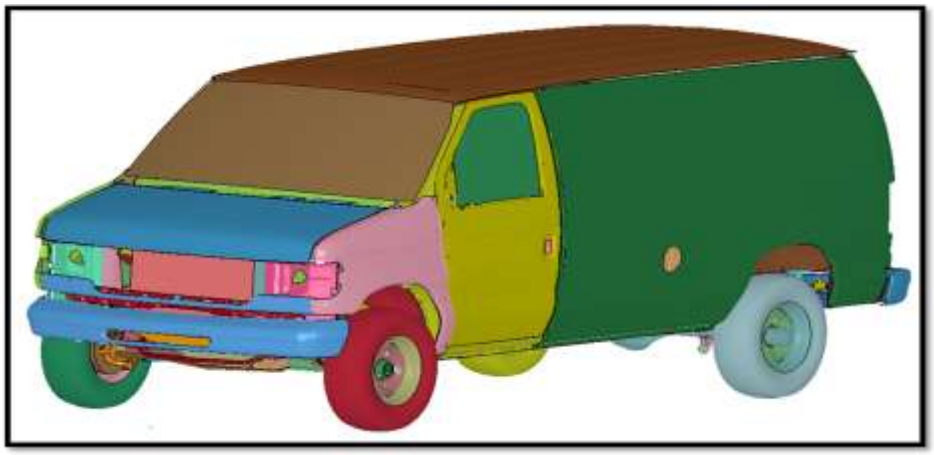

Figure 5.62: FE model of Ford Ecoline

The vehicle FE model has 438 parts; each part of the model depicts different parts of the original vehicle. The material properties of different parts are derived from the coupon testing. Different materials used in this FE model are LOW_DENSITY_FOAM, DAMPER VISCOUS, ELASTIC, PIECEWISE LINEAR PLASTICITY, SPRING_ELASTIC and MODIFIED_ PIECEWISE LINEAR PLASTICITY. There are 300066 elements in the FE model out of which 2 are beam elements, 6 are discrete elements, 278523 are shell elements, 15952 are solid elements. Different parts of the vehicle are constrained by twenty eight revolute joints, twenty eight spherical joints, four universal joints and four thousand six hundred and twenty eight spot

welds. The FE Model is validates the Ford Ecoline NCAP test results and the vehicle is stable at 25, 30, 35, 40 mph. The accelerations of the vehicle and the wall force exerted by this vehicle are comparable to NCAP test results. The Table 5.10 shows the summary of the FE Model.

Table 5.10: FE model summary of Ford Ecoline

Number of Parts	438
Number of Nodes	295555
Number of Solids	15952
Number of Beams	2
Number of Mass Elements	90
Number of Springs	6
Number of Shells	278535
Number of Elements	300066

5.5.2 Crash Simulation

Two vehicles are positioned such that they have full width interaction during collision and the vehicles are placed as close as possible to reduce the computational time. The contact between two vehicles is defined by using "Automatic Surface to surface "card. Static and dynamic friction coefficients are given as 0.3 between the contacts of two vehicles. Rigid wall planar cards are used between the contact of all tires and roads. Initial velocity of 35 mph is given to both vehicles and the simulation termination time of 200 milliseconds is given with a time step of 10 milliseconds. The total computational time for simulation this crash scenario is almost 60 hours. Figure 5.63 shows the results of crash simulation between the two vehicles at different times.

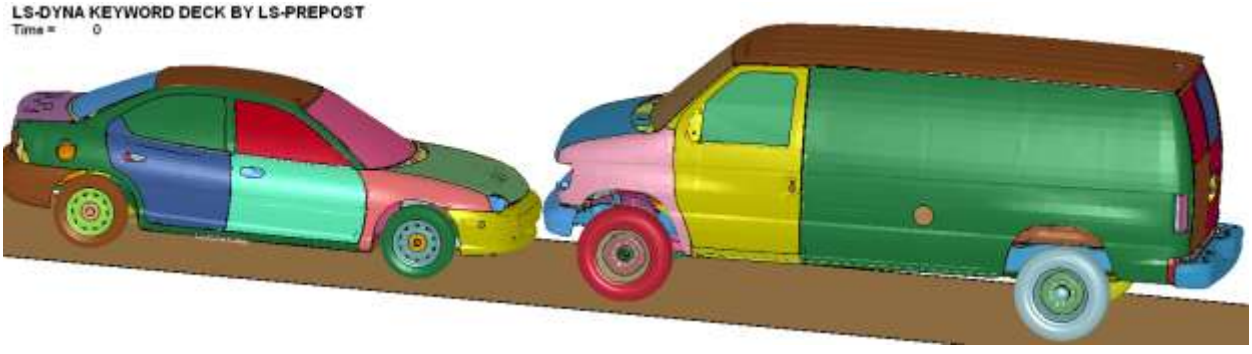

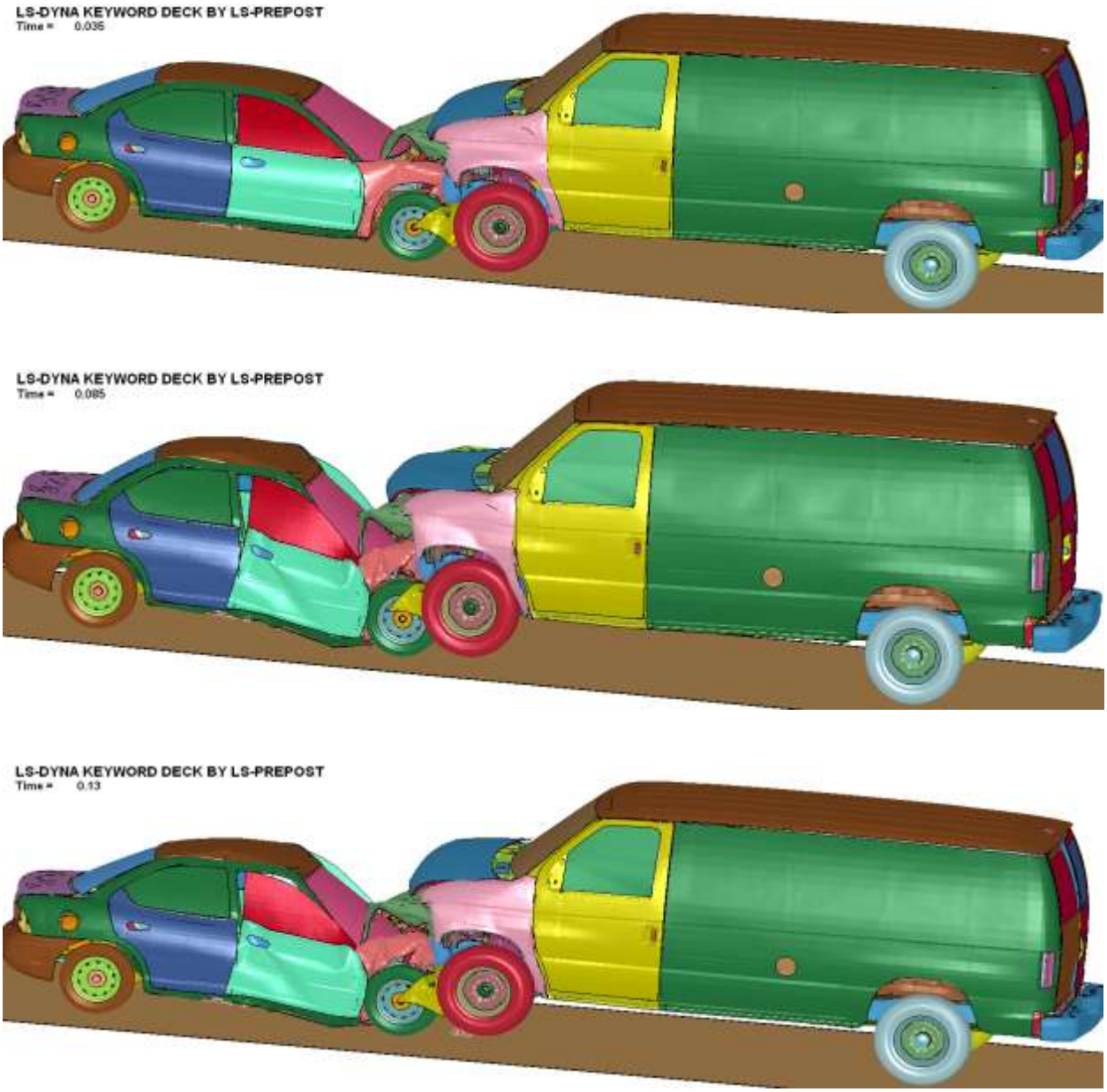

Figure 5.63: Animation of Chevy Ecoline crashing against Dodge Neon

The two vehicles are placed as close as possible to each other to reduce calculation time. The maximum crush between the vehicles happened at 80ms, after which the two vehicle started to come apart. After reaching the maximum crush stage, firewall, driver side A-pillar, foot-well intrusions and accelerations of left and right seat are measured. The Figure 5.64 below shows the intrusions in the firewall of Ecoline.

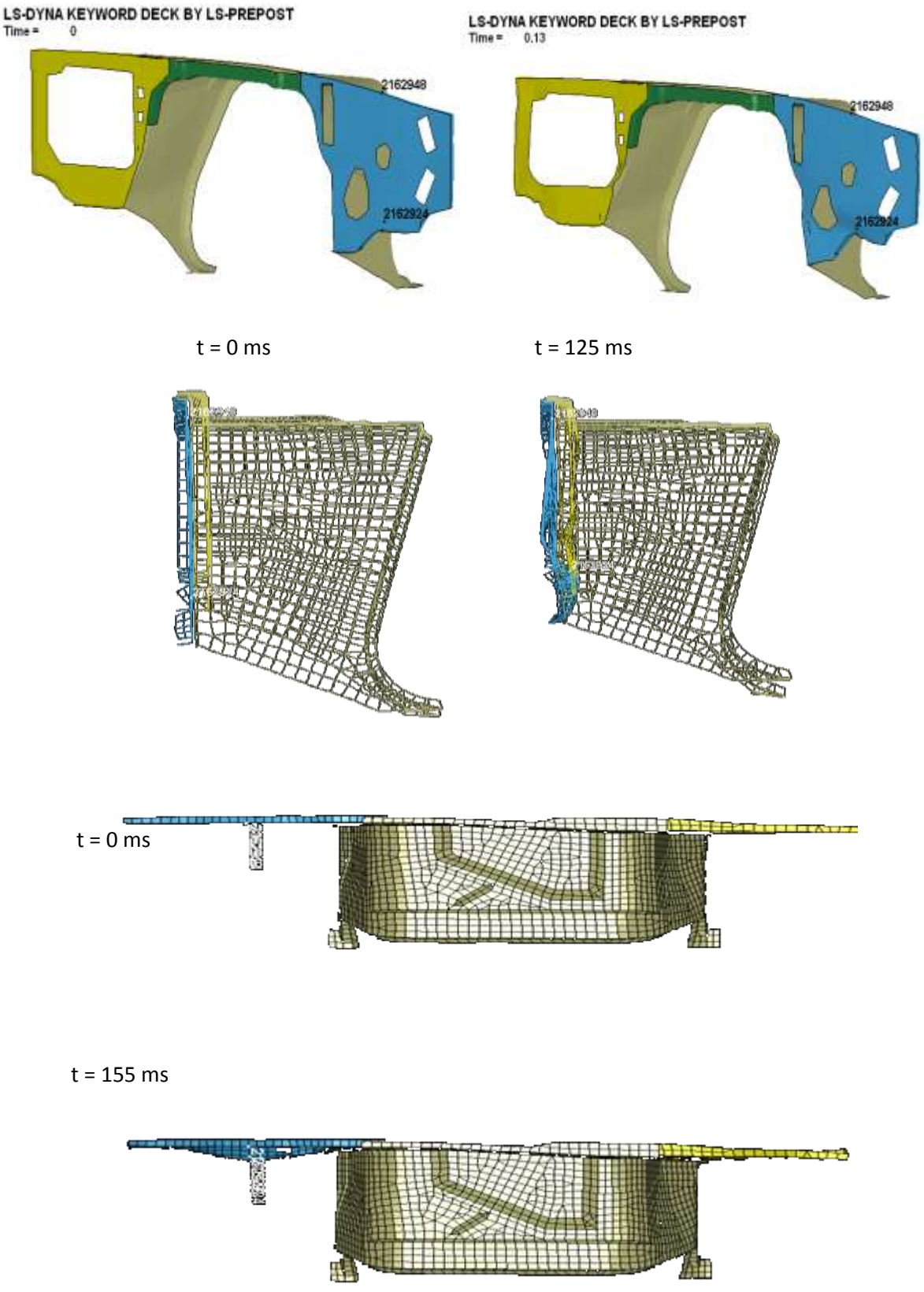

Figure 5.64: Animation sequence showing intrusion in firewall of Ecoline in CASE-V

From Figure 5.64, it is evident that the maximum intrusion occurs approximately at node 2162924. The resultant displacement of the maximum intruded node is shown in the graph below. From the Figure 5.65, maximum intrusion in the firewall of Ecoline in collision with a passenger car is measured as 25 mm.

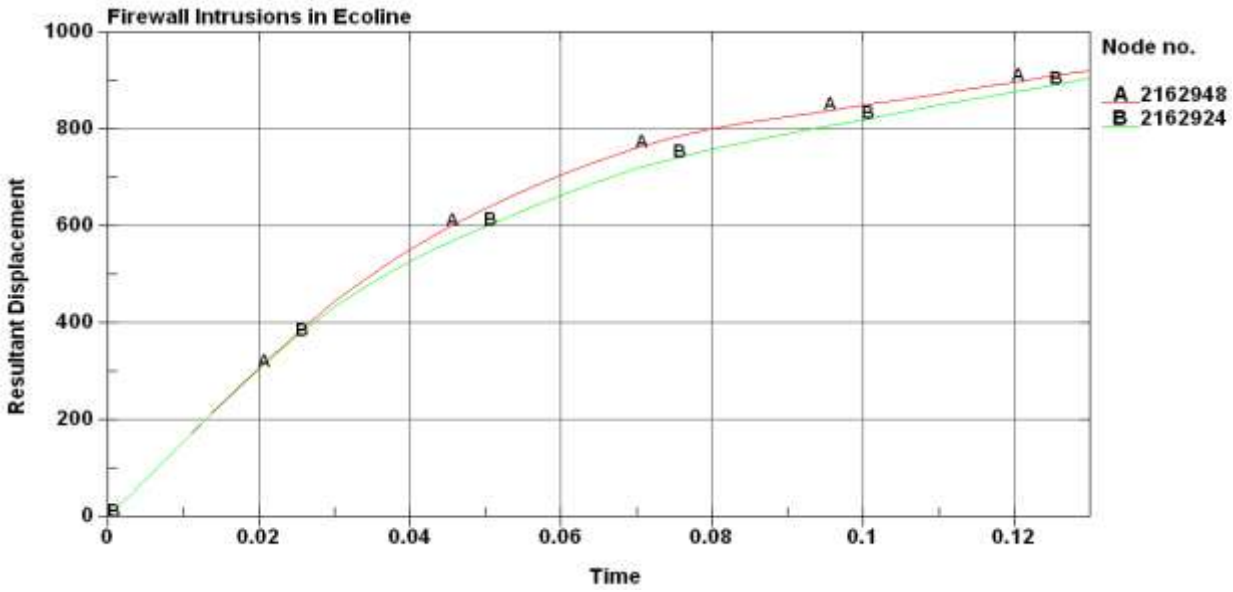

Figure 5.65 Maximum intrusions in firewall of Ecoline in CASE-V

Foot-well Intrusion in Ecoline:

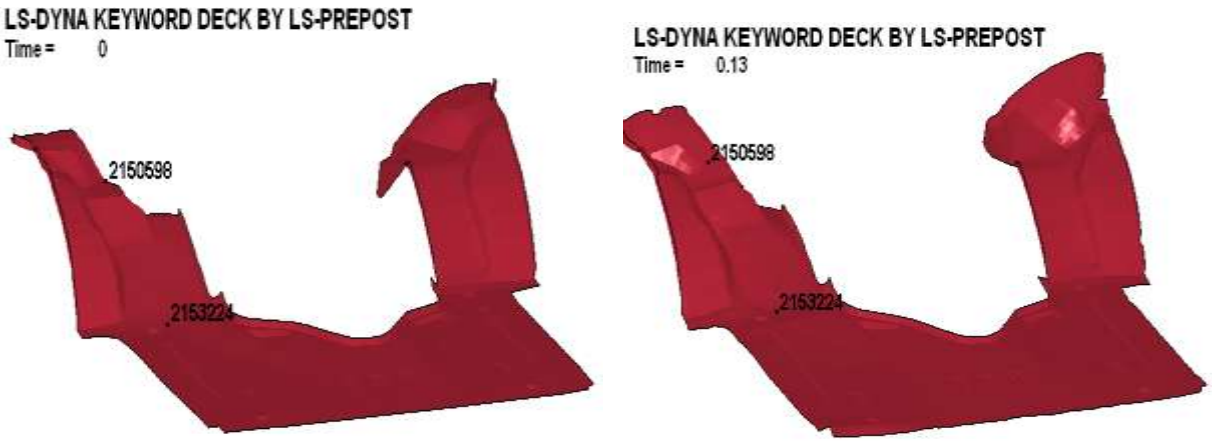

(a): Intrusions in foot-well of Ecoline in CASE-V (isometric view)

Figure 5.66: Animation sequence showing intrusion in foot-well of Ecoline in CASE-V (a) isometric view (b) side view

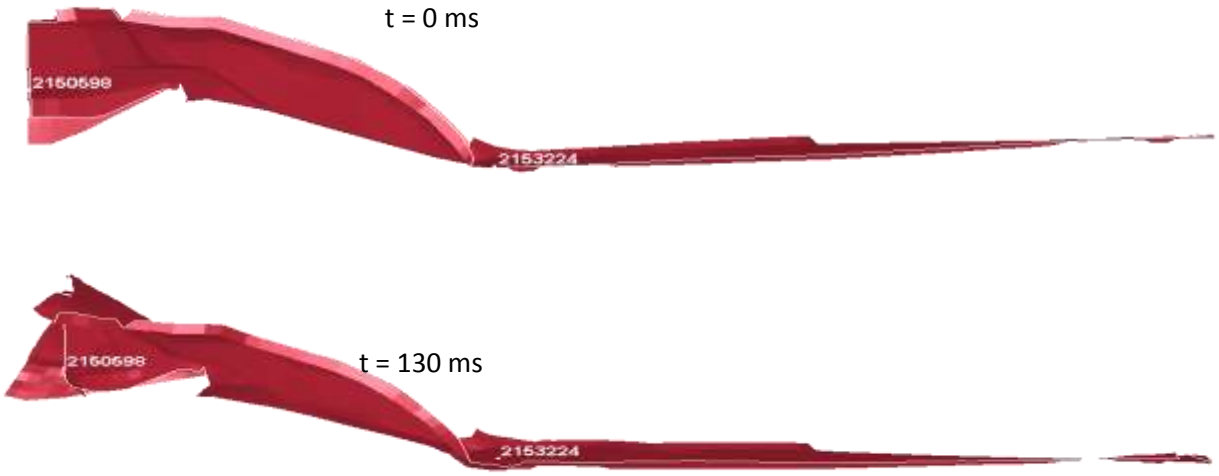

(b): Intrusions in foot-well of Ecoline in CASE-V (side view)

The maximum intrusion in the foot-well of Ecoline occurs at node 2150598. The resultant displacement of this maximum intruded node is shown in the Figure 5.67. From Figure 5.67, the maximum intrusion in the Foot-well of Ecoline in collision with a passenger car is found to be31mm.

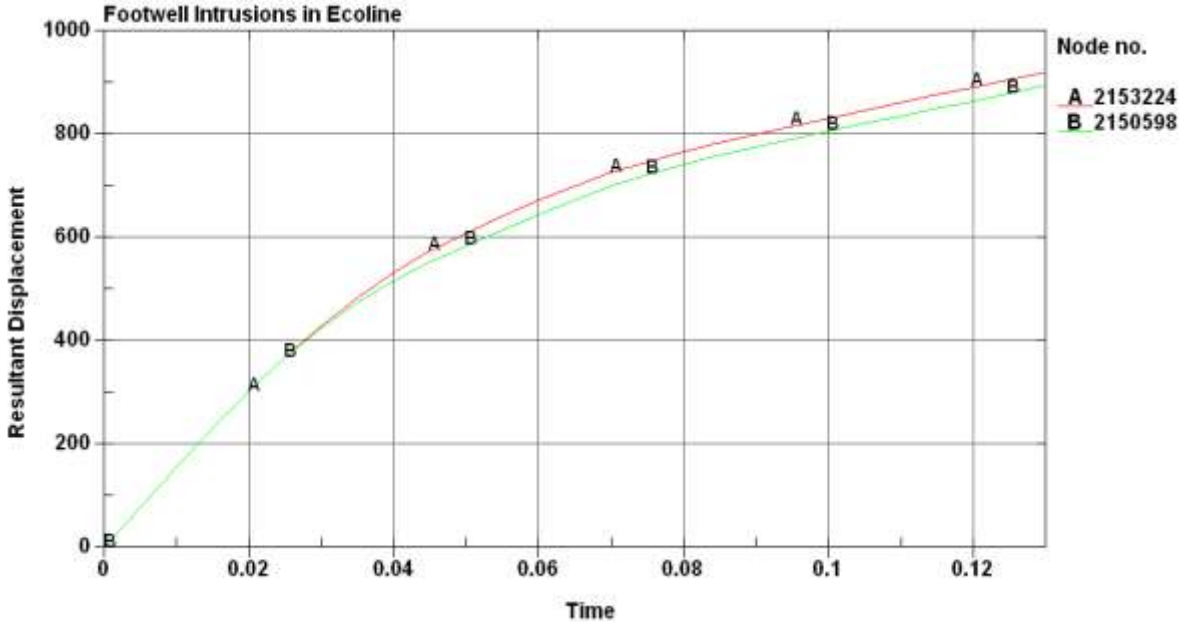

Figure 5.67: Maximum intrusion in foot-well of Ecoline in CASE-V

Driver Side A-pillar Intrusion in Ecoline:

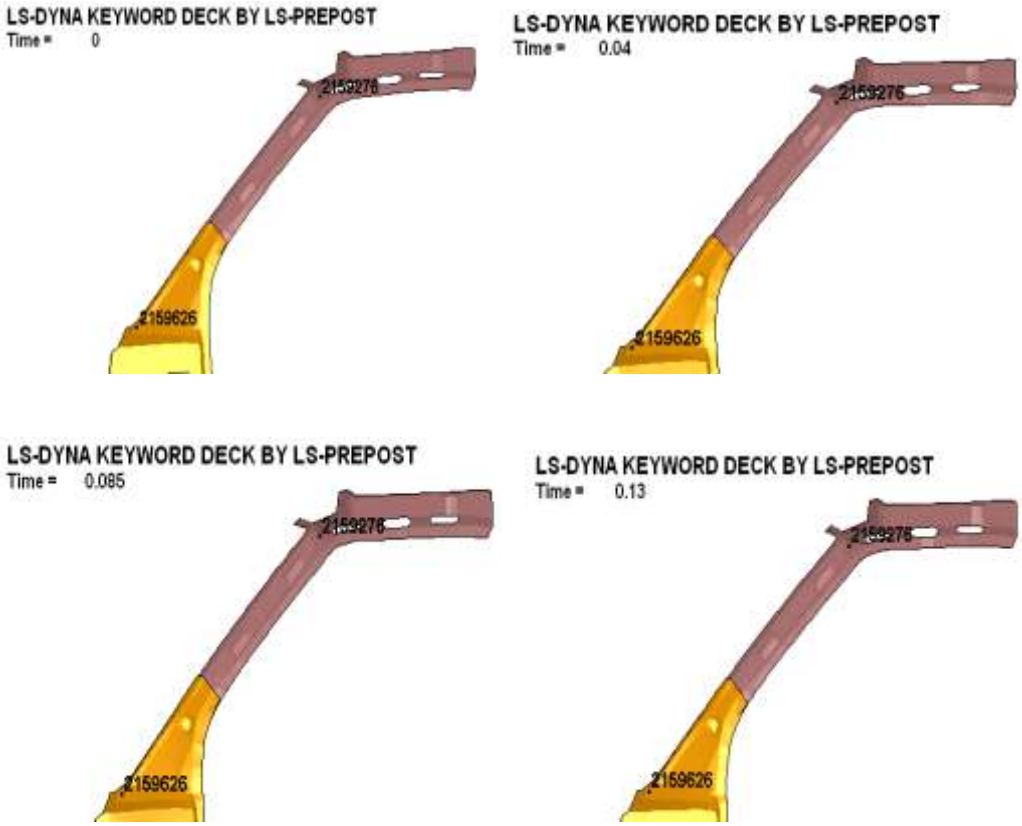

Figure 5.68: Animation sequence showing intrusion in driver side A-pillar of Ecoline in CASE-V

From Figure 5.68, the node which had maximum rearward movement on the A-pillar of the Ecoline is Node #2159626, the maximum displacement of this node is 13 mm. Figure 5.69 shows the displacement of the node with respect to time.

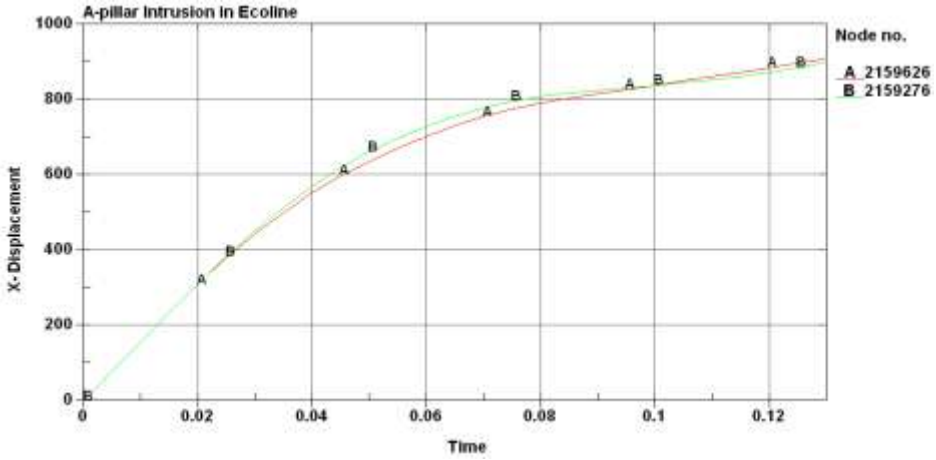

Figure 5.69: Maximum intrusion in driver side A-pillar of Ecoline in CASE-V

Firewall Intrusion in Dodge Neon:

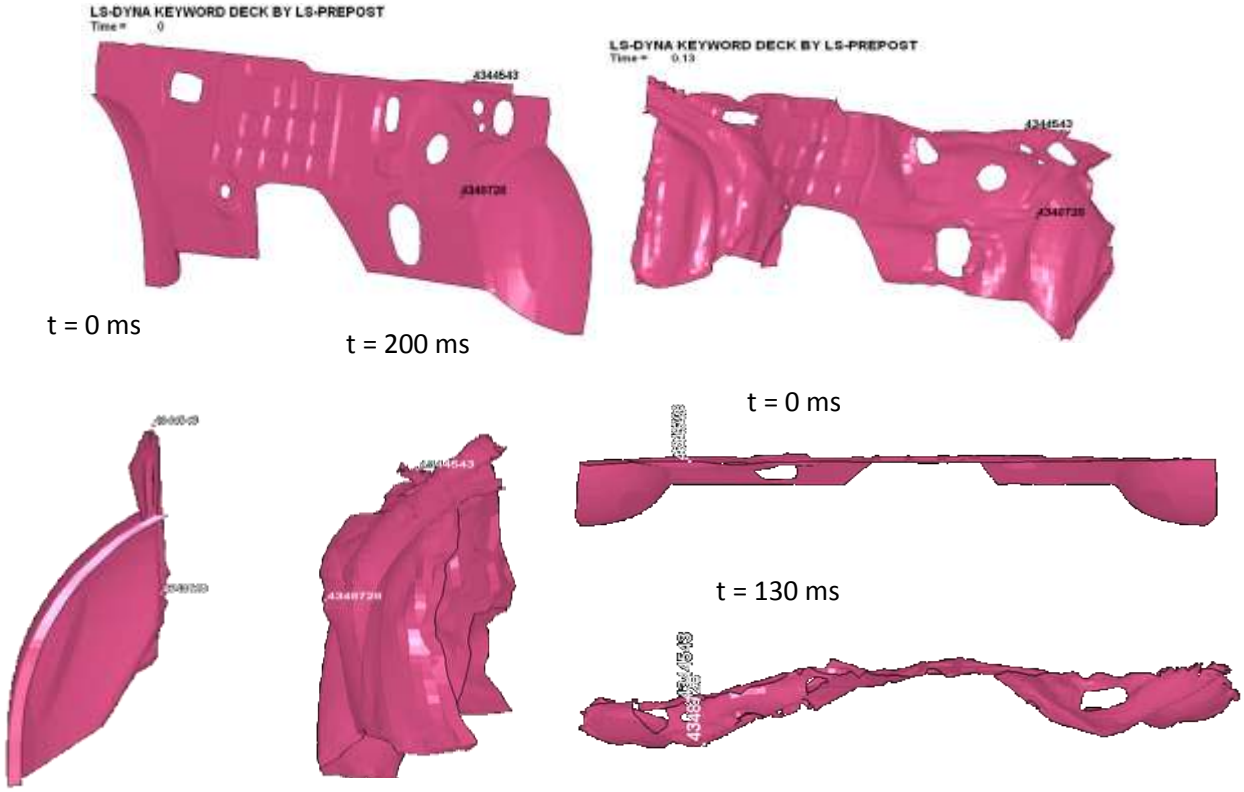

Figure 5.70: Animation sequence showing intrusion in firewall of Neon in CASE-V

From the Figure 5.70 the maximum intrusion in the firewall of the Dodge Neon occurs approximately at Node # 4348728, the maximum displacement of this node is 152 mm, as is shown in the Figure 5.71.

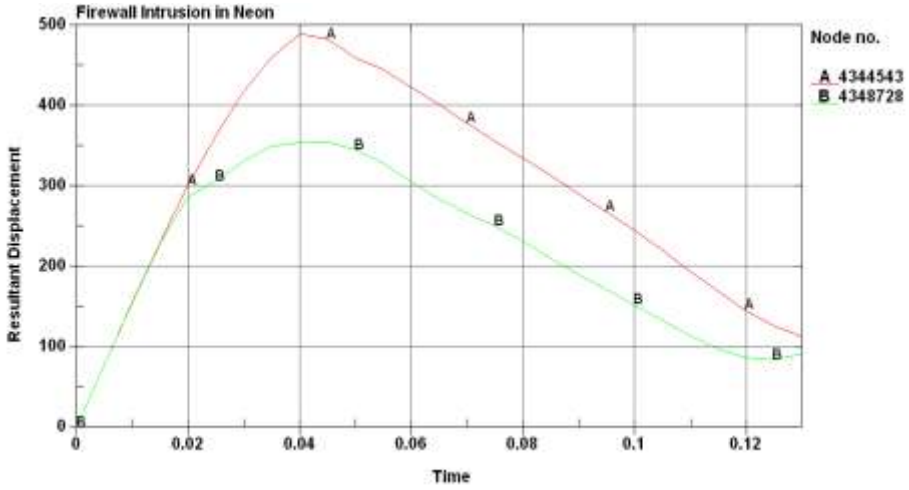

Figure 5.71: Maximum intrusion in firewall of Neon in CASE-V

Foot-well Intrusion in Neon:

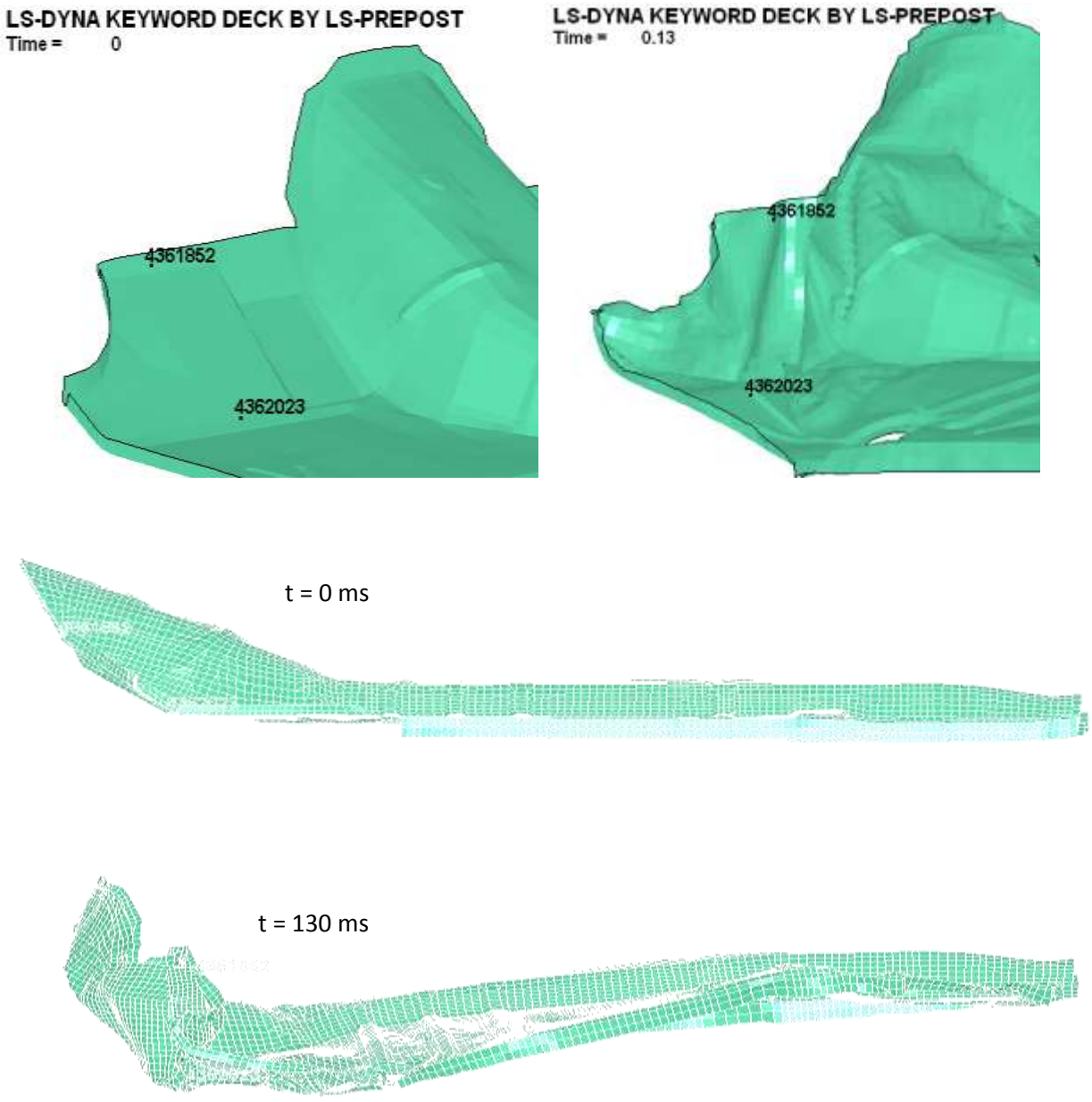

Figure 5.72: Animation sequence showing intrusion in foot-well of Neon in CASE-V

From Figure 5.72, the maximum intrusion in the foot-well of the Dodge Neon occurs approximately at node # 4361852, the maximum displacement of this node is 152 mm, as is shown in the Figure 5.73.

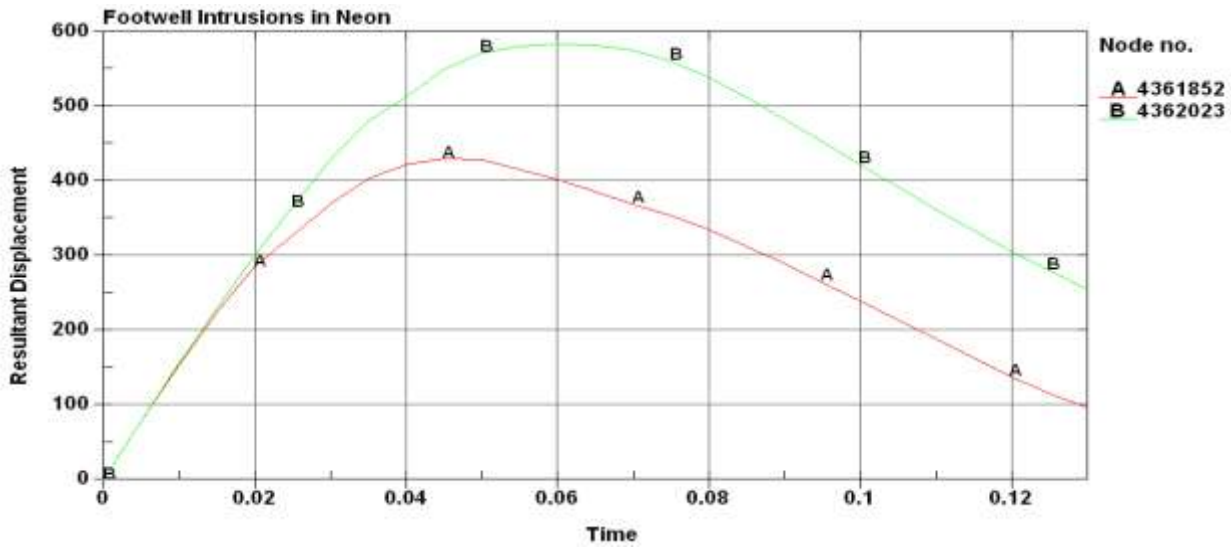

Figure 5.73: Maximum intrusion in foot-well of Neon in CASE-V

Driver side A-Pillar Intrusion in Dodge Neon:

The Figure 5.74 shows the movement of A-pillar during the collision with a full-size van.

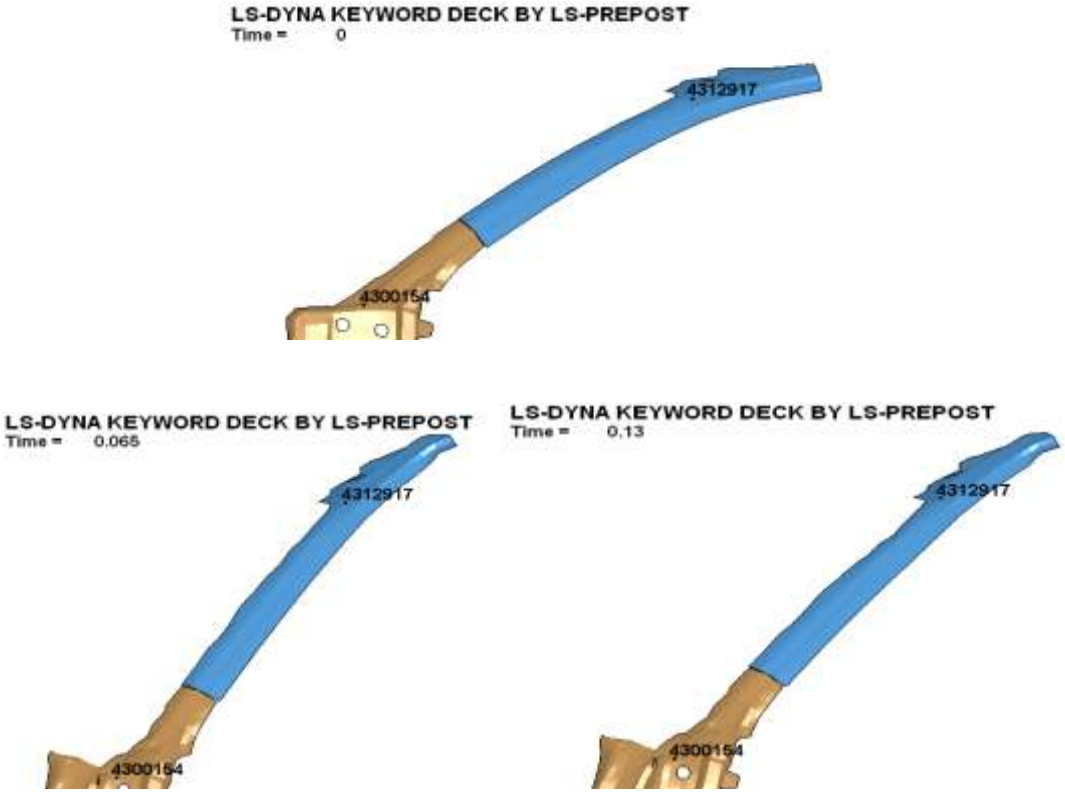

Figure 5.74: Animation sequence showing intrusion in driver side A-pillar of Neon in CASE-V

The node which had maximum rearward movement on the A-pillar of the Dodge Neon is node # 4300154, the maximum displacement of this node is found to be 141mm. Figure 5.75 shows the displacement of the node with respect to time.

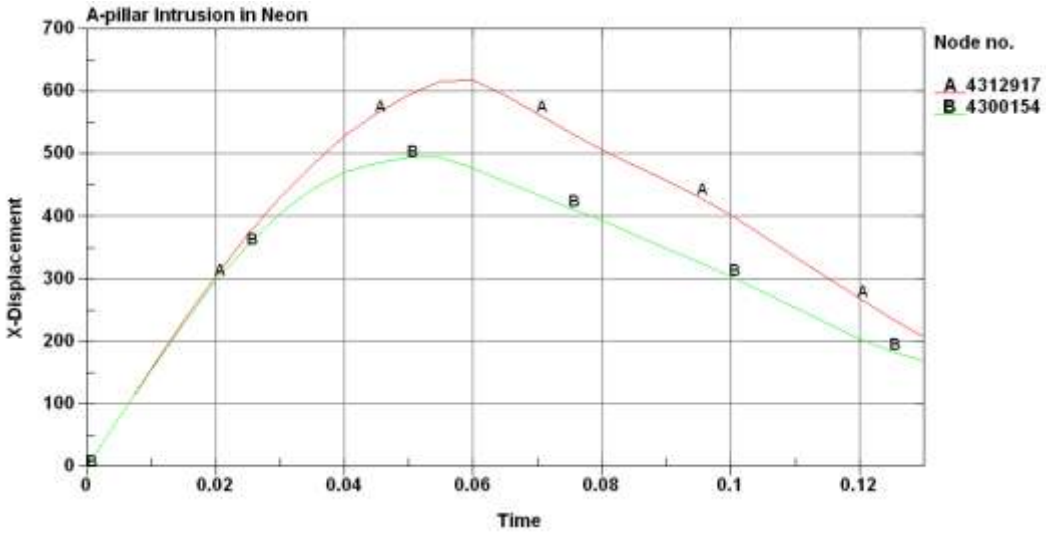

Figure 5.75: Maximum intrusion in driver side A-pillar of Neon in CASE-V

LEFT and RIGHT Seat Acceleration:

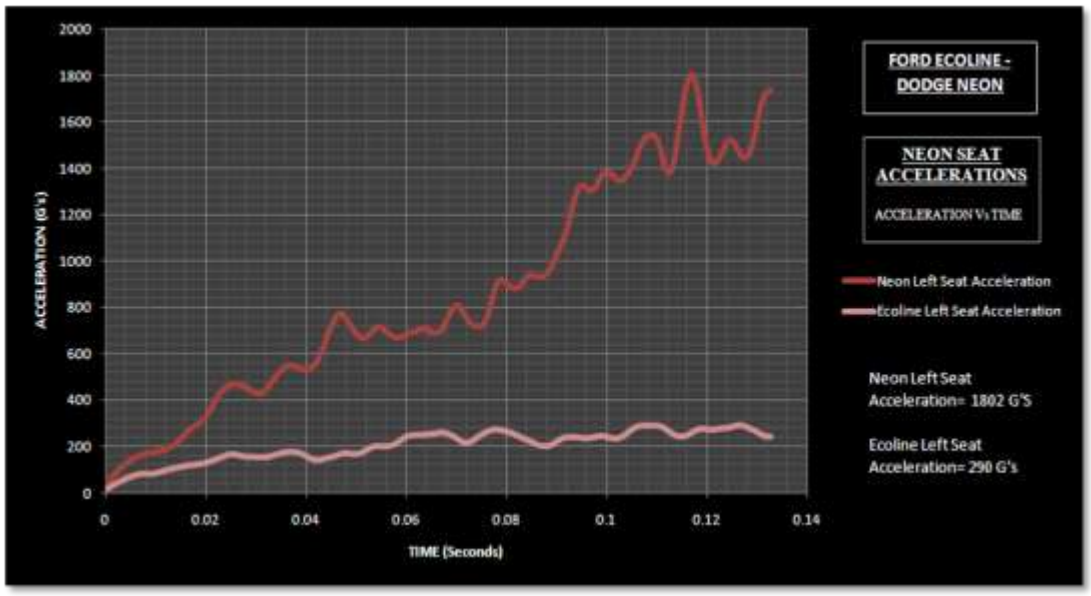

(a): Left seat acceleration in CASE-V

Figure 5.76: Left and Right seat acceleration in CASE-V

(a) Left seat (b) Right seat

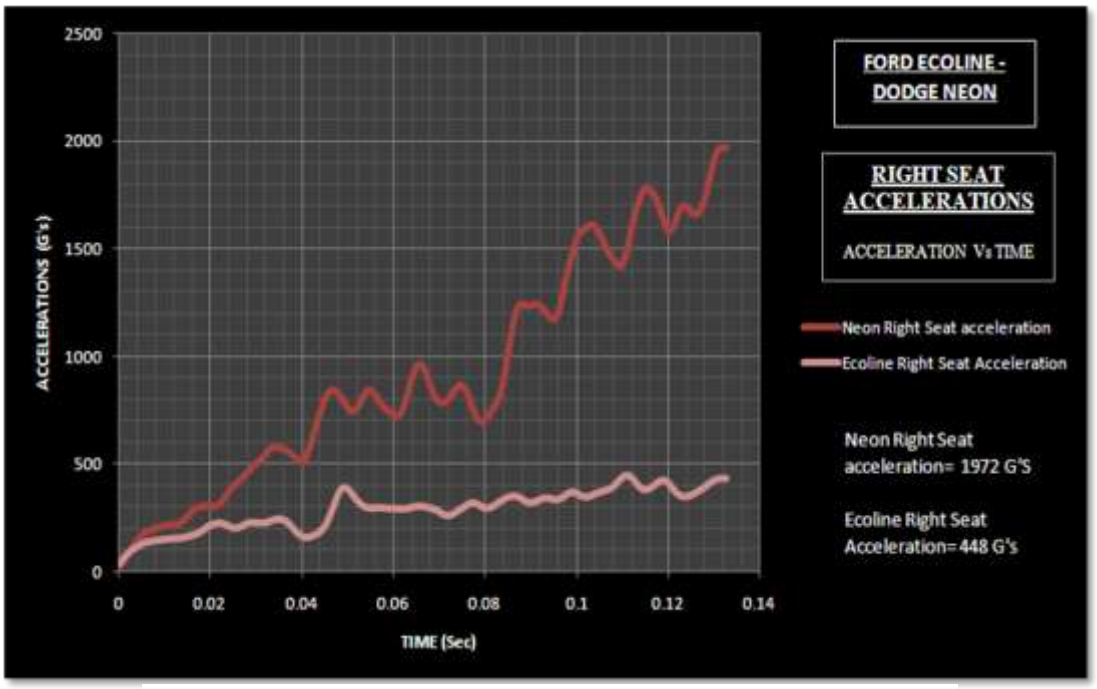

(b): Right seat acceleration in CASE-V

5.5.3 Discussion

In the above crash scenario of Ford Ecoline (representing a full-size van) and Dodge Neon (representing a passenger car), the weight of Ecoline is 2133Kgs, whereas weight of Neon is 1333 Kgs. This difference in weight between the two vehicles will lead to mass incompatibility between them which in turn cause high intrusions in the passenger car than the Full size van. The ride height of Ford Ecoline is approximately 500mm whereas the ride height of Neon is approximately 200mm. This huge difference in the ride height of about 300mm will definitely lead to under-ride of the smaller car into the full size van initially. But as the collision continues two vehicles will move apart from each other because the weigh difference between two vehicles is not very high or the weight of the Ecoline is not high enough to crush Neon under it when Neon under-rides initially. This situation will lead to high fatal injuries to the occupants of passenger car but may not lead to complete collapse of occupant compartment as in above

case IV. Since the Ford Ecoline is bigger vehicle than the Dodge Neon the stiffness of the Ecoline will be high than the Neon leading to stiffness incompatibility. Due to high stiffness of Ecoline, it will force Neon to absorb bulk of the crash energy developed during collision. These three incompatibilities will result in fatal injuries to the occupants in the passenger Car. The Table 5.11 shows the maximum intrusions measured at the locations like firewall, foot-well and driver side A-pillar which can lead to fatal injuries to occupants. The left and right seat accelerations are also measured and tabulated. The Table 5.11 also shows the weight ratio, firewall intrusion ratio, foot-well intrusion ratio, A-pillar intrusion ratio, left and right seat acceleration ratios. The weight ratio is way off from the DFR ratio and the left and right seat accelerations also different to DFR ratio of 1: 6.0. The firewall, foot-well and driver side A-pillar intrusion ratio's of 1: 6.1, 1: 6.0 and 1: 5.9 respectively correlates with DFR ratio of 1: 6.0.

Summary of CASE- V:

Table 5.11: Summary of CASE-V

	Ecoline	Neon
Firewall Intrusion (mm)	25	152
Foot well Intrusion (mm)	31	184
A-pillar Intrusion (mm)	24	141
Left seat Acceleration (G's)	290	1802
Right seat Acceleration (G's)	448	1972

Ford Ecoline : Dodge Neon	Ratio
Ratio of Firewall Intrusion	1: 6.1
Ratio of Foot well Intrusion	1: 6.0
Ratio of A-pillar Intrusion	1: 5.9
Ratio of Left seat Acceleration	1: 6.2
Ratio of Right seat Acceleration	1: 4.4

5.6 Comparative Discussion

Tables 5.12 through 5.14 show the values for the intrusions in mm, accelerations in G's and their ratios in all the five cases described previously. The values are used for comparison and validating the proposed new method of approach.

Table 5.12: Summary of intrusions measured from CASE-I to CASE-V

VEHICLE CATEGORY	FIREWALL		FOOTWELL		A-PILLAR	
Chevy s10-Dodge Neon	S 10	53	S 10	43	S 10	17
	Neon	130	Neon	104	Neon	44
Dodge Caravan-Dodge Neon	Caravan	234	Caravan	48	Caravan	30
	Neon	175	Neon	128	Neon	68
Ford Explorer-Dodge Neon	Explorer	53	Explorer	18	Explorer	31
	Neon	226	Neon	205	Neon	130
Ford F250-Dodge Neon	F 250	116	F 250	23	F 250	13
	Neon	152	Neon	146	Neon	156
Ford Ecoline-Dodge Neon	Ecoline	25	Ecoline	31	Ecoline	24
	Neon	152	Neon	184	Neon	141

Table 5.13: Accelerations measured from CASE-I to CASE-V

VEHICLE CATEGORY	VEHICLE	LEFT SEAT	RIGHT SEAT
Chevy s10-Dodge Neon	Neon	186	159
	S10	223	212
Dodge Caravan-Dodge Neon	Neon	319	236
	Caravan	126	100
Ford Explorer-Dodge Neon	Neon	578	384
	Explorer	37	54
Ford F250-Dodge Neon	Neon	263	228
	F250	62	45
Ford Ecoline-Dodge Neon	Neon	1802	1972
	Ecoline	290	448

Table 5.14: Comparison of objective measures with DFR

OBJECTIVE MEASURE									
VEHICLE CATEGORY	FATALITY RATIO	WEIGHT RATIO	INTRUSIONS				ACCELERATIONS		
			FIREWALL	FOOT-BOARD	A-PILLAR	AVER-AGE	LEFT SEAT	RIGHT SEAT	AVER-AGE
Chevy s10-Dodge Neon	1 : 2.6	0.8 : 1	1 : 2.5	1 : 2.4	1 : 2.5	1: 2.5	1.2 : 1	1.3 : 1	1.2 :1
Dodge Caravan-Dodge Neon	1 : 2.6	1.5 : 1	1.3 : 1	1 : 2.6	1 : 2.4	1: 2.5	1 : 2.5	1 : 2.4	1: 2.4
Ford Explorer-Dodge Neon	1 : 4.3	1.7 : 1	1 : 4.3	1 : 11	1 : 4.2	1: 4.2	1 : 15	1 : 7.0	1: 11
Ford F250-Dodge Neon	1 : 6.2	2.3 : 1	1 : 1.3	1 : 6.3	1 : 12	1: 6.3	1 : 4.3	1 : 5.1	1: 4.7
Ford Ecoline-Dodge Neon	1 : 6.0	1.6 : 1	1 : 6.1	1 : 6.0	1 : 5.9	1: 6.0	1 : 6.2	1 : 4.4	1: 5.3

The Figures 5.77 and 5.78 show the variation of intrusion ratio and acceleration ratio against the statistical Driver Fatality Ratio (DFR).

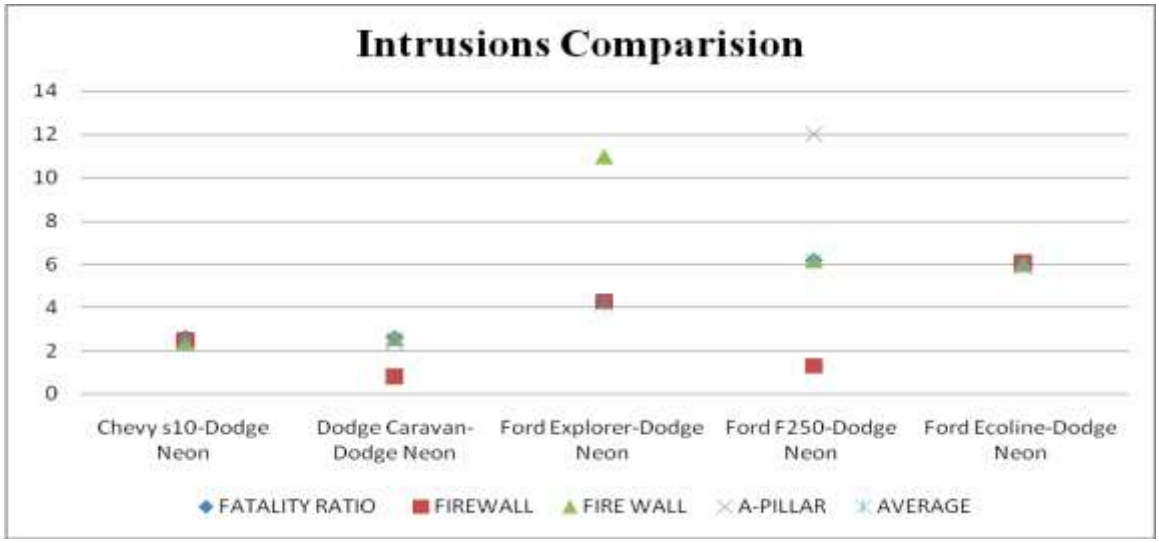

Figure 5.77: Comparison of intrusions ratios against DFR

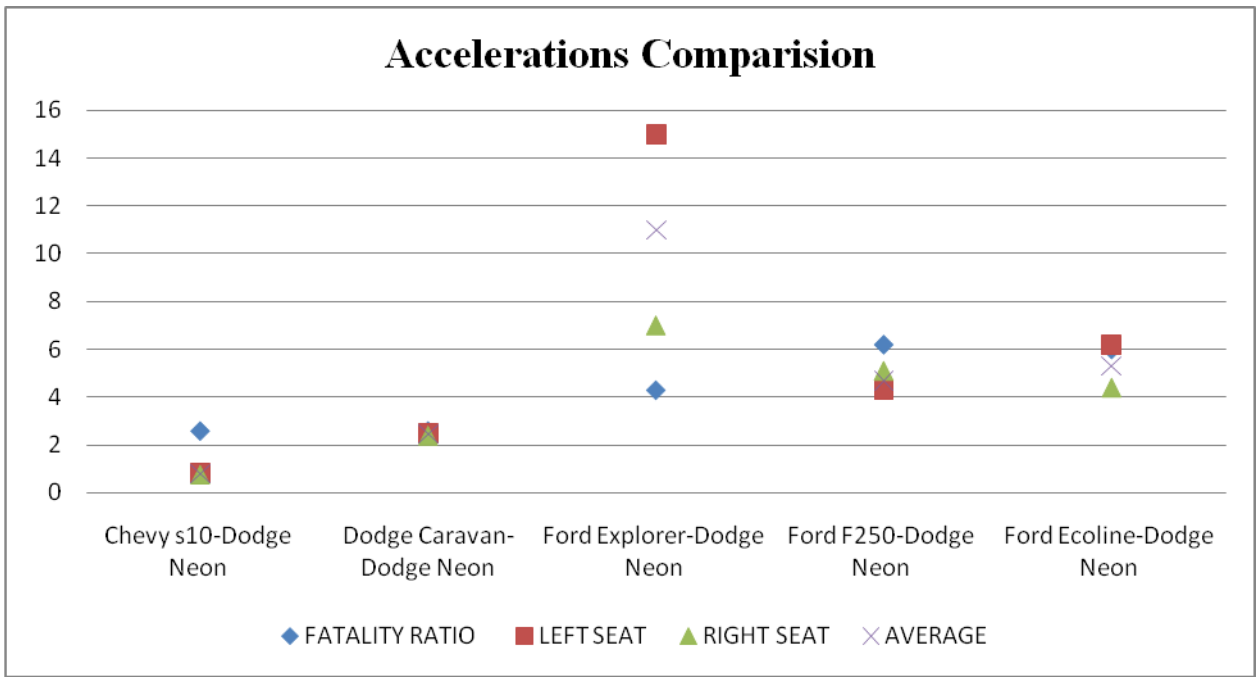

Figure 5.78: Comparison of acceleration ratios against DFR

From the graphs and Tables presented, it can be inferred that the weight ratio of the vehicles involved in collision are completely different from the statistical DFR because of the use of different materials which have different strength to weight ratio. When we compare the subjective measures to predict the DFR, with increase in weight of the vehicle, the stiffness incompatibility between vehicles is increasing in turn. These acceleration ratios are completely different from the DFR. The intrusion ratios at firewall, foot-well and A-pillar show correlation with the DFR. It can be observed from the Figure 5.77, in case I where the three incompatibilities (mass, stiffness and geometric incompatibilities) are within the acceptable range, the produced intrusion ratios completely coincide with the DFR. In case II, the A-pillar and foot-well intrusion ratios are in synchronization with DFR, but the firewall ratio is different from DFR because the frontal geometric structure of Dodge Caravan causes it to experience more intrusions on the firewall than Dodge Neon. In case III, because of high stiffness incompatibility of SUV the foot-

well intrusions differ with DFR but the A-pillar and firewall intrusion ratios are almost the same as DFR. In case IV, the three incompatibilities are extremely high causing the under ride of the smaller car into bigger vehicle producing firewall and A-pillar intrusion ratios different from the DFR. The foot-well ratio though is similar to the DFR. In case V, the three incompatibilities are just enough to produce intrusion ratios at firewall, foot-well and A-pillar which coincide with the value of DFR.

CHAPTER 6

APPLICATION OF PROPOSED METHODOLOGY

After validating the proposed methodology and understanding the impact of different incompatibilities on DFR, these vehicles representing different vehicle classes are selected and the validated methodology is applied on them to evaluate their DFR. Three vehicles selected are Toyota Rav4 representing a wagon style SUV or compact SUV, Chevy C1500 representing a light duty truck category, and a Ford Taurus representing a full-size car. Three different crash simulations are carried out showing the collision of these three cars against Dodge Neon. The proposed new method was then applied on these crash simulations to estimate the DFR of Rav4, C1500 and Taurus.

6.1 Wagon Style SUV (Toyota Rav4) Vs Passenger Car (Dodge Neon)

6.1.1 Model Description

Dodge Neon: Described in Case I.

Toyota Rav4:

The FE model of Toyota Rav4 is developed by National Crash Analysis Center for frontal impacts based on a 1997 model Rav4. This model is validated for frontal impact modes. Figure 6.1 shows the FE Model of the Toyota Rav4 used to represent the wagon style SUV [22].

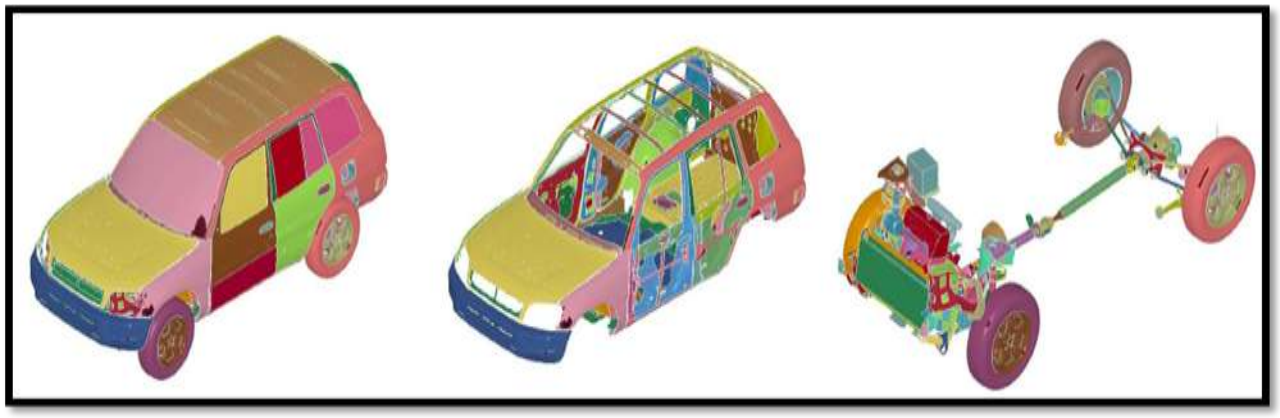

Figure 6.1: Exploded view of Toyota Rav4 FE model

The vehicle FE model has 577 parts; each part of the model depicts different parts of the original vehicle. The material properties of different parts are derived from the coupon testing. Different materials used in this FE model are BLATZ-KO_RUBBER, DAMPER VISCOUS, ELASTIC, MODIFIED_HONEYCOMB,MODIFIED_PIECEWISE_LINEAR_PLASTICITY, PIECEWISE LINEAR PLASTICITY and SPRING_NONLINEAR_ELASTIC. The FE Model is validates the Rav4 NCAP test results and the vehicle is stable at 30, 35, 40 mph. The accelerations of the vehicle and the wall force exerted by this vehicle are comparable to NCAP test results. The Table 6.1 shows the summary of the FE Model.

Table 6.1: FE model summary of Toyota Rav4

Number of Parts	577
Number of Nodes	478624
Number of Solids	21539
Number of Beams	2
Number of Shells	472423
Number of Elements	494117

6.1.2 Crash Simulation

The two vehicles are positioned such that they have full width interaction during collision and the vehicles are placed as close as possible to reduce the computational time. The contact between two vehicles is defined by using “Automatic Surface to surface “card. Static and dynamic friction coefficients are given as 0.3 between the contacts of two vehicles. Rigid wall planar cards are used between the contact of all tires and roads. Initial velocity of 35 mph is given to both vehicles and the termination time of 200 ms is given with a time step of 10 milliseconds. The total computational time for simulation this crash scenario is almost 12 hours. Figure 6.2 shows the results of crash simulation between the two vehicles at different times.

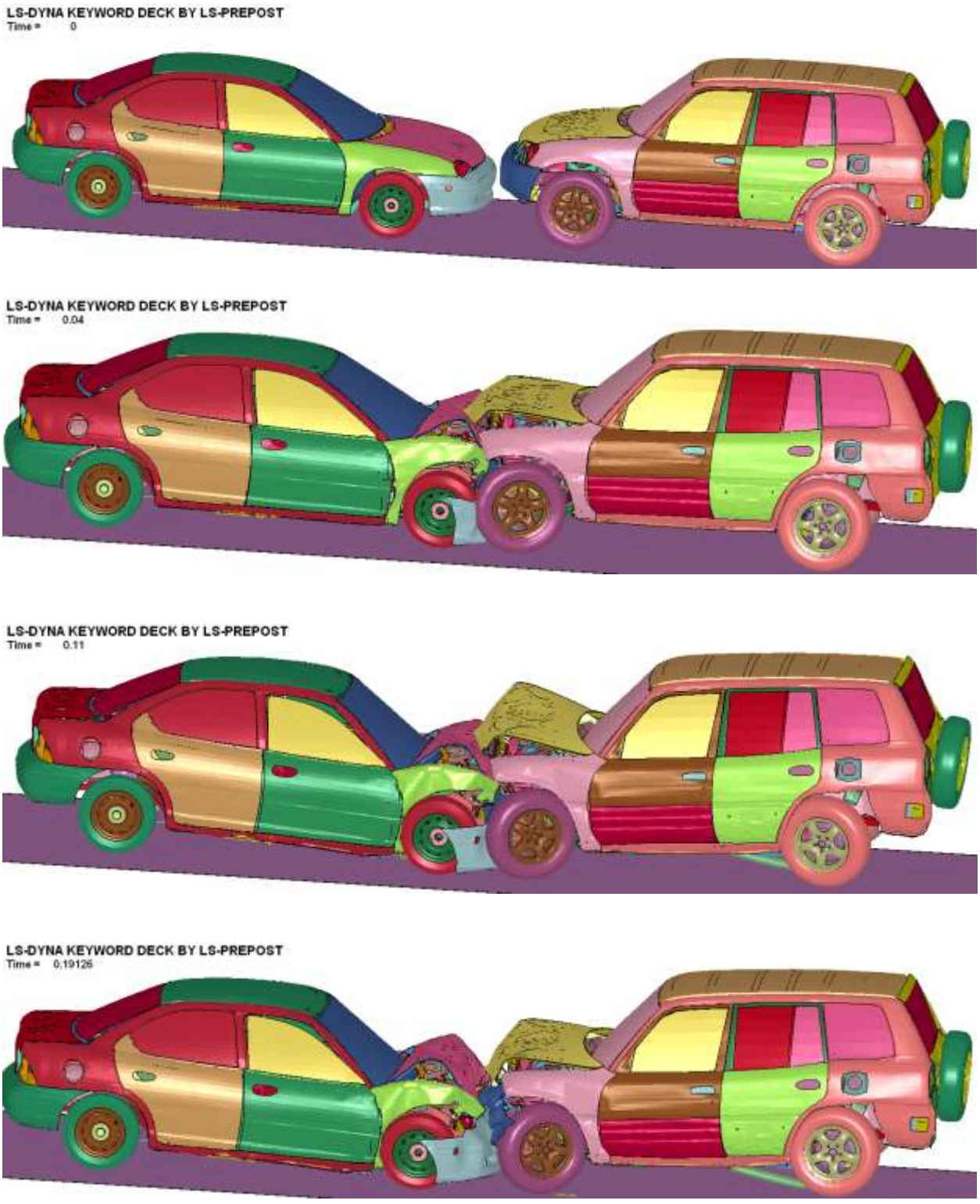

Figure 6.2: Animation of Toyota Rav4 crashing against Dodge Neon

The two vehicles are placed as close as possible to each other to reduce calculation time. The maximum crush between the vehicles happened at 100 ms, after which the two vehicles will start to come apart from each other. After reaching the maximum crush stage, firewall, driver side A-pillar, foot-well intrusions and accelerations of left and right seat are measured. The Figure 6.3 below shows the intrusions in the firewall of Toyota Rav4.

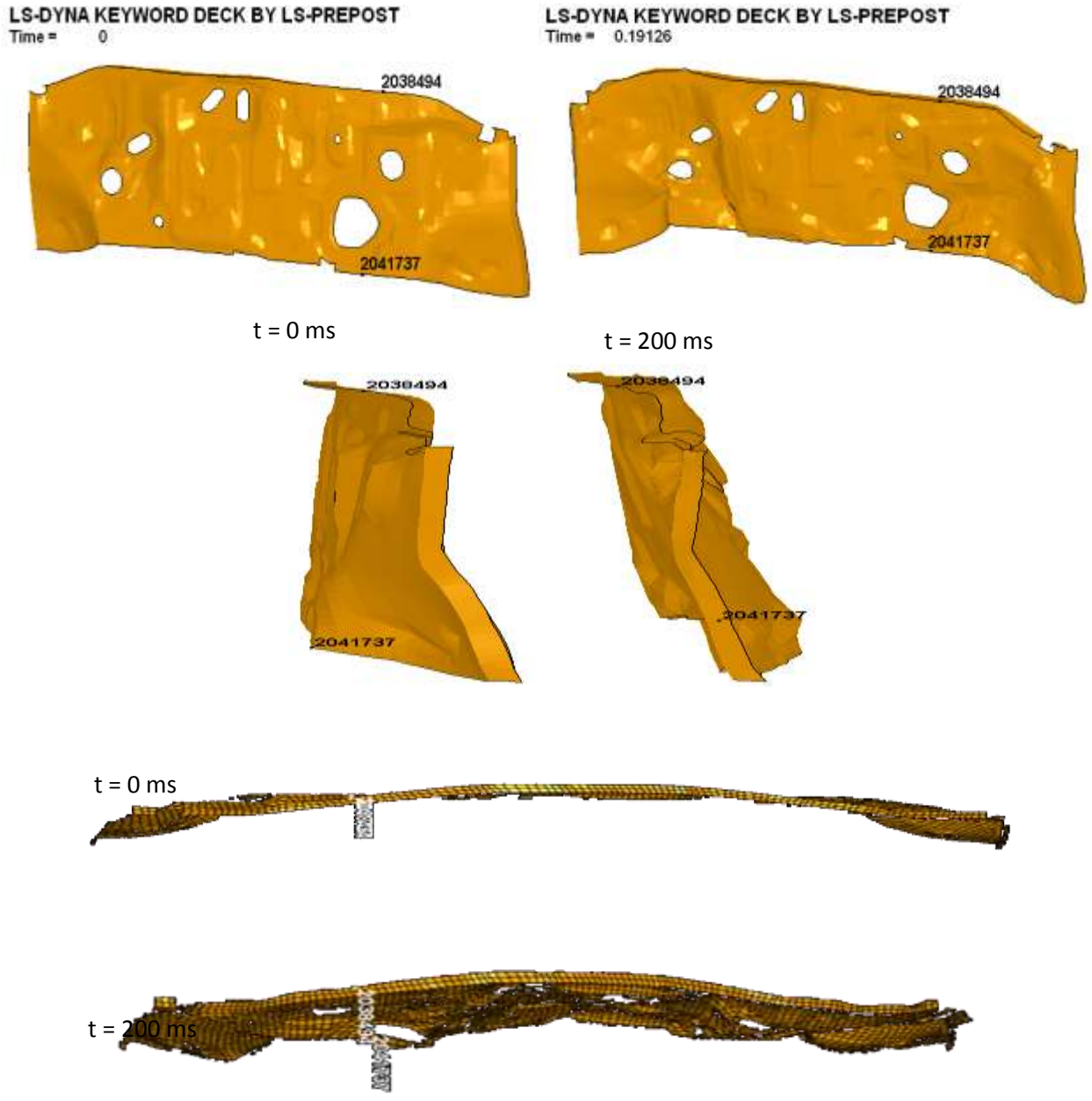

Figure 6.3: Animation sequence showing intrusion in firewall of Rav4 in CASE-VI

From Figure 6.3, it is evident that the maximum intrusion occurs approximately at node 2041737. From Figure 6.4, maximum intrusion in the firewall of Rav4 in collision with a passenger car is measured as 127mm.

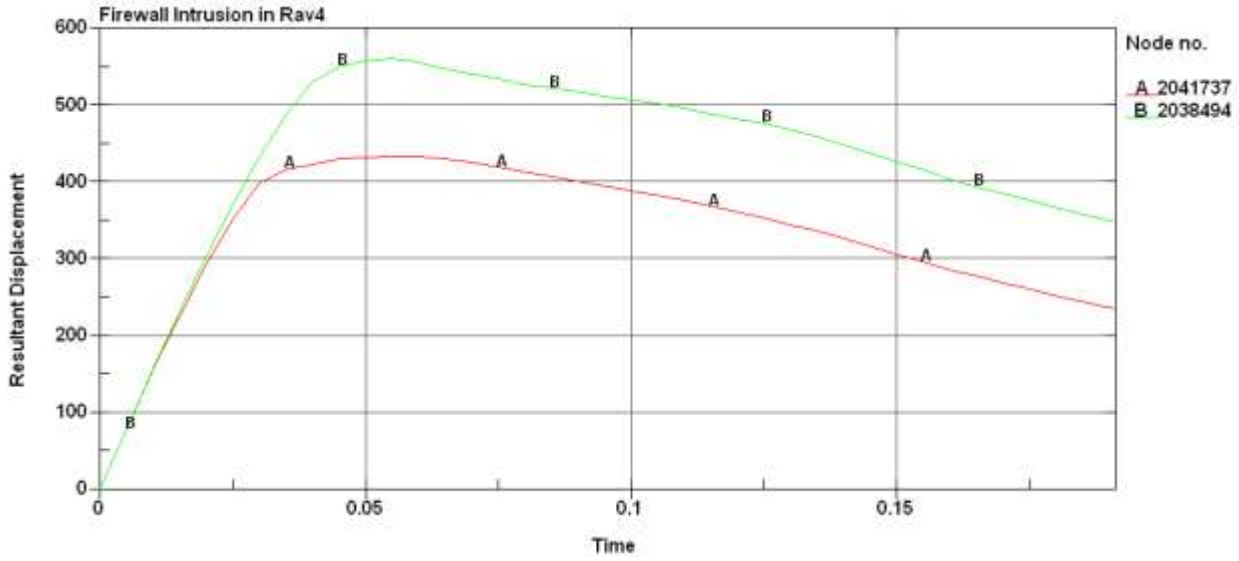

Figure 6.4: Maximum intrusion in firewall of Rav4 in CASE-VI

Foot-well Intrusion in Rav 4:

(a): Intrusion in firewall of Rav4 in CASE-VI (isometric view)

Figure 6.5: Animation sequence showing intrusion in foot-well of Rav4 in CASE-VI
(a) isometric view (b) side view

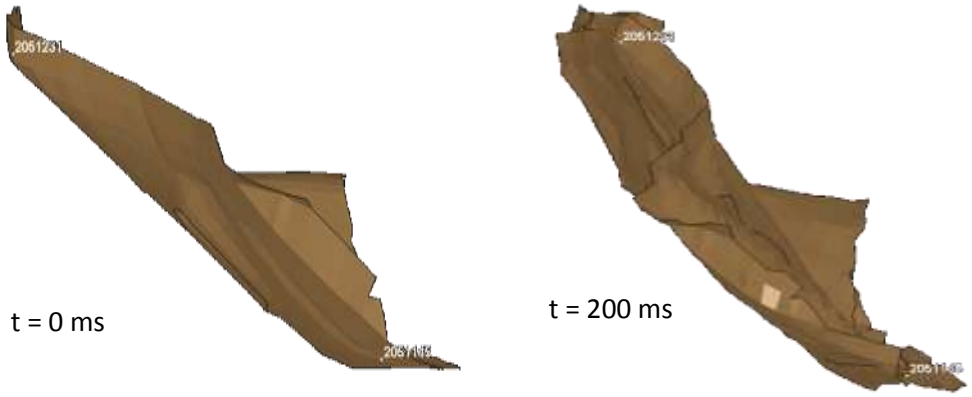

(b): Intrusion in foot-well of Rav4 in CASE-VI (side view)

The maximum intrusion in the foot-well of Rav4 occurs at node 2051231 and the animation sequence of intrusion is shown in the Figure 6.5. The resultant displacement of this maximum intruded node is shown in the Figure 6.6. From Figure 6.6, the maximum intrusion in the foot-well of Rav4 in collision with a passenger car is found to be 85mm.

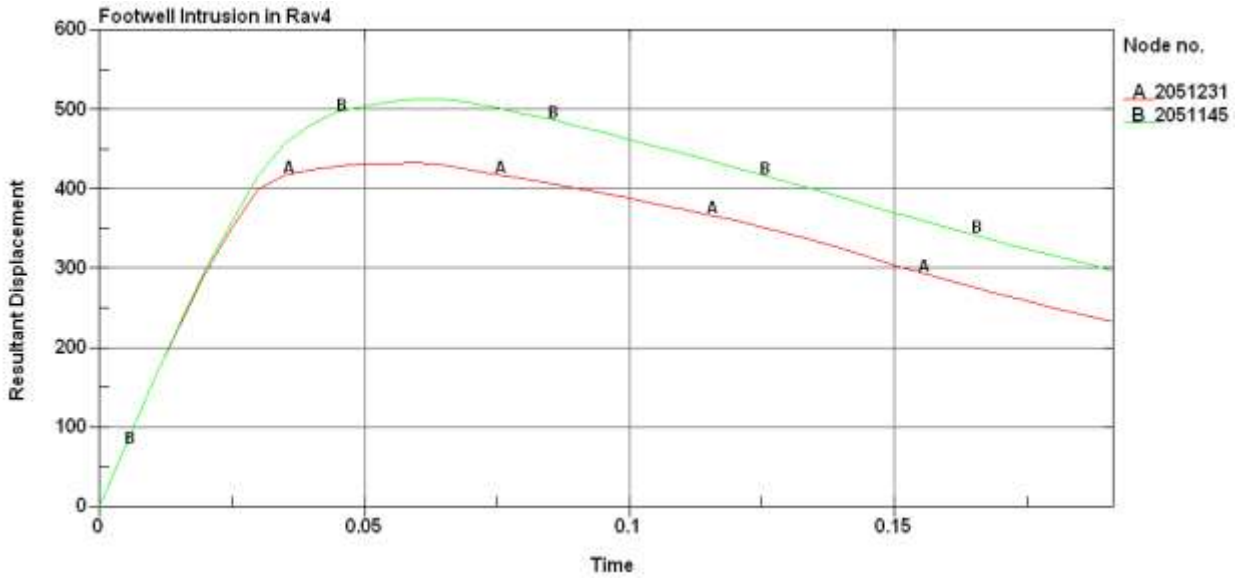

Figure 6.6: Maximum intrusion in foot-well of Rav4 in CASE-VI

Driver side A-Pillar Intrusion in Rav4:

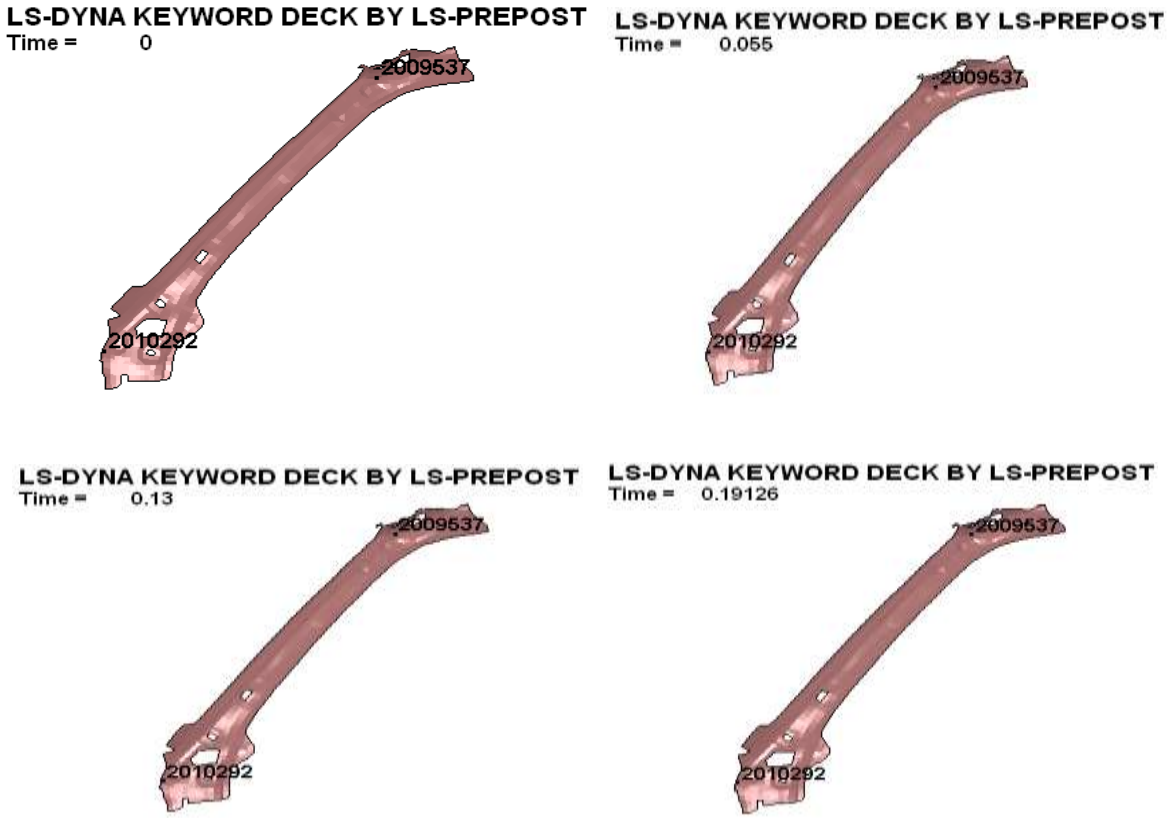

Figure 6.7: Animation sequence showing intrusion in driver side A-pillar of Rav4 in CASE-VI

From the Figure 6.7, the node which had maximum rearward movement on the A-pillar of the Rav4 is Node #2010292, the maximum displacement of this node is 64mm and the Figure 6.8 shows the displacement of the node with respect to time.

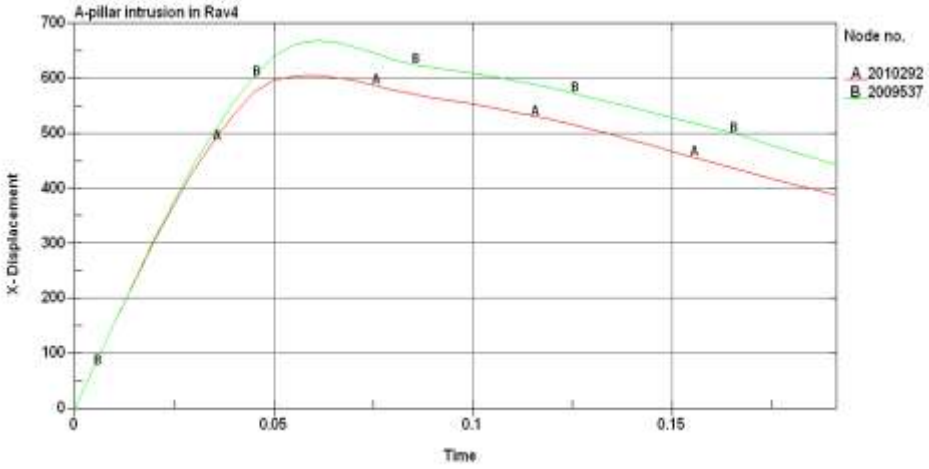

Figure 6.8: Maximum intrusion in driver side A-pillar of Rav4 in CASE-VI

Firewall Intrusion in Dodge Neon:

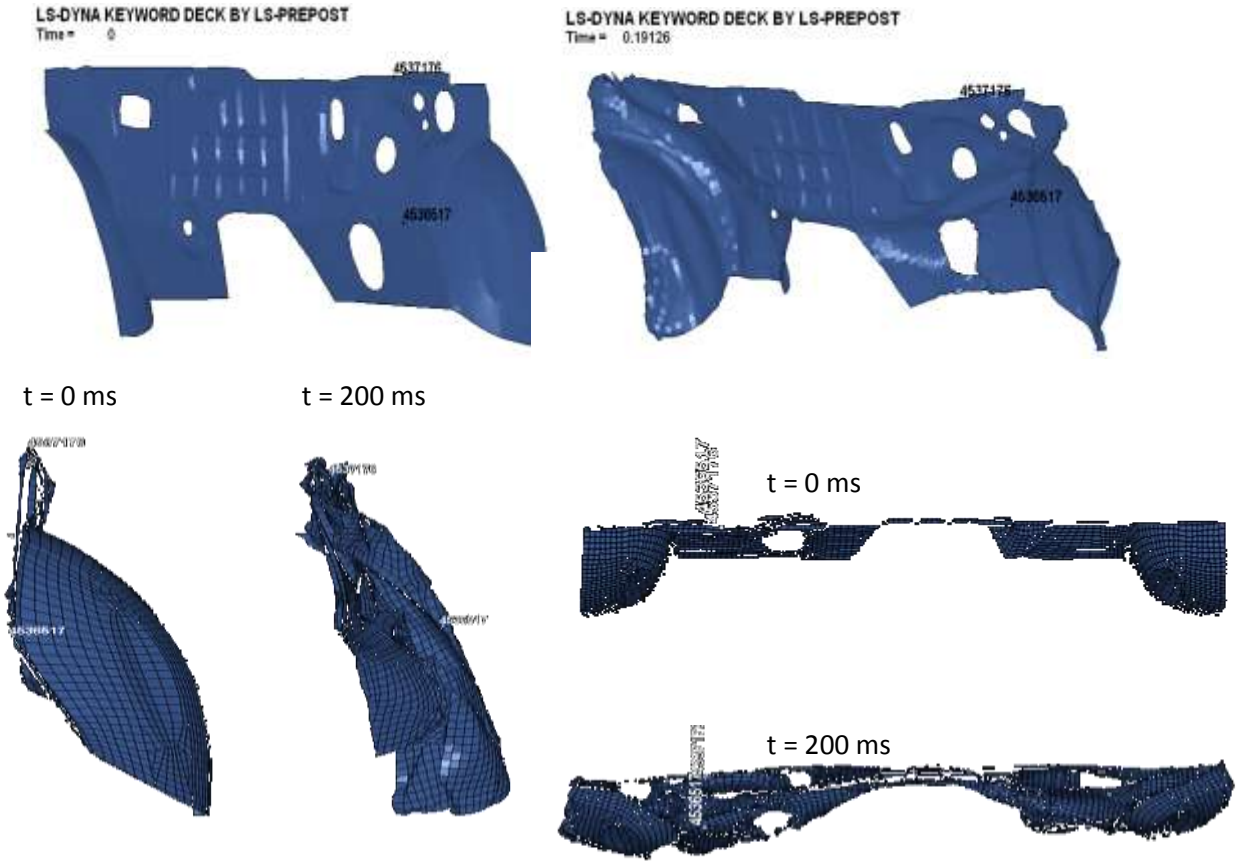

Figure 6.9: Animation sequence showing intrusion in firewall of Neon in CASE-VI

From Figure 6.9, the maximum intrusion in the firewall of Neon occurs approximately at node # 4536517, the maximum displacement of this node is 199 mm, as shown in Figure 6.10.

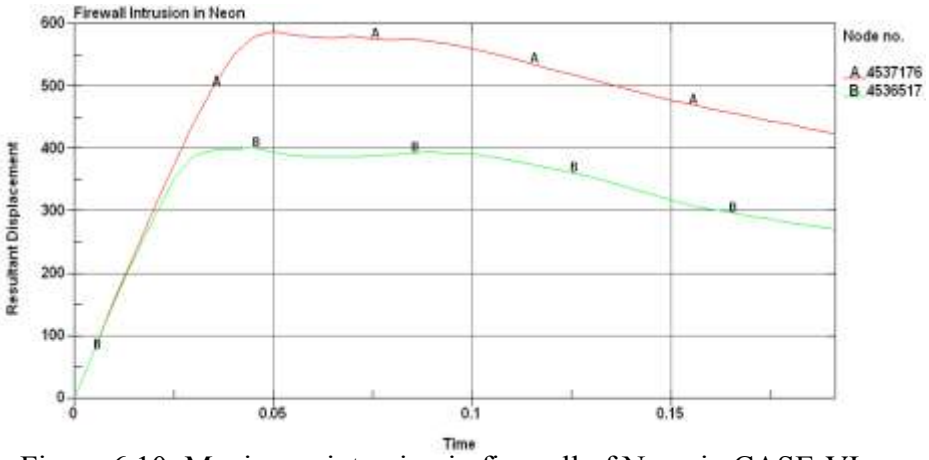

Figure 6.10: Maximum intrusion in firewall of Neon in CASE-VI

Foot-well Intrusion in Neon:

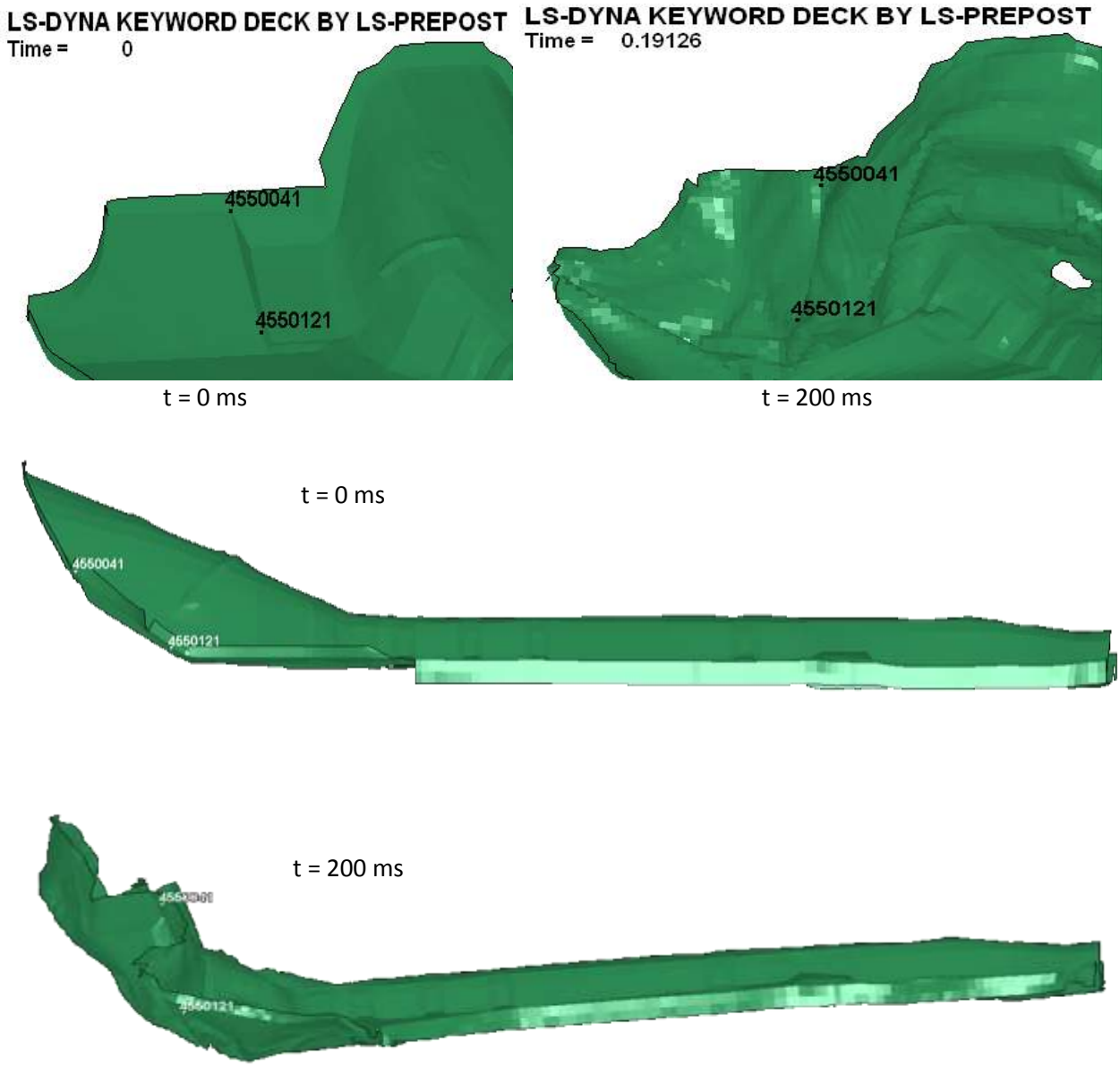

Figure 6.11: Animation sequence showing intrusion in foot-well of Neon in CASE-VI

From Figure 6.11, the maximum intrusion in the foot-well of the Dodge Neon occurs approximately at node # 4550041, the maximum displacement of this node is 148 mm, as shown in Figure 6.12.

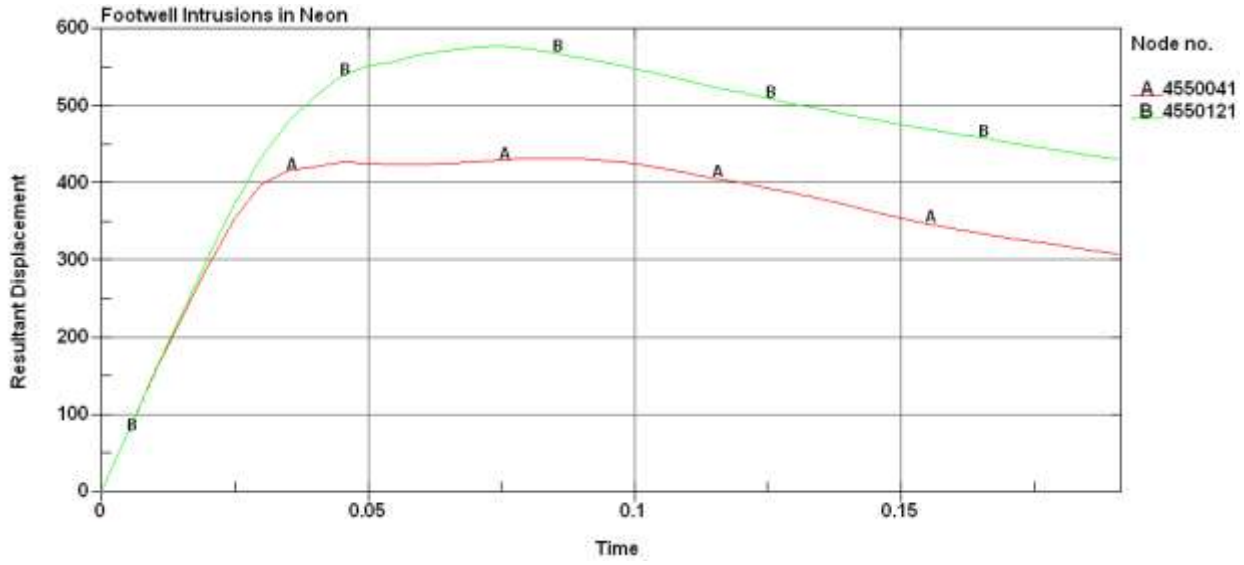

Figure 6.12: Maximum intrusion in foot-well of Neon in CASE-VI

Driver side A-Pillar Intrusion in Dodge Neon:

The Figures 6.13 show the movement of A-pillar during the collision with a compact SUV.

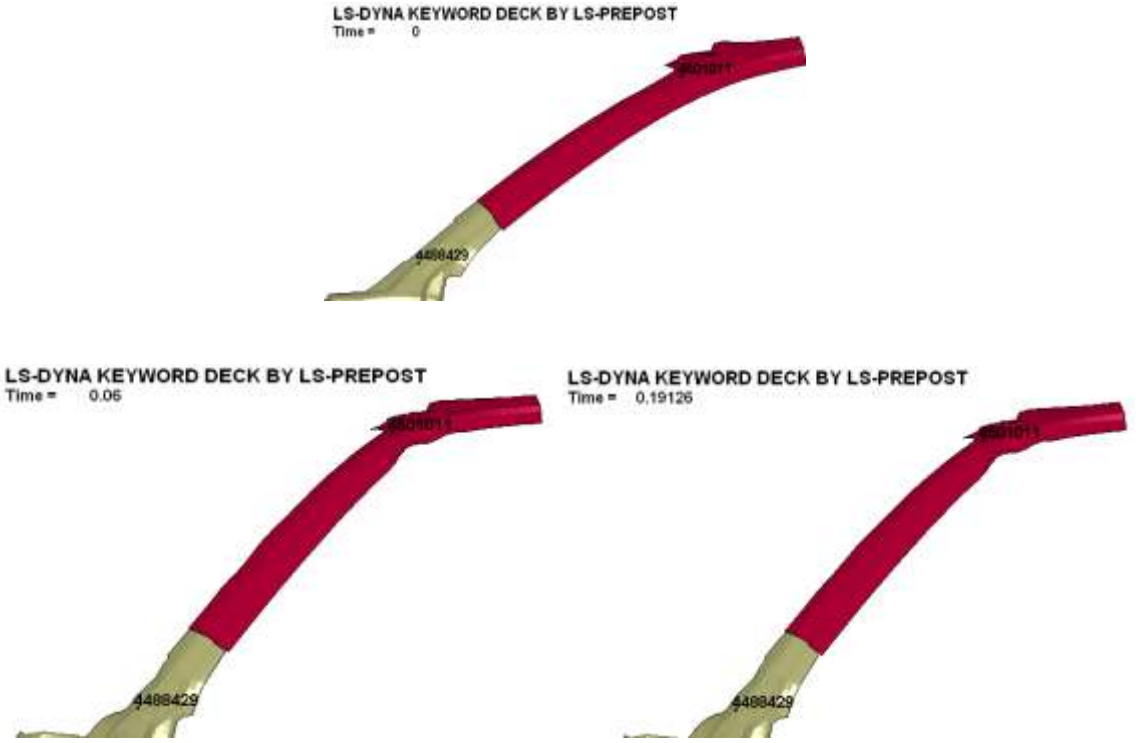

Figure 6.13: Animation sequence showing intrusion in driver side A-pillar of Neon in CASE-VI

The node which had maximum rearward movement on the A-pillar of the Dodge Neon is node # 4488429, the maximum displacement of this node is found to be 68mm. Figure 6.14 shows the displacement of the node with respect to time.

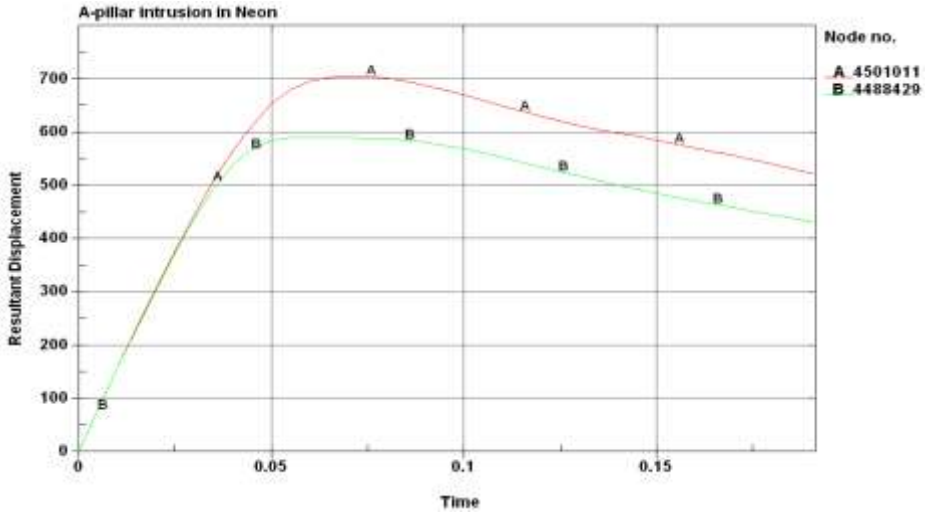

Figure 6.14: Maximum intrusion in driver side A-pillar of Neon in CASE-VI

Figure 6.15 shows the left and right seat acceleration in Toyota Rav4 and Dodge Neon. Figure 6.15 also shows the peak acceleration in the left and right seat of two vehicles.

LEFT and RIGHT Seat Accelerations:

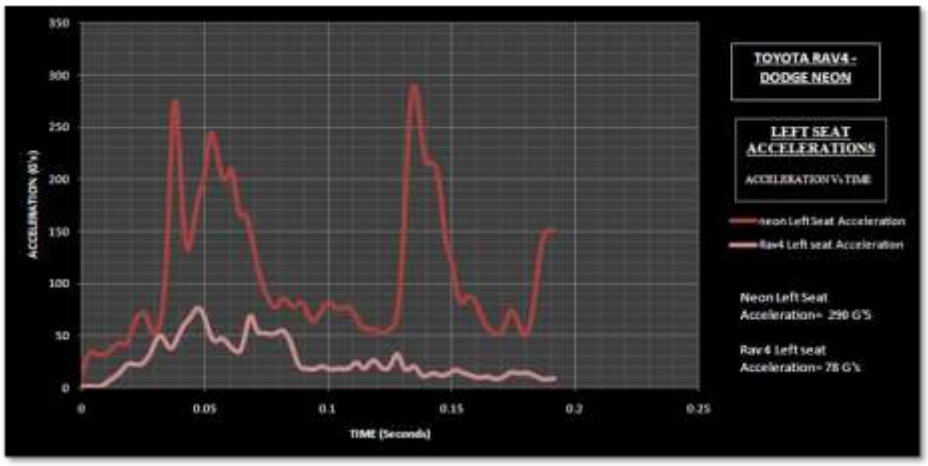

(a): Left seat acceleration in CASE-VI

Figure 6.15: Left and Right seat acceleration in CASE-VI

(a) Left seat (b) Right seat

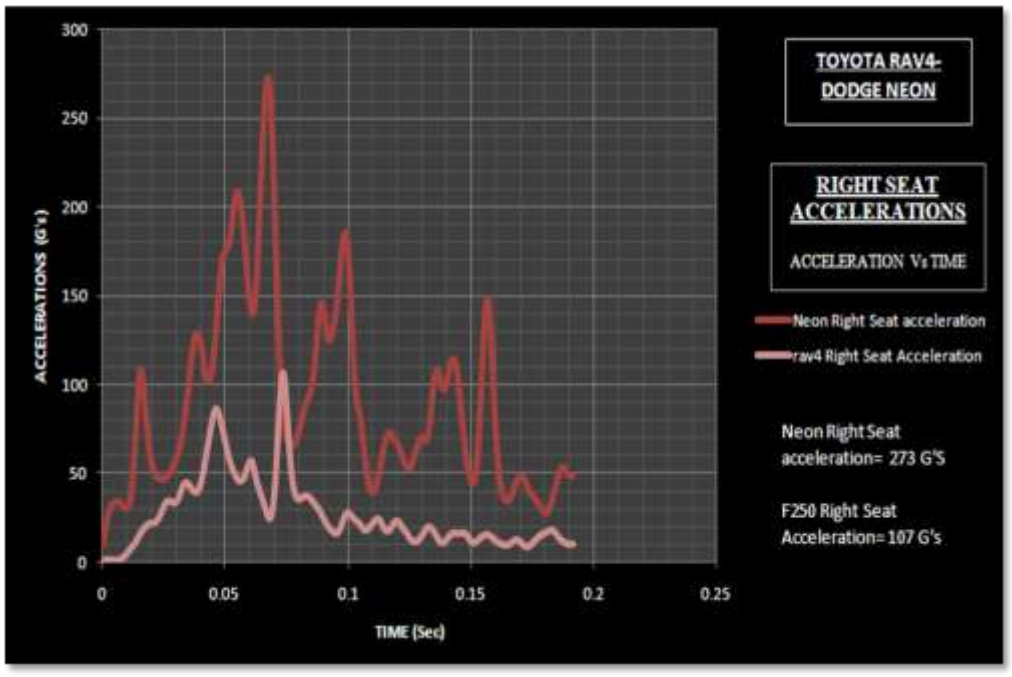

(b): Right seat acceleration in CASE-VI

6.1.3 Discussion

In the crash scenario of Toyota Rav4 against Dodge Neon, the weight ratio of Rav4 against Neon is 1.2: 1. This weight ratio indicates that the difference in weight is not very high where the mass incompatibility leads to complete dominance of one vehicle on the other. The ride height of Rav4 to Neon is in the ratio of 2: 1. The difference in ride height is just enough to prevent rav4 to over ride the passenger car. After running the simulation for 200 ms, maximum intrusions are measured at the firewall, foot-well and A-pillar. Accelerations are measured at the C.G of left and right seats. Table 6.2 shows the intrusions and accelerations measured and, the ratios when both vehicles are compared. The intrusion ratio at firewall of both cars is 1: 1.6; whereas the foot-well intrusion ratio is 1: 1.7; driver side A-pillar intrusion ratio is 1: 1.7. The acceleration ratios at left and right seat are 1: 3.6 and 1: 2.6 respectively. The variation in the acceleration ratios is because of the stiffness incompatibility, thus acceleration ratios are poor estimates for

the DFR. But the intrusion ratios are the same at the firewall, foot-well and at A-pillar follow same pattern. Based on the new method of approach, or can state that the DFR of Toyota Rav4 against passenger car is approximately 1.7: 1.

Summary of Case-VI:

Table 6.2: Summary of CASE-VI

	Rav4	Neon
Firewall Intrusion (mm)	127	199
Foot well Intrusion (mm)	85	148
A-pillar Intrusion (mm)	64	112
Left seat Acceleration (G's)	78	290
Right seat Acceleration (G's)	107	273

Toyota Rav4 : Dodge Neon	Ratio
Ratio of Firewall Intrusion	1: 1.6
Ratio of Foot well Intrusion	1: 1.7
Ratio of A-pillar Intrusion	1: 1.7
Ratio of Left seat Acceleration	1: 3.7
Ratio of Right seat Acceleration	1: 2.6

6.2 Light Duty Truck (Chevy C1500) Vs Passenger Car (Dodge Neon)

6.2.1 Model Description

Dodge Neon: Described in Case I.

Chevy C1500:

The FE model of Chevy C1500 is developed by National Crash Analysis Center for frontal impacts based on a 1994 model C1500. This model can be used for research work in frontal impact modes. The elements size in the frontal portion of the vehicle is very small when compared to the element size in the side and rear portion because the intrusion in these areas is very less during head to head-on collisions. Figure 6.16 shows the FE Model of the Chevy C1500 is used to represent the light duty pick-up truck [22].

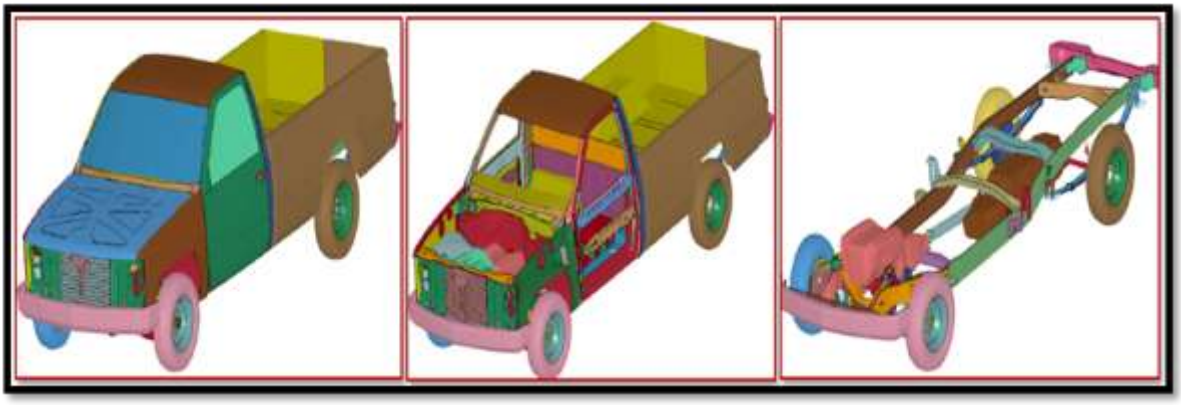

Figure 6.16: Exploded view of Chevy C1500

The vehicle FE model has 251 parts; each part of the model depicts different parts of the original vehicle. The material properties of different parts are derived from the coupon testing. Different materials used in this FE model are BLATZ-KO_RUBBER, DAMPER VISCOUS, ELASTIC,HONEYCOMB,PIECEWISE_LINEAR_PLASTICITY,SPRING_NONLINEAR_EL ASTIC and SPRING_ELASTIC. There are 58313 elements in the FE model out of which 163 are beam elements, 24 are discrete elements, 54565 are shell elements, 3561 are solid elements.

Different parts of the vehicle are constrained by sixteen revolute joints, fourteen spherical joints and five hundred and ninety four spot welds. The FE Model is validates the C1500 NCAP test results and the vehicle is sTable at 30, 35, 40 mph. The accelerations of the vehicle and the wall force exerted by this vehicle are comparable to NCAP test results. The Table 6.3 shows the summary of the FE Model.

Table 6.3: FE model summary of Chevy C1500

Number of Parts	251
Number of Nodes	66586
Number of Solids	3561
Number of Beams	163
Number of Shells	54565
Number of Elements	58313

6.2.2 Crash Simulation

Vehicles are placed as close as possible to reduce time of calculation. The contact between two vehicles is defined by using "Automatic Surface to surface "card. Static and dynamic friction coefficients are given as 0.3 between the contacts of two vehicles. Rigid wall planar cards are used between the contact of all tires and roads. Initial velocity of 35 mph is given to both vehicles and a termination time of 200 milliseconds is given with a time step of 10 milliseconds. The total computational time for simulation this crash scenario is almost 12 hours. Figure 6.17 shows the results of crash simulation between the two vehicles at different time step are show.

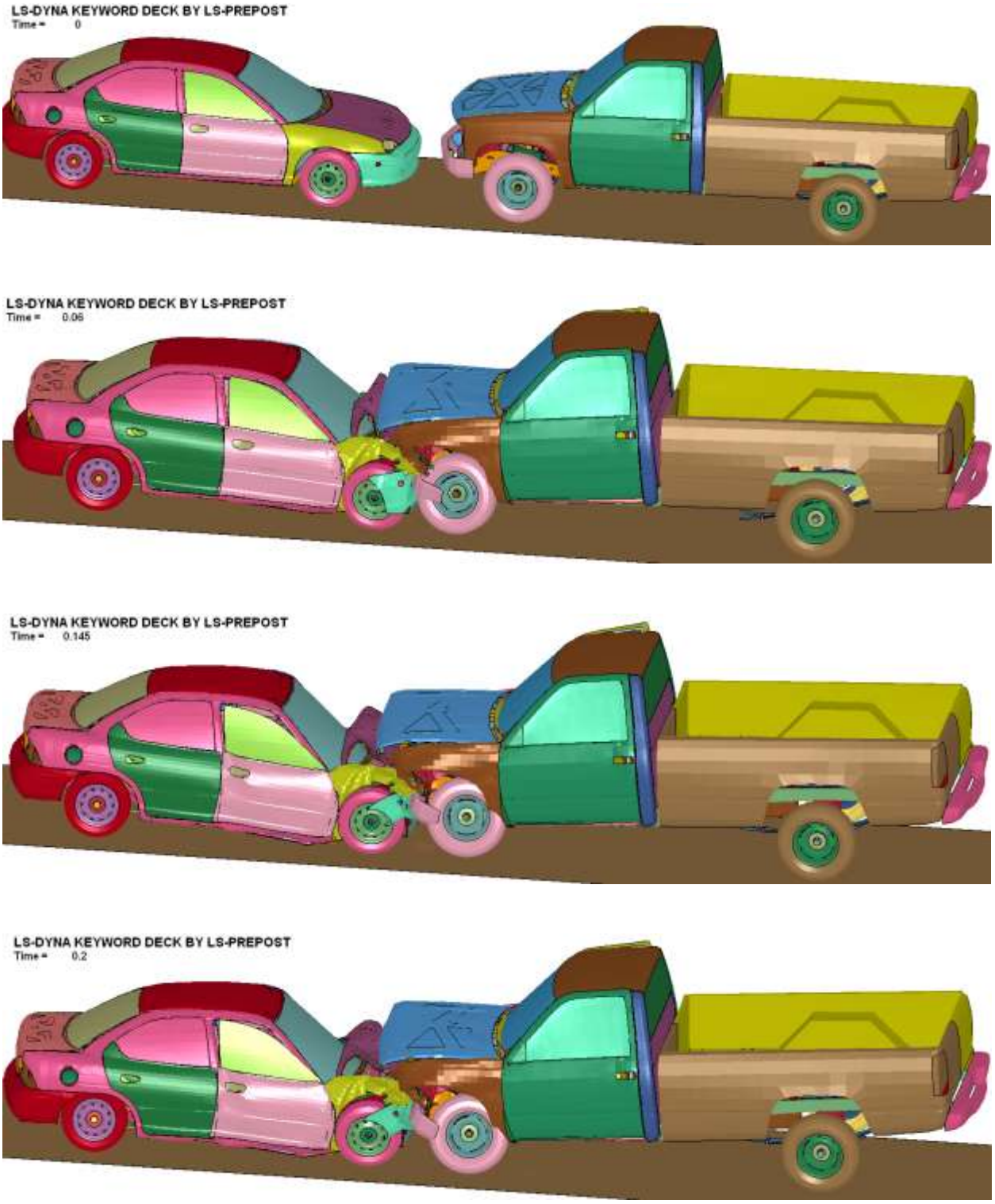

Figure 6.17: Animation of Chevy C1500 crashing against Dodge Neon

The two vehicles are placed as close as possible to each other to reduce calculation time. The maximum crush between the vehicles happened at 100 ms, after which the two vehicles will start to come apart from each other. After reaching the maximum crush stage, firewall, driver side A-pillar, foot-well intrusions and accelerations of left and right seat are measured. The Figure 6.18 below shows the intrusions in the firewall of C1500.

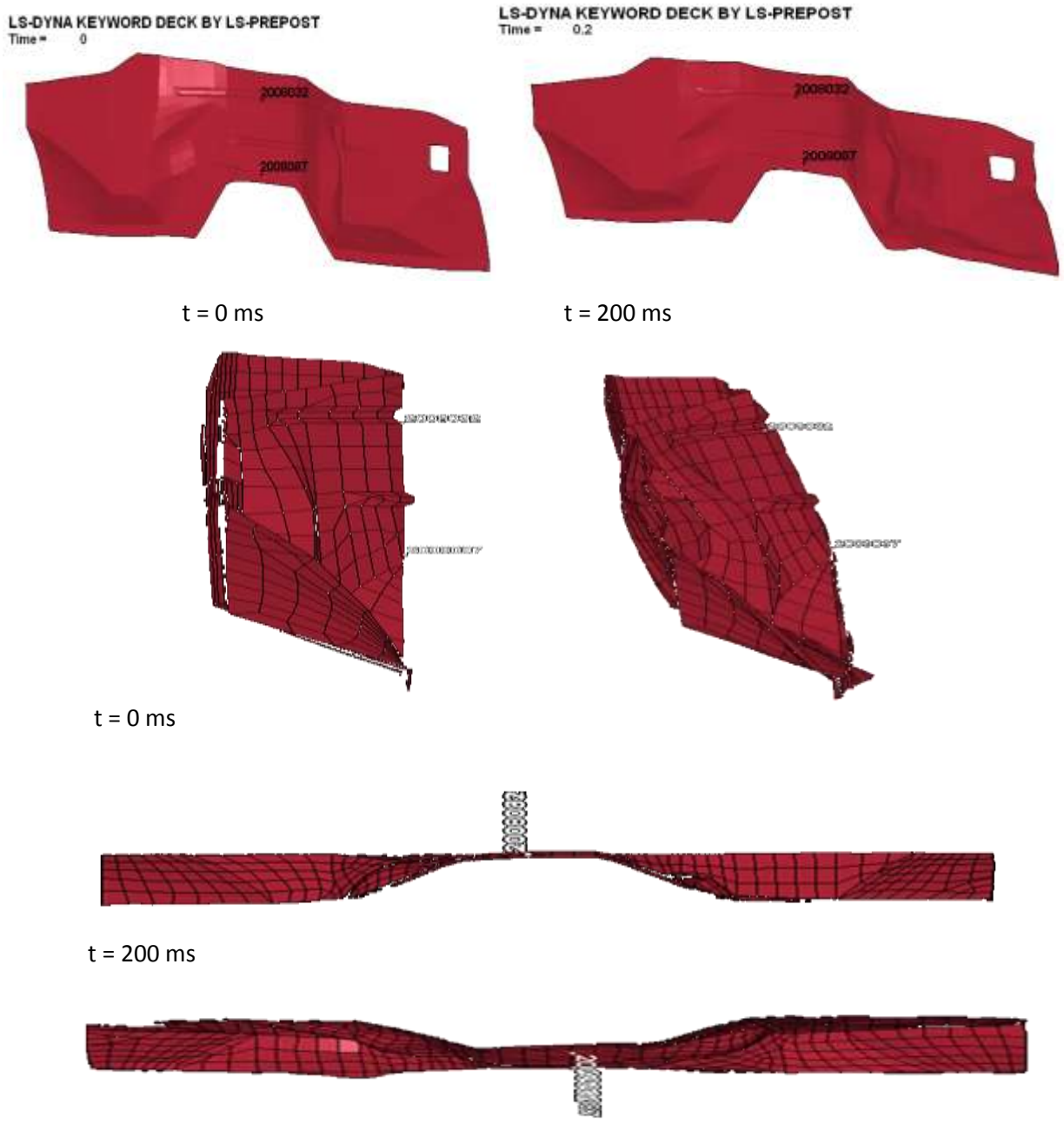

Figure 6.18: Animation sequence showing intrusion in firewall of C1500 in CASE-VII

From Figure 6.18, it is evident that the maximum intrusion occurs approximately at node # 2008087. The resultant displacement of the maximum intruded node is shown in the graph below. From the Figure 6.19, maximum intrusion in the firewall of C1500 in collision with a passenger car is measured as 70 mm.

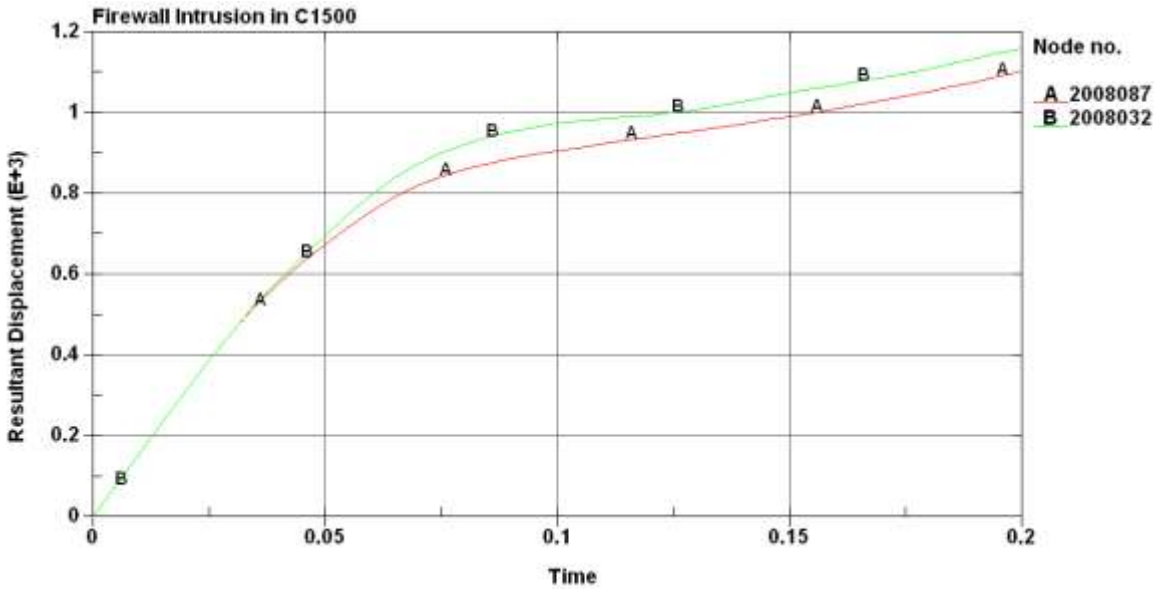

Figure 6.19: Maximum Intrusion in firewall of C1500 in CASE-VII

Foot-well Intrusion in Chevy C1500:

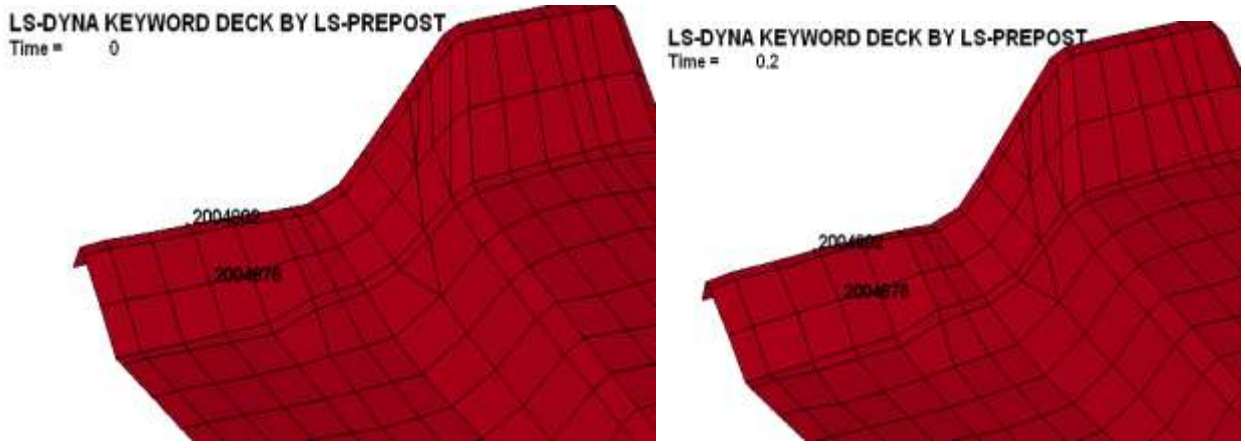

(a): Intrusion in foot-well of C1500 in CASE-VII (isometric view)

Figure 6.20: Animation sequence showing intrusion in foot-well of C1500 in CASE-VII (a) isometric view (b) side view

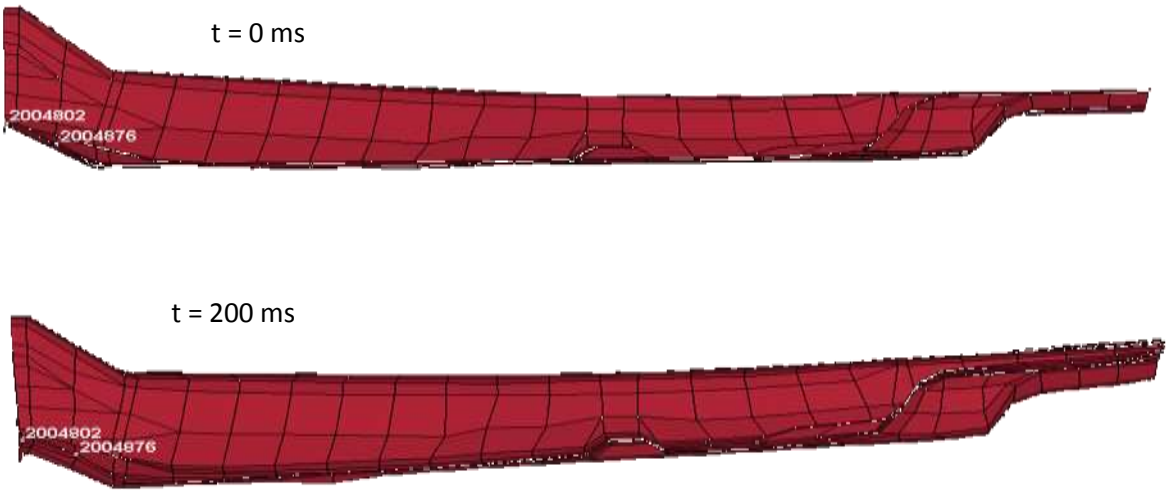

(a): Intrusion in foot-well of C1500 in CASE-VII (side view)

The maximum intrusion in the foot-well of C1500 occurs at node 2004802. The resultant displacement of this maximum intruded node is shown in the Figure 6.21. From Figure 6.22, maximum intrusion in the foot-well of C1500 in collision with a passenger car is 5mm.

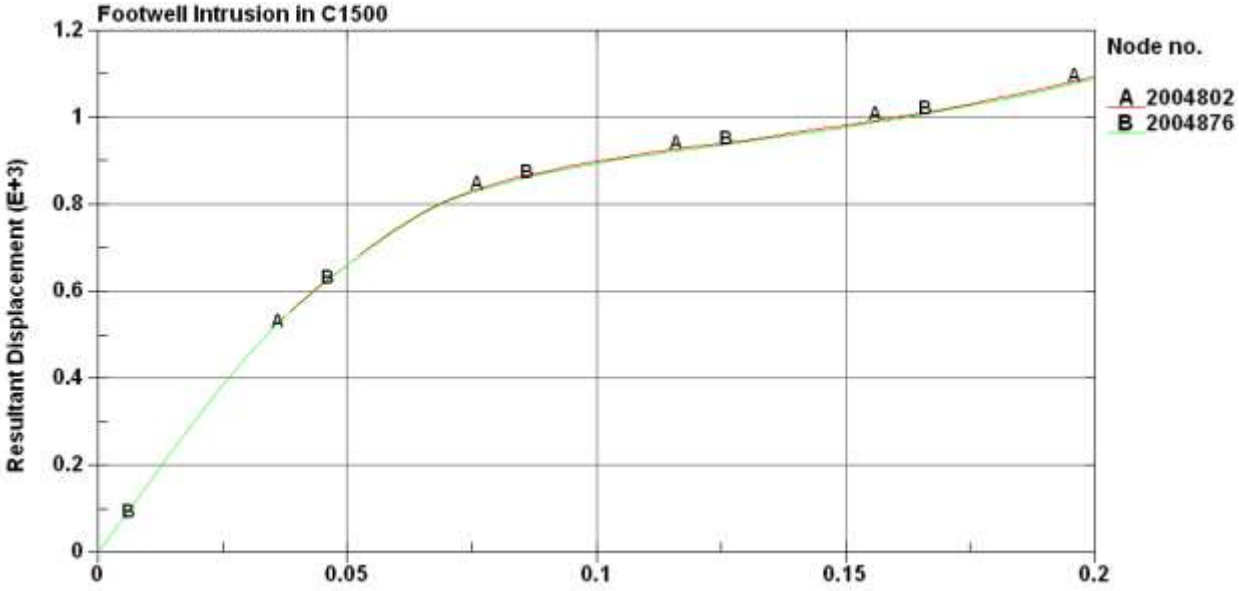

Figure 6.21: Maximum intrusion in foot-well of C1500 in CASE-VII

Driver side A-Pillar Intrusion in C1500:

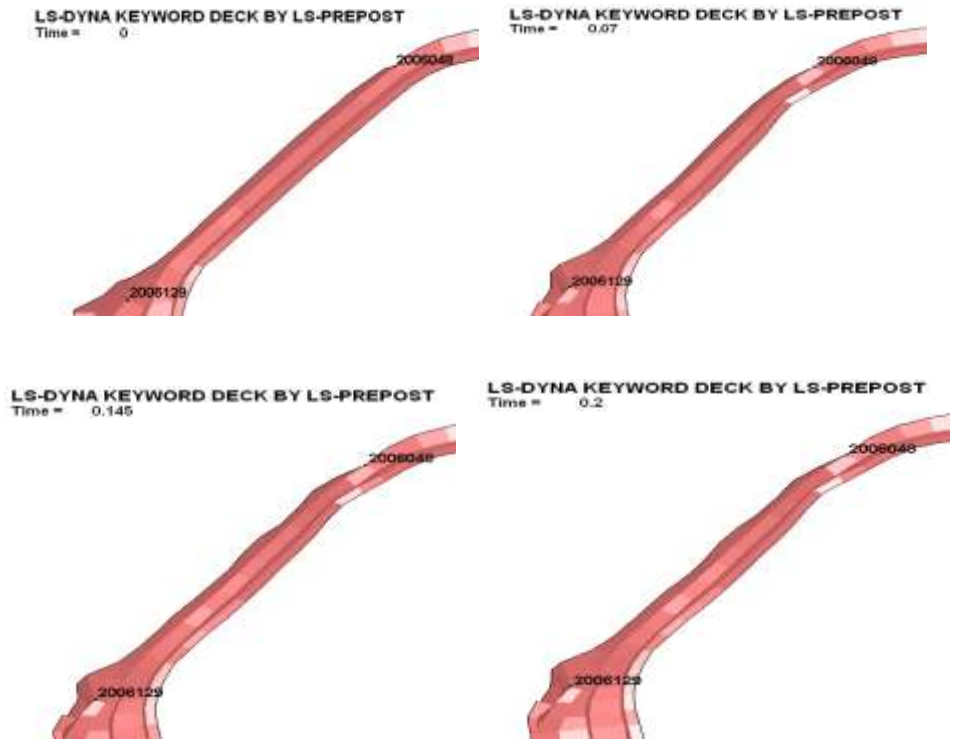

Figure 6.22: Animation sequence showing intrusion in driver side A-pillar of C1500 in CASE-VII

From the Figure 6.22, the node which has maximum rearward movement on the A-pillar of the C1500 is Node #2006048. The maximum displacement of this node is 66mm and the Figure 6.23 shows the displacement of the node with respect to time.

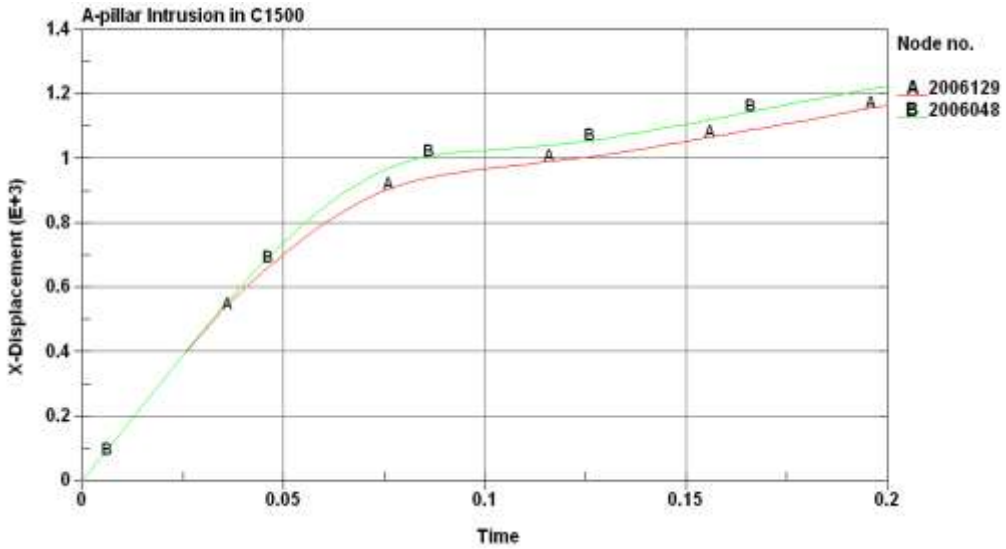

Figure 6.23: Maximum intrusion in driver side A-pillar of C1500 in CASE-VII

Firewall Intrusion in Dodge Neon:

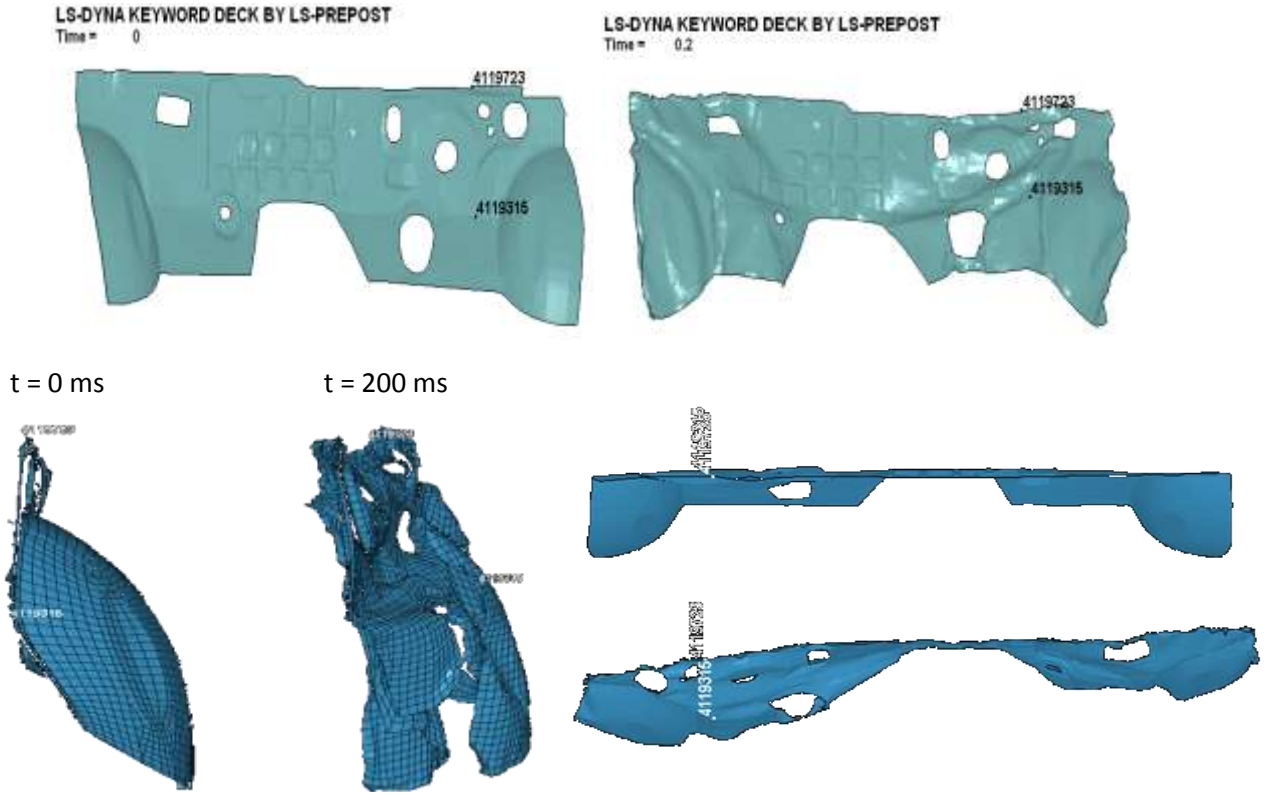

Figure 6.24: Animation sequence showing intrusion in firewall of Neon in CASE-VII

From the Figure 6.24, the maximum intrusion in the firewall of the Dodge Neon occurs approximately at Node # 4119315, the maximum displacement of this node is 190 mm, as is shown in the Figure 6.25.

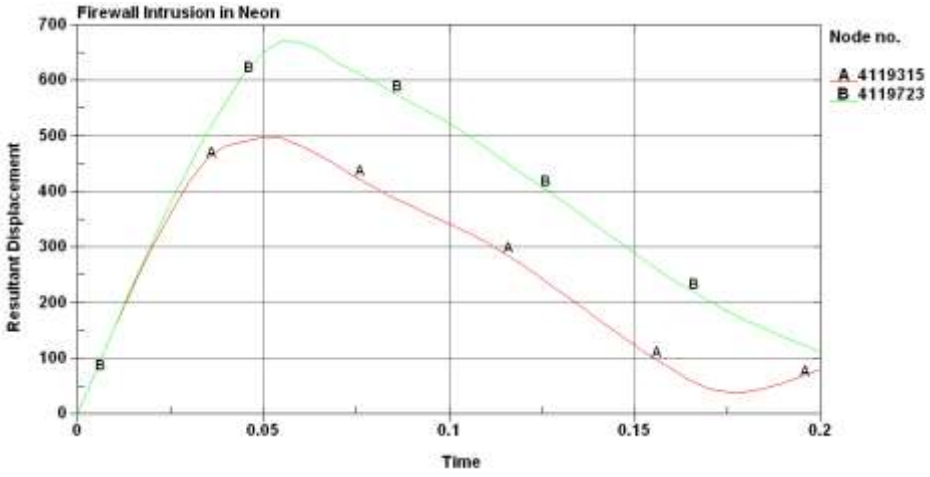

Figure 6.25: Maximum intrusion in firewall of Neon in CASE-VII

Foot-well Intrusion in Neon:

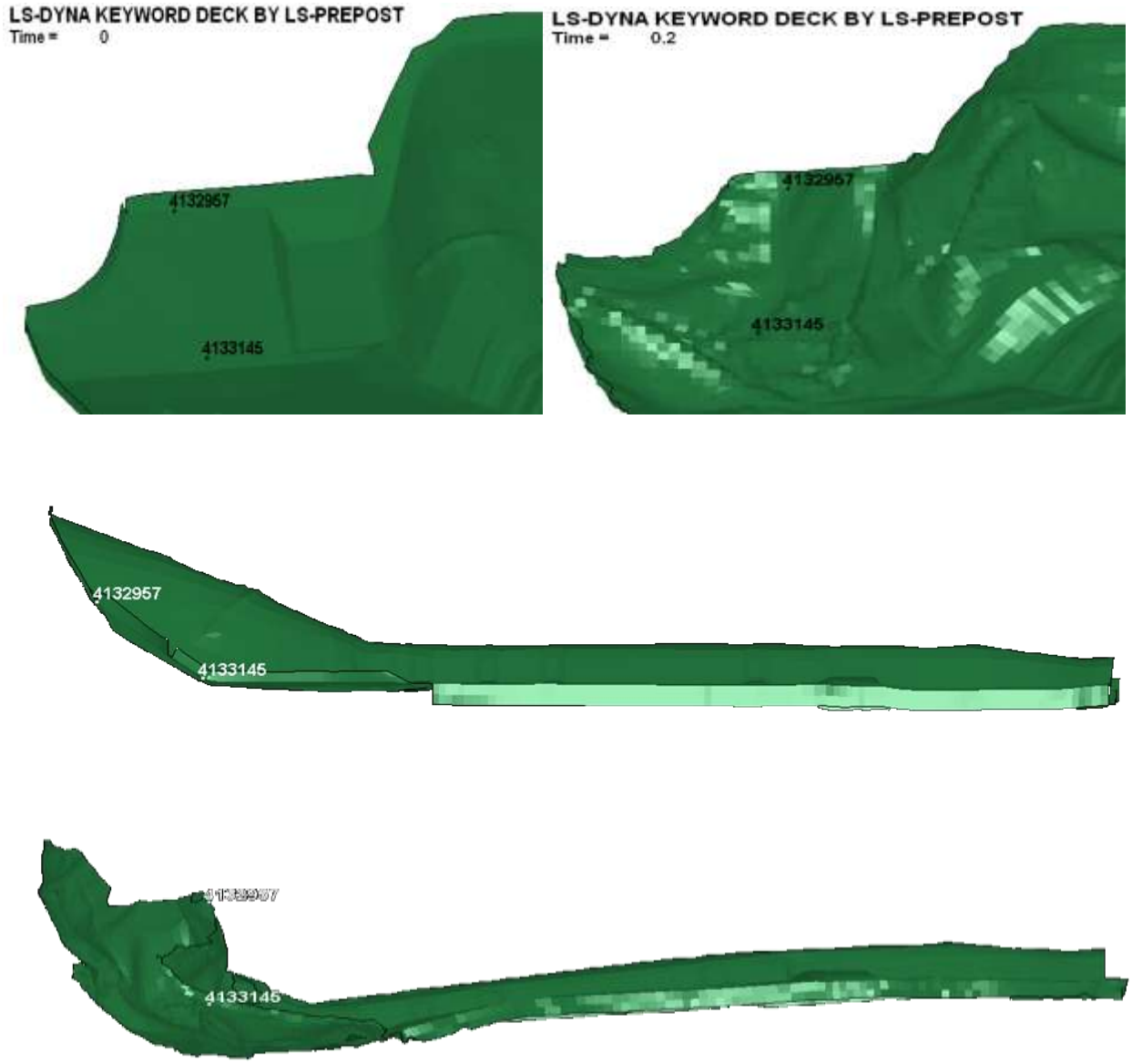

Figure 6.26: Animation sequence showing intrusion in foot-well of Neon in CASE-VII

From Figure 6.26, the maximum intrusion in the foot-well of the Dodge Neon occurs approximately at node # 4132857, the maximum displacement of this node is 192 mm, as is shown in the Figure 6.27.

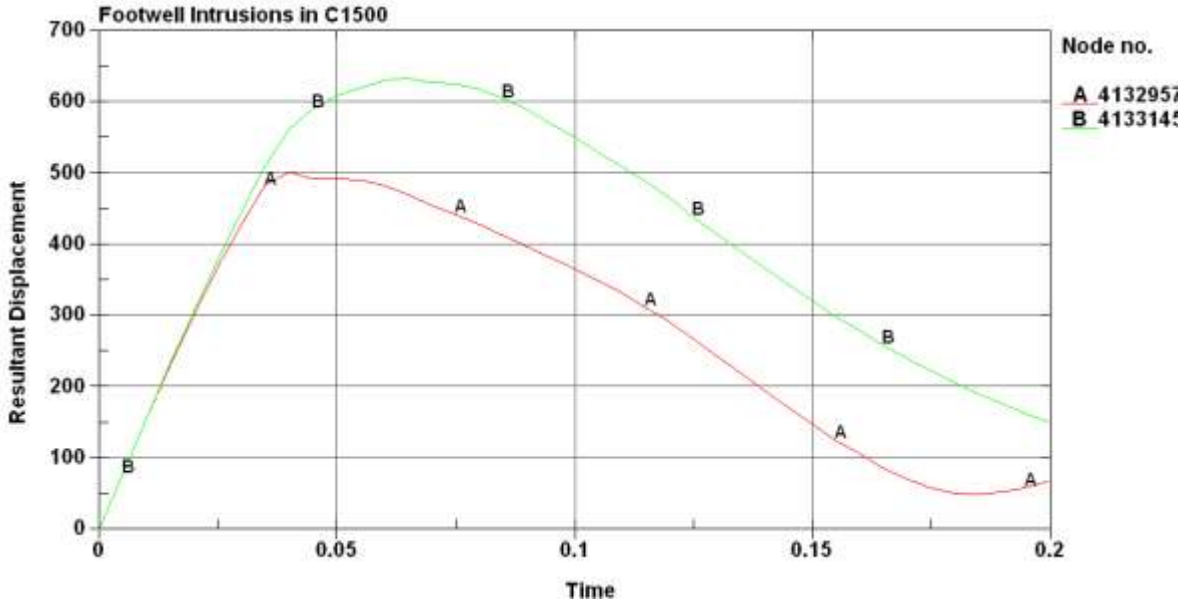

Figure 6.27: Maximum intrusion in foot-well of Neon in CASE-VII

Driver side A-Pillar Intrusion in Dodge Neon:

The Figure 6.28 shows the movement of A-pillar during the collision with a Light Duty Truck.

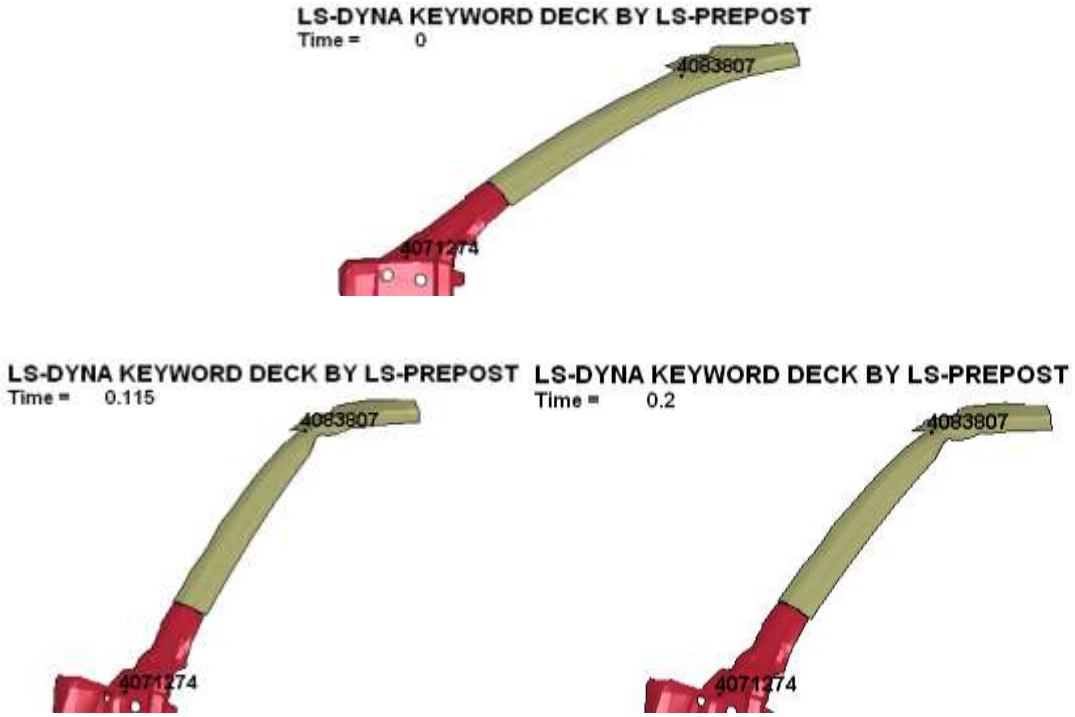

Figure 6.28: Animation sequence showing intrusion in driver side A-pillar of Neon in CASE-VII

The node which had maximum rearward movement on the A-pillar of the Dodge Neon is node #4071274, the maximum displacement of this node is found to be 180mm and the Figure 6.29 shows the displacement of the node with respect to time.

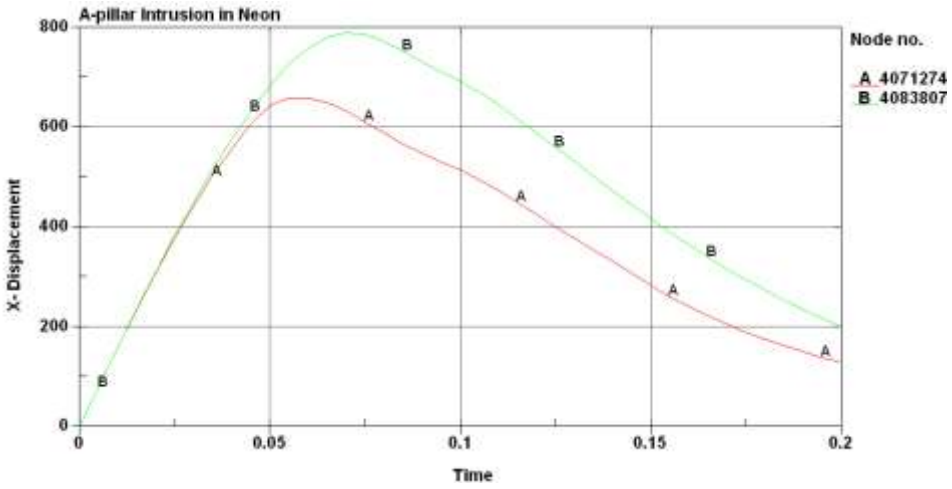

Figure 6.29: Maximum intrusion in driver side A-pillar of Neon in CASE-VII

Figure 6.30 shows the left and right seat accelerations in Chevy C1500 and Dodge Neon. The figure also shows the peak accelerations attained in the two vehicles.

LEFT and RIGHT Seat Accelerations:

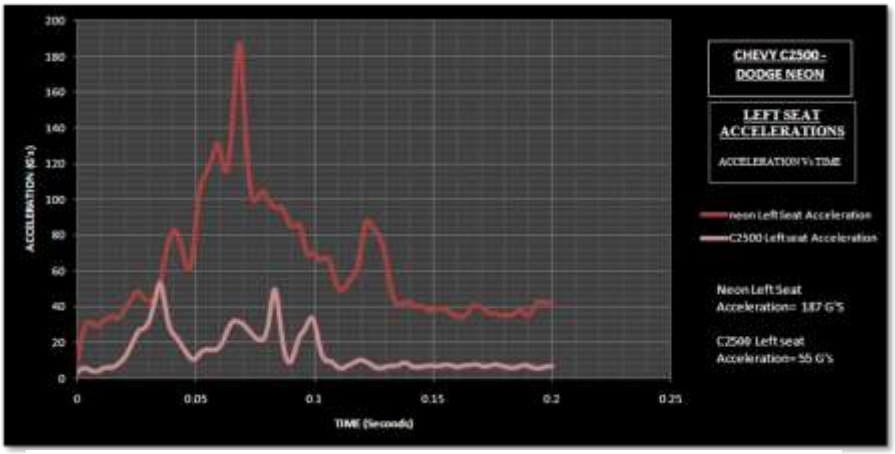

(a): Left seat acceleration in CASE-VII

Figure 6.30: Left and Right seat acceleration in CASE-VII
(a) Left seat (b) Right seat

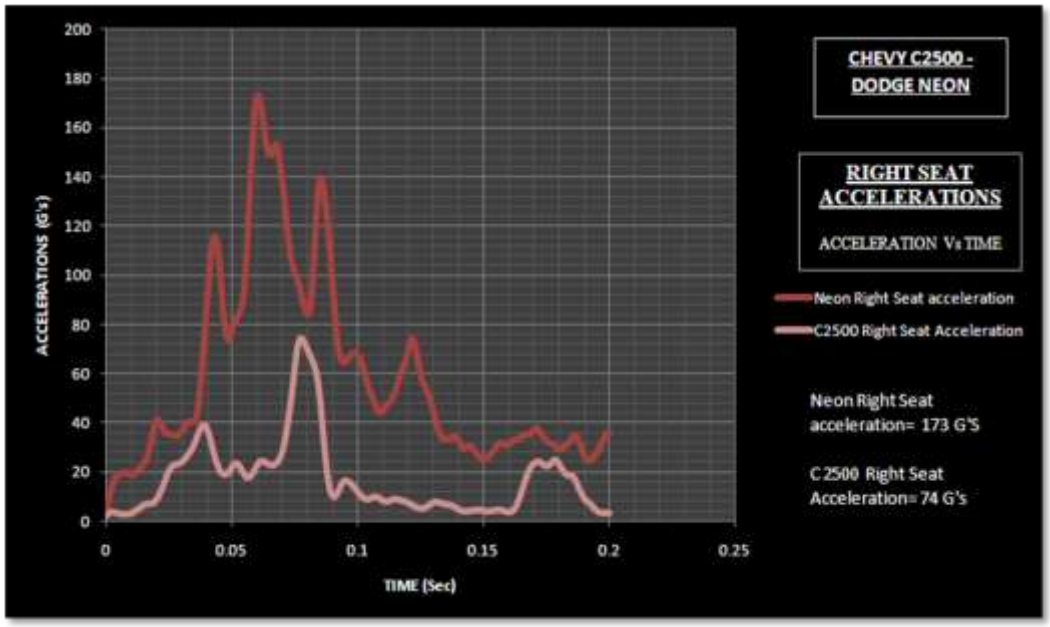

(b): Right seat acceleration in CASE-VII

5.2.3 Discussion

In this crash scenario of Chevy C1500 against the Dodge Neon. The C1500 is a light duty truck, which is stiffer than the passenger car. Hence the acceleration ratios will not follow a particular trend and will not produce consistent results. But the ride height of the pickup is not enough to over-ride on to the passenger car. The weight difference between two vehicles is also within the acceptable range which results in intrusions ratios, which can be used to estimate DFR. The acceleration ratios at the left and right seats C.G are 1: 3.4 and 1: 2.3. These two acceleration ratios do not produce consistent results and cannot be used in estimating DFR. The intrusion ratios of C1500 against Neon at firewall, foot-well and A-pillar are 1: 2.7, 1: 38 and 1:2.7 respectively. All the intrusion ratios, except the foot-well ratio, resulted in same peak value. But in the case of foot-well, the load applied by Neon on C1500 is not that high enough to intrude foot-well of the pickup because of its low weight or ride height or stiffness. From the

Table 6.4, this shows the ratio at all the crucial factors lead to fatal injury to the occupants, or can conclude that the DFR of Chevy C1500 is approximately 1: 2.7 against a passenger car.

Summary of case-VII:

Table 6.4: Summary of CASE-VII

	C1500	Neon
Firewall Intrusion (mm)	70	190
Foot well Intrusion (mm)	05	192
A-pillar Intrusion (mm)	66	180
Left seat Acceleration (G's)	55	187
Right seat Acceleration (G's)	74	173

Chevy C1500 : Dodge Neon	Ratio
Ratio of Firewall Intrusion	1: 2.7
Ratio of Foot well Intrusion	1: 38
Ratio of A-pillar Intrusion	1: 2.7
Ratio of Left seat Acceleration	1: 3.4
Ratio of Right seat Acceleration	1: 2.3

6.3 Full Size Car (Ford Taurus) Vs Passenger Car (Dodge Neon)

6.3.1 Model Description

Dodge Neon: Described in Case I.

Ford Taurus:

The FE model of Ford Taurus is developed by National Crash Analysis Center for frontal impacts based on a 1993 model Taurus. This model can be used for research work in frontal impact modes. The elements size in the frontal portion of the vehicle is very small when compared to the element size in the side and rear portion because the intrusion in these areas is very less during head to head impacts. Figure 6.31 shows the FE Model of the Ford Taurus used to represent the full-size car [22].

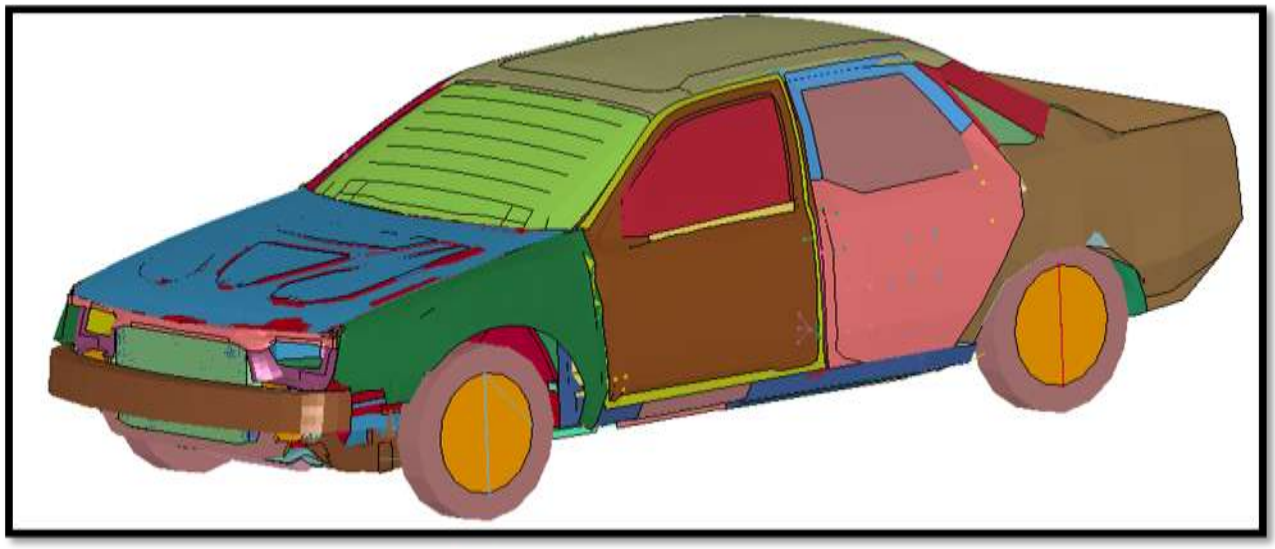

Figure 6.31: FE model of Ford Taurus

The vehicle FE model has 133 parts; each part of the model depicts different parts of the original vehicle. The material properties of different parts are derived from the coupon testing. Different materialsare ELASTIC, HONEYCOMB, RIGID, SPRING_GENERAL_NONLINEAR and PIECE_WISE_LINEAR_PLASTICITY.There are 28402 elements in the FE model out of which 140 are beam elements, 2 are discrete elements, 27873 are shell elements, 348 are solid

elements. Different parts of the vehicle are constrained by one hundred and thirty six Spot welds. The FE Model is validates the Ford Taurus NCAP test results. The Table 6.5 shows the summary of the FE Model.

Table 6.5: FE model summary of Ford Taurus

Number of Parts	133
Number of Solids	348
Number of Beams	140
Number of Shells	27873
Number of Elements	28402

6.3.2 Crash Simulation

The two vehicles are positioned such that they have full width interaction during collision and the vehicles are placed as close as possible to reduce the computational time. The contact between two vehicles is defined by using "Automatic Surface to surface "card. Static and dynamic friction coefficients are given as 0.3 between the contacts of two vehicles. Rigid wall planar cards are used between the contact of all tires and roads. Initial velocity of 35 mph is given to both vehicles and the termination time of 200 milliseconds is given with a time step of 10 milliseconds. The total computational time for simulation this crash scenario is almost 15 hours. Figure 6.32 shows the results of crash simulation between two vehicles at different time steps.

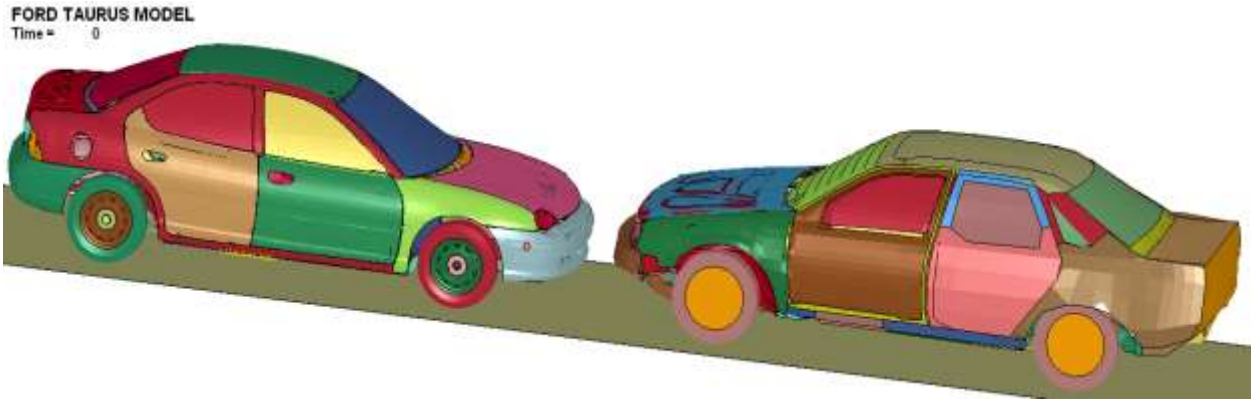

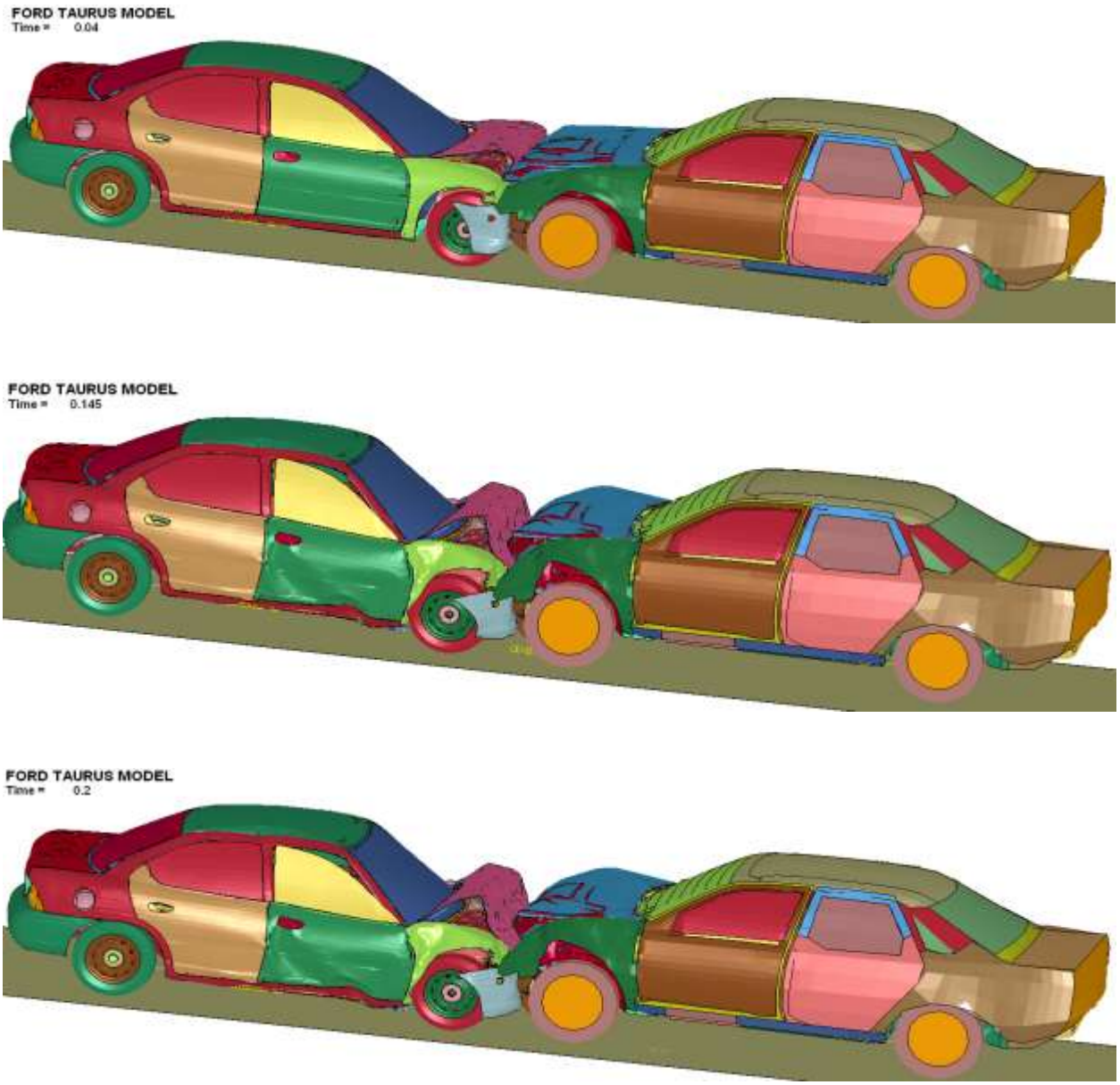

Figure 6.32: Animation of Ford Taurus crashing against Dodge Neon

The two vehicles are placed as close as possible to each other to reduce calculation time. The maximum crush between the vehicles happened at 90 ms, after which the two vehicles will start to come apart from each other. After reaching the maximum crush stage, firewall, driver side A-pillar, foot-well intrusions and accelerations of left and right seat are measured. The Figure 6.33 shows the intrusions in the firewall of Ford Taurus.

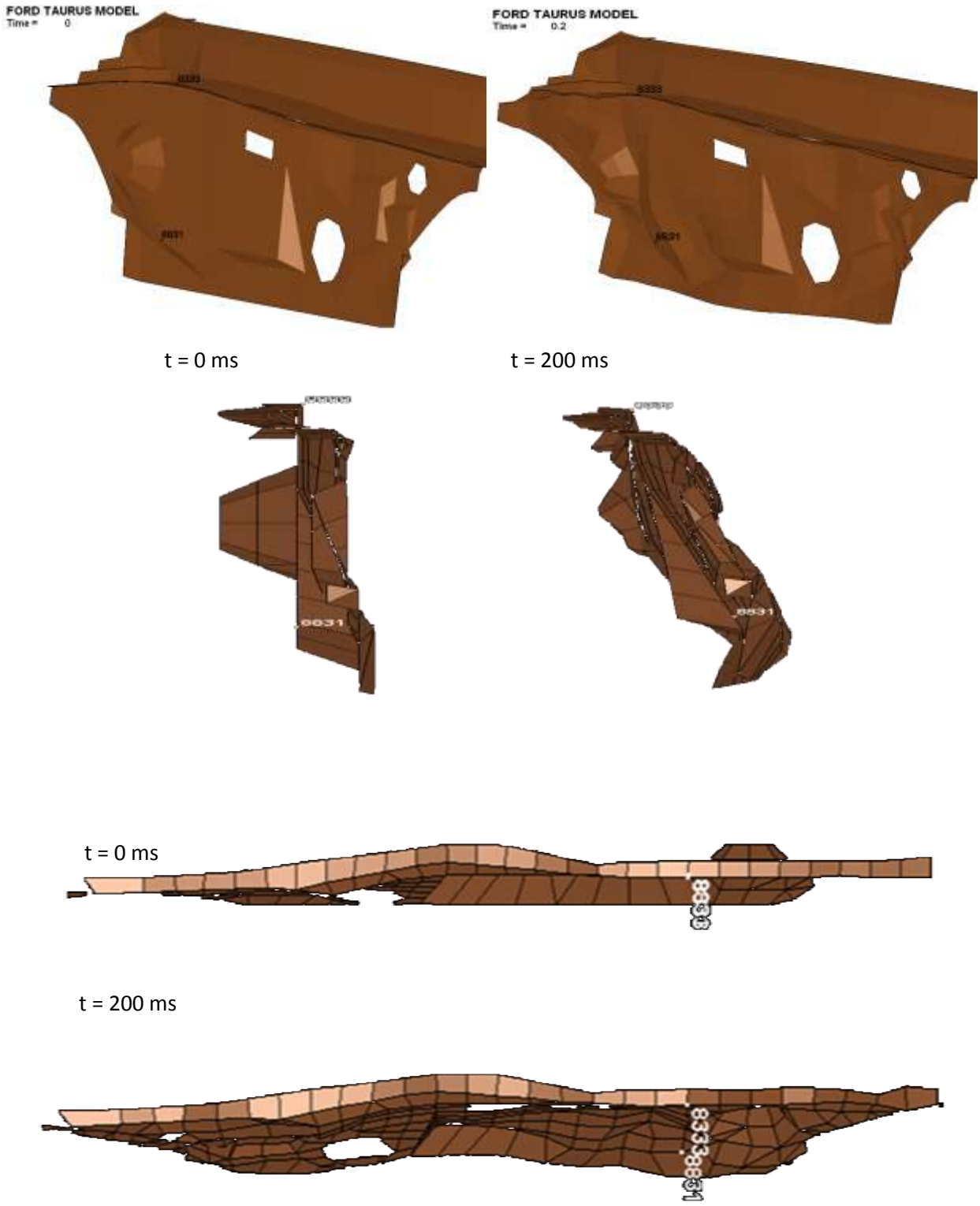

Figure 6.33: Animation sequence showing intrusion in firewall of Taurus in CASE-VIII

From Figure 6.33, it is evident that the maximum intrusion occurs approximately at node 8831. The resultant displacement of the maximum intruded node is shown in the graph below. From the Figure 6.34, maximum intrusion in the firewall of Taurus in collision with a passenger car is measured as 87mm.

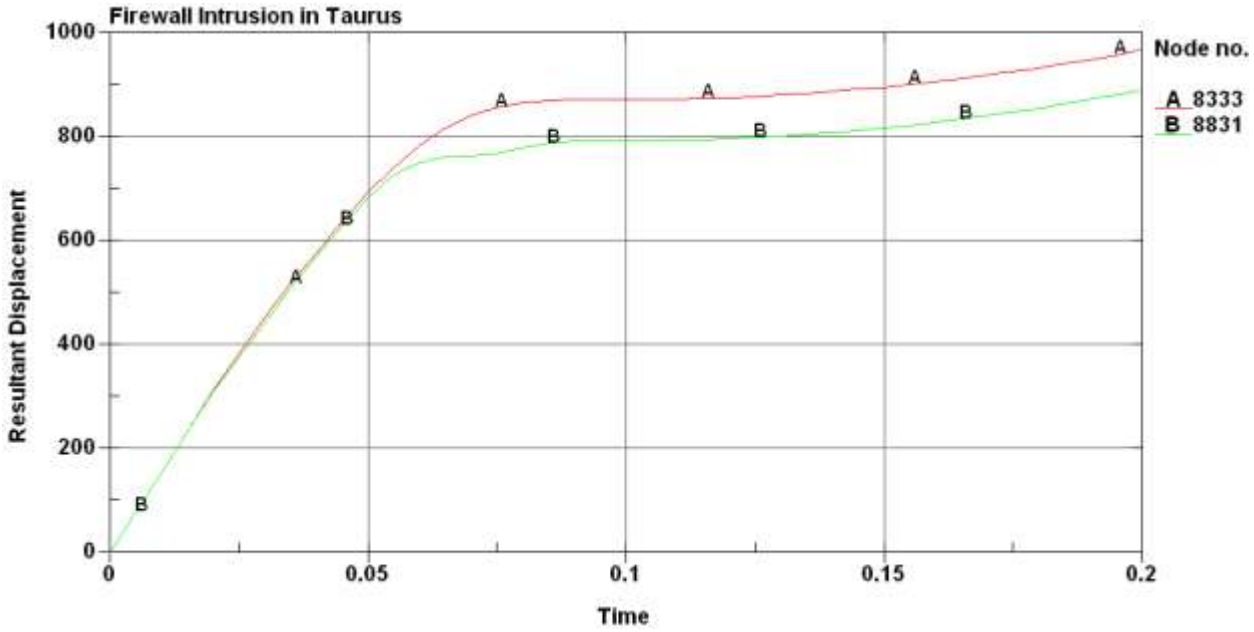

Figure 6.34: Maximum intrusion in firewall of Taurus in CASE-VIII

Foot-well Intrusion in Ford Taurus:

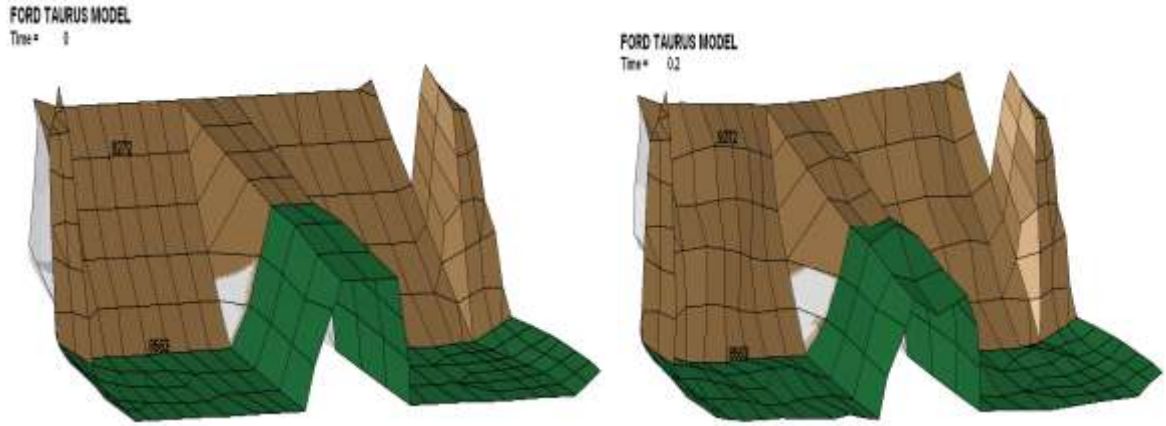

(a): Intrusion in Foot-well of Taurus in CASE-VIII (isometric view)

Figure 6.35: Animation sequence showing intrusion in foot-well of Taurus in CASE-VIII (a) isometric view (b) side view

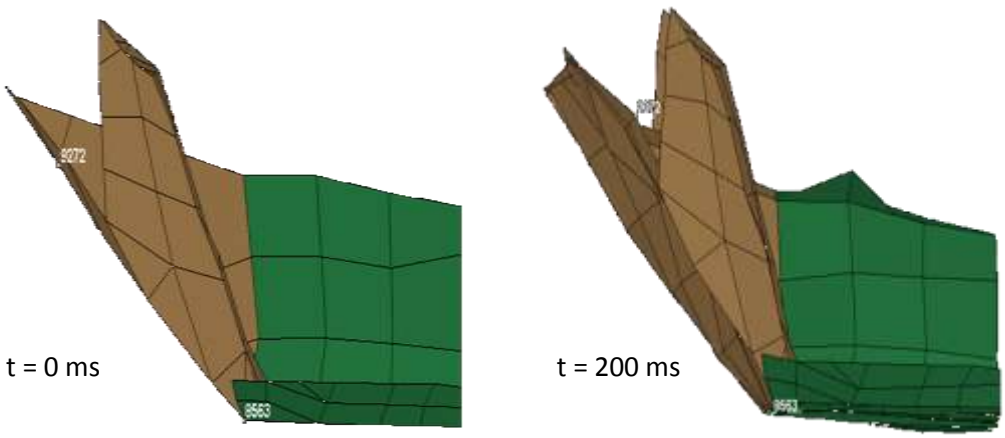

(a): Intrusion in Foot-well of Taurus in CASE-VIII (side view)

The maximum intrusion in the foot-well of Taurus occurs at node 9272 and the Figure 6.35 shows the animation sequence of intrusions. The resultant displacement of this maximum intruded node is shown in the Figure 6.36. From Figure 6.36, the maximum intrusion in the foot-well of Taurus in collision with a passenger car is found to be 57mm.

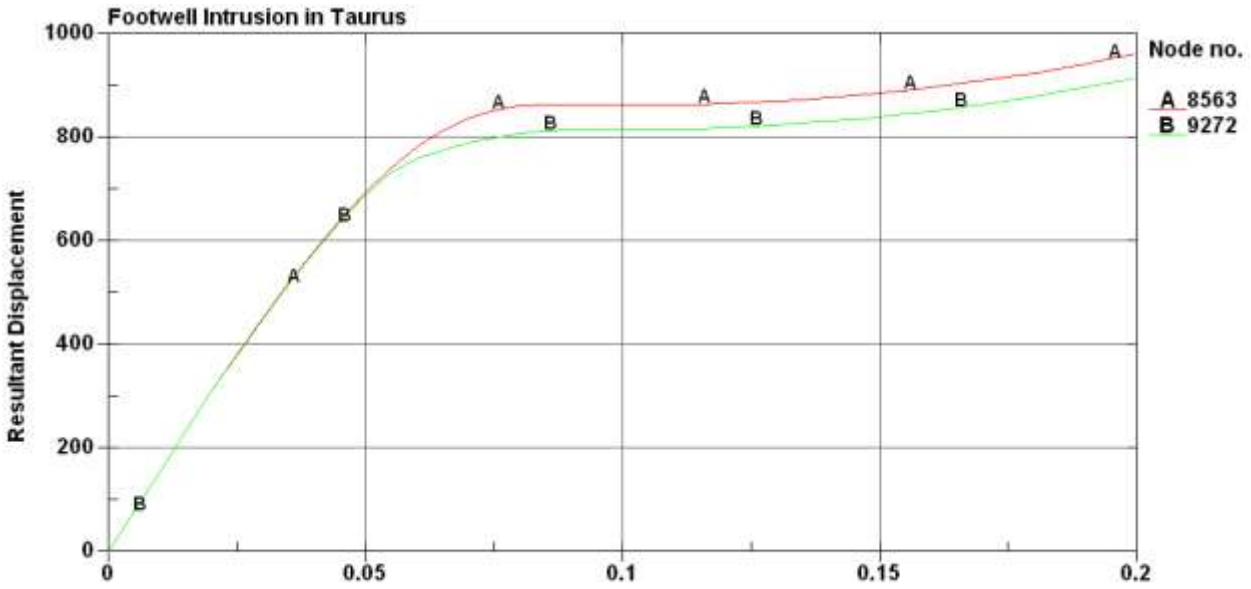

Figure 6.36: Maximum intrusion in foot-well of Taurus in CASE-VIII

Driver side A-Pillar Intrusion in Rav4:

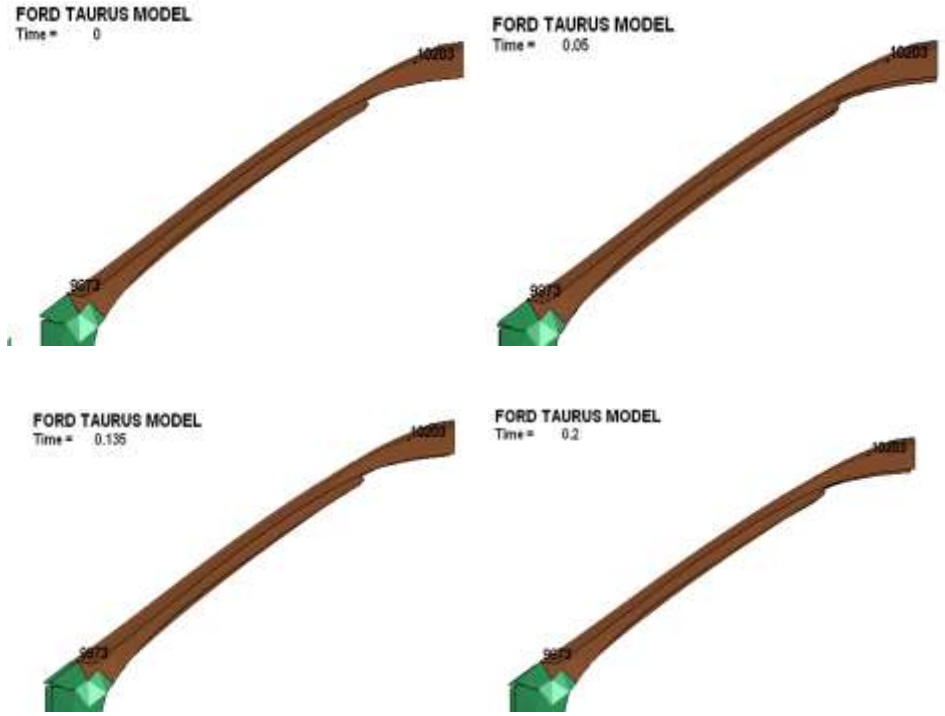

Figure 6.37: Animation sequence showing intrusion in driver side A-pillar of Taurus in CASE-VIII

From the Figure 6.37, the node which had maximum rearward movement on the A-pillar of the Taurus is Node #9873, the maximum displacement of this node is 12mm and the Figure 6.38 shows the displacement of the node with respect to time.

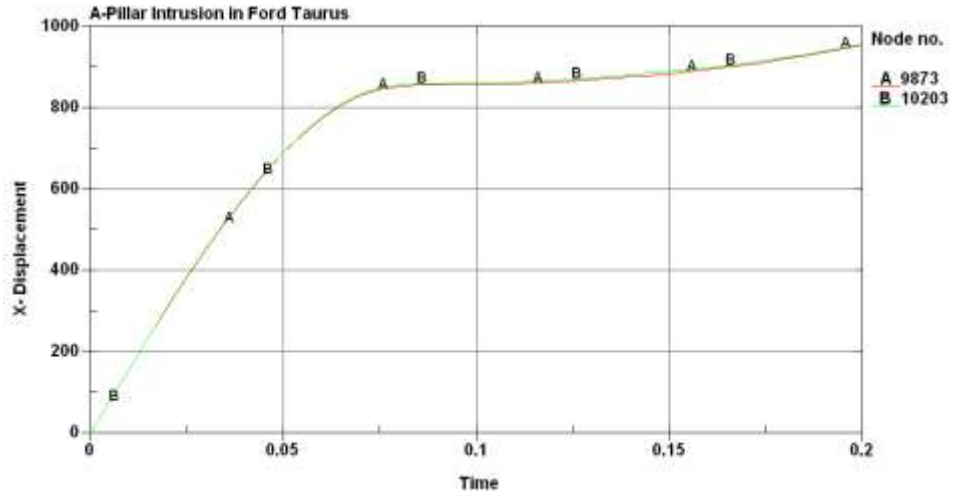

Figure 6.38: Maximum intrusion in driver side A-pillar of Taurus in CASE-VIII

Firewall Intrusion in Dodge Neon:

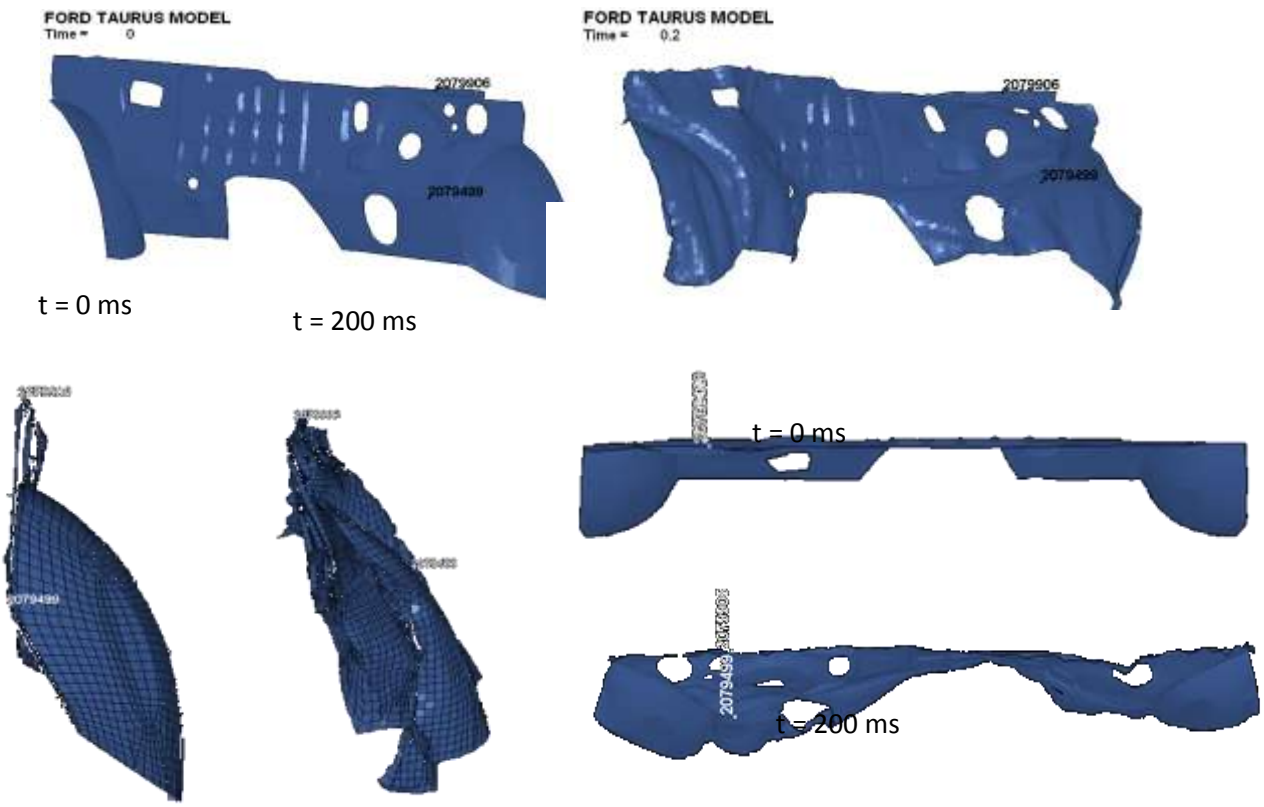

Figure 6.39: Animation sequence showing intrusion in firewall of Neon in CASE-VIII

From the Figure 6.39 the maximum intrusion in the firewall of the Dodge Neon occurs approximately at node # 2079906, the maximum displacement of this node is 193 mm, as is shown in Figure 6.40

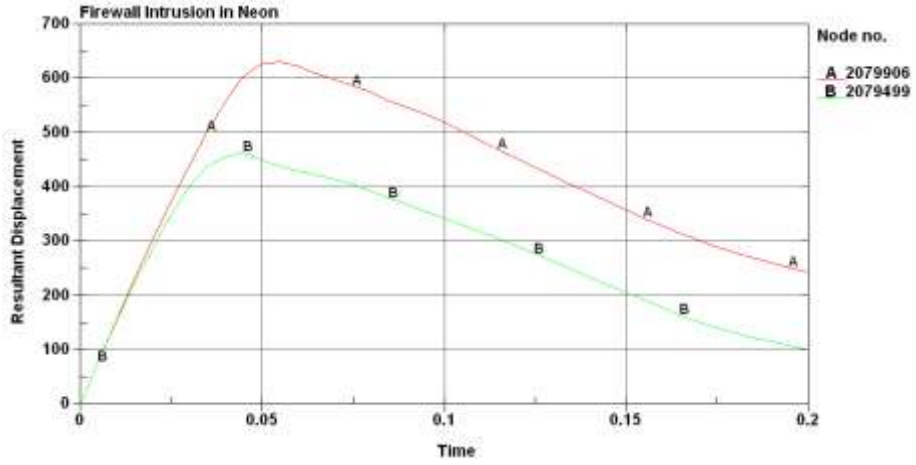

Figure 6.40: Maximum intrusion in firewall of Neon in CASE-VIII

Foot-well Intrusion in Neon:

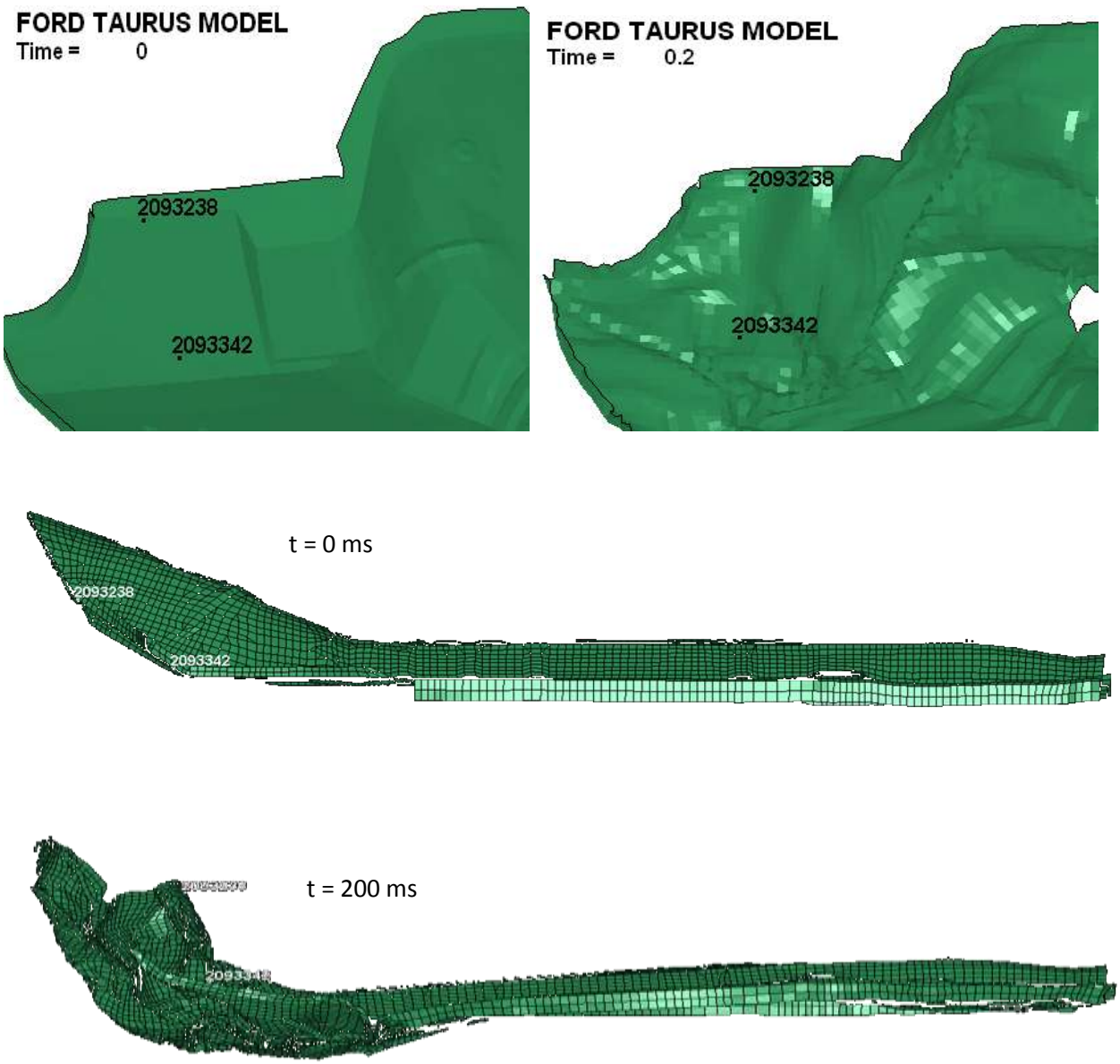

Figure 6.41: Animation sequence showing intrusion in foot-well of Neon in CASE-VIII

From Figure 6.41, maximum intrusion in the foot-well of the Dodge Neon occurs approximately at Node # 2093238, the maximum displacement of this node is 132 mm, as is shown in the Figure 6.42.

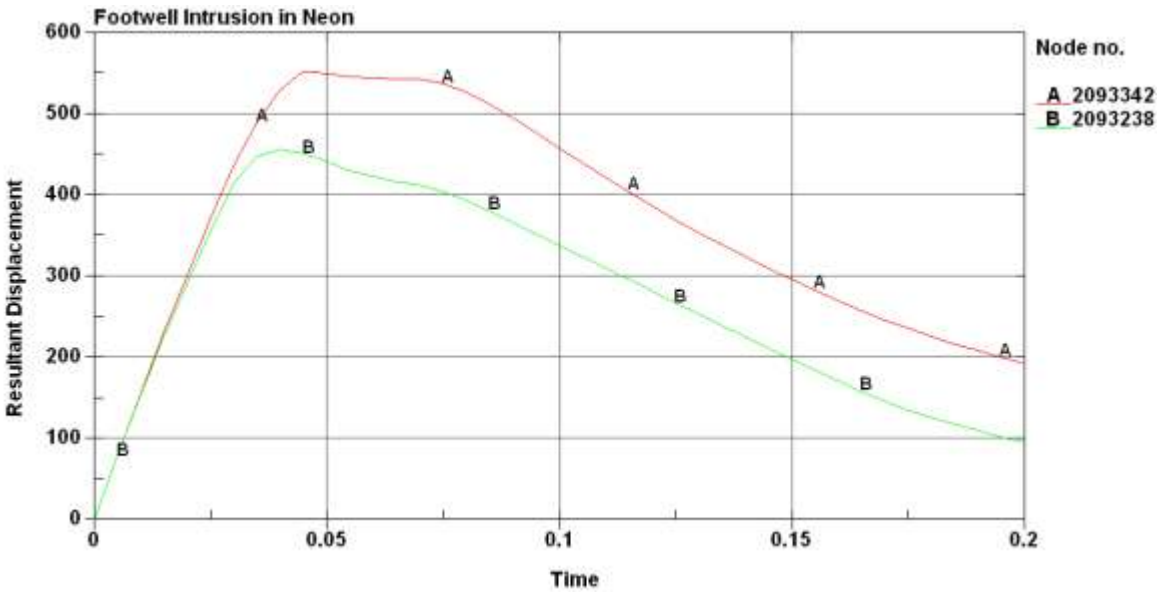

Figure 6.42: Maximum intrusion in foot-well of Neon in CASE-VIII

Driver side A-Pillar Intrusion in Dodge Neon:

The Figures 6.43 show the movement of A-pillar during the collision with a Full-size car.

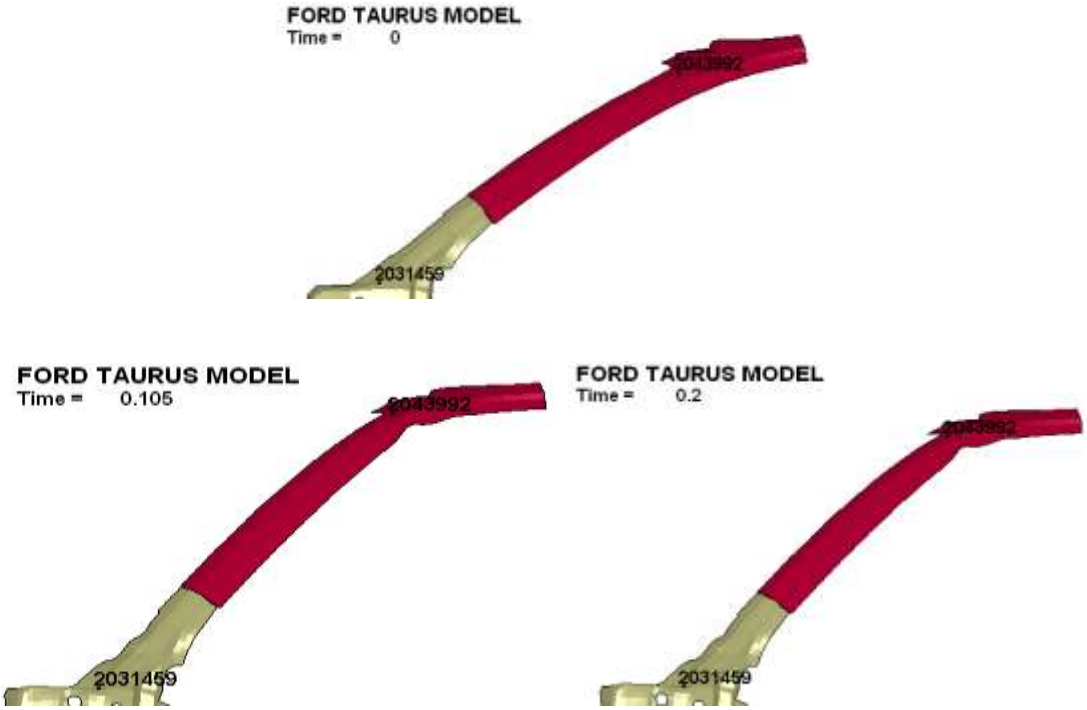

Figure 6.43: Animation sequence showing intrusion in driver side A-pillar of Neon in CASE-VIII

From Figure 6.43, the node which has maximum rearward movement on the A-pillar of the Dodge Neon is node #2031459, the maximum displacement of this node is found to be 113mm and the graph below shows the displacement of the node with respect to time.

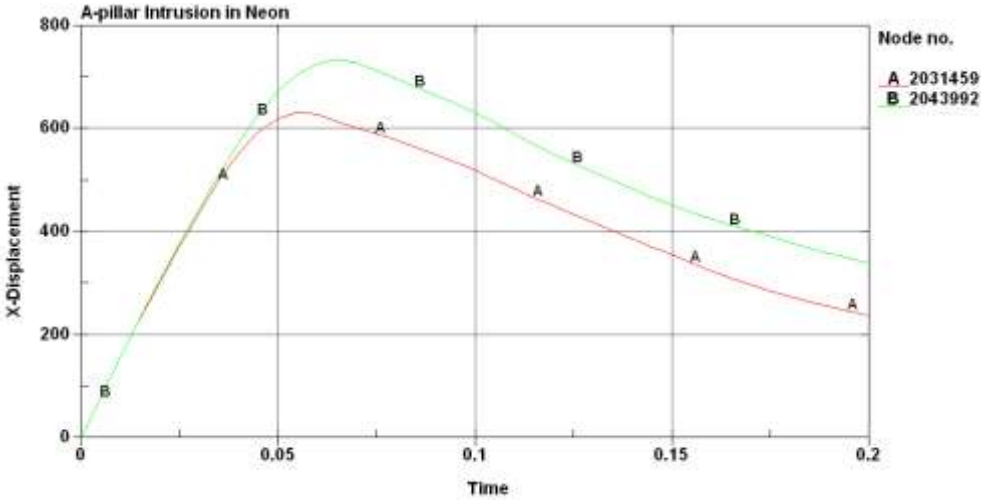

Figure 6.44: Maximum intrusion in driver side A-pillar of Neon in CASE-VIII

Figure 6.45 shows the acceleration in the left and right seats in Ford Taurus and Dodge neon. The peak acceleration in the two vehicles is also shown.

LEFT and RIGHT Seat Accelerations:

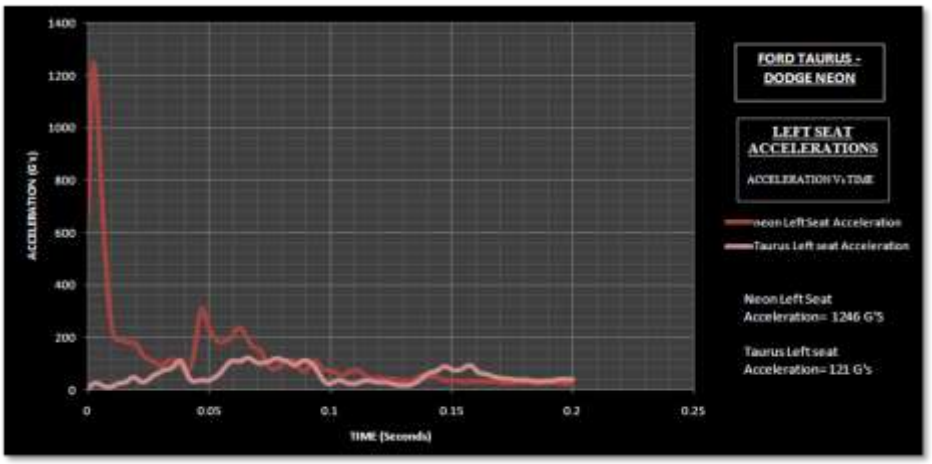

(a): Left seat acceleration in CASE-VIII

Figure 6.45: Left and Right seat acceleration in CASE-VIII

(a) Left seat (b) Right seat

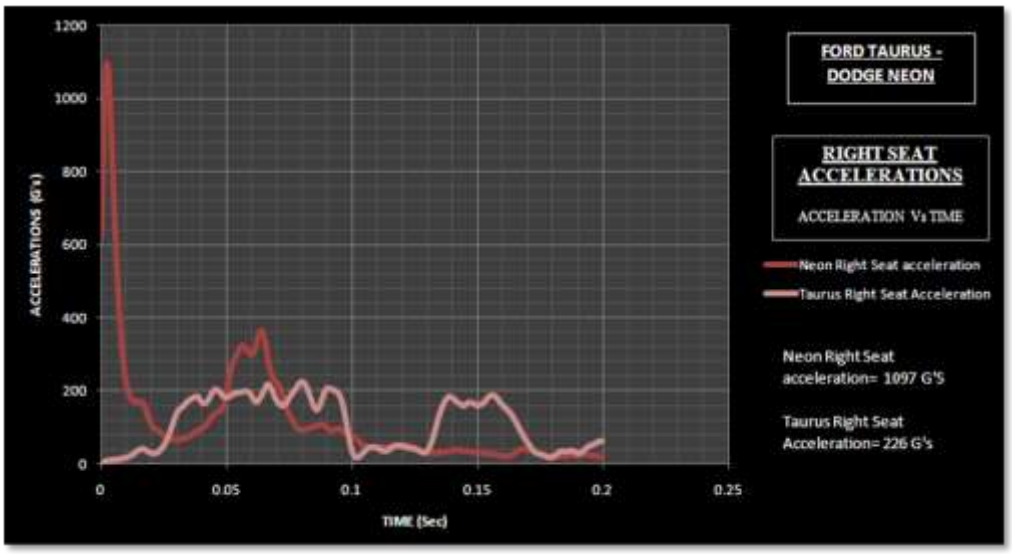

(b): Right seat acceleration in CASE-VIII

6.3.3 Discussion

In this scenario where a full-size car (Ford Taurus) crashing against a mid-size car (Dodge Neon), the weight ratio of these two cars are 1.3: 1 with Taurus being on the heavier side. The ride height of these two cars is almost the same and will not lead to under-ride of Neon into Taurus. By observing these two factors, or can state that in this crash scenario, the geometric and mass incompatibilities will not have any huge role to play. But because of sheer material properties and little difference in weight, the Taurus is stiffer than Neon. This leads to stiffness incompatibility and will result in acceleration ratios, which are completely lopsided. But due to lack of huge effect in the geometric and mass incompatibilities, the maximum intrusion ratios can be used to predict the DFR of Taurus against a mid-size car. The intrusion ratios of the Taurus against Neon at firewall, foot-well and A-pillar are 1: 2.2, 1: 2.3 and 1: 9.4 respectively. In the intrusion ratios, except the A-pillar ratio, resulted in almost the same peak value. But in the case of A-pillar, load applied by the Neon on Taurus is not high enough to intrude A-pillar of the Taurus because of its low weight and ride height. Table 6.6 shows the ratios of crucial factors

which lead to fatal injury to the occupants. Based on the proposed method of approach, the DFR of Ford Taurus is approximately 1: 2.2 against a passenger car.

Summary of case-VIII:

Table 6.6: Summary of CASE-VIII

	Taurus	Neon
Firewall Intrusion (mm)	87	193
Foot well Intrusion (mm)	57	132
A-pillar Intrusion (mm)	12	113
Left seat Acceleration (G's)	121	1246
Right seat Acceleration (G's)	226	1097

Ford Taurus : Dodge Neon	Ratio
Ratio of Firewall Intrusion	1: 2.2
Ratio of Foot well Intrusion	1: 2.3
Ratio of A-pillar Intrusion	1: 9.4
Ratio of Left seat Acceleration	1: 10
Ratio of Right seat Acceleration	1:4.9

6.4 SUMMARY OF RESULTS

The ratios of intrusions, accelerations and weights are tabulated from Tables 6.7 to 6.9. These tables summarize intrusions in the firewall, driver A-pillar, and foot-well and the acceleration in the left and right seats along with weight ratio between two vehicles. All the intrusions are in millimeter and accelerations are measured in G's. The intrusion and acceleration ratios are averaged to state the Driver Fatality Ratio for Rav4, C1500 and Taurus.

Table 6.7: Summary of intrusions measured from CASE-VI to CASE-VIII

VEHICLE CATEGORY	FIREWALL		FOOTWELL		A-PILLAR	
Toyota Rav4 - Dodge Neon	Rav4	127	Rav4	85	Rav4	64
	Neon	199	Neon	148	Neon	112
Chevy C2500- Dodge Neon	C2500	70	C2500	05	C2500	66
	Neon	190	Neon	192	Neon	180
Ford Taurus - Dodge Neon	Taurus	87	Taurus	57	Taurus	12
	Neon	193	Neon	132	Neon	113

Table 6.8: Summary of accelerations measured from CASE-VI to CASE-VIII

VEHICLE CATEGORY	VEHICLE	LEFT SEAT	RIGHT SEAT
Toyota Rav4 - Dodge Neon	Rav4	78	107
	Neon	290	273
Chevy C2500- Dodge Neon	C2500	55	74
	Neon	187	173
Ford Taurus - Dodge Neon	Taurus	121	226
	Neon	1246	1097

Table 6.9: Objective measures of Rav4, C1500 and Taurus against Neon

OBJECTIVE MEASURE								
VEHICLE CATEGORY	WEIGHT RATIO	INTRUSIONS				ACCELERATIONS		
		FIREWALL	FOOTBOARD	A-PILLAR	AVERAGE	LEFT SEAT	RIGHT SEAT	AVERAGE
Toyota Rav4 - Dodge Neon	1.2 : 1	1 : 1.6	1 : 1.7	1 : 1.7	1: 1.7	1 : 3.7	1 : 2.6	1: 3.1
Chevy C1500- Dodge Neon	1.52 : 1	1 : 2.7	1 : 38	1 : 2.7	1: 2.7	1 : 3.4	1 : 2.3	1: 2.8
Ford Taurus - Dodge Neon	1.3 : 1	1 : 2.2	1 : 2.3	1 : 9.4	1: 2.2	1 : 10	1 : 4.9	1: 7.4

By observing Table 6.9, it can be stated that the DFR of Toyota Rav4, Chevrolet C1500 and Ford Taurus are 1: 1.7, 1: 2.7 and 1: 2.2. These DFRs are evaluated based on the proposed new method of approach of chapter 5.

CHAPTER 7

CONCLUSIONS AND RECOMMENDATIONS

7.1 Conclusions

The incompatibility between vehicles in impact can be examined, when the Driver Fatality Ratio data of different vehicles are available against passenger cars. However limitation in collecting statistics during accidents and lack of statistics for new vehicles which are just released in to the market makes it difficult to calculate their Driver Fatality Ratio, and in-turn it will be difficult to study their aggressive behavior against passenger cars. This study was aimed to find a way to predict the Driver Fatality Ratio using computational validated FE models of vehicles in collisions and determining key factors which leads to fatal injuries to occupants of the car during collision.

In this research, the key factors which result in fatal injuries to the occupants were examined. The intrusion in passenger compartment of the occupant, weight of the vehicles and acceleration experienced by the occupants are the three main factors which will lead to fatal injuries. Intrusions and Accelerations and weight measured are Objective Measures. Intrusions were measured according to the IIHS specification. The left and right seat accelerations were measured to check the acceleration experienced by the drivers. Weight ratio is also observed to check whether it has any relation with DFR. Based on these factors a new method of approach is proposed which considers subjective and objective measures.

Different vehicles were selected to represent different category of LTVs and Neon car was selected to represent passenger car and crash simulation were conducted against LTVs to passenger car according to US-NCAP regulations. After the crash simulation maximum Intrusions in the firewall, foot-well and driver side A-pillar intrusion and left and right seat

accelerations were measured during the crash. Ratios of the objective measures were calculated and then compared with the statistical DFR for validation. During the comparison of objective measures it was found out that, new Method of approach works differently for different vehicle combinations. When the three Incompatibilities (mass, stiffness and geometric) are within the acceptable range the new method of approach can directly approximate the DFR, but when one incompatibility dominates the other, then different ratios in proposed methodology will vary. For instance when the stiffness incompatibility is very high between the two vehicles, the ratio of left and right seat acceleration will not produce reliable estimates and in this case Ratio of Intrusion are good estimates of DFR. In the case where the geometric incompatibility is very high, for example a large pick up crashing against a passenger car, it is more likely that the pick-up will over-ride on top of the passenger car. In this scenario the intrusion in the passenger car will produce unreliable estimates and acceleration ratio will also fluctuate because the stiffness of the Pick-up will be very high than passenger car because of huge difference in weight. In this case of geometric incompatibility it will be very hard to estimate the DFR. During validation, it was observed that ratios of intrusions produced consistent results which were identical to statistical DFR values.

After validation, three different vehicles were selected to apply new method of approach and calculate DFR are Toyota Rav4 representing Compact SUV, Chevy C1500 representing light weight Pick-up and Ford Taurus representing Full-size care. These three vehicles were crashed against Dodge neon according to US-NCAP regulation and then new method of approach was applied and DFR of Rav4, C1500 and Taurus are predicted as 1: 1.7, 1: 2.7, 1: 2.2. From the results discussed in this study, it can be concluded that "Ratio of Intrusions" provides better estimate for the DFR when there is no under-ride of smaller car in to bigger vehicle and huge

difference in stiffness. Ratio of Accelerations provides better results when the crash energy developed during collision is absorbed equally between cars involved in collision. This is possible only when two similar vehicles collide against each other. With introduction of composites (which has high strength to weight ratio) it is unlikely that weight ratio can be used to predict DFR. From above statements of pros and cons it can be concluded that Intrusion's at important parts of the passenger cabin can be used in predicting the DFR of the vehicle. DFR is difficult to estimate from the acceleration ratio since acceleration depends on the stiffness of the body. This method is accurate when there is no geometric incompatibility. By observing the intrusion ratio we can approximately predict the DFR of a vehicle during the design stage and make necessary changes to it to decrease the aggressive before it is sent out for production.

7.2 Recommendations

The proposed methodology can be studied more by placing dummy inside the vehicles during crash scenario or designing intruded passenger compartment in MADYMO and then using a dummy to measure the ratios of head, chest, and pelvis injuries in the human/dummy model might give a better estimate of DFR. This study can also be performed in offset and side impact crashes to check whether this proposed methodology can be used to predict DFR of vehicles in offset and side impacts. Designing a full vehicle model in MADYMO using multi bodies can produce decrease calculation time and can be utilized to study the dynamics of the vehicle involved in crash. Further work can also be done in estimating the effect of geometric incompatibility on the fatalities in comparison with the effects of stiffness and mass incompatibilities. This research can further be extended to observe the variation in the objective measures with the addition of pay load or mass of the vehicles because most LTVs usually carry high pay loads.

LIST OF REFERENCES

[1] Gabler H.C., Hollowell W.T., "The Crash Compatibility of Cars and Light Trucks," *Journal of Crash Prevention and Injury Control*, January 2000.

[2] Gabler H.C., Hollowell W.T., "NHTSA'S Vehicle Aggressivity and Compatibility Research Program," U.S. NHTSA, United States, Paper No. 98-S3-O-01, January 2001.

[3] Summers S., Prasad A., Hollowell W.T., "NHTSA's Vehicle Compatibility Research Program," U.S. NHTSA, United States, Paper No. 1999-01-0071, January 1999.

[4] Gabler H.C., Hollowell W.T., "The Aggressivity of Light Trucks and Vans in Traffic Crashes," U.S. NHTSA, Paper No. 980908.

[5] Joksch H., Massie D., Pichier R., "Vehicle Aggressivity: Fleet Characterization Using Traffic Collision Data," DOT HS 808 679, DOT-VNTSC-NHTSA-98-1, year 1998.

[6] Joksch H., "Vehicle Design Versus Aggressivity," Report No. DOT-HS-809-194, April 2000.

[7] Digges K., Eigen A., "Measurements of Stiffness and Geometric Compatibility in Front to Side Crashes," *ESV Conference*, Amsterdam, Holland, Paper No: 349, 2001.

[8] Gabler H.C., Hollowell W.T., "NHTSA'S Vehicle Aggressivity and Compatibility Research Program," U.S. NHTSA, United States, Paper No. 98-S4-O-01, year 2001.

[9] Les M., Morris A., Olsson T., Pettersson J., Holmqvist K., "Vehicle Properties Determining Aggressivity." October 2002.

[10] Summers S., Prasad A., Hollowell W.T., "NHTSA's Research Program for Vehicle Aggressivity and Fleet Compatibility," U.S. NHTSA, United States, Paper No. 249. September 2006.

[11] Gottumukkala V.R.R., "Study of Vehicle Aggressivity in Frontal Crash and Corresponding Occupent Responses," Master of Science Thesis, Wichita State University, July 2003.

[12] Yadav V., "Finite Modelling and Impact Study of a Low-Floor Mass Transit Bus," Master of Science Thesis, Wichita State University, December 2006.

[13] Bhagavathula N.V.S.K., "Protection of Occupants in Car Side Impact Crashes with an External InflaTable Upper Torso Restraint System," Master of Science Thesis, Wichita State University, December 2008.

[14] Krishnamurthy V., "A CAE- Based Study of Reduction of Crash Aggressivity of Pickup Trucks," Thesis submitted to WSU, December 2005.

[15] Maletz M.H., "Comparative Analysis of Structural Crash Behavior and Corresponding Occupant Responses in Vehicle-to-Vehicle impact Scenarios," Master Thesis, Vehicle Safety Institute, Graz University of Technology, Austria, October 2004.

[16] Tay R., "Tin Cans of Assault Vehicles? The Role of Crashworthiness and Non-aggressiveness in Vehicle Safety Design, Promotion and Regulation" *International Association of Traffic and Safety Sciences,* Research, 26(2), 92-98, Year 2002.

[17] Digges K., Eigen.,"Analysis of load Cell Barrier Data to Asses Vehicle Compatibility," SAE Paper No.2000-01-0051, March 2000.

[18] Latin H., Kasolas B., "Bad Designs, Lethal Profits: The Duty to Protect Other Motorists against SUV Collision Risks," Boston University, December 2002.

[19] Gabler H.C., Hollowell W.T., Stucki S.L., Summers S., Hackney J.R.,"Updated Review of Potential Test Procedures for FMVSS No.208," NHTSA, October 1999.

[20] IIHS crash test procedures, www.iihs.org [cited 2010]

[21] US NCAP regulations and crash test procedures, www.nhtsa.gov [cited 2010]

[22] FE models description, www.ncac.com [cited 2010]

[23] Crash test procedures, www.safecar.gov [cited 2010]

[24] LS PrePost and LS Dyna applications, www.lstc.com [cited 2010]

[25] Livermore Software Technology Corporation (May 2007), LS-DYNA Keyword User'a Manual Version 971.

[26] Lankarani H., McCoy M. (2003): Impact Dynamics, Lecture Notes, Wichita State University, January 2010.

[27] Lankarani H., Injury Bio-Mechanics Lecture, Wichita State University. January 2009.

[28] Safecarguide.com: NHTSA- US NCAP, www.safercarguide.com/exp/usncap/idx.htm [cited 2010].

[29] Vehicle Crashworthiness and Occupant Protection, American Iron and Steel Institute. http://www.autosteel.org/AM/Template.cfm?Section=Home&CONTENTID=28388&TEMPLATE=/CM/ContentDisplay.cfm [cited 2010].

[30] Hyde, A.S., "Crash Injuries: How and Why They Happen: A Primer for Anyone Who Cares about People in Cars," Hyde associates. August, 1992.

[31] HyperMesh applications, www.altairhyperworks.com [cited 2010].